SHORT NOTES ON ALASKA GEOLOGY 1997

Professional Report 118

Published by

STATE OF ALASKA
DEPARTMENT OF NATIONAL RESOURCES
DIVISION OF GEOLOGICAL & GEOPHYSICAL SURVEYS

MILTON A. WILTSE
STATE GEOLOGIST
1997

Alaska Department of
NATURAL
RESOURCES

SHORT NOTES ON ALASKA GEOLOGY 1997

Edited by James G. Clough and Frank Larson
Cover design by Ann-Lillian C. Schell

Professional Report 118

Recent research on Alaska geology

Front cover: *View of central Kigluaik Mountains on the Seward Peninsula. Peaks are composed of Thompson Creek Orthogneiss of Late Proterozoic to Early Precambrian age and metamorphosed at upper amphibolite facies conditions about 91 million years ago. Photograph by J.M. Amato.*

Fairbanks, Alaska
1998

STATE OF ALASKA
Tony Knowles, *Governor*

DEPARTMENT OF
NATURAL RESOURCES
John T. Shively, *Commissioner*

DIVISION OF GEOLOGICAL &
GEOPHYSICAL SURVEYS
Milton A. Wiltse
State Geologist and Director

Division of Geological & Geophysical Surveys publications may be inspected at the following locations. Address mail orders to the Fairbanks office.

Alaska Division of Geological &
Geophysical Surveys
Attn: Geologic Communications Section
794 University Avenue, Suite 200
Fairbanks, Alaska 99709-3645
http://wwwdggs.dnr.state.ak.us
dggspubs@dnr.state.ak.us

Department of Natural Resources
Public Information Center
3601 C Street, Suite 200
Anchorage, Alaska 99510

This publication, released by the Division of Geological & Geophysical Surveys, was produced and printed in Fairbanks, Alaska by the University of Alaska Printing Services, at a cost of $9.00 per copy. Publication is required by Alaska Statute 41, "to determine the potential of Alaskan land for production of metals, minerals, fuels, and geothermal resources; the location and supplies of groundwater and construction materials; the potential geologic hazards to buildings, roads, bridges, and other installations and structures; and shall conduct such other surveys and investigations as will advance knowledge of the geology of Alaska."

Foreword

This volume of *Short Notes on Alaska Geology 1997* is the tenth volume in the series begun by the Alaska Division of Geological & Geophysical Surveys (DGGS) in 1976. The *Short Notes* series was started as a vehicle in which to summarize significant observations on Alaska geology that otherwise might not find their way into accessible literature. From the outset an effort has been made to attract the contributions of geologists from the public, private, and academic sectors of Alaska's geologic community.

DGGS has a mandate to advance the knowledge of the geology of Alaska. Clearly, that task is too large to undertake alone. By working together, much more can be accomplished. I would like to reemphasize the inclusive nature of this publication. I strongly encourage readers of this issue to become participants in our next volume. In a very real sense, the *Short Notes* series is a publication of Alaska's entire geologic community.

Authors, as well as readers, benefit from contributions. The publication process is an effective mechanism for clarifying thoughts and eliciting focused comments and pertinent insight from professional peers. Many of you have interesting geologic stories to tell, and all of us would learn from reading about your observations and insights. I know that our colleagues in the private sector are working in areas that are not on the near-term agendas of any government agencies. Our colleagues in academia are pursuing specific problems that are outside the charter of either the private sector or government geologists.

I believe that all those who have contributed to the present issue as authors, reviewers, editors, and publication staff can take a great deal of pride in the fact that they have indeed advanced the state of knowledge of the geology of Alaska. Those of us who are recipients of their work are in their debt.

Sincerely,

Milton A. Wiltse

Milton A. Wiltse
State Geologist and Director

Contents

Geochronologic investigations of magmatism and metamorphism within the Kigluaik Mountains gneiss dome, Seward Peninsula, Alaska
Jeffrey M. Amato and James E. Wright *1*

Composite standard correlation of the Mississippian-Pennsylvanian (Carboniferous) Lisburne Group from Prudhoe Bay to the eastern Arctic National Wildlife Refuge, North Slope, Alaska
John F. Baesemann, Paul L. Brenckle, and Paul D. Gruzlovic *23*

Enigmatic source of oil from Chukchi Sea, northwestern Alaska
Arthur C. Banet and Thomas C. Mowatt *37*

Emsian (late Early Devonian) fossils indicate a Siberian origin for the Farewell Terrane
Robert B. Blodgett *53*

Growth-position petrified trees overlying thick Nanushuk Group coal, Lili Creek, Lookout Ridge Quadrangle, North Slope, Alaska
Paul L. Decker, Gregory C. Wilson, Arthur B. Watts, and David Work *63*

Paleotopographic control on deposition of the lower Kayak Shale, northern Franklin Mountains, Brooks Range, Alaska
David L. LePain *71*

Cooling history of the Okpilak batholith, northeastern Brooks Range, as determined from potassium-feldspar thermochronometry
Julie S. Paegle, Paul W. Layer, and Andrew W. West *87*

First occurrence of a hadrosaur (Dinosauria) from the Matanuska Formation (Turonian) in the Talkeetna Mountains of south-central Alaska
Anne D. Pasch and Kevin C. May *99*

Petrography of the Tingmerkpuk Sandstone (Neocomian), northwestern Brooks Range, Alaska: A preliminary study
Rocky R. Reifenstuhl, Michael D. Wilson, and Charles G. Mull *111*

Lower to Middle Devonian (latest Emsian to earliest Eifelian) conodonts from the Alexander Terrane, southeastern Alaska
Norman M. Savage and Constance M. Soja *125*

Preliminary petrography and provenance of six Lower Cretaceous sandstones, northwestern Brooks Range, Alaska
Marwan A. Wartes and Rocky R. Reifenstuhl *131*

Previous Editions of Short Notes on Alaska Geology *141*

GEOCHRONOLOGIC INVESTIGATIONS OF MAGMATISM AND METAMORPHISM WITHIN THE KIGLUAIK MOUNTAINS GNEISS DOME, SEWARD PENINSULA, ALASKA

by
Jeffrey M. Amato[1] and James E. Wright[2]

ABSTRACT

Geologic mapping and detailed U-Pb geochronologic investigations with monazite and zircon have shown that metamorphism and magmatism are spatially and temporally related in the Kigluaik gneiss dome, exposed in the Kigluaik Mountains, Seward Peninsula, Alaska. Protolith ages from this high-grade metamorphic culmination range from Late Proterozoic through Devonian based on existing fossil data and new U-Pb zircon dates of 678 ± 4 Ma and 555 ± 15 Ma from orthogneiss within the metasedimentary section. A pre-120 Ma blueschist-facies metamorphism that likely affected the entire crustal section was followed by a thermal overprint that increased in metamorphic grade with structural depth from subgreenschist facies to granulite facies. Limited magmatism occurred at ~110-105 Ma based on U-Pb zircon dates from minor orthogneiss bodies, and these highly strained rocks indicate that significant deformation was associated with the thermal overprint. The high-temperature overprint has a minimum age of 91 Ma, based on U-Pb analyses of monazite from orthogneiss and metapelite and from pegmatite derived from partial melting of metasedimentary rocks. Monazite dates of 94-98 Ma may reflect incomplete resetting at 91 Ma. Extensive detailed U-Pb dating of zircon from the mafic root of the Kigluaik pluton using conventional and step-wise HF dissolution techniques yielded a 90 ± 1 Ma intrusive age, suggesting that mantle-derived magmatism was the heat source for high-temperature metamorphism. Diabase dikes cut the pluton, and similar dikes in the country rock intruded at 83 ± 1 Ma, based on $^{40}Ar/^{39}Ar$ dating of biotite and hornblende.

INTRODUCTION

An integral part of the analysis of deformed high-grade gneiss terranes is understanding the temporal relationships between magmatism and metamorphism. In the upper and upper middle crust, peak metamorphic temperatures are often low enough that $^{40}Ar/^{39}Ar$ geochronologic techniques can accurately constrain the timing of metamorphism and associated deformation (Foster and others, 1992). However, in the middle and lower crust, metamorphic temperatures can greatly exceed the Ar closure temperatures for common metamorphic minerals such as mica or amphibole, and $^{40}Ar/^{39}Ar$ dates will give only a minimum age for peak metamorphism. Such is the case in the Kigluaik gneiss dome, a high-grade metamorphic culmination in the Kigluaik Mountains, located on the Seward Peninsula of Alaska (fig. 1). This gneiss dome is cored by a compositionally diverse granitoid pluton that may have provided the heat necessary for upper-amphibolite facies to granulite facies metamorphism, possibly above 750°C in this region (Lieberman, 1988). To test the hypothesis that plutonism may have been a driving force for metamorphism, we have relied on geologic mapping to determine the spatial relationships between the pluton and metamorphic rocks, and on U-Pb dating of zircon to determine the pluton emplacement ages. Because of the high grade of metamorphism, we used U-Pb techniques on monazite, an igneous and metamorphic mineral with a high closure temperature, to attempt to constrain the peak metamorphic age. Tectonic models and a petrogenetic investigation of the Kigluaik pluton can be found in Amato and others (1994), Amato (1995), and Amato and Wright (1997).

This paper summarizes U-Pb dating of Precambrian-Cambrian orthogneisses, U-Pb dating of Cretaceous metamorphism in the gneiss dome, and a detailed step-wise HF dissolution U-Pb experiment on zircon from the Kigluaik pluton, which we conducted after the publication of our initial U-Pb results (Amato and others, 1994). This experiment successfully yielded ages of crystallization for a pluton that presented several analytical difficulties because of the characteristics of its zircon population. We also include $^{40}Ar/^{39}Ar$ data from the youngest magmatic event in the Kigluaik Mountains, the intrusion of a diabase dike swarm.

[1]Department of Geological and Environmental Sciences, Stanford University. Now at Department of Geology and Geophysics, University of Wisconsin, Madison, Wisconsin 53706.
[2]Department of Geology and Geophysics, Rice University, Houston, Texas 77001.

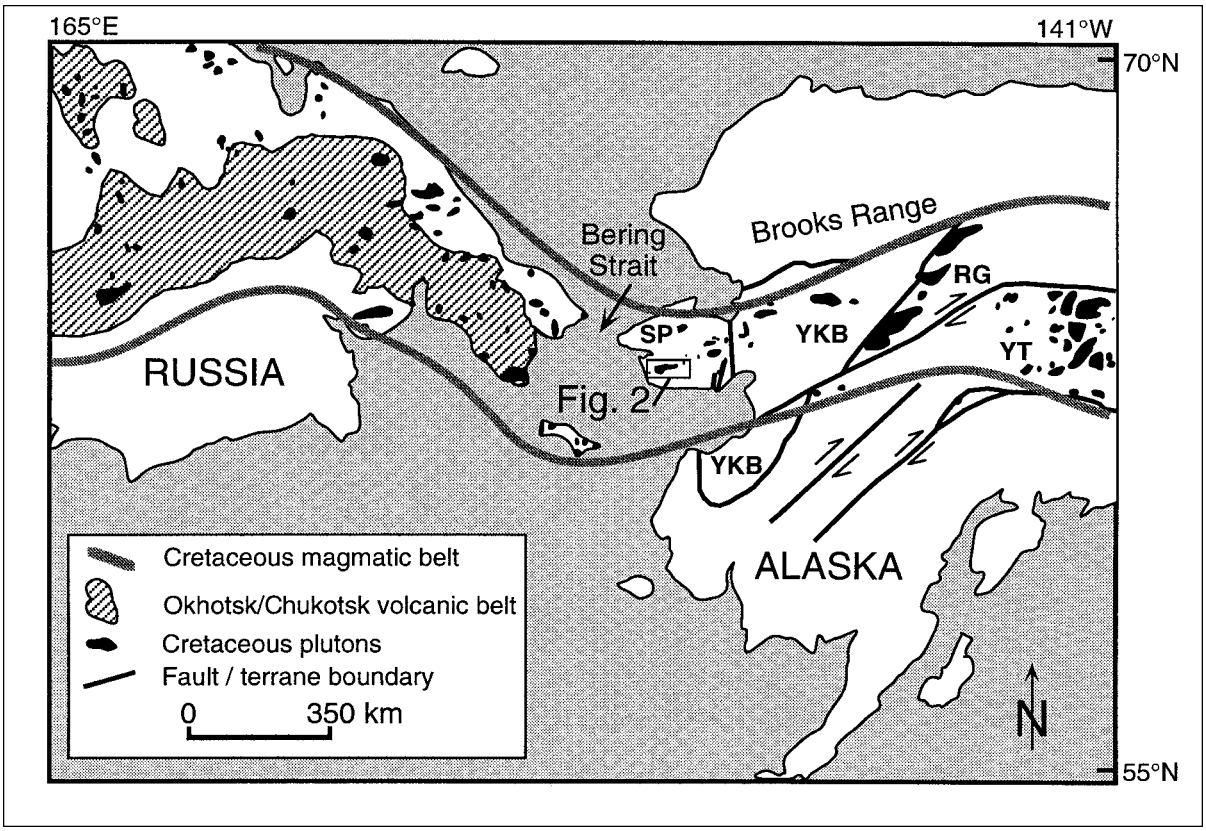

Figure 1. *Regional map showing the boundaries of the Late Cretaceous magmatic belt in the Russian Far East, Seward Peninsula, and interior Alaska. Also shown are the major physiographic elements of northern Alaska. SP= Seward Peninsula, YKB= Yukon-Koyukuk basin, RG= Ruby geanticline, YT= Yukon-Tanana upland.*

GEOLOGIC BACKGROUND

The Kigluaik Mountains gneiss dome is a metamorphic and structural culmination of upper-amphibolite to granulite-facies paragneisses and orthogneisses referred to as the Kigluaik Group (fig. 2) (Moffit, 1913). The gneiss dome is cored by the Kigluaik pluton and flanked by the structurally higher (but lower-grade) Nome Group, which consists of quartzose and pelitic schist, marble, metabasite, and rare felsic orthogneiss (Moffit, 1913; Till and Dumoulin, 1994). Previous studies of the geology of the Kigluaik Mountains include USGS reconnaissance mapping (Brooks and others, 1901; Moffit, 1913; Hummel, 1962; Sainsbury and others, 1972; Till and others, 1986), investigations of metamorphic conditions in the core of the gneiss dome (Lieberman, 1988; Patrick and Lieberman, 1988; Todd and Evans, 1993), and structural and geochronologic studies (Miller and others, 1992; Amato and others, 1994; Amato, 1995).

Both the Kigluaik and Nome Groups have Late Proterozoic to Paleozoic protolith ages (Till and Dumoulin, 1994) and were metamorphosed to blueschist and lower greenschist facies. Relict blueschist-facies minerals found in the Nome Group provide evidence for this high-pressure metamorphic event that likely affected both the Nome and Kigluaik Groups. The first detailed analysis of the age of the blueschist-facies event was by Armstrong and others (1986), who used Rb-Sr isochron and K-Ar ages of whole rock and white mica from Nome Group schists to conclude that the "maximum" of the high-pressure event was pre-160 Ma, and that the rocks reequilibrated during the time span 160 to 100 Ma.

Figure 2. *Simplified geologic and sample locality map of the Kigluaik Mountains, after Amato (1995). Structural data are omitted for clarity. The range forms a doubly plunging antiform or dome, with the dominant axis trending east-west. The Kigluaik pluton is exposed primarily in the west half of the dome. The Nome Group-Kigluaik Group contact is at the biotite-in isograd. Key for U-Pb zircon geochronology samples (see table 1 for exact location of all geochronology samples, including U-Pb monazite samples): 1 = 92.5A-139, 2 = 92.4A-120, 3 = 92.4A-119, 4 = 87AH-58, 5 = 90P12-5, 6 = SP90-6, 7 = 86SB69-1, 8 = 87SB65-5.*

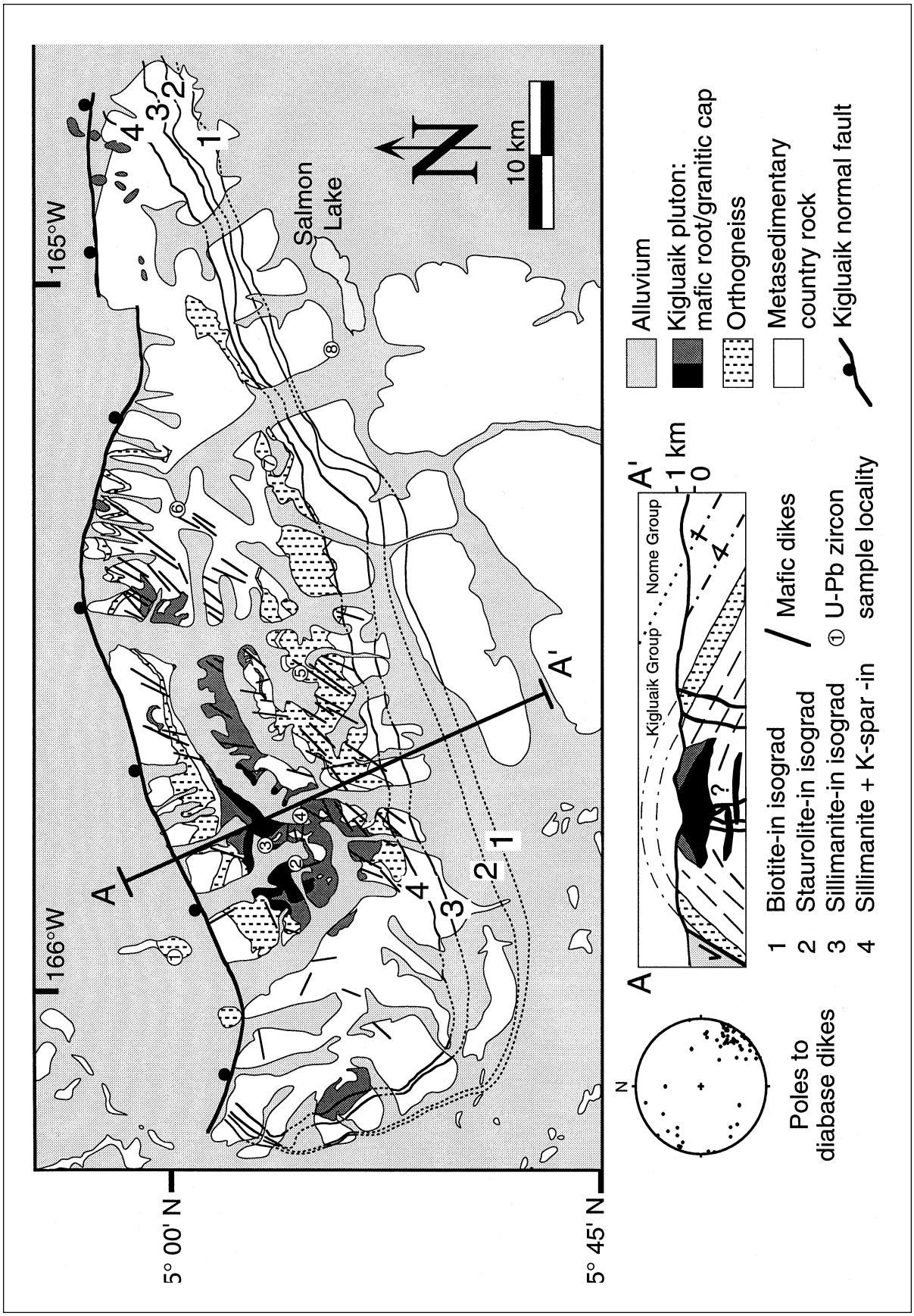
166°W
165°W
5° 00' N
5° 45' N
Salmon Lake
N
10 km
A
A'
1
2
3
4
Alluvium
Kigluaik pluton: mafic root/granitic cap
Orthogneiss
Metasedimentary country rock
Kigluaik normal fault
Kigluaik Group
Nome Group
1 km
0
Mafic dikes
1 Biotite-in isograd
2 Staurolite-in isograd
3 Sillimanite-in isograd
4 Sillimanite + K-spar -in
① U-Pb zircon sample locality
Poles to diabase dikes

A reevaluation of the age of blueschist-facies metamorphism in the Nome Group was reported in Hannula (1993) and Hannula and McWilliams (1995). They extensively sampled Nome Group schists at a variety of structural levels, including schists from localities reported in Armstrong and others (1986), and they used high-precision $^{40}Ar/^{39}Ar$ techniques to date white mica. Samples from the upper part of the structural section yielded plateau ages of 116-125 Ma, which they interpreted as the minimum age for high-pressure metamorphism. White mica from rocks at deeper structural levels that were affected by Cretaceous high-temperature metamorphism yielded disturbed spectra that ranged from 123 Ma to 334 Ma. Hannula and McWilliams (1995) interpreted these old dates as the result of the incorporation of excess ^{40}Ar.

Following the blueschist metamorphism, upper-amphibolite-facies to granulite-facies metamorphism associated with the development of the gneiss dome achieved peak conditions of 800-850°C and 8-10 kbar (Moffit, 1913; Throckmorton and Hummel, 1979; Lieberman, 1988) and caused thermal overprinting of blueschist-facies rocks. Closely spaced Barrovian-type isograds separating the Nome Group from the underlying Kigluaik Group indicate a high metamorphic field gradient, which was originally interpreted as the result of a static, high-temperature overprint associated with the relaxation of isotherms following blueschist-facies metamorphism (Lieberman, 1988; Patrick and Evans, 1989). Other workers, however, have suggested that extensional deformation associated with unroofing of the gneiss dome was responsible in part for telescoping the crustal section and collapsing the isograds (Miller and others, 1992). The dominant foliation and layering within the Kigluaik Group defines an east-west-trending, doubly plunging arch that is cored by the Kigluaik pluton in the western half of the range and cut by a swarm of northeast-striking diabase dikes (fig. 2). Amato and others (1994) proposed that mafic magmatism, represented by gabbro and diorite in the root of the Kigluaik pluton, was the heat source for Late Cretaceous metamorphism.

PROTOLITH AGES FOR METAMORPHIC ROCKS

PREVIOUS WORK

The protoliths for the Nome Group and Kigluaik Group initially were thought to be Precambrian, based on the degree of metamorphism and the lack of fossils (Moffit, 1913). Later maps used the notation "Paleozoic(?)" (Hummel, 1962), but Sainsbury (1969) noted that Early Ordovician fossiliferous limestones in the Nome Group of western Seward Peninsula were underlain by older, unfossiliferous metasedimentary rocks that may be Precambrian. Similarly, it was assumed that the lack of fossils in the underlying Kigluaik Group indicated Precambrian protoliths for the high-grade paragneisses. Till and others (1986) summarized fossil evidence that indicated that Cambrian to Devonian carbonate rocks were present in the Nome Group on the western Seward Peninsula. Rb-Sr model dates from the Nome Group, where an initial $^{87}Sr/^{86}Sr$ for the rocks is assumed and an age is calculated, fall within the range 464 Ma to 538 Ma (Armstrong and others, 1986). Patrick and McClelland (1995) reported U-Pb zircon ages of 676 ± 15 Ma and 681 ± 3 Ma from two felsic orthogneiss bodies that intrude the Nome Group.

The protoliths of the Kigluaik Group are thought to be about the same age as (or possibly older than) those of the Nome Group based on lithologic similarities. Bunker and others (1979) reported a Rb-Sr whole-rock isochron age of 735 Ma from a Kigluaik Group paragneiss, which they interpreted to be the age of high-temperature metamorphism. Armstrong and others (1986) reinterpreted this as a depositional age for the Kigluaik Group protoliths, but cautioned that Rb and Sr mobility during metamorphism likely introduced significant uncertainty. A Rb-Sr whole-rock isochron date of 335 Ma from orthogneisses within both the Nome Group and Kigluaik Group was interpreted as the result of partial resetting of Precambrian ages during Cretaceous metamorphism (Bunker and others, 1979).

NEW U-PB ZIRCON DATA FROM PRECAMBRIAN-PALEOZOIC ORTHOGNEISSES

To obtain a minimum age of the protoliths of the Nome Group and the Kigluaik Group, we dated an orthogneiss from each. In the Nome Group we dated three fractions of zircon from a felsic orthogneiss that crops out near Salmon Lake (sample 87SB65-5; tables 1, 2; figs. 2, 3). Two of the fractions are highly discordant, and the third fraction, which was leached in HF, is nearly concordant. Together, the three fractions define a highly linear array with an upper concordia intercept of 678 ± 4 Ma and a lower concordia intercept of 92 ± 6 Ma. We interpret the upper intercept as the age of the protolith of the orthogneiss. This age is analytically indistinguishable from the ~680 Ma ages obtained by Patrick and McClelland (1995), and is further evidence for the presence of Precambrian rocks within the Nome Group. The lower intercept is evidence of disturbance during Cretaceous metamorphism.

The Kigluaik Group contains larger and more numerous orthogneiss bodies than does the Nome

Table 1. *Geochronology sample locations*

Sample	Latitude (N)	Longitude (W)
87AH-58	64° 56' 00"	165° 44' 15"
87SB65-5	64° 54' 27"	165° 06' 24"
89SB69-1	64° 56' 49"	165° 15' 26"
89SLMC-42	64° 56' 36"	166° 05' 23"
89SLMC-51	64° 51' 59"	166° 00' 16"
89SMC-27	64° 55' 25"	166° 05' 16"
90P12-5	64° 55' 42"	165° 31' 59"
90P8-4c	64° 55' 07"	165° 29' 31"
90P8-9	64° 54' 29"	165° 27' 35"
91G-42	64° 59' 30"	165° 43' 47"
92.1A-9b	65° 01' 36"	165° 36' 21"
92.2A-26b	64° 53' 41"	165° 35' 03"
92.2A-38	64° 53' 45"	165° 37' 45"
92.2A-39c	64° 53' 55"	165° 37' 29"
92.2A-40	64° 55' 00"	165° 37' 19"
92.2A-57	64° 54' 33"	165° 33' 57"
92.3A-101	64° 54' 46"	165° 43' 46"
92.4A-114	64° 53' 41"	165° 39' 08"
92.4A-119	64° 57' 14"	165° 46' 26"
92.4A-120	64° 56' 09"	165° 48' 05"
92.4A-132a	64° 56' 28"	165° 52' 32"
92.4A-132b	64° 56' 28"	165° 52' 32"
92.5A-139	65° 00' 26"	165° 54' 44"
92.NA-106	65° 00' 30"	164° 49' 55"
92.SP-4	64° 56' 43"	166° 08' 39"
92.SP-5	64° 56' 28"	166° 08' 12"

Group; the largest of these is the Thompson Creek orthogneiss (Till, 1980), which is compositionally variable and highly strained. Crosscutting relationships indicate that it was originally an intrusive body. We obtained five U-Pb zircon dates from two rocks within this unit, all of which are highly discordant (table 2; fig. 4). A chord through three analyses of zircon from sample 87SB69-1 has an upper intercept of 555 ± 15 Ma and a poorly defined lower intercept of Cretaceous age. Two analyses from a separate locality within the main orthogneiss body also lie on this chord. It is interesting that all three orthogneisses from the Nome Group are ~680 Ma, and that the orthogneiss within the Kigluaik Group, which underwent both the low and high temperature metamorphic events, yields a younger age. This raises the possibility of a multistage lead-loss history, which might lower the age of the high-grade Thompson Creek orthogneiss. However, given that all five analyses from both samples lie on a well-defined chord, we interpret the upper intercept of 555 ± 15 Ma as the intrusive age of this body. Regardless of the actual protolith age, these data indicate that this orthogneiss body is not representative of the earlier Cretaceous magmatic history in the Kigluaik Mountains.

AGE OF HIGH-TEMPERATURE METAMORPHISM

PREVIOUS WORK

Although Bunker and others (1979) interpreted the 735 Ma isochron from Kigluaik Group paragneiss as the age of high-temperature metamorphism, it is now apparent that this event occurred during the Cretaceous. K-Ar dates of biotite and hornblende from paragneiss, orthogneiss, and amphibolite reported by Turner and Swanson (1981) range from 81 ± 2 Ma to 87 ± 3 Ma. K-Ar analyses of "mafic gneiss" by Sturnick (1984) yielded 84-85 Ma dates. Calvert (1992) dated hornblende from an amphibolite within the Kigluaik Group using $^{40}Ar/^{39}Ar$ techniques. He obtained a plateau date of 86 ± 1 Ma (Calvert, 1992). Because the closure temperature of hornblende to Ar diffusion is thought to be 550°C and the peak metamorphic temperatures were about 700-800°C, this date must be a minimum for peak metamorphism.

NEW U-PB MONAZITE DATA FROM ORTHOGNEISS, METAPELITE, AND PEGMATITE

To more tightly constrain the age of peak metamorphism, we collected numerous samples of orthogneiss, metapelite, and pegmatite for U-Pb dating of monazite. Monazite is a common accessory mineral in metamorphic rocks of staurolite grade or higher, and its closure temperature for the diffusion of Pb is about 725 ± 25°C (Parrish, 1990). Samples from staurolite-grade rocks, which reached maximum temperatures of <600°C, should therefore record the age of peak metamorphism. Unfortunately, all the staurolite-grade samples were barren of monazite. Of the 20 metapelitic rocks collected from levels deeper than the staurolite-in isograd, only six contained monazite. All four of the pegmatite separates yielded abundant monazite, and it was found in seven splits from orthogneiss bodies in the core of the range. Because the rocks that contained monazite may have been heated to ~700°C or higher (Lieberman, 1988), the possibility remains that the U-Pb dates obtained may reflect cooling from peak temperatures that were attained at an earlier time. All the monazite data are reversely discordant on a U-Pb concordia plot (fig. 5), most likely as the result of the incorporation of ^{230}Th during crystallization (e.g., Schärer, 1984; Parrish, 1990).

Ten analyses of monazite were obtained from seven samples of granitic orthogneiss (table 3, fig. 5). Sample 92.5A-139, from a small, highly deformed granitic orthogneiss from the northern part of the range, is compositionally and texturally similar to the Thompson

Table 2. *U-Pb zircon data from Late Proterozoic-Early Paleozoic orthogneiss*

Sample	size[c]	Wt (mg)	Concentration U (ppm)	Concentration $^{206}Pb^{*d}$ (ppm)	Measured ratios[a] $^{206}Pb/^{204}Pb$	Measured ratios[a] $^{207}Pb/^{206}Pb$	Measured ratios[a] $^{208}Pb/^{206}Pb$	Atomic ratios $^{206}Pb^*/^{238}U$	Atomic ratios $^{207}Pb^*/^{235}U$	Atomic ratios $^{207}Pb^*/^{206}Pb$	Ages (Ma)[b] $^{206}Pb^*/^{238}U$	Ages (Ma)[b] $^{207}Pb^*/^{235}U$	Ages (Ma)[b] $^{207}Pb^*/^{206}Pb$	error
Thompson Creek orthogneiss														
89SB69-1	>200l	9.4	583	31.9	7892	0.06017	0.14895	0.06364	0.51185	0.05833	398	420	542	2
89SB69-1	>200	10.6	685	36.0	7143	0.06024	0.14830	0.06114	0.49046	0.05820	382	405	538	2
89SB69-1	<200	11.3	781	37.8	16051	0.05906	0.15272	0.05637	0.45193	0.05815	354	379	535	1
90P12-5	>200	1.3	493	24.7	9524	0.05970	0.13505	0.05827	0.46743	0.05818	365	389	536	2
90P12-5	<200/>325	1.1	537	26.8	5952	0.06062	0.14378	0.05807	0.46585	0.05818	364	388	536	2
Other orthogneiss bodies														
92.5A-139	>200	1.3	1271	39.8	721	0.07670	0.18156	0.03645	0.28405	0.05652	231	254	473	6
92.5A-139	<200/>325	0.8	1536	44.4	268	0.10978	0.26004	0.03364	0.25671	0.05535	213	232	426	15
87SB65-5	>200l	6.1	460	41.1	21978	0.06263	0.19060	0.10393	0.88800	0.06197	637	645	673	1
87SB65-5	>200	7.3	1085	54.4	730	0.07998	0.21956	0.05834	0.48373	0.06014	366	401	608	5
87SB65-5	<200	6.2	1259	60.7	1090	0.07340	0.21084	0.05606	0.46443	0.06008	352	387	607	4

[a]Isotopic compositions corrected for mass fractionation of 0.11%. Sample dissolution and ion exchange chemistry modified from Krough (1973).

[b]Ages calculated by using the following constants: decay constants for ^{235}U and ^{238}U = 9.8485E-10 yr^{-1} and 1.55125E-10 yr^{-1} respectively; $^{238}U/^{235}U$ = 137.88. Precisions on $^{206}Pb^*/^{238}U$ ratios are about 0.2 to 0.3% based on the replicate analysis of two 'standard' zircon fractions. Accuracy of the $^{206}Pb^*/^{238}U$ dates, including uncertainties in spike calibration, is estimated to be within 0.5%. The two-sigma uncertainties in the $^{207}Pb^*/^{206}Pb^*$ ages were calculated from the combined uncertainties in mass spectrometry and an assumed uncertainty of ± 0.1 in the $^{207}Pb/^{204}Pb$ ratio used for the common Pb correction (Mattinson,1987).

[c]>100, <200, etc., refer to size fractions in mesh size. All analyzed zircon fractions consisted of the least-magnetic crystals that could be fractionated on a Frantz magnetic separator. "l" refers to the leachate zircon fraction that was leached for 24 hr in 50% Hf in a Teflon beaker at about 80°C. See Wright and Fahan (1988) and Dilles and Wright (1988) for details of the analytical procedure.

[d]Pb* denotes radiogenic Pb, corrected for common Pb by using the isotopic composition of $^{206}Pb/^{204}Pb$ = 18.6 and $^{207}Pb/^{204}Pb$ = 15.6.

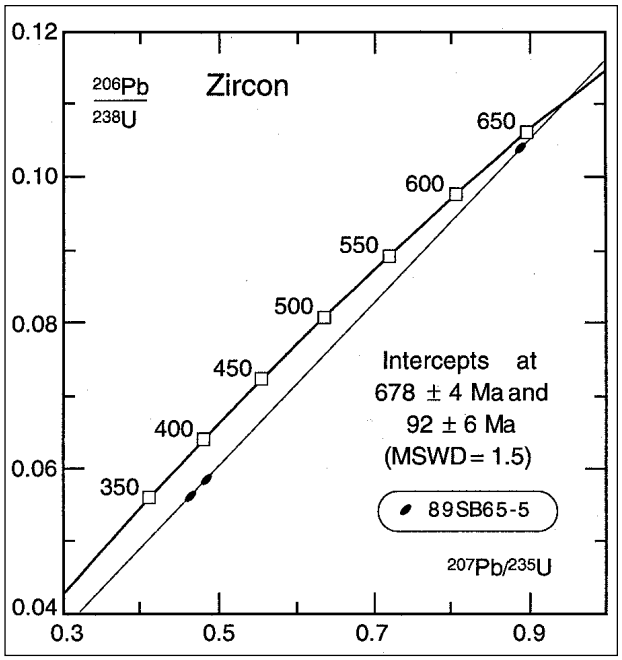

Figure 3. *U-Pb concordia plot showing three analyses of zircon from an orthogneiss in the Nome Group near Salmon Lake. We interpret the upper intercept of 678 ± 4 Ma as the intrusive age for this body. MSWD = mean standard weighted deviation.*

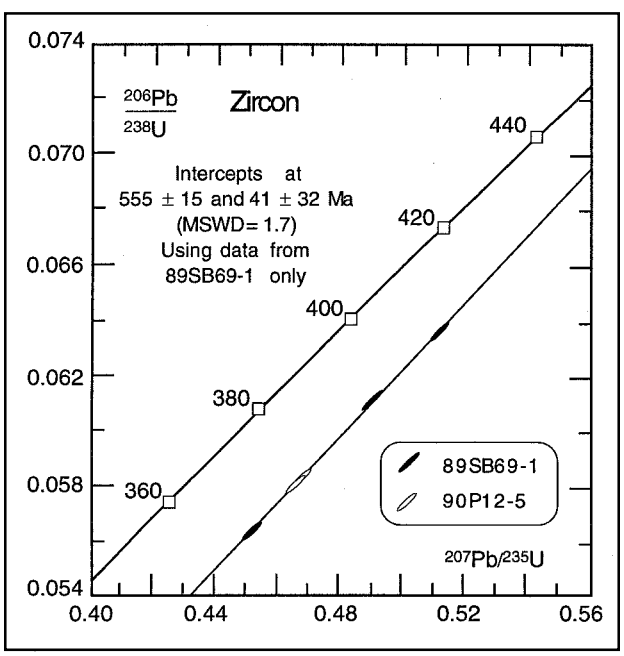

Figure 4. *U-Pb concordia plot showing five analyses of zircon from the Thompson Creek orthogneiss. The upper intercept is about 555 ± 15 Ma, and the lower intercept is poorly defined. The chord shown was drawn by using the data from 89SB69-1 only. If all five points are used, the upper intercept remains 555 ± 15 Ma, with a MSWD of 0.56.*

Creek orthogneiss; it yielded a ^{207}Pb-^{235}U date of 96 Ma. Three of the samples (90P8-4c, 92.2A-38, 92.2A-39c) were taken from the main body of the Thompson Creek orthogneiss, in the southern part of the range. These ^{207}Pb-^{235}U dates range from 98 Ma to 94 Ma. The other three samples (91G-42, 92.4A-132a, 92.4A-132b) were taken from the northern limb of the gneiss dome and may be from the same intrusion as the Thompson Creek orthogneiss (fig. 2). Three of the analyses cluster around 91 Ma, but another analysis (92.4A-132a) from the same outcrop as 92.4A-132b yields a ^{207}Pb-^{235}U date of 94 Ma.

Taken together, the orthogneiss data are complex and difficult to interpret unambiguously. Where two size fractions were analyzed from the same sample, the finer grained fraction yielded the younger date. None of the ^{207}Pb-^{235}U dates are younger than 91 Ma, indicating that 91 Ma is the age of cooling of the complex through the closure temperature of ~725°C. The older dates from monazite in the orthogneiss may reflect incomplete resetting of accessory monazite from the Precambrian-Cambrian igneous protolith. The monazite dates of 91 Ma are all from the orthogneiss in the northern part of the range; moreover, they are also closest to the Kigluaik pluton. The monazite from the biotite-rich 92.4A-132a sample that yielded the only older (94 Ma) date in the northern part of the range may have a slightly different composition. Further work needs to be done to determine the relationship between monazite age, composition, and structural position.

The monazite analyses from metapelitic rocks are generally more concordant than those from the orthogneiss (fig. 5). Seven of the fractions from five rocks collected from throughout the range yield dates between 89 Ma and 92 Ma, overlapping with the ^{207}Pb-^{235}U dates from the some of the younger dates from the orthogneiss. Two fractions of monazite from metapelite collected from the deepest structural levels yielded dates of 95 Ma and 96 Ma. Again, finer grained fractions yielded younger dates.

The pegmatite dikes and lenses found within the Kigluaik Group were derived from partial melting of metapelite during high-temperature metamorphism, an interpretation based on Nd and Sr isotopic data (Amato and Wright, in press). Four of the five fractions of pegmatite yielded ^{207}Pb-^{235}U dates of 90-91 Ma, whereas the finest fraction (< 75 µm) is 86 Ma (fig. 5; table 3).

We believe that because the pegmatite formed during peak metamorphism, the clustering of monazite dates from pegmatite at 90-91 Ma makes the strongest case for peak metamorphism at or

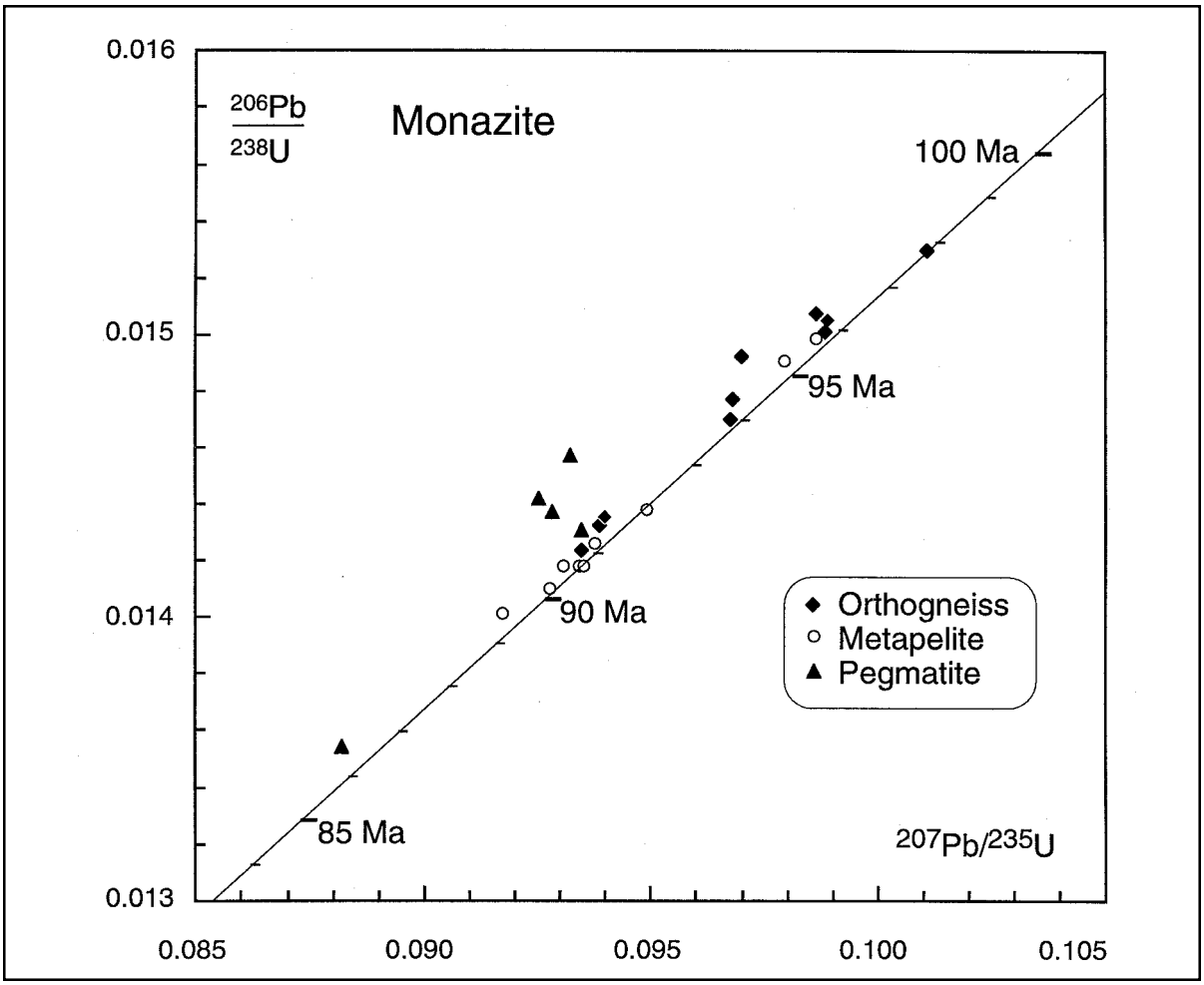

Figure 5. *U-Pb concordia plot showing analyses of monazite from orthogneiss, metapelite, and pegmatite. Clustering of dates around 91 Ma indicates cooling through monazite closure temperature of ~725 °C. Older dates are interpreted as incomplete resetting of detrital and igneous monazite from metapelite and orthogneiss.*

slightly older than 91 Ma. The clustering of ages from monazite from all three rock types at or near 91 Ma and the scarcity of ages younger than 90 Ma further strengthens this interpretation. The older dates from orthogneiss and metapelite may related to inheritance, or possibly they are an indication of a slightly earlier high-temperature metamorphic history of the gneiss dome, as might be suggested by the ~105-110 Ma ages from orthogneiss. We interpret the age of 91 Ma as approximating the attainment of peak temperatures in the range.

AGE OF MAGMATISM

The Cretaceous igneous rocks of the Kigluaik gneiss dome can be divided into three groups: (a) orthogneisses; (b) the undeformed Kigluaik pluton and related dikes; and (c) a diabase dike swarm. The emphasis of this study was dating the undeformed Cretaceous intrusive rocks, as their age was critical in determining the relationship of magmatism to metamorphism.

CRETACEOUS ORTHOGNEISSES

PREVIOUS WORK

In addition to the many older orthogneisses in the Kigluaik Mountains, there are at least two of Cretaceous age. One is a garnet-bearing granitic orthogneiss that was interpreted as being derived from partial melting of metasedimentary rocks (Amato and others, 1994). Three zircon fractions were analyzed and all are significantly discordant. The data collectively lie on a chord with a lower concordia intercept of 105 ± 3 Ma and a poorly defined Late Proterozoic upper concordia intercept (Amato and others, 1994). This unit is fully involved in the deformation and associated metamorphism and corroborates field evidence that much of the high-temperature metamorphic fabric in the gneiss dome formed after intrusion of this orthogneiss.

Table 3. *U-Pb monazite data*

Sample	size[c]	Wt (mg)	Concentration U (ppm)	Concentration $^{206}Pb^{*d}$ (ppm)	Measured ratios[a] $^{206}Pb/^{204}Pb$	Measured ratios[a] $^{207}Pb/^{206}Pb$	Measured ratios[a] $^{208}Pb/^{206}Pb$	Atomic ratios $^{206}Pb^*/^{238}U$	Atomic ratios $^{207}Pb^*/^{235}U$	Atomic ratios $^{207}Pb^*/^{206}Pb$	Ages (Ma)[b] $^{206}Pb^*/^{238}U$	Ages (Ma)[b] $^{207}Pb^*/^{235}U$	Ages (Ma)[b] $^{207}Pb^*/^{206}Pb$	error
Late Proterozoic-Early Paleozoic orthogneiss														
92.5A-139	>100	3.4	2511	32.5	1792	0.05588	8.48101	0.01505	0.09893	0.04767	96	96	83	11
90P8-4c	>200	0.8	5832	76.6	1980	0.05537	4.42066	0.01529	0.10108	0.04795	98	98	97	8
90P8-4c	<200	0.8	5614	72.7	1996	0.05486	4.55970	0.01507	0.09864	0.04748	96	96	74	8
92.2A-38	>200	1.3	3158	41.1	4193	0.05159	5.84525	0.01501	0.09885	0.04777	96	96	88	4
92.2A-38	<200	2.1	1854	90.4	2670	0.05343	6.10166	0.01470	0.09675	0.04775	94	94	87	6
92.2A-39c	<200	2.0	2515	32.4	7283	0.04982	5.84817	0.01477	0.09681	0.04753	95	94	76	4
91G-42	>100	0.3	46063	566.8	6623	0.04975	2.55571	0.01432	0.09387	0.04753	92	91	76	5
92.4A-132a	>100	2.7	7112	91.2	5917	0.04966	3.41023	0.01492	0.09702	0.04717	96	94	58	20
92.4A-132b	>100	3.3	6377	78.9	9552	0.04907	2.29822	0.01435	0.09397	0.04748	92	91	73	5
92.4A-132b	>200	2.9	4240	76.6	9504	0.04927	1.98136	0.01423	0.09348	0.04763	91	91	81	3
Late Proterozoic-Early Paleozoic metapelite														
89SMC-27	>200	0.5	5242	63.5	3876	0.05156	2.23219	0.01409	0.09281	0.04776	90	90	87	7
89SMC-27	<200	0.4	5598	67.4	3485	0.05172	2.27727	0.01401	0.09174	0.04800	90	89	74	7
89SLMC-51	>200	0.8	3780	46.7	3984	0.05159	2.83387	0.01438	0.09496	0.04790	92	92	94	7
89SLMC-51	<200	0.8	3637	44.3	3597	0.05172	2.90422	0.01418	0.09311	0.04763	91	90	81	10
92.1A-9b	>100	3.2	3802	48.9	2110	0.05473	3.19606	0.01498	0.09865	0.04775	96	96	87	2
92.1A-9b	<100/>150	3.4	3668	47.0	2174	0.05446	3.23089	0.01490	0.09798	0.04769	95	95	84	3
92.NA-106	>100	1.0	4888	59.6	4115	0.05134	2.26571	0.01418	0.09343	0.04777	91	91	88	10
92.SP-4	>100	0.8	4853	59.1	2976	0.05278	2.33200	0.01418	0.09356	0.04784	91	91	91	8
92.SP-5	>100	1.1	5155	63.2	3058	0.05251	2.34558	0.01426	0.09381	0.04771	91	91	85	9
Cretaceous pegmatite														
89SLMC-42	>200	0.6	15912	195.6	3623	0.05145	0.65477	0.01431	0.09348	0.04739	92	91	69	8
89SLMC-42	<200	0.5	15632	181.8	1319	0.05843	0.78088	0.01354	0.08823	0.04727	87	86	63	9
92.2A-26b	>100	1.5	7297	90.1	4184	0.04945	4.13198	0.01437	0.09287	0.04688	92	90	43	5
92.2A-57	>200	1.9	4908	60.8	4219	0.05005	5.51343	0.01442	0.09256	0.04656	92	90	27	9
92.4A-114	>100	3.4	9743	122.0	7937	0.04826	2.28607	0.01457	0.09325	0.04641	93	91	19	1

[a]Isotopic compositions corrected for mass fractionation of 0.11%. Sample dissolution and ion exchange chemistry modified from Krough (1973).

[b]Ages calculated by using the following constants: decay constants for ^{235}U and ^{238}U = 9.8485E-10 yr^{-1} and 1.55125E-10 yr^{-1} respectively; $^{238}U/^{235}U$ = 137.88. Precisions on $^{206}Pb^*/^{238}U$ ratios are about 0.2 to 0.3% based on the replicate analysis of two 'standard' zircon fractions. Accuracy of the $^{206}Pb^*/^{238}U$ dates, including uncertainties in spike calibration, is estimated to be within 0.5%. The two-sigma uncertainties in the $^{207}Pb^*/^{206}Pb^*$ ages were calculated from the combined uncertainties in mass spectrometry and an assumed uncertainty of ± 0.1 in the $^{207}Pb/^{204}Pb$ ratio used for the common Pb correction (Mattinson,1987).

[c]>100, <200, etc., refer to size fractions in mesh size.

[d]Pb* denotes radiogenic Pb, corrected for common Pb by using the isotopic composition of $^{206}Pb/^{204}Pb$ = 18.6 and $^{207}Pb/^{204}Pb$ = 15.6.

NEW DATA

The other known Cretaceous orthogneiss is a highly strained metasyenite. This unusual intrusion forms thin layers near the base of the gneiss dome and has been dated at 110 ± 5 Ma (table 4, fig. 6). This age, obtained by W. McClelland of University of California, Santa Barbara, was based on a step-wise dissolution experiment similar to that described in the next section. The age and composition of this unit are remarkably similar to unmetamorphosed potassic plutons within the Yukon-Koyukuk basin and should probably be included in the diffuse belt of alkaline plutonic rocks that stretches from the Yukon-Koyukuk basin to the Darby Mountains, St. Lawrence Island, and Cape Dezhnev, in northeastern Russia (T.P. Miller, 1972).

KIGLUAIK PLUTON

The undeformed Kigluaik pluton is exposed over an area of 100 km^2 in the western part of the gneiss dome (fig. 2). The intrusion consists of a biotite-granite "felsic cap" overlying a gabbro-diorite "mafic root" of unknown volume and extent, along with associated granodioritic rocks. The recognition of mafic rocks within the deeper levels of the gneiss dome raised the possibility that the high-temperature metamorphism was caused by this mantle-derived magmatism (Amato and others, 1994).

The zircon population from the granitic cap includes both opaque dark-brown and opaque white grains, and both are likely metamict. Initial analyses of a representative fraction from each of these grain types (sample 87AH-58) revealed relatively high U concentrations ranging from 5400-7600 ppm (table 3). The $^{206}Pb/^{238}U$ and $^{207}Pb/^{235}U$ dates from each of the two fractions are "concordant" at 83 Ma, but the high U concentration and visible alteration (metamictization) of the zircon grains suggest that Pb loss has likely occurred and that 83 Ma would be a minimum age for the pluton.

This initial attempt led us to direct our efforts toward dating rocks from the mafic root, which was shown by Amato and others (1994) to be coeval with the granitic cap. These rocks would likely contain zircon with a lower uranium concentration and thus be less affected by metamictization and Pb-loss. The two samples we analyzed were from the upper part of the mafic root, in a mingling zone between granitic and granodioritic compositions (Amato and Wright, 1997). These samples, 92.4A-119 and 92.4A-120, are hornblende biotite granodiorite with ~60% SiO_2 and abundant zircon with a range of euhedral shapes from short and stubby to elongate needles. All grains were translucent and honey brown to pink. We analyzed two size fractions (150-200 µm and 75-150 µm) of grains with the lowest magnetic susceptibility from each sample. As expected, in all four fractions the uranium concentration was lower than that in the zircon from the granitic cap, ranging from ~900-1400 ppm (table 3), but discordance between U-Pb and Pb-Pb dates indicated that Pb loss remained a problem. Conventional U-Pb analysis thus did not conclusively provide a crystallization age for the pluton.

In an attempt to reduce the effects of post-crystallization Pb loss, we used a technique developed initially by Krough and Davis (1975), in which zircon fractions are subjected to a mild HF leach to remove internal metamict domains. After leaching, both the leachate (dissolved zircon) and the residue (refractory parts of the grain unaffected by leaching) are analyzed. Mattinson (1984, 1990, 1994) expanded this technique and developed "step-wise dissolution," in which zircons are subjected to a series of progressively longer leaches, with leachate being analyzed after each successive step. After a given number of leaching steps (usually from one to 10), the remaining residue is analyzed. This process has been shown to be successful in "mining out" metamict zones within a zircon with high uranium concentrates, and thus generally gives a more meaningful age. The results of our first leach experiment yielded an age of 92 ± 2 Ma (Amato and others, 1994). However, this procedure was based on only one leach step.

Our latest leach experiment, reported here, followed the procedure of Mattinson (1994) and provides a useful constraint on the age of Late Cretaceous magmatism in the Kigluaik Mountains. We used the 75-150 µm fraction from each of the two granodiorites, and leached them in parallel for times ranging from one day to as long as one month (table 5). The results are displayed in a Tera-Wasserburg plot (fig. 7). ^{238}U release spectra similar to those commonly used to present $^{40}Ar/^{39}Ar$ data show the trend in both the ^{238}U-^{206}Pb and ^{207}Pb-^{206}Pb ages with progressive leaching; they also show the relative amounts of ^{238}U released in each step (fig. 8).

In each sample, the leachate from "early" steps with leach times less than one week gave $^{207}Pb/^{206}Pb$ dates with extremely large errors, resulting from the relatively large amounts of ^{204}Pb (common lead) extracted from the easily dissolved parts of the zircon or along fractures. Back-scattered-electron imaging of zircon from sample 92.4A-120 reveals a core of quartz and feldspar around which is a euhedral zircon (fig. 9). The feldspar is likely the source for the excessive amounts of ^{204}Pb, and the HF leaching would have removed all traces of feldspar by the second leach, thus decreasing the error in the ^{207}Pb-^{206}Pb ratio in subsequent steps.

The leachate from the third and fourth steps in each sample had the youngest $^{206}Pb/^{238}U$ date, and the $^{206}Pb/^{238}U$ dates increased progressively in both samples after the fourth step. This pattern is consistent with the

Table 4. *U-Pb zircon isotopic data and apparent age of syenitic orthogneiss*[a]

Sample	Fraction size[b] (µm)	%U	Wt (mg)	Concentration[c] U	Concentration[c] Pb*/^{204}Pb	Isotopic composition[d] ^{206}Pb/^{207}Pb	Isotopic composition[d] ^{206}Pb/^{208}Pb	Isotopic composition[d] ^{206}Pb/^{238}U	Apparent ages (Ma)[e] ^{206}Pb*/^{235}U	Apparent ages (Ma)[e] ^{207}Pb*/^{206}Pb*	Apparent ages (Ma)[e] ^{207}Pb*/^{238}U	Th-corrected ages (Ma)[f] ^{206}Pb*/^{206}Pb*	Th-corrected ages (Ma)[f] ^{207}Pb*
Sample SP90-6													
a	30-45	n/a	0.4	1179	18.3	12,798	20.243	8.068	98.7	99.2 ± 0.2	112	98.8 ± 0.2	110 ± 1
b	80-100	n/a	2.5	1361	19.7	7,850	19.939	8.483	102.0	102.5 ± 0.2	113	102.1 ± 0.2	111 ± 1
c	145-350	n/a	1.7	2034	29.0	6,657	19.815	9.586	101.0	101.5 ± 0.2	112	101.1 ± 0.2	110 ± 1
d	145-350	n/a	1.0	2174	34.4	9,915	20.098	8.384	101.2	101.7 ± 0.2	113	101.3 ± 0.2	111 ± 2
e	145-350A	n/a	0.4	362	5.8	5,920	19.677	7.937	102.4	103.0 ± 0.2	116	102.5 ± 0.2	114 ± 2
Partial dissolution results													
L1-1	n/a	65.9%	n/a	11,141	170.5	4,481	19.413	8.902	98.8	99.3 ± 0.3	110	98.9 ± 0.3	109 ± 2
L1-2	n/a	31.8%	n/a	5,381	84.6	31,179	20.478	13.029	104.0	104.6 ± 0.2	117	104.1 ± 0.2	115 ± 2
L1-3	n/a	2.2%	n/a	366	6.5	43,391	20.407	9.370	114.3	115.1 ± 0.3	132	114.4 ± 0.2	130 ± 2
R1	n/a	0.1%	n/a	15	0.4	1,764	16.639	2.862	139.7	147.7 ± 0.3	279	139.7 ± 0.3	278 ± 3
T1	145-350	n/a	6.3	2683	41.6	n/a	n/a	n/a	100.8	101.3 ± 0.3	113	100.9 ± 0.3	112 ± 2
L2-1	n/a	27.9%	n/a	891	17.3	3,042	18.550	7.373	123.1	124.5 ± 3.0	151	123.2 ± 0.4	150 ± 2
L2-2	n/a	2.8%	n/a	89	1.2	2,177	18.062	7.282	86.1	87.7 ± 0.2	129	86.2 ± 0.2	128 ± 5
L2-3	n/a	56.2%	n/a	1,795	25.7	39,381	20.527	11.186	93.6	94.5 ± 0.1	116	93.7 ± 0.2	115 ± 1
R2	n/a	13.2%	n/a	421	7.1	41,572	20.564	10.137	109.0	109.2 ± 0.1	113	109.1 ± 0.2	112 ± 2
T2	145-350	n/a	2.5	1279	20.5	n/a	n/a	n/a	103.7	104.7 ± 0.2	128	103.7 ± 0.3	126 ± 2

[a]All analyses were performed by W.C. McClelland at the University of California, Santa Barbara. Work was funded by National Science Foundation grant EAR91-18394 awarded to B.E. Patrick.

[b]a, b, etc. designate conventional fractions; A designates conventional fractions abraded to 30 to 60% of original diameter; L1-1, L1-2, etc. designate leachate steps; R designates digestion of final residue; T designates mathematically recombined steps and residue. All fractions were washed in warm 3N HNO_3 and 3N HCl for 15 min each, spiked with ^{205}Pb-^{235}U tracer, and dissolved in a 50% HF>>14N HNO_3 solution within 3 ml Savillex™ capsules placed in 125 ml TFE Teflon™ lined Parr acid digestion bomb. Dissolution schedule for experiments: 1-1 = 30 hr at 80°C; 1-2 = 24 hr at 180°C; 1-3 = 24 hr at 210°C; 2-1 = 6 hr at 80°C; 2-2 = 12 hr at 80°C; 2-3 = 12 hr at 170°C. Residues and conventional fractions were dissolved in 60 hr at 245°C. Following evaporation and dissolution in HCl, Pb and U for all fractions were separated following techniques modified from Krogh (1973). Pb and U were combined and loaded with H_3PO_4 and silica gel onto single degassed Re filaments. Isotopic compositions of Pb and U were determined through static collection on a Finnigan-MAT 261 multicollector mass spectrometer by using an ion counter for collection of the ^{204}Pb beam. All zircon fractions are nonmagnetic on Frantz magnetic separator at 1.8 amps; 15° forward and 1° side slopes.

[c]Pb* is radiogenic Pb expressed as ppm for conventional analyses and as nanograms for partial dissolution steps. U is expressed as ppm for conventional analyses and as nanograms and percent of total U for partial dissolution steps.

[d]Reported ratios corrected for fractionation (0.125 ± 0.038%/AMU) and spike Pb. Ratios used in age calculation were adjusted for 10 to 20 picograms of blank Pb with isotopic composition of ^{206}Pb/^{204}Pb = 18.6, ^{207}Pb/^{204}Pb = 15.5, and ^{208}Pb/^{204}Pb = 38.4, 2 picograms of blank U, 0.25 ± 0.049%/AMU fractionation for UO_2, and initial common Pb with isotopic composition approximated from Stacey and Kramers (1975) and assigned uncertainty of 0.1 to initial 207Pb/204Pb.

[e]Uncertainties reported as 2 sigma. Decay constants: ^{238}U=1.5513 E-10, 235U=9.8485 E-10; ^{238}U/^{235}U = 137.88.

[f]A 75% ± 25% efficiency in ^{230}Th exclusion during zircon crystallization is assumed; ^{207}Pb/^{206}Pb and ^{206}Pb/^{238}U ratios have been adjusted accordingly. Age assignments presented are derived from Th-corrected ratios.

n/a = not applicable.

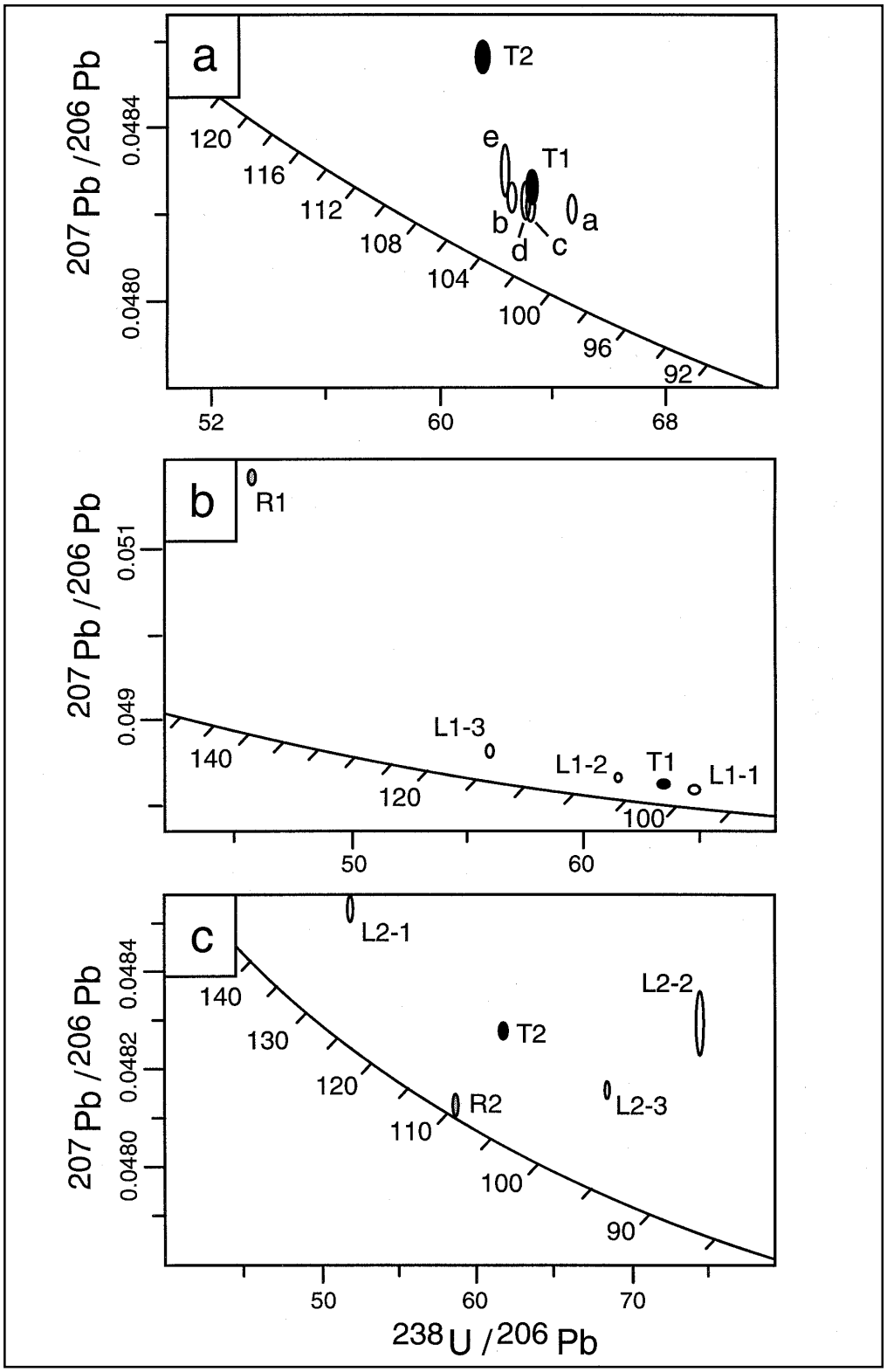

Figure 6. *U-Pb Tera-Wasserburg plots of (a) conventional and (b, c) partial dissolution data from metasyenite. Error ellipses are plotted at 95% confidence level and labeled according to analysis as listed in table 1. The zircon systematics suggest that this unit suffers from the effects of both Pb-loss and the presence of inherited components. The inferred crystallization age for this sample is 110 ± 5 Ma, based on the residue results from partial dissolution experiment 2.*

Table 5. *U-Pb zircon data from the Kigluaik pluton*

					Measured ratios[a]			Atomic ratios			Ages (Ma)[b]			
Sample	**size[c]**	**Wt (mg)**	**U[d] (ppm)**	**^{206}Pb*[e] (ppm)**	**^{206}Pb/^{204}Pb**	**^{207}Pb/^{206}Pb**	**^{208}Pb/^{206}Pb**	**^{206}Pb*/^{238}U**	**^{207}Pb*/^{235}U**	**^{207}Pb*/^{206}Pb**	**^{206}Pb*/^{238}U**	**^{207}Pb*/^{235}U**	**^{207}Pb*/^{206}Pb**	**error**
							Felsic cap							
87AH-58	>200db[f]	3.6	5372	60.0	3135	0.05256	0.15880	0.01300	0.08517	0.04787	83	84	93	3
87AH-58	>200w[f]	2.2	7584	84.5	2078	0.05512	0.15440	0.01297	0.08591	0.04804	83	84	101	4
							Mafic root							
92.4A-119	>100	10.2	1371	18.0	1502	0.05757	0.27785	0.01127	0.07419	0.04777	72	73	88	4
92.4A-119	>200	11.5	1421	18.3	2786	0.05302	0.25569	0.01133	0.07456	0.04773	73	73	86	6
92.4A-119	sdl1[g]		22.7	0.34	136	0.15515	0.15659	0.01509	0.09826	0.04722	97	95	61	40
92.4A-119	sdl2		3.7	0.05	4425	0.05117	0.33262	0.01252	0.08258	0.04785	80	81	92	8
92.4A-119	sdl3		7.4	0.08	11364	0.04955	0.32567	0.01116	0.07426	0.04826	72	73	112	18
92.4A-119	sdl4		10.3	0.11	27027	0.04902	0.30740	0.01095	0.07320	0.04849	70	72	123	8
92.4A-119	sdl5		8.5	0.10	10526	0.04963	0.28451	0.01142	0.07595	0.04824	73	74	111	13
92.4A-119	sdl6		7.0	0.08	8130	0.04970	0.26206	0.01213	0.08010	0.04789	78	78	94	6
92.4A-119	sdl7		6.9	0.09	15873	0.04879	0.24616	0.01284	0.08472	0.04786	82	83	93	2
92.4A-119	sdr		54.1	0.75	100000	0.04797	0.20548	0.01406	0.09267	0.04782	90	90	90	1
92.4A-120	>100	10.0	920	14.3	699	0.06890	0.29014	0.01293	0.08529	0.04786	83	83	92	6
92.4A-120	>200	12.8	928	13.3	1168	0.06040	0.26110	0.01234	0.08135	0.04781	79	79	90	3
92.4A-120	sdl1		4.2	0.06	45	0.37542	1.06054	0.01415	0.09134	0.04823	91	89	40	173
92.4A-120	sdl2		1.0	0.02	374	0.32431	37.74682	0.01645	0.10735	0.04733	105	104	66	39
92.4A-120	sdl3		2.0	0.03	1996	0.05534	0.36411	0.01256	0.08312	0.04798	81	81	98	12
92.4A-120	sdl4		3.1	0.04	4831	0.05117	0.34315	0.01167	0.07741	0.04812	75	76	105	16
92.4A-120	sdl5		3.7	0.04	2786	0.05333	0.31319	0.01200	0.07951	0.04805	77	78	102	10
92.4A-120	sdl6		2.3	0.03	4098	0.05139	0.27162	0.01263	0.08325	0.04780	81	81	89	14
92.4A-120	sdr		46.0	0.64	50000	0.04809	0.20830	0.01398	0.09211	0.04780	90	90	89	1

[a]Isotopic compositions corrected for mass fractionation of 0.11%. Sample dissolution and ion exchange chemistry modified from Krough (1973).

[b]Ages calculated by using the following constants: decay constants for ^{235}U and ^{238}U = 9.8485E-10 yr^{-1} and 1.55125E-10 yr^{-1} respectively; ^{238}U/^{235}U = 137.88. Precisions on ^{206}Pb*/^{238}U ratios are about 0.2 to 0.3% based on the replicate analysis of two 'standard' zircon fractions. Accuracy of the ^{206}Pb*/^{238}U dates, including uncertainties in spike calibration, is estimated to be within 0.5%. The two-sigma uncertainties in the ^{207}Pb*/^{206}Pb* ages were calculated from the combined uncertainties in mass spectrometry and an assumed uncertainty of ± 0.1 in the ^{207}Pb/^{204}Pb ratio used for the common Pb correction (Mattinson,1987).

[c]>100, <200, etc., refer to size fractions in mesh size. All analyzed zircon fractions consisted of the least-magnetic crystals that could be fractionated on a Frantz magnetic separator. "l" refers to the leachate zircon fraction that was leached for 24 hr in 50% Hf in a Teflon beaker at about 80°C. See Wright and Fahan (1988) and Dilles and Wright (1988) for details of the analytical procedure.

[d]Concentration from unleached samples reported as ppm, concentration from leached samples reported as nanomoles.

[e]*Denotes radiogenic Pb, corrected for common Pb by using the isotopic composition of ^{206}Pb/^{204}Pb = 18.6 and ^{207}Pb/^{204}Pb = 15.6.

[f]"db" and "w" are dark brown and white zircon.

[g]"sdl1" is the first step in the dissolution experiment, and "r" is the residue. Procedure followed that reported in Mattinson (1994). Leach duration: step 1= 1 hr, step 2 = 3 hr, step 3 = 24 hr, step 4 = 3 days, step 5 = 1 week, step 6 = 2 weeks, step 7 = 4 weeks.

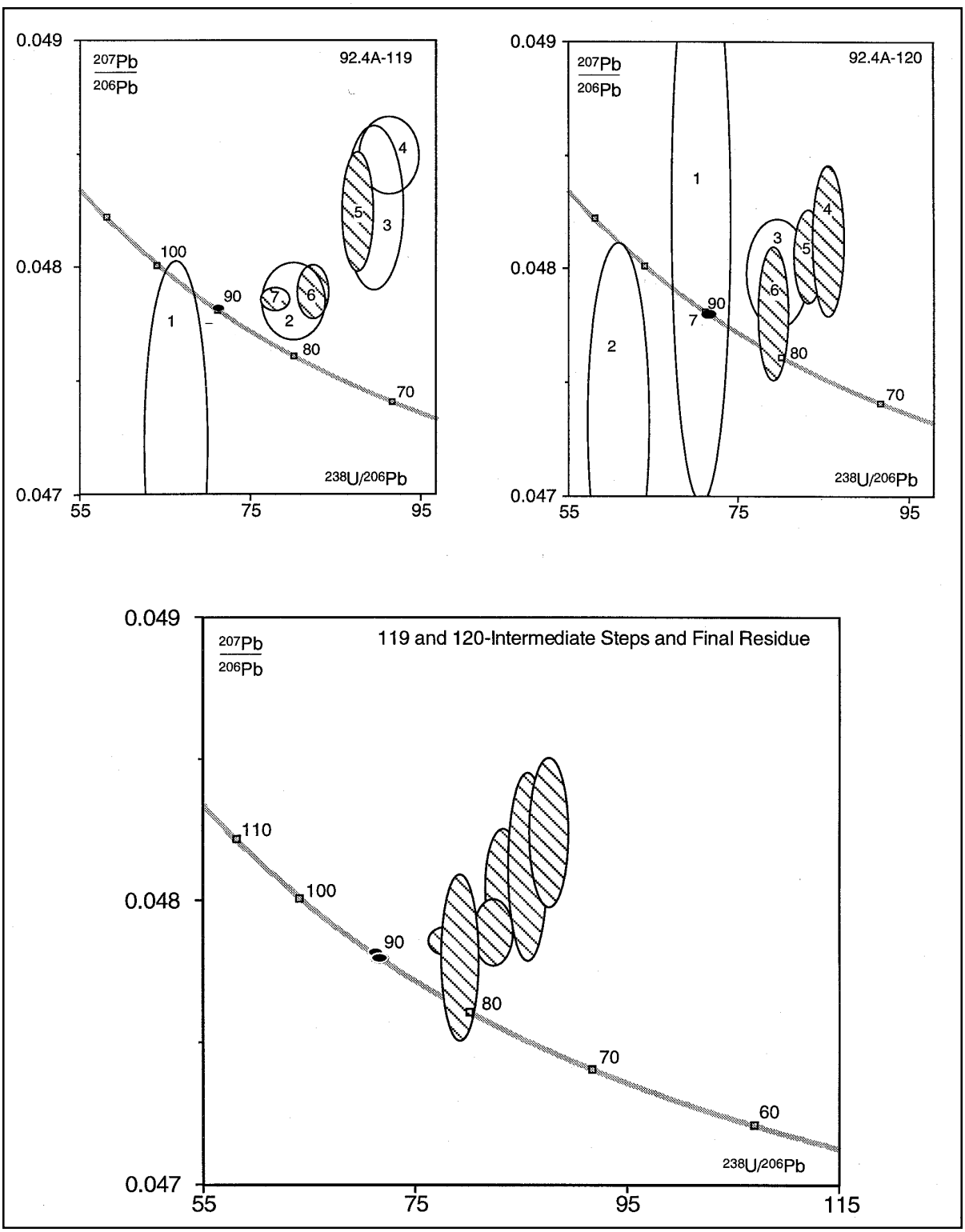

Figure 7. *U-Pb Tera-Wasserburg plot of step-wise dissolution experiment on zircon fractions from the Kigluaik pluton. Early, short-term steps (open ellipses) have high errors owing to large amounts of common Pb. Intermediate steps (striped ellipses) begin to approach concordia, and final steps (solid ellipses) are concordant at 90 ± 1 Ma. We have followed the convention of assigning errors on the* $^{206}Pb/^{238}U$ *dates based on the degree of leaching involved: ± 5% for "early" steps, ± 2% for intermediate steps, and ± 1% for the residue. These data indicate that the zircons contain inherited components and encountered Pb-loss.*

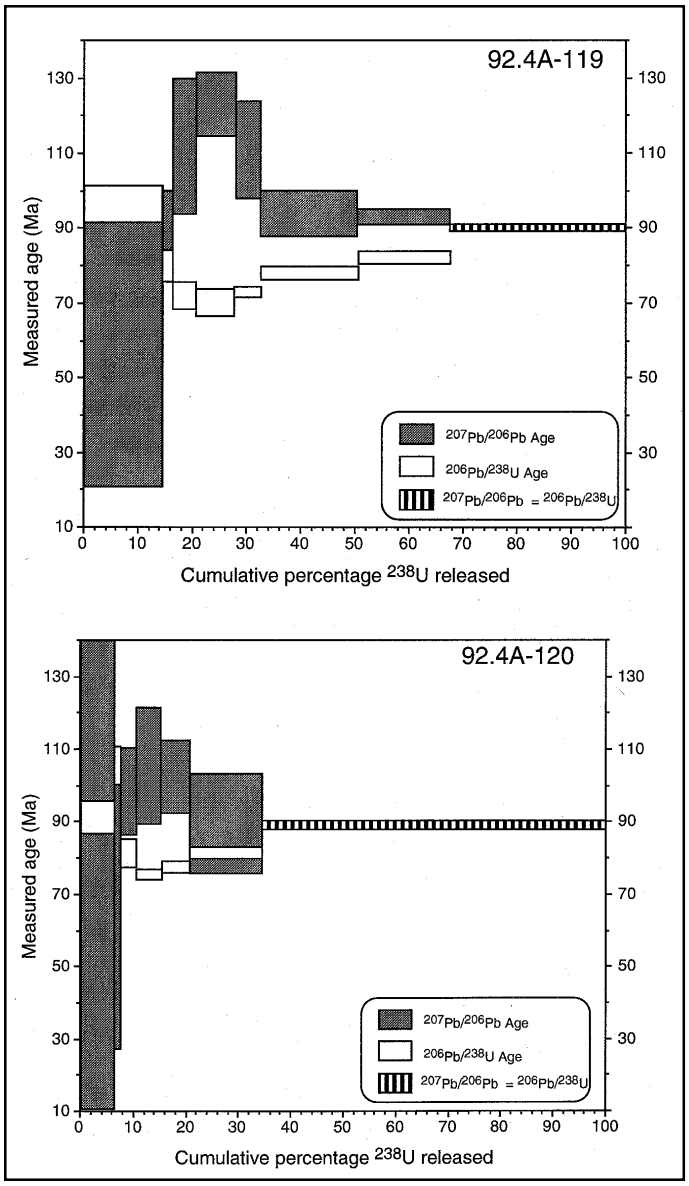

Figure 8. *^{238}U release spectra show the progressively converging ^{207}Pb/^{206}Pb and ^{206}Pb/^{238}U dates. Step 4 of 92.4A-119 is outside the analytical uncertainty of the later steps and indicates a small inherited component that is likely present in the zircon population from both samples.*

more easily leached domains being affected by Pb loss. The residue analyses from both samples were internally concordant and also agreed with each other within error: sample 92.4A-119 gave an age of 89 ± 1 Ma and sample 92.4A-120 gave an age of 90 ± 1 Ma.

For sample 92.4A-120, all the ^{207}Pb-^{206}Pb dates are within error. The fourth leach step from sample 92.4A-119 has a ^{207}Pb-^{206}Pb date of 123 ± 8, which is outside the analytical uncertainty for the final three steps. This suggests that there must be an older component in this zircon population. The later steps do not show evidence for this older component, and therefore it was probably leached out entirely during the experiment.

The zircon systematics from the Kigluaik pluton are complex. The zircons from the granitic cap have extremely high uranium concentrations and are visibly metamict. The zircons from granodiorite within the mafic root contain (a) numerous visible inclusions, (b) cores of feldspar with a high concentration of ^{204}Pb, (c) an inherited component of unknown age, and (d) they were affected by Pb loss. The step-wise dissolution procedure "sees through" these complexities by progressively removing domains within the zircon that were affected by inheritance or lead loss (or both) and the residue analysis yielded a concordant age. On the basis of this experiment, we now believe that the granodiorite crystallized at 90 ± 1 Ma, an age that is close to our estimate of 91 Ma for the age of peak metamorphism.

DIABASE DIKES

A shoshonitic diabase dike swarm cuts all units within the core of the Kigluaik gneiss dome. These dikes range from alkali basalt (~48% SiO_2) to trachyte (~63% SiO_2) and are compositionally and isotopically similar to the mafic root of the pluton. Field evidence of diabase cutting across the pluton (Amato, 1995) showed that the dikes represented the youngest magmatic event within the Kigluaik Mountains.

To better constrain the age of the dike swarm, Amato, in collaboration with A. Calvert and P. Gans (Calvert and others, manuscript in preparation), dated biotite and hornblende from dikes at two structural levels (tables 6-8; fig. 10). Biotite from the deepest sample, 92.3A-101, yielded a date of 82.5 ± 0.5 Ma, slightly younger than a 84 ± 0.6 Ma biotite date from sample 92.2A-40, collected from an outcrop 2-3 km structurally higher than 92.3A-101. Because biotite has a relatively low closure temperature for argon (~300°C), this may be a "cooling age" rather than an intrusive age. It would be preferable to date hornblende, which has a higher closure temperature (~550°C). Although many of the dikes crystallized magmatic hornblende, typically this mineral was highly altered to actinolite and therefore was unsuitable for ^{40}Ar/^{39}Ar dating. Of nearly 40 thin sections examined, only one dike (sample 92.2A-40) contained fresh hornblende. This dike also had a trend nearly orthogonal to the typical N. 30° E. trend of most of the dikes in the

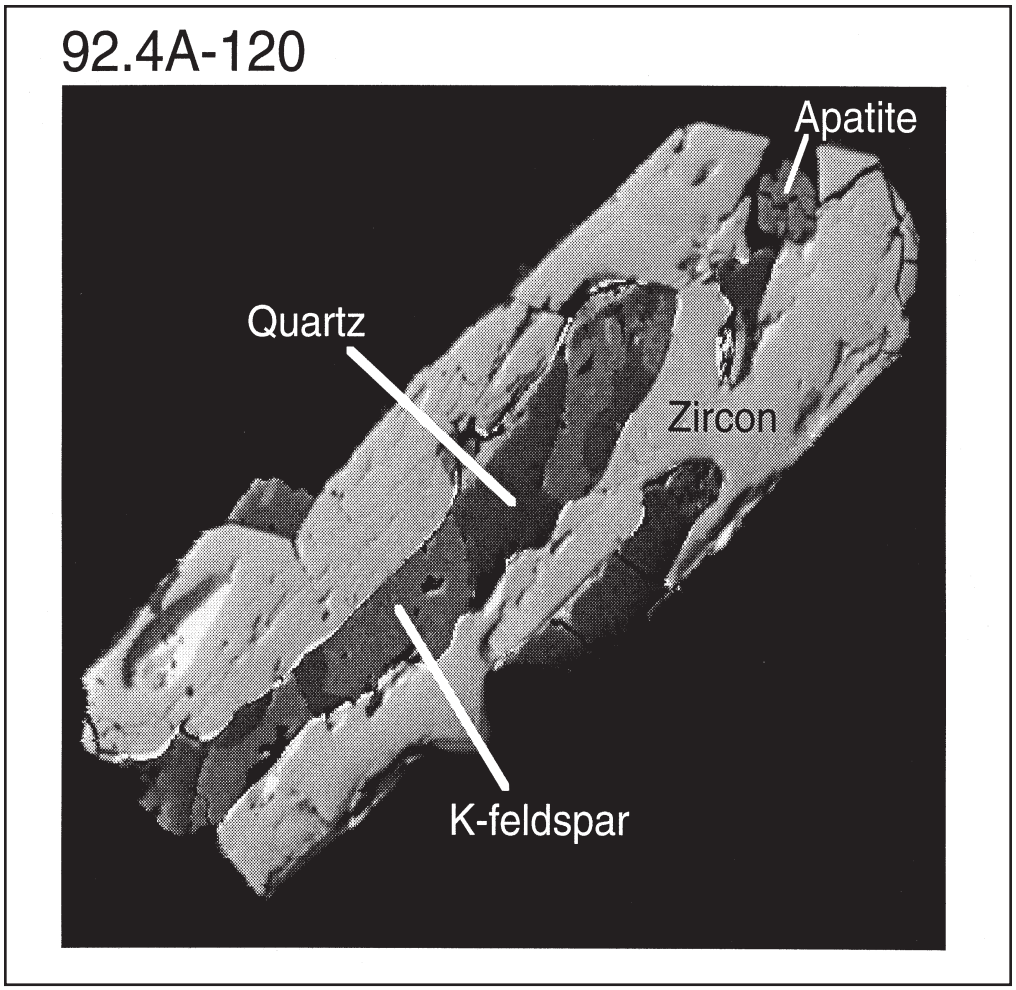

Figure 9. *Back scattered electron image of a zircon crystal with a core of K-feldspar and quartz. Euhedral crystal of apatite is an inclusion. The feldspar within the core is likely the source of the high concentration of ^{204}Pb in the early leach steps.*

Table 6. *^{40}Ar/^{39}Ar data for 92.3A-101 biotite*

T (°C)	40(mol)	^{40}Ar/^{39}Ar	^{37}Ar/^{39}Ar	^{36}Ar/^{39}Ar	K/Ca	Σ^{39}Ar	^{40}Ar*	Age (Ma)	error
640	3.40E-14	5.5566	0.0391	0.0081	13.0	0.060	0.700	71.7	0.5
785	6.00E-14	6.3818	0.0187	0.0016	26.0	0.182	0.933	82.1	0.2
900	6.20E-14	6.4826	0.0290	0.0008	17.0	0.312	0.967	83.3	0.2
1010	9.00E-14	6.4746	0.0574	0.0009	8.5	0.498	0.961	83.2	0.2
1070	8.10E-14	6.4290	0.0300	0.0003	16.0	0.671	0.986	82.7	0.2
1125	1.20E-13	6.4066	0.0274	0.0002	18.0	0.930	0.994	82.4	0.1
1155	2.40E-14	6.4357	0.0626	0.0001	7.8	0.982	0.996	82.8	0.4
1260	1.20E-14	6.7438	0.1084	0.0096	4.5	1.000	0.705	86.6	1.3

J=0.0072940.
Total fusion age (TFA) = 82.14 ± 0.13 Ma (including J).
Weighted mean plateau age (WMPA) = 82.51 ± 0.12 Ma (including J).
Steps used: 640, 785, 900, 1010, 1070, 1125, 1155, 1260 (100% Σ^{39}Ar).
40(mol) = moles corrected for blank and reactor-produced ^{40}Ar.
Σ^{39}Ar is cumulative, ^{40}Ar* = radiogenic fraction.

Table 7. *$^{40}Ar/^{39}Ar$ data for 92.2A-40 biotite*

T (°C)	40(mol)	$^{40}Ar/^{39}Ar$	$^{37}Ar/^{39}Ar$	$^{36}Ar/^{39}Ar$	K/Ca	$\Sigma\ ^{39}Ar$	$^{40}Ar^*$	Age (Ma)	error
640	1.10E-13	6.1604	0.0318	0.0057	15	0.126	0.787	79.3	0.2
750	1.50E-13	6.5188	0.0165	0.0008	30	0.311	0.968	83.8	0.1
845	1.00E-13	6.5348	0.0138	0.0004	36	0.445	0.984	84.0	0.2
925	6.50E-14	6.5919	0.0331	0.0007	15	0.528	0.970	84.7	0.2
990	8.50E-14	6.5710	0.0293	0.0006	17	0.637	0.977	84.5	0.2
1050	1.70E-13	6.5043	0.0178	0.0005	28	0.859	0.979	83.6	0.1
1090	7.70E-14	6.4935	0.0250	0.0007	20	0.958	0.972	83.5	0.2
1125	3.00E-14	6.5028	0.0365	0.0008	13	0.996	0.969	83.6	0.3
1155	3.20E-15	6.6258	0.1840	0.0066	2.7	1.000	0.776	85.1	3.4
1190	7.30E-16	7.1438	0.3944	0.0514	1.2	1.000	0.321	91.6	35.8
1260	2.00E-15	12.1946	0.1554	0.3053	3.2	1.000	0.119	153.7	85.8

J=0.0072940.
Total fusion age (TFA) = 83.35 ± 0.12 Ma (including J).
Weighted mean plateau age (WMPA) = 83.61 ± 0.12 Ma (including J).
Inverse isochron age = 84.38 ± 0.25 Ma. (MSWD =13.59; $^{40}Ar/^{36}Ar$=230.4 ± 9.6).
Steps used: 640, 750, 845, 925, 990, 1050, 1090, 1125, 1155, 1190, 1260 (100% $\Sigma^{39}Ar$).
40(mol) = moles corrected for blank and reactor-produced ^{40}Ar.
$\Sigma^{39}Ar$ is cumulative, $^{40}Ar^*$ = radiogenic fraction.

Table 8. *$^{40}Ar/^{39}Ar$ data for 92.2A-40 hornblende*

T (°C)	40(mol)	$^{40}Ar/^{39}Ar$	$^{37}Ar/^{39}Ar$	$^{36}Ar/^{39}Ar$	K/Ca	$\Sigma^{39}Ar$	$^{40}Ar^*$	Age (Ma)	error
500	5.70E-15	3.1020	2.3380	0.0839	0.21	0.006	0.113	30.3	6.8
600	6.00E-15	8.1651	1.0690	0.0080	0.46	0.023	0.782	78.6	1.7
700	1.10E-14	8.2710	0.7739	0.0040	0.63	0.057	0.881	79.6	0.9
800	1.20E-14	8.2343	1.2517	0.0032	0.39	0.096	0.909	79.2	0.7
850	7.30E-15	8.3642	2.5489	0.0039	0.19	0.119	0.900	80.5	1.2
900	1.40E-14	8.6365	6.3912	0.0057	0.08	0.161	0.883	83.0	0.9
940	9.00E-14	8.6147	6.8770	0.0044	0.07	0.444	0.926	82.8	0.3
970	1.20E-13	8.6063	6.8254	0.0028	0.07	0.827	0.973	82.7	0.2
1000	3.00E-14	8.6190	6.7869	0.0025	0.07	0.929	0.982	82.9	0.4
1030	1.30E-14	8.4723	7.9193	0.0040	0.06	0.970	0.943	81.5	0.9
1060	6.20E-15	9.0778	16.4258	0.0059	0.03	0.989	0.958	87.2	1.4
1100	1.50E-15	8.8735	10.6681	0.0050	0.05	0.994	0.939	85.2	5.3
1140	1.60E-15	8.2314	11.0659	0.0046	0.04	0.999	0.950	79.2	4.8
1180	4.00E-16	8.7651	9.5927	0.0157	0.05	1.000	0.695	84.2	30.6

J=0.0054530.
Total fusion age (TFA)= 83.35 ± 0.12 Ma (including J).
Weighted mean plateau age (WMPA)= 83.61 ± 0.12 Ma (including J).
Inverse isochron age = 84.38 ± 0.25 Ma. (MSWD =13.59; $^{40}Ar/^{36}Ar$=230.4 ± 9.6).
Steps used: 640, 750, 845, 925, 990, 1050, 1090, 1125, 1155, 1190, 1260 (100% $\Sigma^{39}Ar$).
40(mol) = moles corrected for blank and reactor-produced ^{40}Ar.
$\Sigma^{39}Ar$ is cumulative, $^{40}Ar^*$ = radiogenic fraction.

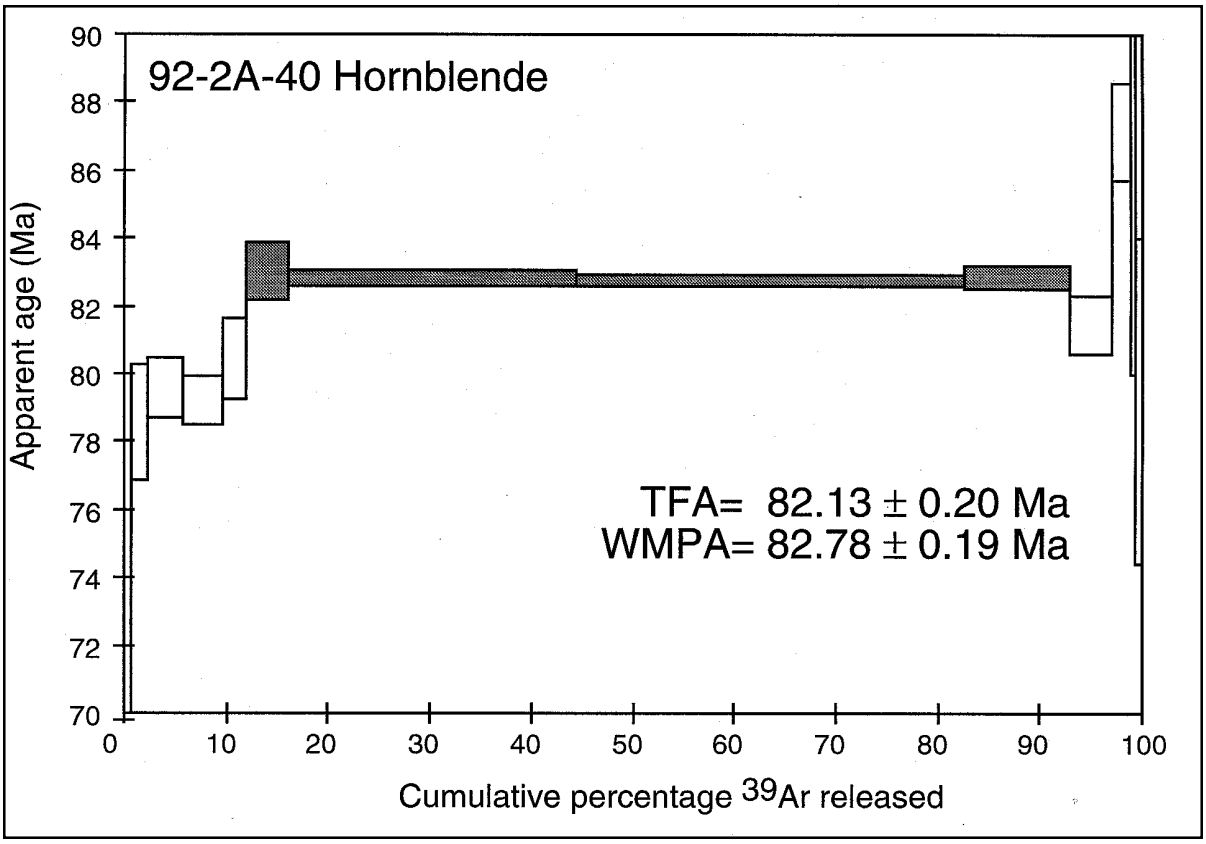

Figure 10. *$^{40}Ar/^{39}Ar$ release spectra for hornblende from a diabase dike. Inferred age of 83 ± 1 Ma for the dikes is based on the weighted mean plateau age (WMPA) using the shaded steps and the total fusion age (TFA) for this sample, together with the biotite ages from this sample and 92.3A-101.*

core, raising the possibility that it was a slightly younger dike that escaped hydrothermal alteration associated with the crystallizing pluton. This sample yielded a plateau date of 82.8 ± 0.4 Ma. This is slightly younger than the biotite date from the same sample. On the basis of the near concordance of the hornblende and biotite Ar dates from sample 92.2A-40, we believe that 83 ± 1 Ma is the best estimate of the age of the diabase dike swarm.

DISCUSSION

The relationship between magmatism and high-temperature metamorphism is important in the interpretation of the Cretaceous tectonic history of the Kigluaik Mountains. If magmatism was largely felsic and post-tectonic, it may be unnecessary to invoke a new tectonic event following blueschist metamorphism. In this case, magmatism could be related to the relaxation of isotherms as was suggested by Patrick and Lieberman (1988). If magmatism was syn-tectonic, there may have been a separate episode of tectonism that postdated the earlier high-pressure event. Although the age of the inception of blueschist metamorphism on Seward Peninsula is unknown, it must have occurred previous to 120 Ma (Hannula and McWilliams, 1995).

The presence of highly deformed igneous rocks of 105 Ma indicates that there must have been deformation associated with the post-blueschist-facies high-temperature metamorphism, and therefore this event was not a static overprint related to thermal reequilibration (Amato and others, 1994). This argument also was made on the basis of the structural geology of the isograd zone (Miller and others, 1992) and is strengthened by the better dated 110 ± 5 metasyenite.

The discovery of mafic plutonic rocks at the base of the Kigluaik pluton led to the suggestion that processes other than anatexis were important in its formation (Amato and others, 1994; Amato and Wright, 1997). But was the pluton the actual heat source for metamorphism? To answer this, we must critically evaluate the geochronologic data, because although coeval magmatism and metamorphism do not necessarily indicate a cause and effect, the presence of mafic magmas of the same age as the surrounding metamorphic rocks would be compelling evidence for magmatically induced metamorphism.

There are uncertainties about the actual peak temperatures in the metamorphic rocks used for U-Pb monazite dating, but estimates of 700-750°C (Lieberman, 1988) are near the closure temperature of 725 ± 25°C for the diffusion of Pb in monazite. The older monazite dates obtained from orthogneiss and paragneiss are likely the result of incomplete resetting of preexisting monazite (either igneous or detrital). This incomplete resetting implies that the temperatures either did not get significantly higher than the closure temperature or that if they did they did not stay high for long. Our estimate of 91 Ma must be a minimum for the age of attainment of peak temperatures, but it is difficult to imagine that temperatures stayed above 700°C between the time of the intrusion of the Cretaceous orthogneisses at 110-105 Ma and 91 Ma. Additionally, because of the composition and small volume of these orthogneisses, it is unlikely that they contributed significantly to the heat budget for high-temperature metamorphism.

However, the pluton has a mafic root that would make it a candidate for transporting heat from the mantle into the middle crust during a Cretaceous event. Because we know that there was significant deformation associated with this event (based on the deformation of the orthogneiss), we would expect the pluton to show some evidence of strain if it were the heat source. In fact the pluton is largely undeformed and cross cutting, though weakly deformed dikes were observed. If the metamorphism has a minimum age of 91 Ma, and the pluton is 90 ± 1 Ma, it probably intruded toward the end of the metamorphic deformational event. Our interpretation is that there may be other mafic intrusions below the gneiss dome that may be slightly older than the Kigluaik pluton and that these intrusions would be "responsible" for the elevated temperatures. Geophysical data would be required to test this hypothesis. In this scenario, the Kigluaik pluton is a late-stage representative of a longer, perhaps episodic magmatic event, a "last-gasp" intrusion that reveals the influence of mafic magmatism on the Cretaceous high-temperature metamorphism. The presence of the compositionally similar diabase dike swarm at 83 ± 1 Ma is further evidence of episodic mafic magmatism in the gneiss dome.

CONCLUSIONS

Geochronologic investigations relying primarily on U-Pb dating of zircon and monazite and $^{40}Ar/^{39}Ar$ dating of amphibole and mica allow us to make the following conclusions about the geologic history of the Kigluaik gneiss dome:

- A new U-Pb zircon date of 678 ± 4 Ma from a Nome Group orthogneiss confirms that ~680 Ma orthogneisses are common within the Nome Group and that the country rock must be in part Precambrian. A new U-Pb zircon date of 555 ± 15 Ma from a Kigluaik Group orthogneiss is interpreted as a crystallization age.
- Although the data are complex, U-Pb dating of monazite from orthogneiss, metapelite, and pegmatite suggest that peak high-temperature metamorphism in the gneiss dome has a minimum age of 91 Ma, an interpretation based primarily on the clustering of dates from pegmatite interpreted to have formed by partial melting of metasedimentary rocks during peak metamorphism.
- The earliest documented Cretaceous magmatism is represented by two orthogneiss bodies dated at 110 ± 5 Ma (this paper) and ~105 Ma (Amato and others, 1994).
- A step-wise dissolution experiment on zircon from the Kigluaik pluton indicates that the zircon population was affected by both inheritance and Pb loss. The experiment yielded concordant ages of 90 ± 1 Ma, which we interpret as the crystallization age.
- The youngest Cretaceous igneous event was the intrusion of a diabase dike swarm, dated at 83 ± 1 Ma by using $^{40}Ar/^{39}Ar$ techniques on biotite and hornblende.
- The temporal association of magmatism and metamorphism indicates that mafic magmatism beginning before 90 Ma resulted in high-temperature metamorphism of the gneiss dome. While the Kigluaik pluton may not have been the actual heat source for metamorphism, it may represent the latest stages of a more protracted, episodic mafic magmatic history in the region, represented at the exposed crustal levels by the 90-Ma pluton and the 83-Ma dike swarm.

ACKNOWLEDGMENTS

This work constitutes part of Amato's Ph.D. dissertation at Stanford University. Fieldwork was supported by NSF grant EAR-90-18922 to E.L. Miller, a GSA John T. Dillon award (1991), GSA Penrose award (1992), and a Stanford School of Earth Sciences McGee Fund grant to Amato. Acquisition of U-Pb

geochronologic data was supported by NSF grant EAR-91-17419 to J.E. Wright. Amato was supported in part by NSF grant OPP-95-00241 to P. Layer, D. Stone, and K. Fujita. W.C. McClelland and B.E. Patrick generously provided U-Pb data for the metasyenite, work supported by NSF grant EAR91-18394 awarded to Patrick. Argon data was collected by Amato in collaboration with A.T. Calvert and P.B. Gans at UC-Santa Barbara. This project was based on fieldwork carried out by Amato, Gans, Calvert, T.A. Little, K.A. Hannula, Miller, J. Toro, and Wright, assisted by J.Y. Amory and L. Symchych. Reviews by McClelland and C. Hanks are greatly appreciated.

REFERENCES CITED

Amato, J.M., 1995, Tectonic evolution and petrogenesis of the Kigluaik gneiss dome, Seward Peninsula, Alaska: An integrated structural and geochemical study of extensional processes in mid-crustal rocks: Stanford, Stanford University, Ph.D. dissertation, 150 p., 10 pls., 37 figs.

Amato, J.M., and Wright, J.E., 1997, Petrogenesis of the Kigluaik pluton: An isotopic study of Late Cretaceous arc-related potassic magmatism in northern Alaska: Journal of Geophysical Research, v. 102, p. 8065-8084.

Amato, J.M., Wright, J.E., Gans, P.B., and Miller, E.L., 1994, Magmatically induced metamorphism and deformation in the Kigluaik gneiss dome, Seward Peninsula, Alaska: Tectonics, v. 13, p. 515-527.

Armstrong, R.L., Harakal, J.E., Forbes, R.B., Evans, B.W., and Thurston, S.P., 1986, Rb-Sr and K-Ar study of metamorphic rocks of the Seward Peninsula and Southern Brooks Range, Alaska: Geological Society of America Memoir 164, p. 184-203.

Brooks, A.H., Richardson, G.B., and Collier, A.J., 1901, A reconnaissance of the Cape Nome and adjacent gold fields of Seward Peninsula, Alaska, in 1900, *in* U.S. Geological Survey Reconnaissances in Cape Nome and Norton Bay regions, Alaska, in 1900, 185 p.

Bunker, C.M., Hedge, C.E., and Sainsbury, C.L., 1979, Radioelement concentrations and preliminary radiometric ages of rocks of the Kigluaik Mountains, Seward Peninsula, Alaska: U.S. Geological Survey Professional Paper 1129-C, 11 p.

Calvert, A.T., 1992, Structural evolution and thermochronology of the Kigluaik Mountains, Seward Peninsula, Alaska: Stanford, Stanford University, M.S. dissertation, 50 p.

Dilles, J.H., and Wright, J.E., 1988, The chronology of early Mesozoic arc magmatism in the Yerington District of western Nevada and its regional implications: Geological Society of America Bulletin, v. 100, p. 644-652.

Foster, D.A., Miller, C.F., Harrison, T.M., and Hoisch, T.D., 1992, $^{40}Ar/^{39}Ar$ thermochronology and thermobarometry of metamorphism, plutonism, and tectonic denudation in the Old Woman Mountains area, California: Geological Society of America Bulletin, v. 104, p. 176-191.

Hannula, K.A., 1993, Relations between deformation, metamorphism, and exhumation in the Nome Group blueschist-greenschist terrane, Seward Peninsula, Alaska: Stanford, Stanford University, Ph.D. dissertation, 171 p.

Hannula, K.A., and McWilliams, M.O., 1995, Reconsideration of the age of blueschist facies metamorphism on the Seward Peninsula, Alaska, based on phengite $^{40}Ar/^{39}Ar$ results: Journal of Metamorphic Geology, v. 13, p. 125-139.

Hummel, C.H., 1962, Preliminary geologic map of the Nome D-1 quadrangle, Seward Peninsula, Alaska, U.S. Geological Survey Miscellaneous Investigations Field Studies Map MF-248, scale 1:63,360.

Krough, T.E., 1973, A low-contamination method for hydrothermal decomposition of zircon and extraction of U and Pb for isotopic age determinations: Geochimica et Cosmochimica Acta, v. 37, p. 485-494.

Krough, T.E., and Davis, G.L., 1975, Alteration in zircons and differential dissolution of altered and metamict zircon: Carnegie Institution Washington Yearbook, v. 74, p. 619-623.

Lieberman, J.E., 1988, Metamorphic and structural studies of the Kigluaik Mountains, Western Alaska: Seattle, University of Washington, Ph.D. dissertation, 192 p.

Mattinson, J.M., 1984, Labile Pb in young, high-uranium zircons: Geological Society of America Abstracts with Programs, v. 16, p. 559.

———1987, U-Pb ages of zircon: A basic examination of error propagation: Chemical Geology, v. 66, p. 151-162.

———1990, Petrogenesis and evolution of the Salinian magmatic arc, *in* Anderson, J.L., ed., The nature and origin of Cordilleran magmatism: Geological Society of America Memoir 174, p. 237-250.

———1994, A study of complex discordance in zircons using step-wise dissolution techniques: Contributions to Mineralogy and Petrology, v. 116, p. 117-129.

Miller, E.L., Calvert, A.T., and Little, T.A., 1992, Strain-collapsed metamorphic isograds in a sillimanite gneiss dome, Seward Peninsula, Alaska: Geology, v. 20, p. 487-490.

Miller, T.P., 1972, Potassium-rich alkaline intrusive rocks of western Alaska: Geological Society of America Bulletin, v. 83, p. 2111-2128.

Moffit, F.H., 1913, Geology of the Nome and Grand Central Quadrangles, Alaska: U.S. Geological Survey Bulletin 533, 140 p.

Parrish, R.R., 1990, U-Pb dating of monazite and its application to geologic problems: Canadian Journal of Earth Sciences, v. 27, p. 1431-1450.

Patrick, B.E., and Evans, B.W., 1989, Metamorphic evolution of the Seward Peninsula blueschist terrane: Journal of Petrology, v. 30, p. 531-555.

Patrick, B.E., and Lieberman, J.E., 1988, Thermal overprint on blueschists of the Seward Peninsula: The Lepontine in Alaska: Geology, v. 16, p. 1100-1103.

Patrick, B.E., and McClelland, W.C., 1995, Late Proterozoic granitic magmatism on Seward Peninsula and a Barentian origin for Arctic Alaska-Chukotka: Geology, v. 23, p. 81-84.

Sainsbury, C.L., 1969, Geology and ore deposits of the central York Mountains, western Seward Peninsula, Alaska: U.S. Geological Survey Bulletin 1287, 101 p.

Sainsbury, C.L., Hummel, C.L., and Hudson, T., 1972, Reconnaissance geologic map of the Nome Quadrangle, Seward Peninsula, Alaska: U.S. Geological Survey Open-File Report 72-326, 28 p., 1 sheet, scale 1:250,000.

Schärer, U., 1984, The effect of initial ^{230}Th disequilibrium on young U-Pb ages: The Makalu case, Himalaya: Earth and Planetary Science Letters, v. 67, p. 191-204.

Stacey, J.S., and Kramers, J.D., 1975, Approximation of terrestrial lead isotope evolution by a two-stage model: Earth and Planetary Science Letters, v. 26, p. 207-221.

Sturnick, M.A., 1984, Metamorphic petrology, geothermobarometry, and geochronology of the eastern Kigluaik Mountains, Seward Peninsula, Alaska: Fairbanks, University of Alaska, Ph.D. dissertation, 175 p.

Throckmorton, M.L., and Hummel, C.L., 1979, Quartzofeldspathic, mafic, and ultramafic granulites identified in the Kigluaik Mountains, Seward Peninsula, Alaska, U.S. Geological Survey Circular 804-B, p. 70-72.

Till, A.B., 1980, Crystalline rocks of the Kigluaik Mountains, Seward Peninsula, Alaska: Seattle, University of Washington, M.S. dissertation, 97 p.

Till, A.B., and Dumoulin, J.A., 1994, Geology of Seward Peninsula and Saint Lawrence Island, *in* Plafker, George, and Berg, H.C., eds., The Geology of Alaska, The Geology of North America, v. G-1: Boulder, Geological Society of America, p. 141-152.

Till, A.B., Dumoulin, J.A., Gamble, B.M., Kaufman, D.S., and Carroll, P.I., 1986, Preliminary geologic map and fossil data, Solomon, Bendeleben, and Southern Kotzebue quadrangles, Seward Peninsula, Alaska: U.S. Geological Survey Open-File Report 86-276.

Todd, C.S., and Evans., B.W., 1993, Limited fluid-rock interaction at the marble-gneiss contacts during Cretaceous granulite-facies metamorphism, Seward Peninsula, Alaska: Contributions to Mineralogy & Petrology, v. 114, p. 27-41.

Todt, W.A., and Büsch, W., 1981, U-Pb investigations of zircons from pre-Variscan gneisses I. A study from the Schwarzwald, West Germany: Geochimica et Cosmochimica Acta, v. 45, p. 1789-1810.

Turner, D.L., and Swanson, S.E., 1981, Continental rifting: a new tectonic model for the central Seward Peninsula, *in* Wescott, S.E., and Turner, D.L., eds., Geothermal reconnaissance survey of central Seward Peninsula, Alaska: University of Alaska Geophysical Institute Report UAG R-284, p. 7-36.

Wright, J.E., and Fahan, M.R., 1988, An expanded view of Jurassic orogenesis in the western United States Cordillera: Middle Jurassic (pre-Nevadan) regional metamorphism and thrust faulting within an active arc environment, Klamath Mountains, California: Geological Society of America Bulletin, v. 100, p. 859-876.

This page has intentionally been left blank.

COMPOSITE STANDARD CORRELATION OF THE MISSISSIPPIAN-PENNSYLVANIAN (CARBONIFEROUS) LISBURNE GROUP FROM PRUDHOE BAY TO THE EASTERN ARCTIC NATIONAL WILDLIFE REFUGE, NORTH SLOPE, ALASKA

by

John F. Baesemann,[1] Paul L. Brenckle,[2] and Paul D. Gruzlovic[3]

ABSTRACT

Composite standard treatment of microfossil-occurrence data provides a detailed biostratigraphic scheme to correlate Middle Mississippian to Middle Pennsylvanian depositional events within the Alapah and Wahoo Limestones of the Lisburne Group between Prudhoe Bay and the western and eastern areas of the Arctic National Wildlife Refuge (ANWR). Lisburne deposition in ANWR, which preceded that at Prudhoe Bay, spans about the same time interval but is represented by differing rock thicknesses which reflect local variations in paleotopography, sedimentation, and post-Lisburne erosion. Reservoir-quality dolomites occur widely across the study area in the upper Alapah Limestone and a coeval lower Alapah dolomite zone can be identified in the ANWR sections. The change from Alapah to Wahoo sedimentation began in western ANWR, then spread to eastern ANWR and finally to Prudhoe Bay. Numerous progradational shallowing-upward cycles or parasequences characterize the Wahoo Limestone in northeastern Alaska. Chronostratigraphic comparison of parasequence occurrences between western ANWR and Prudhoe Bay shows that few of these parasequences correlate, suggesting that local sedimentary and tectonic processes, rather than eustasy, controlled their formation. The Arctic seaway through Alaska has long been thought to be the only pathway for migration of Late Mississippian and Pennsylvanian calcareous foraminifers from Eurasia into North and South America, and vice versa. New information indicates that intermittent Early to Middle Pennsylvanian highstands may have linked North Africa and western Europe to South America, opening up auxiliary routes for the exchange of faunas.

INTRODUCTION

The possibility (Crow and Williams, 1987) of world-class hydrocarbon reserves under the North Slope in the Arctic National Wildlife Refuge (ANWR) prompted this study to refine correlation of the Alapah and Wahoo Limestones, the two formations comprising the Mississippian-Pennsylvanian (Carboniferous) Lisburne Group in northeastern Alaska. Detailed measurement and sampling of outcrops at Clarence River and Katakturuk River within eastern and western ANWR, respectively, and of cores from the Sohio Sag Delta 6 well at Prudhoe Bay (fig. 1) provided comprehensive lithostratigraphic and biostratigraphic control to predict the probable subsurface stratigraphy in the ANWR coastal plain, where no well data were available to us. Conodont and calcareous microfossil (foraminifers, algae, *incertae sedis*) occurrences were used to construct a local composite standard for graphic correlation. This methodology produced a tightly constrained chronostratigraphic framework for extrapolating microfossil ranges from section to section, determining age relationships of formational contacts, determining the continuity of dolomite zones (the principal reservoir rocks) within the Alapah Limestone, and correlating Wahoo parasequences.

GEOLOGIC SETTING

The Lisburne Group is a marine, predominantly carbonate sequence extending across Arctic Alaska into Canada. Deposition began to the south during the Osagean (Tournaisian) in a deeper water setting and became progressively shallower as the sequence transgressed northward to an ancient shoreline along the edge of the present-day Barrow Arch (Bird and Jordan, 1977; Bird, 1980). In northeastern Alaska the Lisburne is represented by the Alapah and Wahoo Limestones of

[1]Amoco Corporation, Exploration and Production Technology Group, P.O. Box 3092, Houston, Texas 77253.
[2]Consultant, 1 Whistler Point Road, Westport, Massachusetts 02790.
[3]Delta Environmental Consultants, Inc., 5401 West Kennedy Blvd., Suite 400, Tampa, Florida 33609.

Meramecian to Atokan (Visean to Bashkirian) age. The three Lisburne sections (fig. 2) of this study share many lithologic similarities, although variation in sedimentation rates, intraformational erosion, pre-Lisburne topography, and the amount of downcutting along the post-Lisburne unconformity account for local differences in thickness and lithofacies. Detailed Lisburne descriptions for this region can be found, for example, in Armstrong (1974), Armstrong and Mamet (1974, 1975), Bird and Jordan (1977), Watts and others (1994), Krumhardt and others (1996), and Harris and others (1997).

Alapah sedimentation at Prudhoe Bay and Clarence River conformably transgressed the paralic-continental facies of the Mississippian (Tournaisian-Visean) Endicott Group. Katakturuk River was situated on a positive feature, the Sadlerochit high (Armstrong, 1974; Armstrong and Mamet, 1974; Mamet and Armstrong, 1984); here the Alapah lies directly on Lower Paleozoic rocks. The area evidently remained mildly positive throughout the Late Paleozoic because the Lisburne section at Katakturuk River is considerably thinner than at the other localities and the Wahoo section is one of the thinnest regionally for that formation.

The Alapah Limestone is composed of a transgressive-regressive sequence. The lower part contains dolomite, algal limestone, and peloidal-skeletal packstone-grainstone, deposited in intertidal to restricted platform environments, that pass gradationally into bryozoan-pelmatozoan limestones formed in an open-platform setting. The upper Alapah represents the regressive part of the sequence and was deposited in restricted platform to intertidal environments. It is composed dominantly of skeletal mudstone-wackestone-packstone, spiculitic dolomite, and dolomite containing cryptalgal laminations, fenestral fabric, and solution-collapse breccia. Silicified and calcitized evaporite nodules are widespread throughout the regressive phase.

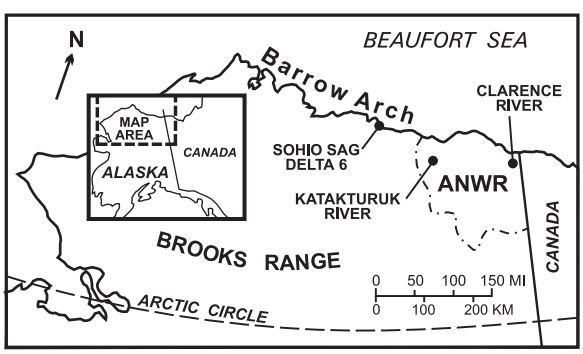

Figure 1. *Location of study areas in northeastern Alaska. Generalized stratigraphic columns for each area are illustrated in figure 2 and geographic coordinates are given in the Locality Register. ANWR=Arctic National Wildlife Refuge.*

The formation is thickest at Clarence River, which contains the deepest water Alapah deposits of the three studied sections. The greater depth is indicated by the interspersed encrinites and recessive, argillaceous bryozoan packstone-wackestone throughout much of the unit, accompanied by reduced numbers of foraminifers that would have thrived in a shallower shelf setting. The uppermost Alapah beds at the Katakturuk River section are recrystallized limestones (fig. 2) (Harris and others, 1997, fig. 2). They may have originated as cave fillings derived from dissolution along a pre-Wahoo exposure surface (Watts and others, 1994) or from some local tectonic event (Wood and Armstrong, 1975). Whatever the origin, there is no obvious gap or repetition in the faunal succession associated with the interval.

The Wahoo in outcrop has been divided informally into lower and upper members (Watts and others, 1994). The formational contact between the Alapah and Wahoo is placed between the dark gray, recessive weathering dolomite-limestone of the Alapah and the light-gray weathering, cliff-forming bryozoan-pelmatozoan grainstone-packstone-wackestone of the lower Wahoo member. The latter unit is transgressive and represents a return to open-marine sedimentation following the last restrictive episode at the top of the Alapah. The appearance of slope-forming, yellow- to orange-weathering dolomite at the top of the cliffs marks the base of the upper Wahoo member. Although parasequences are present within both Wahoo members, those in the upper member are generally thinner and form a characteristic ledge and slope topography. The resistant, ledge-forming beds are composed of skeletal and oolitic grainstones, and in the upper part of the member they also contain algal (*Donezella*) biostromes (Mamet and deBatz, 1989) and oncolitic ("*Osagia*") shoals. The absence of the latter deposits in the Katakturuk River section is probably related to differential post-Lisburne erosion.

ALAPAH DOLOMITES

According to C.E. Bartberger (written commun., 1986), upper Alapah dolomites ("medial dolomite" of Bird and Jordan, 1977) are the most porous and permeable facies within the Lisburne Group at the Prudhoe Bay field. These beds are negligible hydrocarbon producers because they generally lie beneath the oil-water contact, and most Lisburne production comes from fractured Wahoo carbonates higher in the column (Jameson, 1994). In the appropriate geologic setting the dolomites could be a viable exploration target (Dolton and others, 1987). One of the objectives of this study, therefore, was to determine the

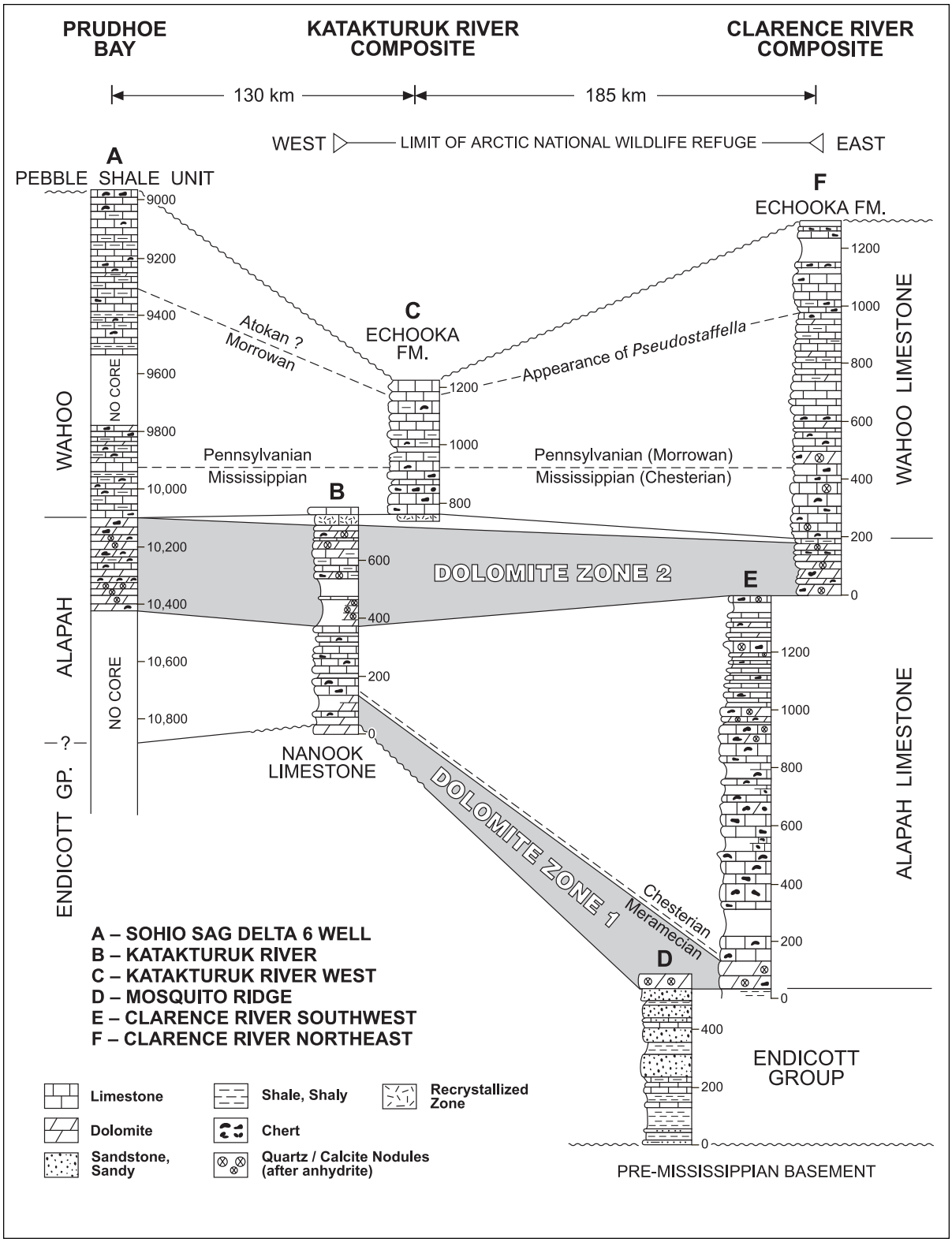

Figure 2. *Regional cross section of the Lisburne Group tied to the Mississippian-Pennsylvanian boundary (= first occurrence of the conodont* Declinognathodus noduliferus *subspp.). Katakturuk River outcrop sections are adjacent and were measured continuously. The three Clarence River outcrop sections are not close together and were measured separately. Thickness or depth on stratigraphic columns is in feet.* Pseudostaffella *at the Morrowan-Atokan(?) boundary refers to the foraminiferal subgenus* Pseudostaffella (Pseudostaffella).

extent of dolomitization in ANWR outcrops. Mesozoic erosion is thought to have removed much of the Lisburne under the coastal plain (Bird and others, 1987). If only a remnant of the Lisburne is preserved in the ANWR subsurface, it would be the Alapah, including possibly the prospective dolomites. Both the Clarence River and Katakturuk River sections contain lower and upper dolomite zones within the Alapah (fig. 2). The upper zone is stratigraphically in the same position as at Prudhoe Bay, but it is unknown if a lower zone is present at Prudhoe because our study of the Sag Delta 6 well was confined to cored intervals that did not include the lower Alapah.

COMPOSITE STANDARD-GRAPHIC CORRELATION

The timing of depositional and erosional events is critical to understanding the development of Lisburne stratigraphy on the North Slope and we used the composite standard-graphic correlation technique pioneered by Shaw (1964) to correlate the three sections. This methodology has been explained further in papers by Miller (1977), Edwards (1984, 1989, 1991, 1995), and Carney and Pierce (1995). A composite standard was developed by initially graphing the Sag Delta 6 well against the Katakturuk River section (fig. 3), the designated standard reference section. The oldest (base) and youngest (top) occurrences of taxa common to both localities were plotted on an X-Y coordinate grid on which the vertical and horizontal axes represent the thicknesses of the two sections. The most reliable bases in the crossplotted array of points on the grid were used to draw a line of correlation (LOC) that was used to determine time-equivalent horizons on both axes. Initial graphing permitted fossil range data from the Sag Delta well to be combined (composited) with those from Katakturuk River, including all taxa from both sections, not just those in common. This integrated information became the X axis, or composite standard, of a new crossplot (fig. 4) to correlate against the Clarence River sections on the Y axis. The composite standard axis was assigned a linear scale of time units (composite standard units, or CSU) tied to the age of appearance or disappearance of key taxa, and the relative timing of stratigraphic events was then extrapolated from one section to another.

In figure 3 the LOC was defined by appearances of the conodont species *Declinognathodus noduliferus* and the foraminiferal subgenus *Pseudostaffella* (*Pseudostaffella*). Both taxa occur with their evolutionary antecedents [*Gnathodus girtyi simplex* and *Pseudostaffella* (*Semistaffella*), respectively] at the three localities, and their appearances are deemed to be synchronous within the limits of resolution of the biostratigraphic data. The first occurrence of *D. noduliferus* within the lower Wahoo member marks the base of the Morrowan Series (Pennsylvanian System) and that of *P.* (*Pseudostaffella*) in the upper Wahoo approximates the base of the Atokan Series (Middle Pennsylvanian).

The LOC in figure 4 is composed of an upper segment defined by the same taxa as in figure 3 and a lower segment extending from the base of *D. noduliferus* to the top of the conodont form genus *Apatognathus*. There is a slight change in slope between the two segments, indicating minor differences in rock accumulation rates. *Apatognathus* disappeared within the late Meramecian in the lower Alapah at Katakturuk River and Clarence River, but its presence at Prudhoe Bay could not be confirmed because core of appropriate age was not available for study.

Figure 5 illustrates stratigraphic implications interpreted from the LOCs in figures 3 and 4. The Lisburne outcrops at Katakturuk and Clarence rivers cover nearly the same time interval whereas Lisburne deposition began later in the Sag Delta 6 well, closer to the Late Mississippian shoreline. The Katakturuk River section (fig. 2) is considerably thinner than the Lisburne at the other two localities because it was deposited on the Sadlerochit high, where Lisburne sedimentation rates were probably slower and diastems more numerous. Furthermore, the older age of the top of the Wahoo Limestone at Katakturuk River (fig. 5) suggests greater erosion here along the post-Lisburne unconformity. This interpretation is supported by the appearance of the conodonts *Neognathodus* and *Neogondolella* in the uppermost Wahoo at Sag Delta 6 and *Neognathodus* from the same level at Clarence River. Neither genus was found in the upper Wahoo at Katakturuk River, where the taxa would be expected if these beds are time-equivalent to the other sections. The Wahoo interval above the appearance of *Pseudostaffella* is also much thinner at Katakturuk River than at the other localities (fig. 2), which is another indication of local differential erosion.

The lower Alapah dolomite zone (figs. 2, 5) was deposited almost synchronously between Clarence River and Katakturuk River, but the composite standard indicates that lower Alapah dolomite in the Sag Delta well, if present, would be appreciably younger than and, therefore, probably discontinuous with the one in ANWR. The upper Alapah dolomite zone represents a widespread regression across the North Slope. Deposition of this interval began at Katakturuk River and persisted there the longest on the Sadlerochit high, although the youngest dolomites are found in the Sag Delta 6 well. The Alapah-Wahoo contact (fig. 5) is time

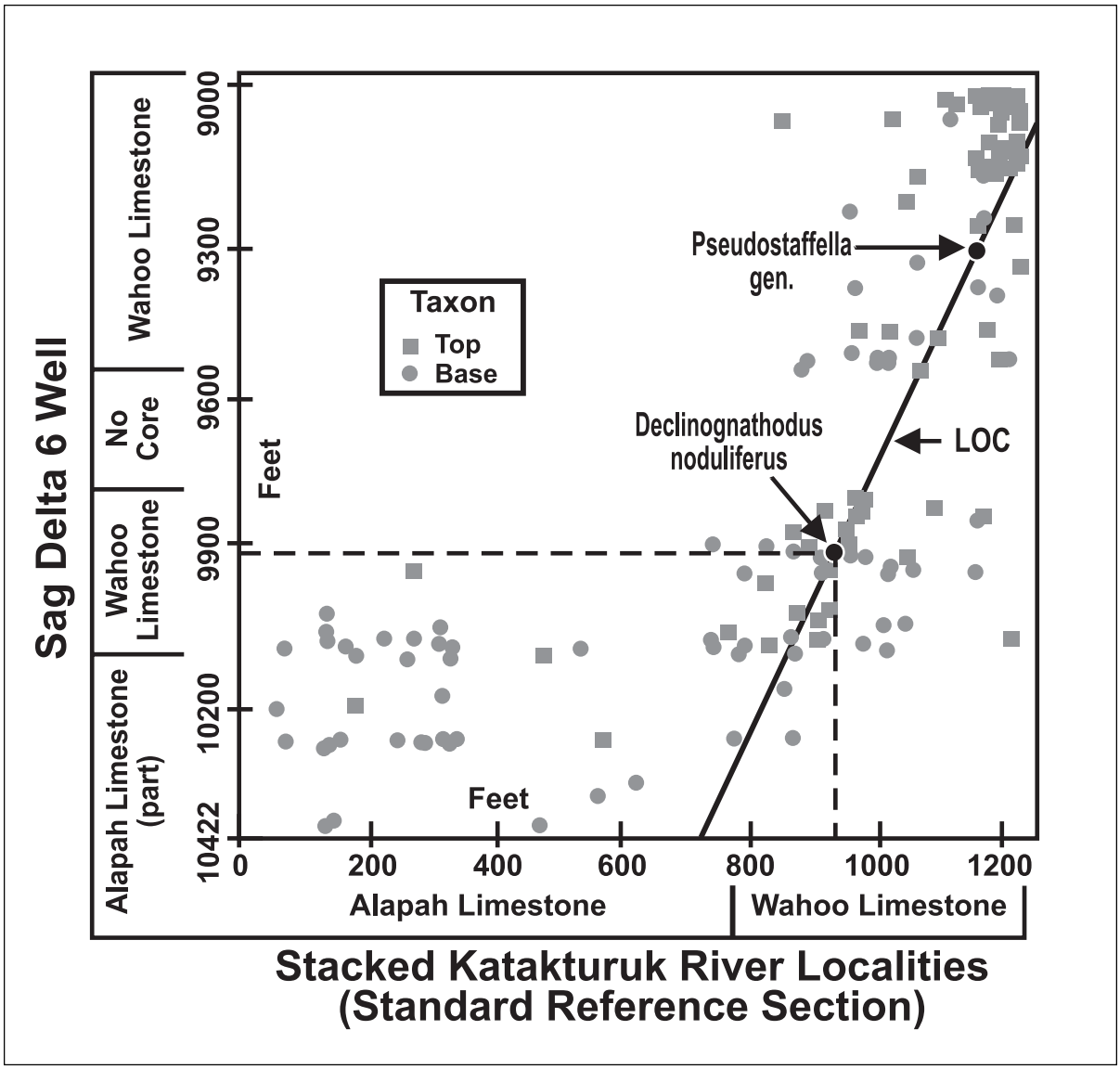

Figure 3. *Graphic correlation crossplot of stratigraphic occurrences of conodonts and calcareous microfossils from the Sag Delta 6 well vs the Katakturuk River composite section. The dashed lines extending from the line of correlation (LOC) at the base of* D. noduliferus *intersect the vertical and horizontal axes at the position where the species first occurs in the two localities. In a similar manner the LOC can be used to find other equivalent horizons. Taxon names other than those defining the LOC are not included in this or figure 4 to reduce clutter on the diagrams. Base = oldest occurrence of a taxon; top = youngest occurrence.*

transgressive. Lower Wahoo lithologies occur first at Katakturuk River and spread diachronously to Clarence River and finally Sag Delta.

WAHOO PARASEQUENCE CORRELATION

Pennsylvanian strata worldwide exhibit large-scale, transgressive-regressive sequences and classic, small-scale parasequences whose origins have been linked to eustatic sea-level changes controlled by Gondwanan glacial episodes (for example, Ross and Ross, 1985a; Veevers and Powell, 1987). If these sequences truly reflect global eustacy, they should be correlative over wide areas. Indeed, claims have been made that Wahoo parasequences are closely correlative across the North Slope (B. L. Mamet, written commun. to J. R. Groves, March 1987) and represent the same parasequences seen in coeval rocks in Nevada (Carr and Budd, 1987).

To test their local continuity, we determined the number of Wahoo parasequences at Katakturuk River and Sag Delta 6 and correlated the Katakturuk

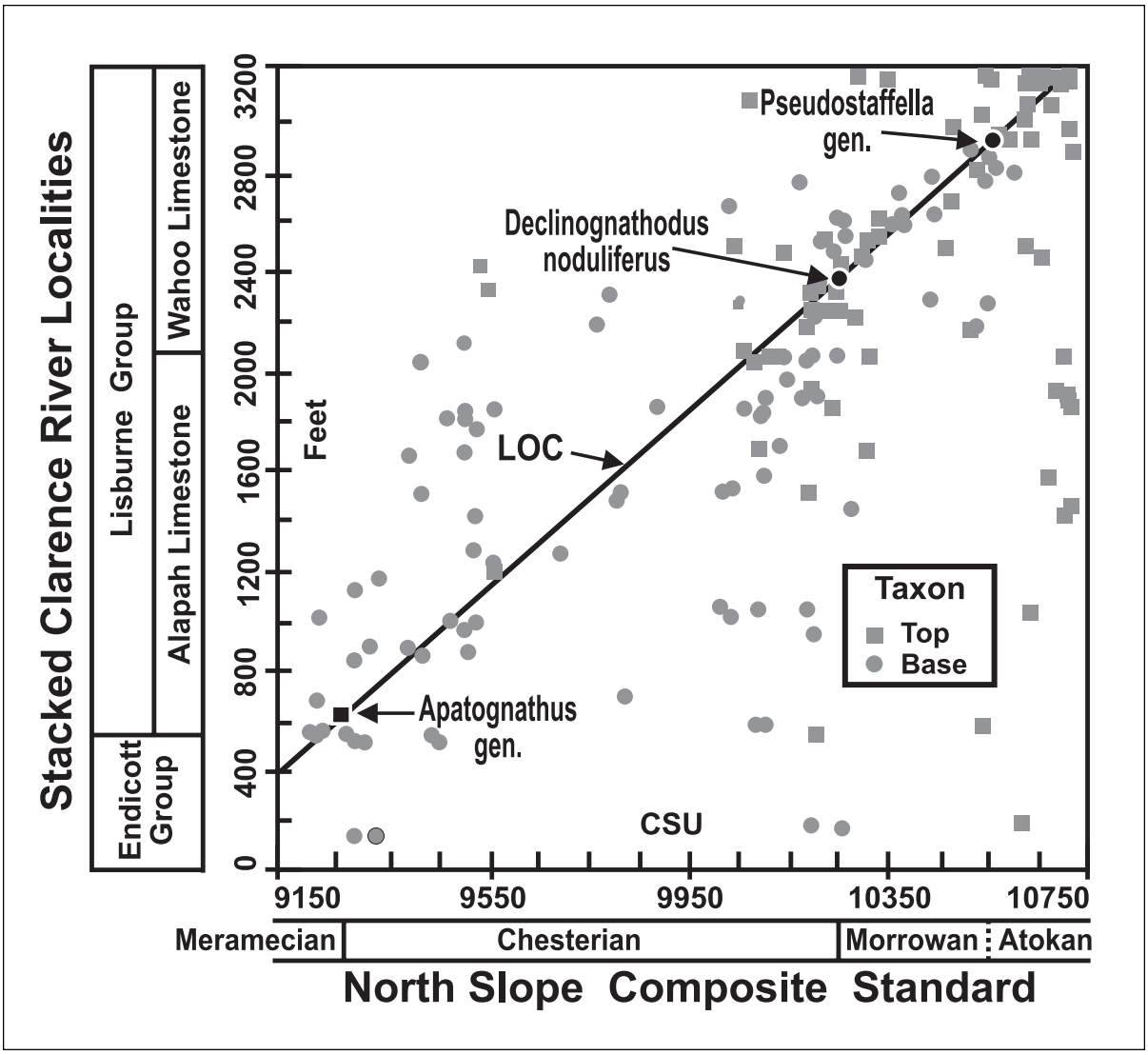

Figure 4. *Graphic correlation crossplot of conodont and calcareous microfossil occurrences at the Clarence River composite section vs microfossil ranges composited from the Sag Delta 6 well and the Katakturuk River composite section. Horizontal axis is a linear time scale expressed as composite standard units (CSU). LOC = line of correlation; base = oldest occurrence of a taxon; top = youngest occurrence.*

parasequence boundaries to the equivalent stratigraphic position in the Sag Delta well based on the LOC shown in figure 3. The results (fig. 6) show 17 Wahoo parasequences at Katakturuk River compared to 29 in the Sag Delta well, excluding the uncored interval in the upper Wahoo. The fewer parasequences at Katakturuk are in part attributable to greater erosion along the post-Lisburne unconformity, but the discrepancy in number and thickness between the two localities suggests that local tectonism strongly modified any eustatic control on sedimentation.

The Wahoo Limestone at Prudhoe Bay was deposited in a northeast-trending depression called the Canning sag (Armstrong, 1974). Subsidence within this basin provided the accommodation space to develop the relatively thick and numerous parasequences seen in the Sag Delta well. In contrast, Katakturuk deposition was on the Sadlerochit high. Here, slower sedimentation and diastems at the Mississippian-Pennsylvanian boundary (Harris and others, 1997) and probably at other horizons account for the thinner and fewer preserved parasequences. Furthermore, graphic correlation (figs. 3, 6) shows that the basal one to two parasequences at Katakturuk River are time-equivalent to the upper Alapah dolomite beds at Sag Delta 6. This correlation agrees with the local paleogeography, as the Prudhoe Bay area at that time was proximal to the shore (Jameson, 1994), whereas Katakturuk River was in a more seaward

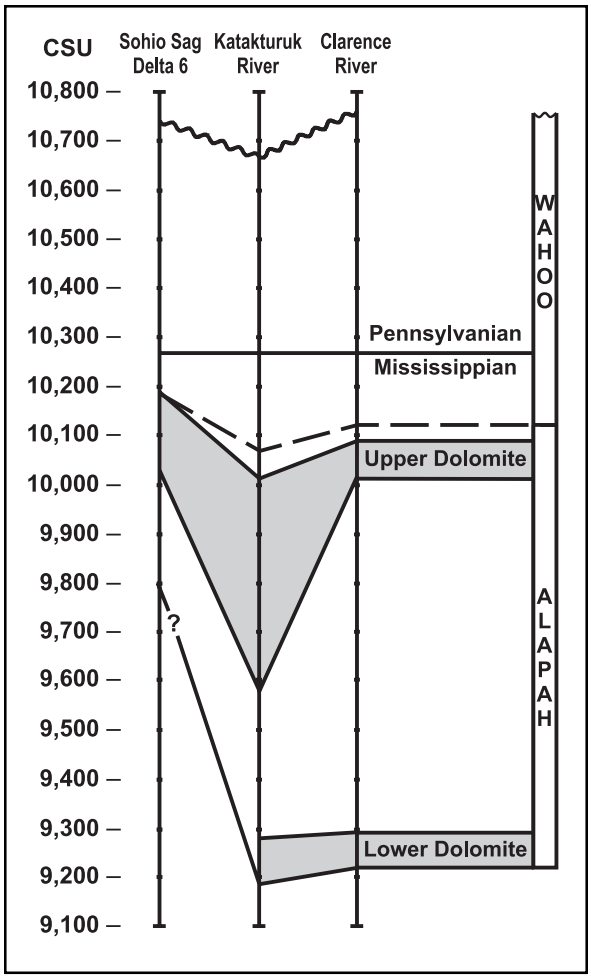

Figure 5. *Composite standard chronostratigraphic correlation of major Lisburne stratigraphic events across the study area. Composite standard units (CSU) represent time lines.*

position. Most parasequences are autocyclic. Few can be matched across the North Slope—much less the distance separating northern Alaska from the southern United States.

BIOSTRATIGRAPHY AND BIOGEOGRAPHY

CALCAREOUS MICROFOSSILS

Calcareous microfossils have long played a prominent role in dating the Lisburne Group within Arctic Alaska (for example, Armstrong and Mamet, 1974, 1975, 1977; Mamet and Armstrong, 1972, 1984) but, for various reasons, interpretations based on these microfossils have provided discrepant results for local and regional correlation (Krumhardt and others, 1996; Harris and others, 1997). Nevertheless, the Lisburne microfossil succession is generally consistent across northeastern Alaska and can provide a fairly reliable scheme for local Mississippian-Pennsylvanian correlation. The order of appearance and, to a lesser extent, disappearance of these microfossils produces an operational basis for correlating the Lisburne regionally (fig. 7). The relationship to coeval strata within sub-Arctic North America is complicated because of the absence of key taxa or migration between the two regions.

The Endicott Group, examined only at the Mosquito Ridge section (fig. 2), contains scarce Meramecian calcareous microfossils because of the mostly siliciclastic lithologies. Alapah biotas are also sparse because of the predominant dolomites, relatively deeper water argillaceous carbonates, and covered intervals in outcrop; they range from late Meramecian to late Chesterian. Diversity and abundance increase in the lower Wahoo member, and algae and foraminifers proliferate in the upper Wahoo, where pervasive shallow-water shelf environments are most favorable for their development. The Mississippian-Pennsylvanian (Chesterian-Morrowan) boundary falls near the top of the lower Wahoo member and the Morrowan-Atokan(?) boundary within the upper Wahoo member. The calcareous microfossil succession at Katakturuk River, which is representative of the Lisburne localities studied herein, is discussed and illustrated in Harris and others (1997).

Arctic foraminiferal faunas in both Alaska and Canada are more closely related to Eurasia than to the rest of North America, although there are enough similarities for intracontinental correlation. Paleogeographic and paleoenvironmental conditions in the Late Mississippian-Pennsylvanian (Ross and Ross, 1985b) prevented some Arctic taxa from migrating into sub-Arctic North America and delayed others so that appearances are commonly diachronous (Harris and others, 1997). For example, *Globivalvulina*, which is a reliable marker for the base of the Pennsylvanian in the conterminous United States (Mamet, 1975), first occurs in the upper Alapah Limestone, well below the Mississippian-Pennsylvanian boundary in northeastern Alaska (figs. 2, 7). Conversely, *Millerella marblensis* and *M. pressa* are common near the base of the Pennsylvanian in the sub-Arctic Americas, where they originated, but are so rare in the Arctic that they have little biostratigraphic use.

Pseudostaffella (Pseudostaffella) is another case in point. Its appearance defines the Morrowan-Atokan boundary across North America (Mamet, 1975; Groves, 1986). The taxon developed in Eurasia (Groves, 1988) through the lineage *Plectostaffella-Pseudostaffella* (*Semistaffella*)-*Pseudostaffella* (*Pseudostaffella*), which is also present in northeastern Alaska. However,

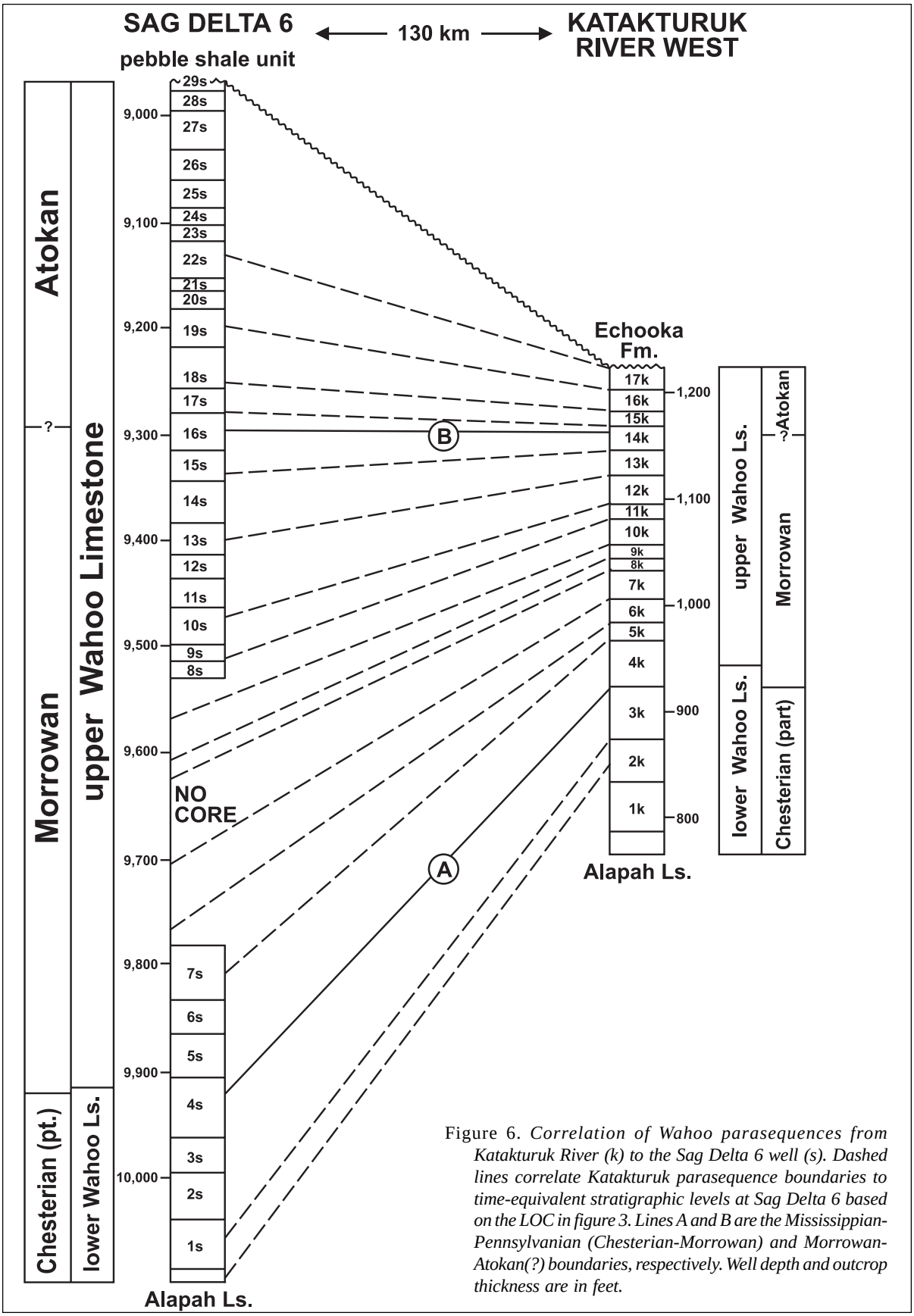

Figure 6. *Correlation of Wahoo parasequences from Katakturuk River (k) to the Sag Delta 6 well (s). Dashed lines correlate Katakturuk parasequence boundaries to time-equivalent stratigraphic levels at Sag Delta 6 based on the LOC in figure 3. Lines A and B are the Mississippian-Pennsylvanian (Chesterian-Morrowan) and Morrowan-Atokan(?) boundaries, respectively. Well depth and outcrop thickness are in feet.*

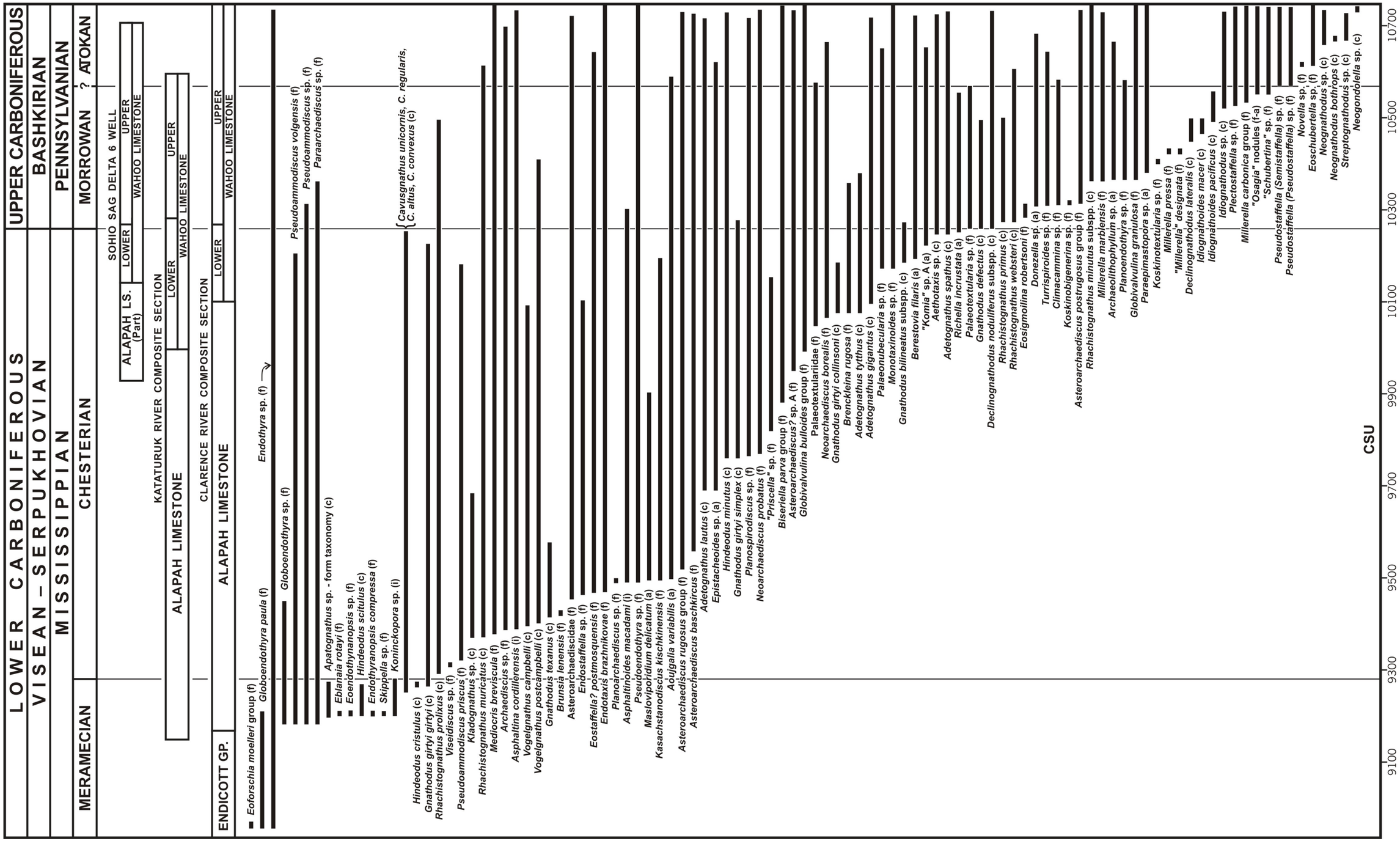

Figure 7. *Selected conodont and calcareous microfossil ranges composited from occurrences at Sag Delta 6, Katakturuk River and Clarence River. Range lines extend between first and last positive occurrences that were used to position the bases and tops in figures 3 and 4. Top of Meramecian placed at last occurrence of* Koninckopora *at Katakturuk River and* Apatognathus *at Clarence River, base of Pennsylvanian at first occurrence of* Declinognathodus noduliferus *subspecies and base? of Atokan at first occurrence of* Pseudostaffella (Pseudostaffella). *The lengths of the stratigraphic columns at the top of the figure are scaled to relative time (CSU), not thickness. CSU = Composite standard units, c = conodont, f = foraminifer; a = alga, i =* incertae sedis.

P. Pseudostaffella) appears without its evolutionary antecedents in sub-Arctic North America, suggesting a later arrival in that area (Groves, 1988). If this is true, a *Pseudostaffella*-based Morrowan-Atokan boundary must be diachronous between Alaska and southern North America, accounting for the uncertainty in placement of that boundary in this paper.

The distinctness of Arctic Carboniferous foraminiferal assemblages from sub-Arctic North America and their affinities to Eurasia have been recognized for some time (Mamet and Belford, 1968; Armstrong and Mamet, 1977). Ross (1967) proposed Eurasian-Arctic and Midcontinent-Andean realms to characterize the differences between the Old and New World faunas. Ross and Ross (1985b) postulated that during the Late Mississippian-Pennsylvanian the Arctic shelf was the primary migration route for Eurasian forms into North and South America (fig. 8) and that the temperate to colder Arctic waters prevented unrestricted entry into the New World, accounting for the compositional differences between realms.

New evidence suggests that at least for the Early to Middle Pennsylvanian there may have been migration routes also from North Africa and western Europe to South America, most likely associated with intermittent highstand incursions into the Amazonian seaway (fig. 8). Altiner and Savini (1995) reported a possible connection in the Morrowan after discovering *Plectostaffella* in northern Brazil. They also found specimens of the pseudovidalinid foraminifer *Asselodiscus* from upper Atokan rocks. Both of these Eurasian genera occur in the Arctic (Groves and others, 1994; Henderson and others, 1995). Because they are unknown elsewhere in North America, it is unlikely that they migrated into South America from that direction. Amoco unpublished collections from outcrops along the Macuma River in Ecuador and from wells in Peru contain *Plectostaffella*, *Pseudostaffella* (*Pseudostaffella*), and *P.* (*Semistaffella*).

These highstand migration routes may have provided an opportunity for native American taxa to enter Eurasia. Villa Otero (1995, pl. 1, figs. 22, 24) illustrated *Millerella marblensis* from Bashkirian (Early-Middle Pennsylvanian) rocks in the Cantabrian Mountains of Spain. The same faunas contain *Pseudostaffella* (*Pseudostaffella*), *P.* (*Semistaffella*) (Villa Otero, 1995, pl. 5, figs. 9-12) and probable *Plectostaffella* (Villa Otero, written commun. to Brenckle, April 1996). It would seem more plausible to bring *M. marblensis* into Europe directly from South America than to propose a circuitous migration around the Arctic shelf.

CONODONTS

Lisburne conodont biostratigraphy from northeastern Alaska is discussed in detail by Krumhardt and others (1996) and Harris and others (1997). These authors include systematics and discussions of ranges and environmental associations. The latter paper includes a description of the Katakturuk River conodont faunas. Virtually all Lisburne conodont taxa (fig. 7) have been reported from the Midcontinent, Appalachian, and Cordilleran areas of the United States, where assemblages are more diverse. Because the ranges of some taxa vary between northeastern Alaska and sub-Arctic North America, current sub-Arctic North American conodont zonal schemes do not apply to the Lisburne. Krumhardt and others (1996) and Harris and others (1997) used a simplified Lisburne conodont zonal scheme that reflects these differences in faunas and ranges.

In this study the Mississippian-Pennsylvanian (Chesterian-Morrowan) boundary is defined at the three sections by the appearance of the conodont *Declinognathodus noduliferus* subspecies which also defines the Mid-Carboniferous boundary inter-continentally (Lane and others, 1985; Brenckle and others, 1997). The Morrowan-Atokan (Early-Middle Pennsylvanian) boundary is picked at the base of the foraminiferal subgenus *Pseudostaffella* (*Pseudostaffella*). The appearance of this subgenus may not be synchronous between northeastern Alaska and sub-Arctic North America as discussed in the preceding calcareous microfossil section. Conodont evidence does not totally clarify this issue but suggests that the amount of diachroneity is not substantial. In sub-Arctic North America, the conodont genus *Idiognathodus* first occurs below *P.* (*Pseudostaffella*) (Lane and others, 1972), but in Eurasia (for example, Nemirovskaya and Alekseev, 1995) the order of appearance is reversed. If the base of *Idiognathodus* represents a time line, *P.* (*Pseudostaffella*) was delayed in entering sub-Arctic North America. In all Lisburne conodont localities *Idiognathodus* appears above *P.* (*Pseudostaffella*) except at Clarence River, where a single specimen of the conodont was found in the upper Wahoo member below that foraminifer. It may be argued that *P.* (*Pseudostaffella*) is out of sequence at Clarence River, but the shallow water environments of the upper Wahoo are much more hospitable for calcareous foraminifers than conodonts. *Pseudostaffella* (*Pseudostaffella*) is common throughout the upper Wahoo and its appearance is probably synchronous, whereas that of *Idiognathodus* is variable because of generally unfavorable conodont facies. Environmental factors apparently restricted the appearance of *Idiognathodus* below *P.* (*Pseudostaffella*) in the Lisburne in contrast to sub-Arctic North America where the conodont genus occurs abundantly and consistently from the beginning of its range. Nevertheless, the evidence indicates that the stratigraphic succession of the two taxa

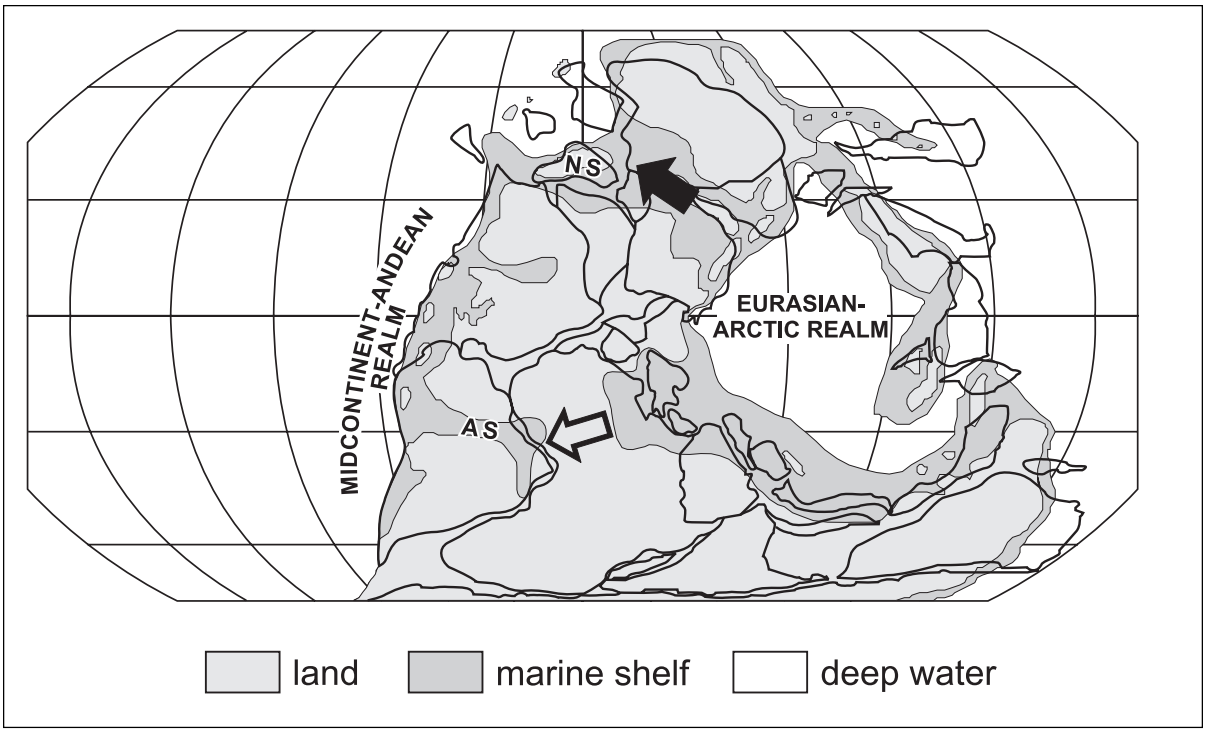

Figure 8. *Middle Pennsylvanian paleogeographic reconstruction modified from Golonka and others (1994). Solid arrow represents the major (Arctic) pathway across the North Slope (NS) for migration of calcareous microfossils from Eurasia into the North American-Andean Realm during the Late Mississippian and Pennsylvanian. Open arrow represents direction of possible intermittent incursions of calcareous microfossils into the Amazonian seaway (AS) from North Africa and western Europe during the Early to Middle Pennsylvanian.*

is the same within North America. Since this is the case, the age discrepancy in the appearance of *P.* (*Pseudostaffella*) between sub-Arctic North America and Alaska is considerably less than that between sub-Arctic North America and Eurasia.

LOCALITY REGISTER

Sohio Sag Delta 6 well, NE1/4 SE1/4 sec. 2, T. 11 N., R. 15 E., Beechey Point B-3 Quadrangle Map, U.S. Geological Survey, 1955, scale 1: 63,360. Core samples were taken from the upper Alapah and Wahoo Limestones; 219 samples were analyzed for microfossils.

Katakturuk River section, western Sadlerochit Mountains: SW1/4 SW1/4 sec.19, T. 3 N., R. 27. E., Mt. Michelson C-3 Quadrangle Map, U.S. Geological Survey, 1955, scale 1: 63,360. The section, measured along the west river bank, begins at the base of the Alapah Limestone and ends at the Alapah-Wahoo-Limestone contact at the top of the recrystallized zone; 116 samples were analyzed for microfossils.

Katakturuk River West section, western Sadlerochit Mountains: SE1/4 SE1/4 sec. 24, T. 3 N., R. 26 E., Mt. Michelson C-3 Quadrangle Map, U.S. Geological Survey, 1955, scale 1: 63,360. The section, a continuation of the Katakturuk River locality about 0.4 km to the east, begins in the recrystallized zone at the top of the Alapah Limestone and continues through the overlying Wahoo Limestone into the basal beds of the overlying Echooka Formation; 155 samples were analyzed for microfossils.

Mosquito Ridge section, eastern Brooks Range: SW1/4 NW1/4 sec. 13 and SE1/4 NE1/4 & NE1/4 SE1/4 sec. 14, T. 1 N., R. 44 E., Demarcation Point B-1 Quadrangle Map, U.S. Geological Survey, 1956, scale 1: 63,360. The section consists of the basal Alapah Limestone and the underlying Endicott Group. It is located on a southeast-facing hillside about 6 km northwest of the Clarence River Southwest section; 19 samples were analyzed for microfossils.

Clarence River Southwest section, eastern Brooks Range: W1/2 SE1/4 sec. 21 and NE1/4 NW1/4 & NW1/4 NE1/4 sec. 28, T. 1 N., R. 45 E., Demarcation Point B-1 Quadrangle Map, U.S. Geological Survey, 1956, scale 1: 63,360. The section begins at the Endicott-Alapah contact on the upper part of a south-facing hillside and continues down the north-facing dip slope of that hill until it ends in the upper Alapah along the Clarence River; 158 samples were analyzed for microfossils.

Clarence River Northeast section, eastern Brooks Range: W1/2 SE1/4 & NE1/4 SW1/4 sec. 22, T. 1 N., R. 45 E., Demarcation Point B-1 Quadrangle Map, U.S. Geological Survey, 1956, scale 1: 63,360. The section is on a south-facing cliff along the right bank of the Clarence River 1 km east of the Clarence River Southwest section. It begins in the upper Alapah Limestone and continues to the overlying Wahoo Limestone-Echooka Formation contact; 172 samples were analyzed for microfossils.

ACKNOWLEDGMENTS

We thank many people and institutions for their support and assistance in this study: H.R. Lane for initiating the research; C.E. Bartberger for help in measuring, describing, and sampling the Katakturuk River sections and sharing his knowledge of Lisburne depositional environments; J.A. Babcock for assisting in fieldwork at the Clarence River sections; A.A. Bakke for measuring and describing the Mosquito Ridge section and for field assistance at the other Clarence River sections; J.G. Clough and other Alaska Division of Geological & Geophysical Surveys (DGGS) personnel for orienting us at the Katakturuk and Clarence River sections; M.I. Pavlicek for helping identify conodonts in the Sag Delta 6 well; J.R. Groves for identifying calcareous microfossils in the Clarence River Northeast section; C.G. Mull for clarifying some aspects of North Slope stratigraphic terminology; P. Fullbright and M. Schendel for drafting the figures; R.W. Pierce for commenting on an earlier version of the paper; A.P. Krumhardt and R.L. Ravn for thoughtful reviews of the submitted manuscript; DGGS for arranging logistics for Clarence River fieldwork; Sohio for permitting us to examine and sample the Sag Delta 6 cores in 1986; British Petroleum for permitting us to publish the results from these cores; and Amoco Corporation for providing logistical support for the Katakturuk and Clarence River fieldwork in 1985 and 1987 and for permitting Baesemann and Brenckle to publish this paper.

REFERENCES CITED

Altiner, D., and Savini, R., 1995, Pennsylvanian Foraminifera and biostratigraphy of the Amozonas and Solimões basins (North Brazil): Revue de Paléobiologie, v. 14, no. 2, p. 417-453.

Armstrong, A.K., 1974, Carboniferous carbonate depositional models, preliminary lithofacies and paleotectonic maps, Arctic Alaska: American Association of Petroleum Geologists Bulletin, v. 58, no. 4, p. 621-645.

Armstrong, A.K., and Mamet, B.L., 1974, Carboniferous biostratigraphy, Prudhoe Bay State 1 to northeast Brooks Range, Arctic Alaska: American Association of Petroleum Geologists Bulletin, v. 58, no. 4, p. 646-660.

Armstrong, A.K., and Mamet, B.L., 1975, Carboniferous biostratigraphy, northeastern Brooks Range, Arctic Alaska: U.S. Geological Survey Professional Paper 884, 29 p.

———1977, Carboniferous microfacies, microfossils, and corals, Lisburne Group, Arctic Alaska: U.S. Geological Survey Professional Paper 849, 144 p.

Bird, K.J., 1980, Petroleum exploration of the North Slope, Alaska, *in* Mason, J.F., ed., Petroleum geology in China: Principal lectures presented to the United Nations International meeting on petroleum geology, Beijing, March 1980: Tulsa, PennWell Publishing Company, p. 233-248.

Bird, K.J., Griscom, S.B., Bartsch-Winkler, S., and Giovannetti, D.M., 1987, Chapter 7. Petroleum reservoir rocks, *in* Bird, K.J., and Magoon, L.B., eds., Petroleum geology of the northern part of the Arctic National Wildlife Refuge, northeastern Alaska: U.S. Geological Survey Bulletin 1778, p. 79-99.

Bird, K.J., and Jordan, C.F., 1977, Lisburne Group (Mississippian and Pennsylvanian), potential major hydrocarbon objective of Arctic Slope, Alaska: American Association of Petroleum Geologists Bulletin, v. 61, no. 9, p. 1493-1512.

Brenckle, P.L., Baesemann, J.F., Lane, H.R., West, R.R., Webster, G.D., Langenheim, R.L., Brand, U., and Richards, B.C., 1997, Arrow Canyon, the Mid-Carboniferous boundary stratotype: *in* Brenckle, P.L., and Page, W.R., leaders, Paleoforams '97 guidebook: Post-conference field trip to the Arrow Canyon Range, southern Nevada USA: Cushman Foundation for Foraminiferal Research, Supplement to Special Publicatin No. 36, p. 13-32.

Carney, J.L., and Pierce, R.W., 1995, Graphic correlation and composite standard databases as tools for the exploration biostratigrapher, *in* Mann, K.O., and Lane, H.R., eds., Graphic correlation: SEPM (Society for Sedimentary Geology) Special Publication 53, p. 23-43.

Carr, T.R., and Budd, D.A., 1987, Sequence stratigraphic concepts applied to Early Pennsylvanian shelf carbonates: Geological Society of America Abstracts with Programs, v. 19, no. 7, p. 612.

Crow, P., and Williams, B., 1987, Arctic National Wildlife Refuge: Will it be leased or locked up?: Oil and Gas Journal, February 2, p. 12-15.

Dolton, G.L., Bird, K.J., and Crovelli, R.A., 1987, Chapter 22: Assessment of in-place oil and gas resources, *in* Bird, K.J., and Magoon, L.B., eds., Petroleum geology of the northern part of the Arctic National Wildlife Refuge, northeastern Alaska: U.S. Geological Survey Bulletin 1778, p. 277-298.

Edwards, L.E., 1984, Insights on why graphic correlation (Shaw's method) works: Journal of Geology, v. 92, p. 583-597.

———1989, Supplemental graphic correlation: A powerful tool for paleontologists and nonpaleontologists: Palaios, v. 4, p. 127-143.

———1991, Quantitative biostratigraphy, *in* Gilinsky, N.L., and Signor, P.W., eds., Analytical paleobiology, short course in paleontology, no. 4: The Paleontological Society, University of Tennessee, Knoxville, p. 39-58.

Edwards, L.E., 1995, Graphic correlation: Some guidelines on theory and practice and how they relate to reality, *in* Mann, K.O., and Lane, H.R., eds., Graphic correlation: SEPM (Society for Sedimentary Geology) Special Publication 53, p. 45-50.

Golonka, J., Ross, M.I., and Scotese, C.R., 1994, Phanerozoic paleogeographic and paleoclimatic modeling maps, *in* Embry, A.F., Beauchamp, B., and Glass, D.J.,eds., Pangea: Global environments and resources: Canadian Society of Petroleum Geologists Memoir 17, p. 1-47.

Groves J.R., 1986, Foraminiferal characterization of the Morrowan-Atokan (lower Middle Pennsylvanian) boundary: Geological Society of America Bulletin, v. 97, p. 346-353.

———1988, Calcareous foraminifers from the Bashkirian stratotype (Middle Carboniferous, South Urals) and their significance for intercontinental correlations and the evolution of the Fusulinidae: Journal of Paleontology, v. 62, no. 3, p. 368-399.

Groves, J.R., Nassichuk, W.W., Rui, L, and Pinard, S., 1994, Middle Carboniferous Fusulinacean biostratigraphy, northern Ellesmere Island (Sverdrup Basin, Canadian Arctic Archipelago): Geological Survey of Canada Bulletin 469, 55 p.

Harris, A.G., Brenckle, P.L., Baesemann, J.F., Krumhardt, A.P., and Gruzlovic, P.D., 1997, Comparison of conodont and calcareous microfossil biostratigraphy and lithostratigraphy of the Lisburne Group (Carboniferous), Sadlerochit Mountains, northeast Brooks Range, Alaska, *in* Dumoulin, J.A., and Gray, J.L., eds., Geologic studies in Alaska by the U.S. Geological Survey, 1995: U.S. Geological Survey Professional Paper 1574, p. 195-219.

Henderson, C.M., Pinard, S., and Beauchamp, B., 1995, Biostratigraphic and sequence stratigraphic relationships of Upper Carboniferous conodont and foraminifer distribution, Canadian Arctic Archipelago: Bulletin of Canadian Petroleum Geology, v. 43, no. 2, p. 226-246.

Jameson, J., 1994, Models of porosity formation and their impact on reservoir description, Lisburne field, Prudhoe Bay, Alaska: American Association of Petroleum Geologist Bulletin, v. 78, p. 1651-1678.

Krumhardt, A.P., Harris, A.G., and Watts, K.F., 1996, Lithostratigraphy, microlithofacies, and conodont biostratigraphy and biofacies of the Wahoo Limestone (Carboniferous), eastern Sadlerochit Montains, northeast Brooks Range, Alaska: U.S. Geological Survey Professional Paper 1568, 58 p.

Lane, H.R., Bouckaert, J., Brenckle, P., Einor, O.L., Havlena, V., Higgins, A.C., Yang J., Manger, W.L., Nassichuk, W., Nemirovskaya, T., Owens, B., Ramsbottom, W.H.C., Reitlinger, E.A., and Weyant, M., 1985, Proposal for an international Mid-Carboniferous boundary: 10th International Congress of Carboniferous Stratigraphy and Geology, Madrid, l983, Compte rendu, v. 4, p. 323-339.

Lane, H.R., Sanderson, G.A., and Verville, G.J., 1972, Uppermost Mississippian-basal Middle Pennsylvanian conodonts and fusulinids from several exposures in the south-central and southwestern United States: 24th International Geological Congress, Montreal, Section 7, Paleontology, p. 549-555.

Mamet, B.L., 1975, Carboniferous Foraminifera and Algae of the Amsden Formation (Mississippian and Pennsylvanian) of Wyoming: U.S. Geological Survey Professional Paper 848-B, 18 p.

Mamet B.L., and Armstrong A.K., 1972, Lisburne Group, Franklin and Romanzof Mountains, northeastern Alaska, in Geological Survey Research 1972: U.S. Geological Survey Professional Paper 800-C, p. C127-C144.

———1984, The Mississippian-Pennsylvanian boundary in the northeastern Brooks Range, Arctic Alaska: 9th International Congress of Carboniferous Stratigraphy and Geology, Champaign-Urbana, 1979, Compte rendu, v. 2, p. 428-436.

Mamet, B.L., and Belford, D.J., 1968, Carboniferous Foraminifera, Bonaparte Gulf Basin, northwestern Australia: Micropaleontology, v. 14, no. 3, p. 339-347.

Mamet, B., and deBatz, R., 1989, Carboniferous microflora, Lisburne Group, Sadlerochit Mountains, Alaska: 11th International Congress of Carboniferous Stratigraphy and Geology, Beijing, 1987, Compte rendu, v. 3, p. 50-60.

Miller, F.X., 1977, The graphic correlation method in biostratigraphy, *in* Kauffman, E.G., and Hazel, J.E., eds., Concepts and methods in biostratigraphy: Stroudsburg, Pennsylvania, Dowden, Hutchinson, and Ross, p. 165-186.

Nemirovskaya, T.I., and Alekseev, A.S., 1995, The Bashkirian conodonts of the Askyn section, Bashkirian Mountains, Russia: Bulletin de la Société belge de Géologie, v. 103, fasc. 1-2, p. 109-133.

Ross, C.A.,1967, Development of fusulinid (Foraminiferida) faunal realms: Journal of Paleontology, v. 41, p. 1341-1354.

Ross, C.A., and Ross, J.R.P., 1985a, Late Paleozoic depositional sequences are synchronous and world-wide: Geology, v. 13, p. 194-197.

———1985b, Carboniferous and Early Permian biogeography: Geology, v. 13, p. 27-30.

Shaw, A.B., 1964, Time in Stratigraphy: New York, McGraw-Hill, 365 p.

Veevers, J.J., and Powell, C.M., 1987, Late Paleozoic glacial episodes in Gondwanaland reflected in transgressive-regressive depositional sequences in Euramerica: Geological Society of America Bulletin, v. 98, p. 475-487.

Villa Otero, E., 1995, Fusulinaceos carboniferos del este de Asturias (N de Espanã): Biostratigraphie du Paléozoïque, Université Claude Bernard Lyon I, Centre des Sciences de la Terre, v. 13, 261 p.

Watts, K.F., Harris, A.G., Carlson, R.C., Eckstein, M.K., Gruzlovic, P.D., Imm, T.A., Krumhardt, A.P., Lasota, D.K., Morgan, S.K., Enos, P., Goldstein, R., Dumoulin, J.A., and Mamet, B.L., 1994, Analysis of reservoir heterogeneities due to shallowing-upward cycles in carbonate rocks of the Carboniferous Wahoo Limestone of northeastern Alaska: U.S. Department of Energy Report, Contract DE-AC22-89BC14471, 433 p.

Wood, G.V., and Armstrong, A.K., 1975, Diagenesis and stratigraphy of the Lisburne Group limestones of the Sadlerochit Mountains and adjacent areas, northeastern Alaska: U.S. Geological Survey Professional Paper 857, 47 p.

ENIGMATIC SOURCE OF OIL FROM CHUKCHI SEA, NORTHWESTERN ALASKA

by
Arthur C. Banet, Jr.[1] and Thomas C. Mowatt[2]

ABSTRACT

North Slope exploration is expanding to the Chukchi Sea. Thus far, five wells have been drilled in this vast province. This drilling has yielded noncommercial discoveries of gas or oil in four wells, drilled on the initially perceived most-promising prospects. With some modification, the major stratigraphic depositional systems of the North Slope persist offshore. However, indigenous and primary reservoir properties are limited to the Neocomian Breakup Sequence sandstones, rather than the Ellesmerian reservoirs of the Prudhoe Bay area found downsection.

Of the known North Slope oil-source rocks, geochemistry shows that the predominantly carbonate Shublik Formation is the richest source rock of the Chukchi area. However, the Chukchi oil does not correlate well with the Prudhoe oil suite which is also derived from the Shublik. Instead, the chemistry of the Chukchi oil indicates it is derived from marine clastic rocks. Drilling in the Chukchi Sea shows that none of the potential marine clastic rocks have sufficient organic richness or kerogens to generate oil.

INTRODUCTION

The United States' portion of Chukchi Outer Continental Shelf (OCS) encompasses some 130,000 km,^{2} located between northwestern Alaska and the Chukhotsk Peninsula and south of latitude 73° (fig. 1). It is entirely north of the Arctic Circle and probably the most remote part of OCS to explore. Onshore exploration drilling began in the 1950s around Barrow and spread southwest. Government-sponsored drilling and, later, drilling by industry, took place during the 1970s and 1980s. Gas shows were common but development is limited to the Barrow area. To date, five wells have tested the offshore.

REGIONAL GEOLOGY

Across the North Slope, Proterozoic through upper Devonian basement rock consists of various schist, quartzite, carbonate, and argillite lithologies. In the Chukchi area, regionally extensive carbonate depositional sequences attain thicknesses of several thousand meters. Basement complex is shallowest in the subsurface along the present-day coastline. From the Pt. Barrow area, it plunges southeast as the Barrow Arch, which is a series of Late Jurassic to Early Cretaceous uplifts which formed concordantly with rifting events (fig. 2). Generally, the North Slope's prerift, south-dipping sediments are uplifted and truncated to varying extents on the arch's south flank (fig. 3).

Basement rocks are unconformably overlain by the northerly-derived Ellesmerian sequence (Lerand, 1973). Upper Mississippian through Triassic Ellesmerian rocks include carbonate, shale, and predominantly quartzitic sandstone. These sediments covered a south-facing, passive continental margin. Exploratory drilling near the coast has revealed much about proximal depositional environments (versus correlative distal depositional environments, as exposed in the Brooks Range). The Sadlerochit and Endicott sands are important reservoirs at Prudhoe Bay; Lisburne carbonates are of less importance. The Ellesmerian section is uplifted and truncated from highs along the Barrow Arch.

The Jurassic through Lower Cretaceous "Breakup Sequence" records the transition from northerly to southerly derived sedimentation. Onshore, the coarse-grained members are restricted to the Barrow Arch and are found in the subsurface along the present coast. They are known as (or correlative to) Carman and Hardwick's Barrovian Sequence (1981) [Craig and others (1985), Rift Sequence; and Hubbard and others (1987), Beaufortian Sequence]. Where preserved, the Breakup Sequence records the effects of rifting events that initiated formation of the Arctic basin (fig. 1). The Lower Cretaceous unconformity refers to the culmination stage of uplift, truncation of the Ellesmerian section, and some basement lithologies along the Barrow Arch during the rifting events on the North Slope. However, within the

[1]Bureau of Land Management, Anchorage, Alaska 99507.
[2]Consultant, Port Orford, Oregon 97465.

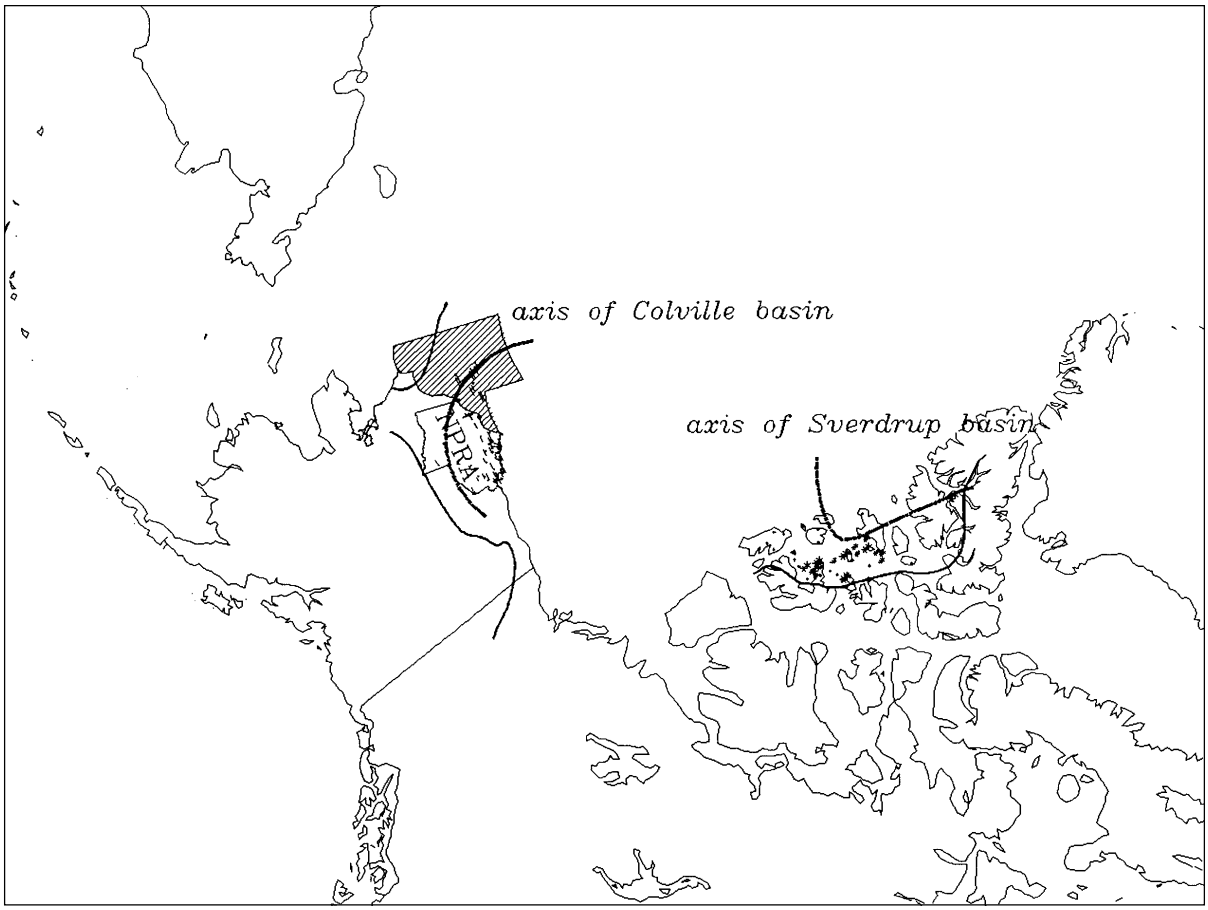

Figure 1. *Location map showing Alaska, NPRA, Arctic Canada, U.S. Chukchi (shaded), and axes of Colville and Sverdrup Basins (dashed).*

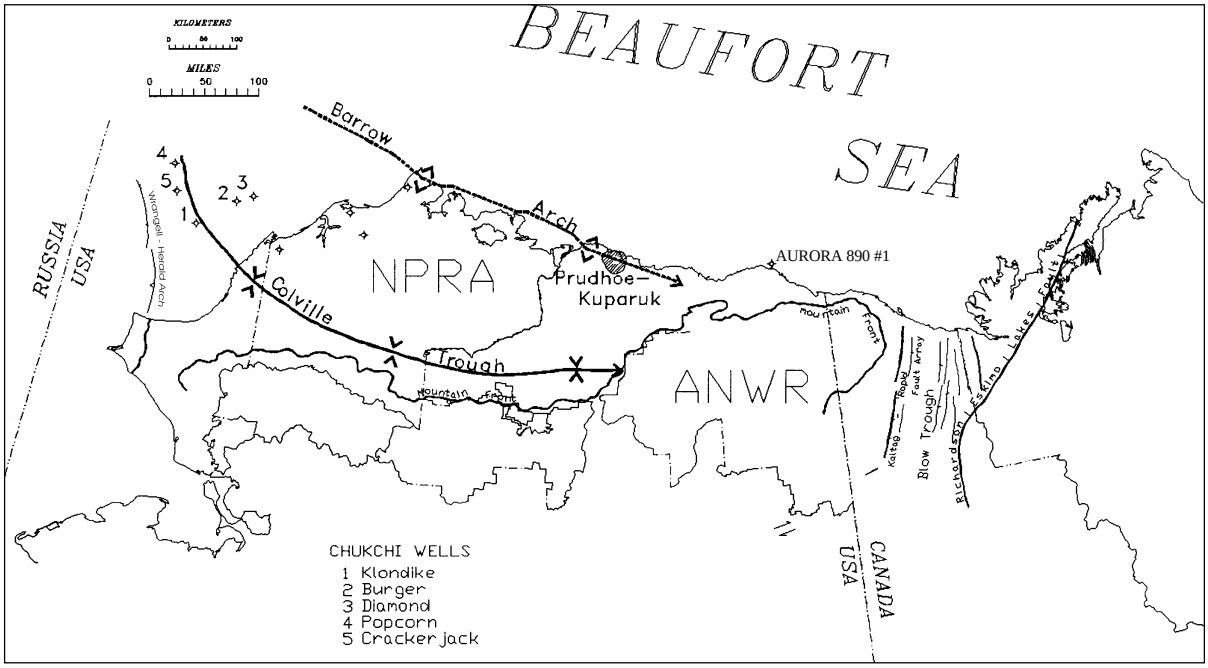

Figure 2. *Major tectonic features of Arctic Alaska and adjacent Canada.*

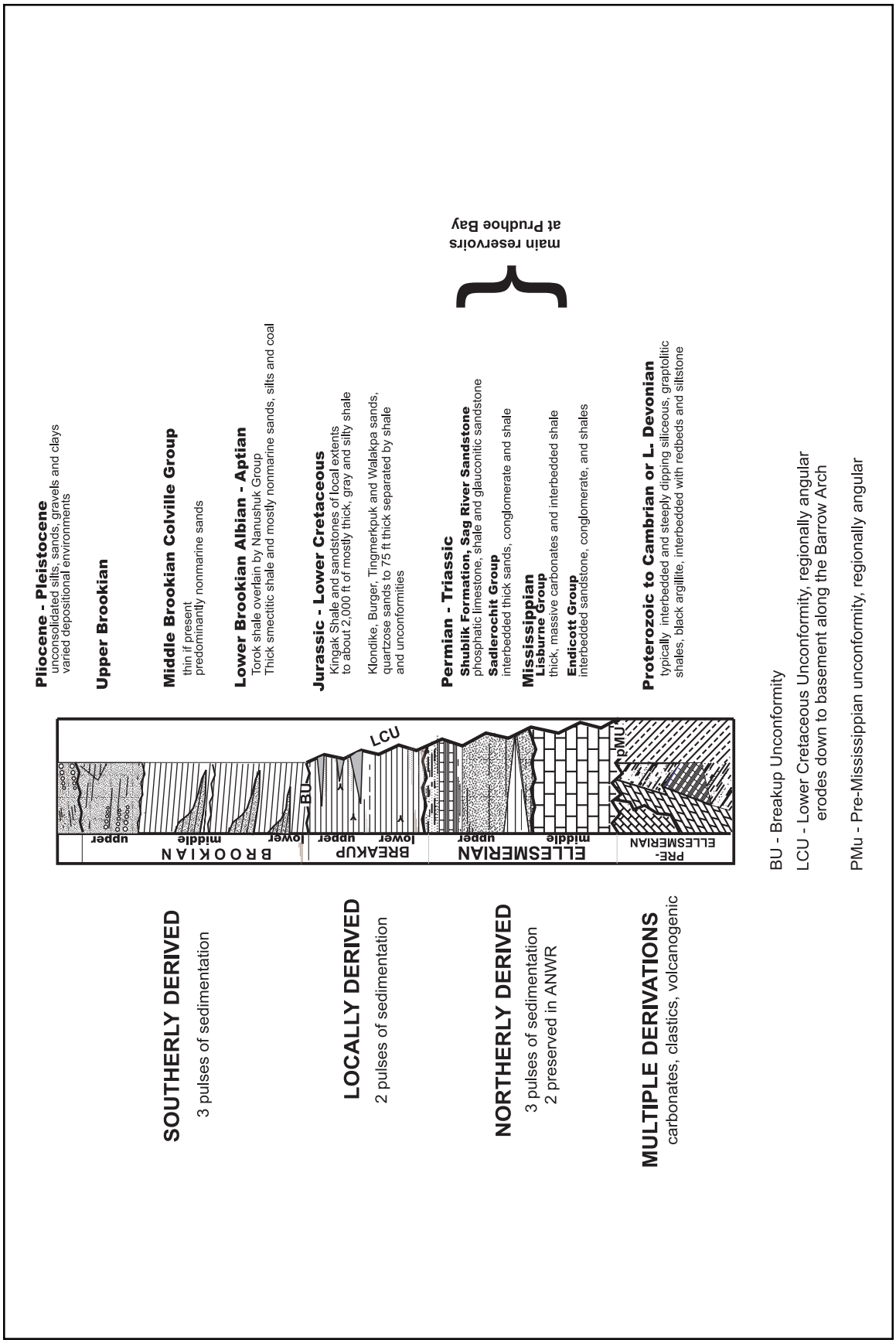

Figure 3. *Generalized stratigraphy of northwestern Alaska.*

Breakup Sequence, local and internal unconformities within the Jurassic Kingak Shale are numerous and usually of limited lateral extents, indicating lesser events.

Breakup Sequence sands having reservoir potential are thinner than and less areally extensive than Prudhoe Bay area reservoirs. These sands record deposition directed from several isolated and ephemeral highs. They are petrographically mature quartz arenites and similar to the Sadlerochit Group and Endicott Group reservoirs at Prudhoe Bay.

In contrast, subsequent southerly derived Brookian sequence (Lerand, 1973) depositional sequences consist mostly of shale and chert litharenites. These are predominantly regressional depositional sequences which extend from onshore through the entire Chukchi area. Hubbard and others (1987) describe regional Brookian sedimentation consisting of distinct pulses of east-northeast-trending clastics. After filling the Colville Trough, their distal portions overstep the Barrow Arch and fill both the Chukchi and Beaufort platforms. The Torok Formation (Aptian) and mostly nonmarine Nanushuk Group (Albian) record Lower to middle Cretaceous sedimentation in the western part of the North Slope. Upper Cretaceous through Lower Eocene middle Brookian rocks overlie the Nanushuk Group and are restricted to the central and eastern parts of the North Slope. Post-Middle Eocene, upper Brookian clastics overlie the Nanushuk Group in the Chukchi and Middle Brookian rocks to the east.

CHUKCHI GEOLOGY

Recent exploration drilling in the Chukchi Sea has penetrated middle Ellesmerian Lisburne Group carbonates of Late Mississippian age. Seismic data indicates these carbonates are very thick in the Chukchi Sea, as are the underlying clastic units and older carbonates (Thurston and Theiss, 1987). Three exploration wells have encountered upper Ellesmerian, late Permian clastic rocks. These fine-grained sediments correlate in age to the major reservoirs of the Prudhoe Bay field, the Sadlerochit Group. Drilling data shows the sands have appreciable thicknesses where encountered. However, these Sadlerochit lithologies lack appreciable reservoir characteristics in this part of the Chukchi Sea.

The Triassic Shublik Formation is the main source rock for the Prudhoe Bay oil (Seifert and others, 1979). Logs from the Chukchi Sea and across the North Slope describe the Shublik Formation as interbedded silty limestone or limy siltstone and shale with abundant fossils and phosphate nodules. In the Prudhoe Bay area, kerogens from carbonate facies provide the high sulfur content, high metals content, high diasterane content and the diagnostic biomarker 28,30-bisnorhopane. The Shublik Formation present in the Chukchi Sea is lithologically similar and has very good source-rock characteristics.

Jurassic through Lower Cretaceous Breakup Sequence sands and shales overlie the Ellesmerian section. Unlike the onshore part of the North Slope, the pre-Bajocian part of the Kingak Shale has been widely eroded from the Chukchi platform. The upper Kingak Shale is also comparatively thin and is missing from the Diamond well (fig. 2). In the Lower Cretaceous section, sands are mostly fine grained, well sorted quartzose sublitharenites–quartz litharenites. Medium- to coarse-grained fabrics and detrital clays are subordinate. There are also traces of chert, argillaceous clasts, and carbonate grains (Mowatt and others, 1995). Typically, these Breakup Sequence sands rest on or are stratigraphically near the Lower Cretaceous unconformity.

Brookian sediments are interbedded, predominantly fine- to coarse-grained chert litharenites, siltstones, and shale from marine through lacustrine and coal-bearing environments. Lower Brookian rocks range from post rifting lower to mid-Cretaceous and overlie the Breakup Sequence across the Chukchi (Thurston and Theiss, 1987). These are equivalent to the Nanushuk Group and Torok Formations. Onshore, these units crop out in tight symmetrical folds that form the Brooks Range foothills. Offshore, correlative rocks crop out at the sea floor. Pre-faulting burial has generated subbituminous coal throughout the section. Offshore exploration drilling shows the basal Tertiary section has impressive reservoir potential with thick sandstones, up to 165 m (Sherwood and others, 1995). The overlying upper Brookian consists of loosely consolidated sands, silts, and clay.

GEOCHEMISTRY

The Prudhoe oil is the most significant oil type on the North Slope in terms of volume, geographic extents, and economic development potential. It is the yardstick to which all other North Slope oils are compared. Prudhoe oils (table 1) are found between Barrow and the Pt. Thompson area and are restricted to the subsurface of the coastal plain. Prudhoe oil does not occur at seeps or oil-stained sandstones. The geochemical signature indicates it is a marine oil type, derived from the Shublik and Kingak Formations and Pebble Shale unit (Seifert and others, 1980; Magoon and Claypool, 1981). Thermally mature and nonbiodegraded, it has high sulfur content (greater than 1%), high metals (Ni and V) contents, ^{13}C isotopes between about -29.0 $^{0}/_{00}$ and -30.5 $^{0}/_{00}$, and API gravities ranging from 20° to about 40° (averaging about 25°). Biomarker hopane and sterane contents are present in low concentrations and pristane:phytane ratios are about 1.0 (table 1).

Table 1. *Geochemical data for western North Slope oils (modified from Hughes and Holba, 1986; and Banet, 1994)*

Type	Sample	Well	Depth (ft)	Reservoir	Age	API	%S	Ni ppm	V ppm	V:V + Ni	% Sat	pr/ph
Umiat	80	Seabee #1	5,366-5,394	Torok	K	52.6	0.01	0.2	0.2	0.50	90.7	12.00
Umiat	105	Well A	14,126-14,144	not listed	K	39.6	0.23	2.6	0.3	1.10	64.7	1.43
Umiat	108	Umiat #4	299	Nanushuk	K	36.5	0.06	4.5	0.5	0.10	69.3	1.77
Transitional	AYZ	Hemi Springs #1	7,196-7,245	Kuparuk	K	34.4	0.25	6.0	2.2	0.27	51.8	2.17
Transitional	GGN	Gwydyr Bay S #1	10,053-10,105	Sadlerochit	Tr	33.6	0.30	9.0	4.3	0.32	55.9	1.74
Mixed[a]	DZG	Mikkelsen Bay St. #1	10,468-10,550	Colville	K	33.2	0.83	8.5	6.9	0.45	48.1	1.18
Mixed[a]	76	S Barrow 20	1,629-1,639	Pebble Shale	K	28.8	0.21	4.2	4.7	0.53	64.8	1.32
Prudhoe/Transitional	CGN	W Kuparuk St #1	8,880-8,924	Shublik	Tr	28.0	0.60	10.0	21.6	0.68	46.3	1.49
Transitional	BHW	Hemi Springs #1	9,538-9,582	Sadlerochit	Tr	27.8	0.22	2.9	1.1	0.28	57.1	1.56
Prudhoe	CGM	Sag River St #1	8,890-9,008	Sadlerochit	Tr	27.0	1.01	9.9	22.5	0.69	40.0	1.53
Prudhoe	DZF	N Kuparuk St #1	8,890-8,984	Sadlerochit	Tr	26.0	1.00	11.2	22.2	0.66	42.3	1.42
Prudhoe	GGK	N Kuparuk St #1	3,708	Colville sandstone	KT	25.8	1.00	9.3	18.9	0.67	32.7	1.44
Prudhoe	75	Put River D-3	10,417-10,536	Sadlerochit	Tr	24.9	0.99	8.4	16.7	0.66	43.5	1.42
Prudhoe	BCY	Kuparuk River 1Y-2	7,638-8,012	Kuparuk	K	23.9	1.67	21.7	58.0	0.73	38.9	1.30
Umiat	79	Simpson core test	near surface	Nanushuk	K	23.0	0.24	1.2	0.7	0.64	58.0	1.57
Prudhoe	GGM	Foggy Is Bay St #1	10,092-10,209	Lisburne	Mi s	23.1	1.27	22.8	40.9	0.78	38.1	1.45
Prudhoe	GGL	Mikkelsen Bay St #1	11,870-12,200	Lisburne	Mi s	22.7	1.28	30.8	71.1	0.70	35.1	1.10
Prudhoe	77	S Barrow 19	2,200-2,245	Sag River sandstone	Jur	21.1	1.34	21.2	20.8	0.50	48.1	1.22
Prudhoe	GGJ	Kavearak Pt #1	3,794-3,845	Ugnu sandstone	T	20.9	1.56	14.8	35.4	0.71	39.0	1.56
Prudhoe	DZE	Pt. Thompson #1	12,063-13,050	Thompson sandstone	K	20.0	1.16	23.8	58.6	0.71	36.0	1.35
Prudhoe	DZC	Well B	not listed	not listed	K	12.4	0.87	17.0	48.4	0.74	29.3	1.18
Prudhoe	ASN	Mukluk OCS-Y-0334	7,360-7,385	Kuparuk River	K	12.1	na	na	na	- -	28.3	1.54
Prudhoe (altered)	81	J.W. Dalton #1	8,568-8,665	Lisburne	Mi S	6.5	3.12	43.9	141.1	0.76	23.5	1.37
Chukchi		Klondike	9,916	Shublik	Tr	35.3	0.18	- -	- -	- -	66.2	1.92
Chukchi		Burger	5,560-5,665	Breakup	K	46.4	0.4	0.9	0.35	0.28	64.1	1.84

[a]Prudhoe and Umiat.
n/a = Not available.
- - = No data.

The Shublik Formation is a marine carbonate facies rich in sapropelic organic material. Phosphate nodules and shale are common; Shublik kerogens contributed the high sulfur content, high metal content, and triterpane biomarker parts of the Prudhoe oil (Banet, 1994). The Kingak kerogens are a likely source of diasteranes in the Prudhoe oil and also modified its isotopic signature. Pebble Shale kerogens, where thermally mature, also contribute both diasteranes and the extended hopane fraction to the Prudhoe biomarker spectra that are absent from the other two source rocks (fig. 4).

The Umiat oil is another oil type found primarily in NPRA and commonly compared to the Prudhoe oil (Magoon and Claypool, 1981). Its chemical characteristics indicate it has been generated from a marine clastic source with no carbonate input (table 1). Diasterane and tricyclic contents suggest it is more thermally mature than the Prudhoe oil. Umiat oil is found in both wells and seeps in the foothills and on the coastal plain.

Exploration drilling shows that correlative source-rock lithologies are present throughout the Chukchi shelf. Figure 5 shows the general area where these pre-Brookian source rocks are projected to be thermally mature. Total Organic Carbon (TOC) values are high enough to suggest there is good source-rock potential in the Pebble Shale unit, Kingak Shale, and Shublik Formations (fig. 6). There is also unexpected organic richness in the underlying Sadlerochit Group equivalent lithology.

Geophysical and lithologic logs describe the potential source rock units at Klondike well. Compared with the Prudhoe Bay area, both the Pebble Shale unit and Kingak Shale are silty and thin. Lithological

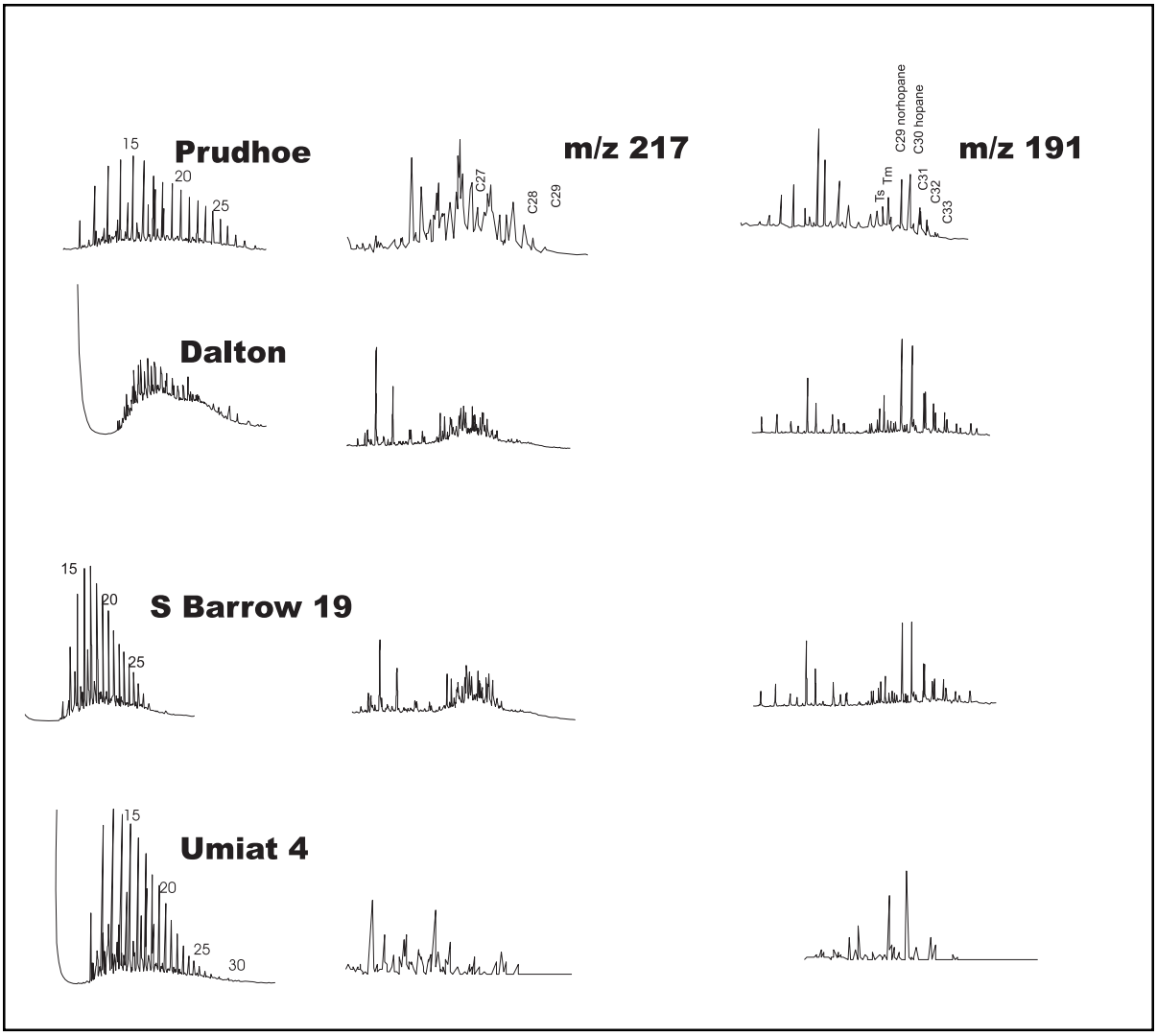

Figure 4. *Comparison of gas chromatographs (first column) and biomarker spectra (m/z 217 and m/z 191) from NPRA (modified from Magoon and Claypool, 1985). m/z = mass/charge.*

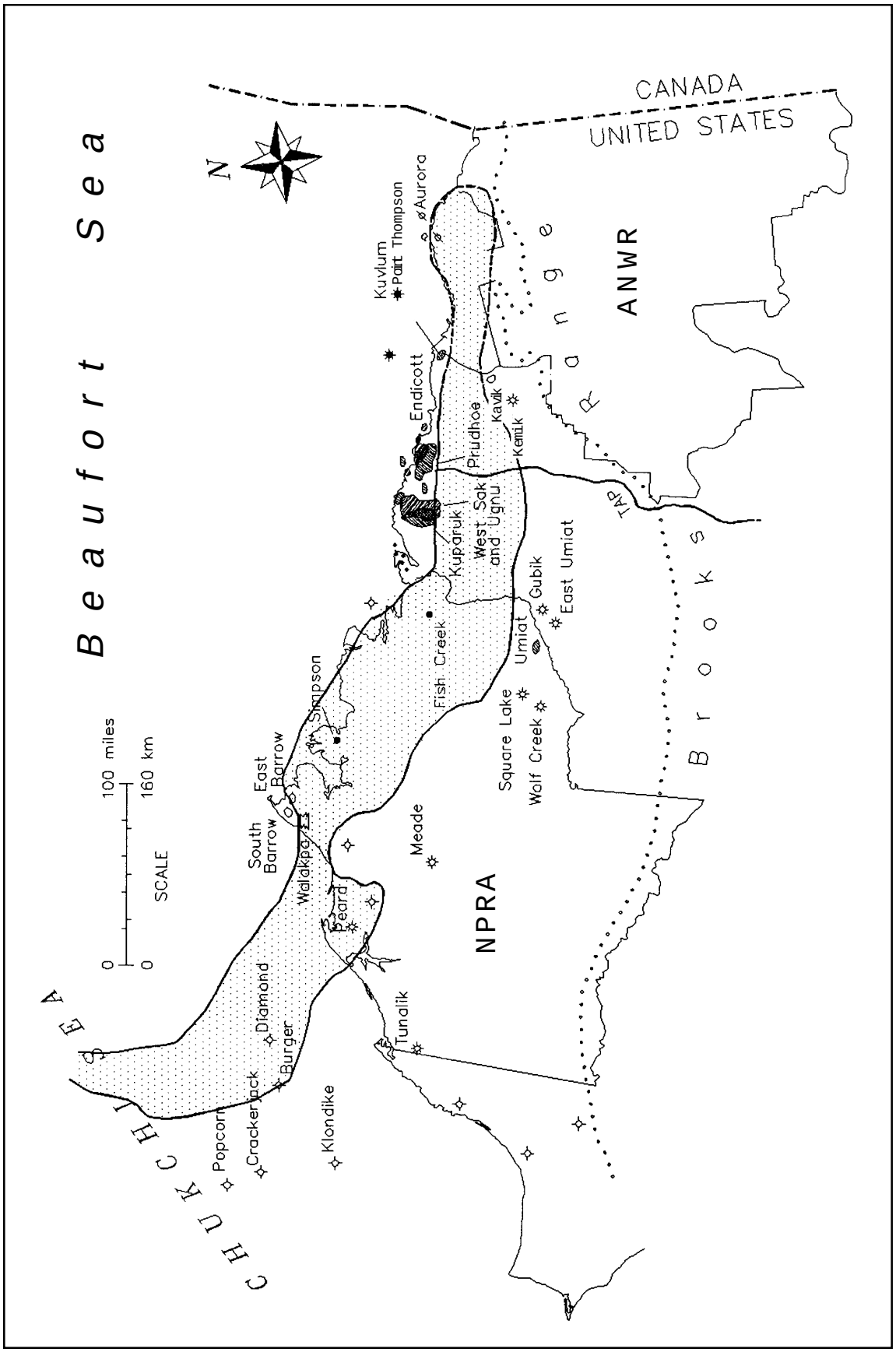

Figure 5. *Extents of thermally mature Shublik and Kingak Formations between truncation and* R_O*>1.35% (modified from Thurston and Theiss, 1987).*

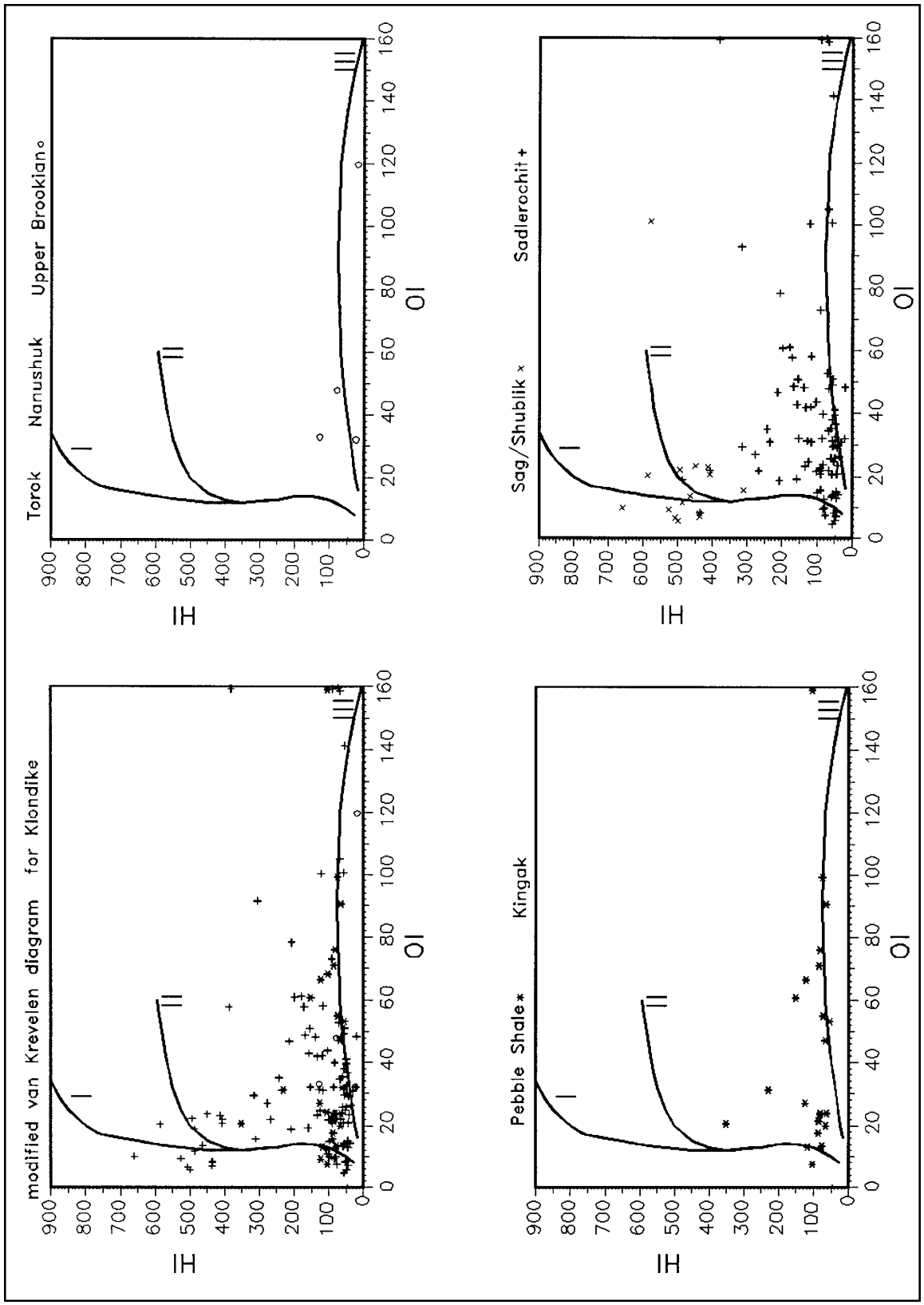

Figure 6. *Modified Van Krevelen diagrams for source rocks at Klondike well showing Type I, II, and III kerogens. HI = hydrogen index; OI = oxygen index.*

descriptions show the Shublik Formation consists of fossiliferous and interbedded, mixed carbonate, shale, and siltstone lithologies. The siltstone is typically chalky and the shale is dark gray, fissile, organic-rich, and oily. Forams are common. This also describes the Shublik Formation near Prudhoe Bay.

All three Prudhoe oil type source rocks are present across the Chukchi Sea. They also have sufficient organic carbon contents to be considered good source rocks. However, analysis of the Klondike well shows type I and II kerogens mostly in the Shublik Formation (fig. 6). In contrast, the Pebble Shale and Kingak Shale have predominantly type III kerogens with no oil-source potential. They show significantly less source potential than most areas on the North Slope. Thus, only the Shublik Formation and perhaps some facies of the Sadlerochit Group have enough hydrogen-rich kerogens to have generated hydrocarbons for this area of the Chukchi.

OIL

Oil was recovered from the Shublik Formation at 3,022 m depth from the Klondike well (OCS-Y-1482) during a drill bit change. Examination of the logs suggests oil is also present in a Breakup Sequence sandstone at 2,492-2,507 m. However, there were no tests. At the Burger well (OCS-Y-1413), repeat-formation tests yielded hydrocarbons from a Breakup Sequence sandstone between 1,695 and 1,727 m. Abundant dry gas and a few milliliters of liquid hydrocarbon were recovered (table 2); so far, these are the only data available.

Geochemically, the oil from the Klondike well and the minuscule amount from the Burger well share similarities, even though they have different API gravities (Banet, 1994). Figures 7 and 8 show the Chukchi oil has ^{13}C ratios with a range suggestive of marine sources and overall biomarker distributions similar to the Prudhoe oils. Most significantly though, they lack the major geochemical characteristics common to marine carbonate source rock such as the Shublik. Chukchi oil differences from the Prudhoe type oils include lower sulfur content (much less than 1%), lower metals content, higher pristane:phytane ratios (greater than 1.5), lower V:/V+Ni ratios and aromatics:saturates:NSO ratios, and higher API gravity (tables 1, 2). The high API gravity and diasterane content suggest these oils are thermally altered.

Many of the geochemical characteristics are similar to Umiat oils, i.e. derived from marine clastic source rocks. However, the biomarker distributions of the Chukchi and Umiat oils are dramatically different (Banet, 1994). Chukchi oil has higher sterane:diasterane ratios than those of Umiat oils. Chukchi oil spectra at m/z 191 have a well-developed series of extended hopanes. There is a diagnostic peak for 28,30-bisnorhopane and Ts greater than Tm. These are not found in Umiat oils. In addition, Chukchi oil spectra differ from those of Prudhoe oil at m/z 191. These spectra show that the Chukchi oil has fewer tricyclics, C_{29} much less than C_{30} hopane, and Ts equal to or greater than Tm (figs. 4, 9). Chukchi oils have the chemical characteristics of being derived from a marine clastic source. However, the geochemical data and source-rock

Table 2. *Comparison of geochemical data*

	Kuparuk	**Prudhoe**	**Umiat**	**Klondike**	**Burger**
Depth	1,770-1,920	2,560-2,745	to 300	3,022	1,695
Reservoir	Kuparuk	Sadlerochit	Nanushuk	Triassic[a]	Breakup
Temperature	65	93	<32	95	52
Gas cap	no	yes	no	no	yes
API gravity	24	22-32	19-39.2	35.3	32-57
% Sulfur	1.67	0-79-1.49	0.04-0.29	0.18	0.04-0.06
Gas:oil ratio	450	730	- -	- -	- -
% saturates	38.9	38.9	67	66.2	70.5
% aromatics	55.1	54.4	33	26.1	11.0-21.3
pr/ph	<1.50	1.0	>1.5	1.9	1.4-1.7
CPI	1.0-1.5	0.97	1.02-1.05	- -	- -
Ni	21.7	10-30	0.2-4.5	- -	0.9
V	58.0	20-60	0.2-0.7	- -	0.35
V:V+Ni	0.73	.62-.74	0.11	- -	0.28
^{13}C ppt	-30.2	-29.89	- -	-30.56	-28.3
Triterpanes tri/pent	0.63	0.11-0.27	0.51	0.57	- -

[a]Logs show oil in Breakup Sequence sand recoved from Triassic.
- - = No data.

analyses show it is not derived from the same source as the Umiat oils.

This, then, is the enigma of the Chukchi oil. Whereas its chemical signature indicates it is derived from a marine clastic source-rock, none of the marine shales in the Chukchi have kerogens with sufficient properties to have produced oil. Only the Shublik Formation has sufficient organic carbon, requisite kerogen types, and necessary thermal maturity to be the source of the oil, as it is around Prudhoe Bay. However, the Chukchi oil is dramatically different. Parrish (1987) describes regional variations within the Shublik Formation lithology; however, her projections of the Shublik depositional facies and the log interpretations suggest there is no difference between the Shublik Formation where it is thermally mature in the Chukchi Sea and around Prudhoe Bay. This suggests the Shublik Formation generates two distinctly different oils from the same source lithologies.

One possible explanation may come from considering a proposed prerift geometry of the Arctic (Tailleur, 1973). A clockwise rerotation of the land masses closes the Arctic basin and restores the original positions of the sediment sources This reconstructed rerotation juxtaposes the North Slope Colville and Sverdrup basins (fig. 8). Embry and others (1994) show

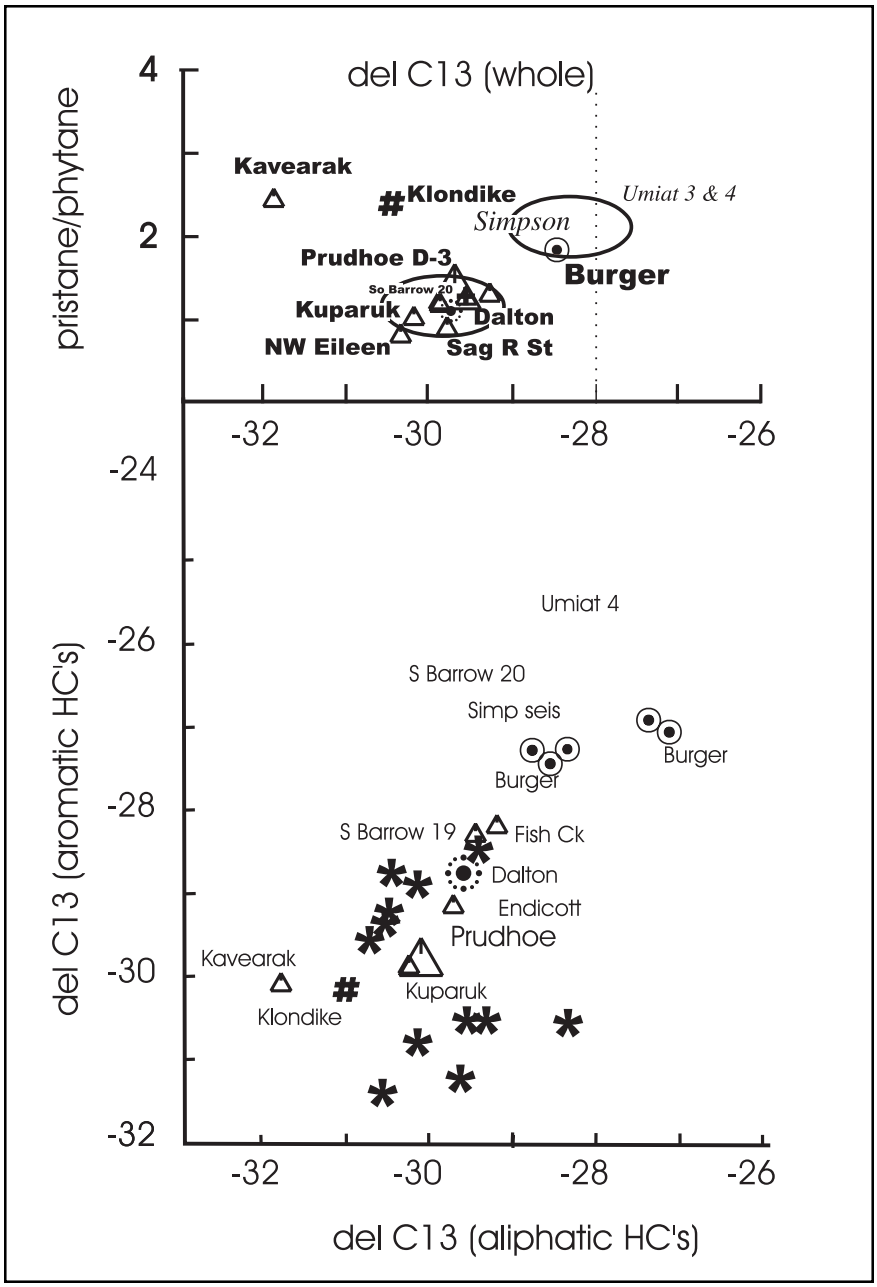

Figure 7. *Isotope ratios for Prudhoe, Umiat, Chukchi, and Sverdrup Basin (*) oils.*

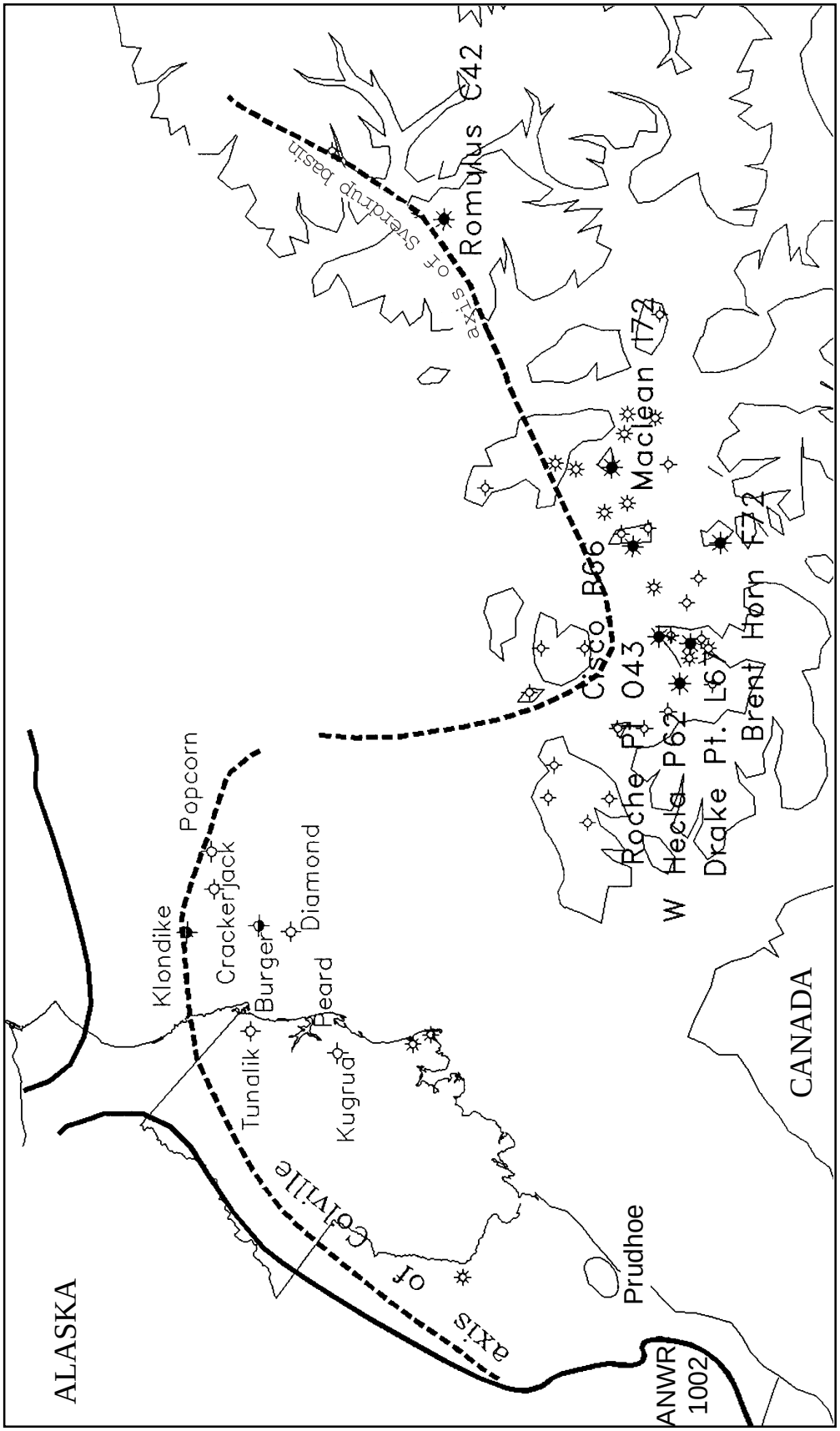

Figure 8. *Rotated and closed Arctic Basin showing relationships between Chukchi Basin and Sverdrup basin.*

stratigraphic and paleontologic correlations that support prerift similarities between the Tunalik well in western NPRA and the Canadian Arctic Islands, Brock I-20, and Cape Norem A-80 wells in the Sverdrup Basin.

Brooks and others (1992) and Curiale (1992) demonstrate that the Sverdrup oils and condensates are from a single genetic family and originate from organic-rich facies within the Triassic Schei Point Group. Geochemical variations reflect differences in thermal effects (Curiale, 1992). Limestone, calcareous sandstone, and black organic-rich shale compose the source rocks of the Schei Point Group (Stuart-Smith and Wennekers, 1977). These lithologic descriptions correspond well with those for the Shublik Formation.

Table 3 and figure 9 show the geochemical analyses and biomarker distributions for the Sverdrup Basin oils. Sulfur contents are low, metals contents are low, pristane:phytane ratios and saturates:aromatics:NSO ratios are also similar to those of the Chukchi oil. In addition, the biomarker spectra are nearly identical, including low triterpane content, no C_{28}-C_{30} bisnorhopanes, C_{29} much less than C_{30} hopane, and a well-developed extended hopane series. The concentration of Ts is greater than the concentration of Tm in only these and the Chukchi oils of the ten types identified on the North Slope. These oil and source-rock correlations are as well supported by the available data as any of the current oil-oil and oil-source rock correlations on the North Slope (Banet, 1994).

By considering the rerotation of the Arctic Basin, the spatial relationship between the Chukchi oil and the Shublik Formation assumes a new perspective.

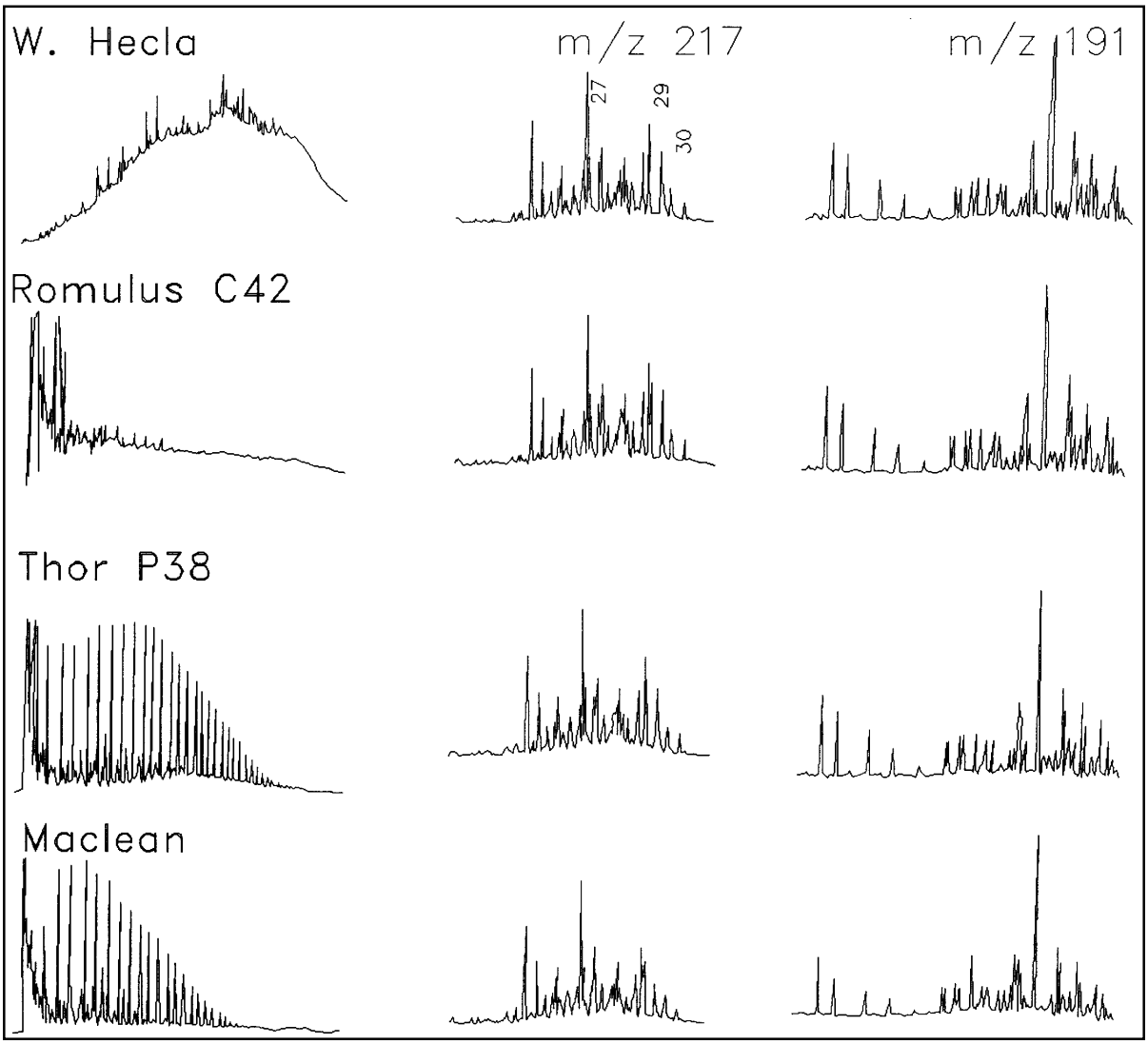

Figure 9. *Comparison of gas chromatographs (first column) and biomarker spectra (m/z 217 and m/z 191) from Sverdrup Basin. m/z = mass/charge.*

Table 3. *Geochemical data from selected Sverdrup Basin oils*

Well	Interval	API	pr/ph	%S	V	oil	Aliph	aro	Ts/TM	tri/pent	C_{27} C_{28} C_{29}
Cisco B66	6,879-6,906	- -	1.6	- -	- -	30.4	31.7	29.5	47.3	1.28	41:22:37
Cisco B66	6,903-6,916	- -	1.35	.43	- -	31.0	31.0	29.8	8.00	1.15	34:23:43
Drake Pt. L67	4,599-4,737	18-24	- -	.01	- -	29.1	30.1	28.9	2.42	0.89	37:22:40
Roche Pt. 0434	5,980-9,035	- -	1.44	.14	.01	29.2	30.4	28.6	4.50	3.35	37:24:39
Romulus C42	3,386-3,425	28	- -	- -	.1	30.0	30.6	29.2	2.45	1.52	41:20:39
Romulus C42	9,324-9,400	>45	1.7	.53	- -	29.2	29.5	28.4	1.76	1.44	39:22:39
W. Hecla P62	3,096-3,530	18-22	- -	.70	5.8	29.2	30.4	29.0	2.83	0.71	34:21:45
Best Horn F72A	10,039-10,686	- -	1.04	.45	.01	30.2	30.6	29.7	- -	3.23	36:13:51
Bent Horn N72	10,500-10,538	47	1.15	.06	.02	30.1	30.6	29.5	- -	- -	- -
Maclean I72	5,804-5817	- -	2.28	.04	- -	30.3	30.7	30.2	1.00	0.26	31:19:50
Maclean I72	5,879-5,892	- -	1.40	.10	- -	30.7	31.2	30.6	4.19	0.62	37:21:42
Thor P38	12,697-12,762	40	1.41	.13	.06	0.0	30.6	28.4	2.17	0.43	36:21:43

- - = No data.

Lithological and subsequent geochemical relationships may be more closely related between the Chukchi Sea and Sverdrup Basin areas than between the Chukchi Sea and Prudhoe Bay areas. This intriguing relationship suggests that the Shublik Formation is a potential source rock with vast regional extents like none other in the Arctic. Consequently the demonstrated Ellesmerian(!) petroleum system in operation around the Prudhoe Bay area may only be a small part of its true potential.

Despite the good geochemical fit between the Chukchi and Sverdrup oils, the enigma of the Shublik Formation as a source rock still remains. On a regional scale, the Shublik Formation retains its lithological character. But despite its persistent carbonate facies, this organic-rich unit generates two distinctly different oils.

SUMMARY

Oil discovered in the exploration of the Chukchi Sea has been generated from kerogens from the carbonate and clastic facies of the Shublik Formation. None of the other possible source rocks in the Chukchi Sea have enough kerogens to have generated oil. Although the Shublik Formation is the major source of the Prudhoe Bay oils, the Chukchi oil is dramatically different. It does not have the high metal contents, high sulfur contents, or pertinent biomarkers found in carbonate source rocks of the Prudhoe oils—thus the geochemical enigma.

Regional considerations indicate the important paleontologic, stratigraphic and lithologic correlations between the pre-Lower Cretaceous section of the Chukchi area and the Sverdrup Basin of the Canadian Arctic Islands. Both areas have an upper Triassic, phosphatic carbonate and shale unit—organic-rich units which are oil source rocks. A comparison between the Chukchi oil and Sverdrup Basin oils supports these correlations. Whatever ultimate mechanism for creating the Arctic basin may be deciphered, the juxtaposition of the Chukchi area to the Sverdrup Basin also suggests the vastness of the Shublik Formation as the most important and productive regional source rock for oil.

REFERENCES CITED

Banet, A.C., Jr., 1994, A comparison of crude oil chemistry on America's North Slope Chukchi Sea-Mackenzie Delta: U.S. Bureau of Land Management Alaska Technical Report 17, 66 p., 4 sheets.

Brooks, P.W., Embry, A.F., Goodarzi, F., and Stewart, R., 1992, Geochemical studies of the Sverdrup Basin (Arctic Islands), Part 1: Organic geochemistry and biological marker geochemistry of the Schei Point Group (Triassic) and recovered oils: Bulletin of Canadian Petroleum Geology, v. 40, p. 173-187.

Carman, G.J., and Hardwick, Peter, 1983, Geology and regional setting of the Kuparuk River Oil Field: American Association of Petroleum Geologists Bulletin, v. 67, no. 6, p. 1014-1031.

Craig, J.D., Sherwood, K.W., and Johnson, P.P., 1985, Geologic report for the Beaufort Sea Planning Area: Regional geology, petroleum geology and environmental geology: U.S. Minerals Management Service Outer Continental Shelf Report MMS 85-0111, 192 p.

Curiale, J.A., 1992, Molecular maturity parameters within a single oil family; a case study from the Sverdrup Basin, Arctic Canada, *in* Moldowan, J.M., Albrecht, P., and Philp, R.P., eds., Biological markers in sediments and petroleum; a tribute to Wolfgang K. Seifert: Englewood Cliffs, NJ, Prentice Hall, p. 275-300.

Embry, A.F., Mickey, M.B., Haga, Hideyo, and Wall, J.H., 1994, Correlation of the Pennsylvanian-Lower Cretaceous succession between northwest Alaska and southwest Sverdrup Basin: Implications for Hanna Trough Stratigraphy, *in* Thurston, D.K., and Fujita, Kazuya, eds., 1992 Proceedings International Conference on Arctic Margins: U.S. Minerals Management Service study, MMS 94-0040, p. 105-110.

Hubbard, R.J., Edrich, S.D., and Rattey, R.P., 1987, Geologic evolution and hydrocarbon habitat of the 'Arctic Alaskan Microplate' *in* Tailleur, I.L., and Weimer, Paul, eds., Alaskan North Slope geology: Bakersfield, CA, Pacific Section, Society of Economic Paleontologists and Mineralogists, Book 50, v. 2, p. 797-830.

Lerand, Monti, 1973, Beaufort Sea, *in* McCrossan, R.G., ed., The future petroleum provinces of Canada—Their geology and potential: Canadian Society of Petroleum Geologists Memoir 1, p. 315-386.

Magoon, L.B., 1988, Identified petroleum systems in the United States—1990, *in* Magoon, L.B. ed., The petroleum system—Status of Research and Methods, 1990, U.S. Geological Survey Bulletin 1912, 88 p.

Magoon, L.B., and Claypool, G.E., 1985, Alaska North Slope oil/rock correlation study: American Association of Petroleum Geologists Studies in Geology, no. 20, 682 p.

——1981, Two types of oil on North Slope, implications for exploration: American Association of Petroleum Geologists Bulletin, v. 65, p. 644-652.

Moore, T.E., Wallace, W.K., Bird, K.J., Karl, S.M., Mull, C.G., and Dillon, J.T., 1992, Stratigraphy, structure, and geologic synthesis of northern Alaska: U.S. Geological Survey Open-File Report 92-330, 189 p., 1 sheet, scale 1:500,000.

Mowatt, T.C., and Banet, A.C., Jr., 1994, Petrography and petrology of the Tapkaurak and Oruktalik Sands, Aurora Well, Beaufort Sea, northeast Alaska: U.S. Bureau of Land Management Alaska Open File Report 51, 40 p., 3 sheets.

Mowatt, T.C., Mull, C.G., Banet, A.C., Wilson, M.D., and Reeder, J.W., 1995, Petrography of Neocomian sandstones in western Brooks Range, and Tunalik, Klondike and Burger wells, northwestern Arctic Slope-Chukchi Sea (abs.): San Francisco, CA, American Association of Petroleum Geologists Bulletin, v. 79, p. 594.

Parrish, J.T, 1987, Lithology, geochemistry, and depositional environment of the Triassic Shublik Formation, northern Alaska, *in* Tailleur, I.R., and Weimer, P., eds., Alaskan

North Slope geology: Bakersfield, CA, Pacific Section, Society of Economic Paleontologists and Mineralogists, Book 50, v. 1, p. 391-397.

Powell, T.G., 1978, An assessment of the hydrocarbon source rock potential of the Canadian Arctic Islands: Geological Survey of Canada Paper 83-31, 82 p.

Seifert, W.K., Moldowan, J.M., and Jones, R.W., 1980, Application of biological marker chemistry to petroleum exploration: John Wiley & Sons, Chichester, International, Proceedings—Tenth World Petroleum Congress, Bucharest, Rumania (1979), no. 10, v. 2, p. 425-440.

Sherwood, K.W., Craig, J.D., and Lothamer, R.T., 1995, Oil and gas exploration, U.S. Chukchi Shelf (abs.): San Francisco CA, Abstracts with Program, American Association of Petroleum Geologists, Pacific Section, May 3-5, 1995, p. 52.

Stuart-Smith, J.H., and Wennekers, J.N.H., 1977, Geology and hydrocarbon discoveries of Canadian Arctic Islands: American Association of Petroleum Geologists Bulletin, v. 61, p. 1-27.

Tailleur, I.R., 1973, Probable rift origin of Canada Basin, Arctic Ocean, *in* Pitcher, M.G., ed., Arctic Geology: American Association of Petroleum Geologists Memoir 19, p. 526-535.

Thurston, D.K., and Theiss, L.A., 1987, Geologic Report for the Chukchi Sea Planning Area: Minerals Management Service Outer Continental Shelf Report 87-0046, p. 193.

This page has intentionally been left blank.

EMSIAN (LATE EARLY DEVONIAN) FOSSILS INDICATE A SIBERIAN ORIGIN FOR THE FAREWELL TERRANE

by
Robert B. Blodgett[1]

INTRODUCTION

Recent years have witnessed the rise of the hypothesis that nearly all of Alaska, as well as much of the western Cordillera of North America, is composed of numerous discrete, accreted tectonostratigraphic terranes (Coney and others, 1980; Jones and others, 1981, 1982, 1986, 1987; Nokleberg and others, 1994). The only exception to this in Alaska is represented by the small triangular area of the Nation Arch in east-central Alaska (fig. 1). This area is composed primarily of Precambrian and Paleozoic rocks that represent a continuation of similar rocks exposed farther to the east in the Ogilvie Mountains of the Yukon Territory. The autochthoneity of these east-central Alaskan Paleozoic rocks is supported by both lithic continuity and paleontological evidence. Faunal evidence for this is especially notable in Early Devonian age strata, as these contain faunas typical of North American miogeoclinal and cratonic strata in northwestern and Arctic Canada.

In this paper, however, attention is focused on newly acquired faunal data of important biogeographic significance from late Early Devonian (Emsian) age strata of two terranes, the Nixon Fork and Mystic, situated in west-central and southwestern Alaska. These terranes, along with Dillinger terrane, were recognized by Decker and others (1994) to be genetically related and were reduced in rank to subterranes of a larger terrane, termed the Farewell terrane (fig. 1). Other terranes in interior Alaska such as the Minchumina, East Fork, and Livengood are also probably genetically related to the Farewell terrane, and together represent a locally highly deformed continental margin sequence composed primarily of Neoproterozoic to Paleozoic strata. Previous interpretation of the gross lithostratigraphy and faunal affinities of the most well-studied subterrane, the Nixon Fork, has previously been suggested to indicate either fragmentation from or lithic continuity with northwestern Canada (Blodgett, 1983; Churkin and others, 1984; Blodgett and Clough, 1985; Rohr and Blodgett, 1985; Abbott, 1995). Newly acquired biogeographic data from Emsian (late Early Devonian) strata of the Farewell terrane, along with reconsideration of the affinities of faunas and floras of other time intervals (Middle Cambrian, Late Ordovician, and Permian), now have convinced the author that this continental margin sequence originated from the Siberian continent, rather than northwestern North America.

DEVONIAN BIOGEOGRAPHY

The study of Devonian marine biogeography has been the subject of considerable attention in the literature for nearly 30 years now. Most of these studies have relied on three primary groups: brachiopods (Boucot, 1974, 1975; Boucot and others, 1969; Johnson, 1970, 1971; Johnson and Boucot, 1973; Savage and others, 1979; Wang Yu and others, 1984); rugose corals (Oliver, 1973, 1976, 1977; Oliver and Pedder, 1979, 1984; Pedder and Oliver, 1990); and trilobites (Ormiston, 1972, 1975; Kobayashi and Hamada, 1975; Eldredge and Ormiston, 1979). Other faunal groups have also been studied to a lesser degree [that is, gastropods (Blodgett, 1992; Blodgett and others, 1988, 1990; Forney and others, 1981); and ostracodes (Copeland and Berdan, 1977; Berdan, 1990)], but are in virtually full agreement with established biogeographic patterns shown by the more common and better studied faunal groups mentioned above.

The highest level of provincialism in Devonian marine faunas occurred during the later two stages (Pragian and Emsian) of the Early Devonian (Boucot, 1975, 1988; Blodgett and others, 1988). Both before and after, the levels of provincialism vary from moderate to low, with the Middle Devonian evincing steadily declining levels of endemism from the Eifelian into the succeeding Givetian. The Late Devonian, including both the Frasnian and Famennian, is considered to be characterized by a remarkably high level of cosmopolitanism at the generic level, although undoubtedly detailed future study will still show distinct biogeographic provinces on the basis of the distribution of both species and some genera.

Rich, abundant, diverse megafaunas are known from both early Middle (Eifelian) and early Late (Frasnian) Devonian faunas of the Farewell terrane. The Eifelian faunas were thought to show their strongest similarities

[1]Department of Zoology, Oregon State University, Corvallis, Oregon 97331.

with those of northwestern Canada (Blodgett, 1983, 1992; Blodgett and others, 1990), although strong affinities are also noted to Siberia and the Urals (Baxter and Blodgett, 1994). Frasnian faunas of the Farewell terrane show close biogeographic ties to western North America, Novaya Zemlya, Taimyr, and Kolyma (Blodgett and Gilbert, 1992a; W.K. Braun *in* Blodgett, 1983, p. 128). Differentiation between Siberia and northwestern Canadian faunas during the Middle and Late Devonian is difficult, because both areas share many of the same genera, due to the moderate to low level of endemism during this time interval. To better differentiate faunas biogeographically between these areas, it is best to use evidence from the middle and late Early Devonian (Pragian and Emsian), when global endemism was relatively high. Unfortunately, until recently virtually no biogeographically useful collections of these ages were available to the author from this terrane. At this time, however, biogeographically distinctive Emsian collections have been examined from two localities, which now indicate strong Siberian and Uralian—rather than western or Arctic Canadian—affinities and origin for this terrane.

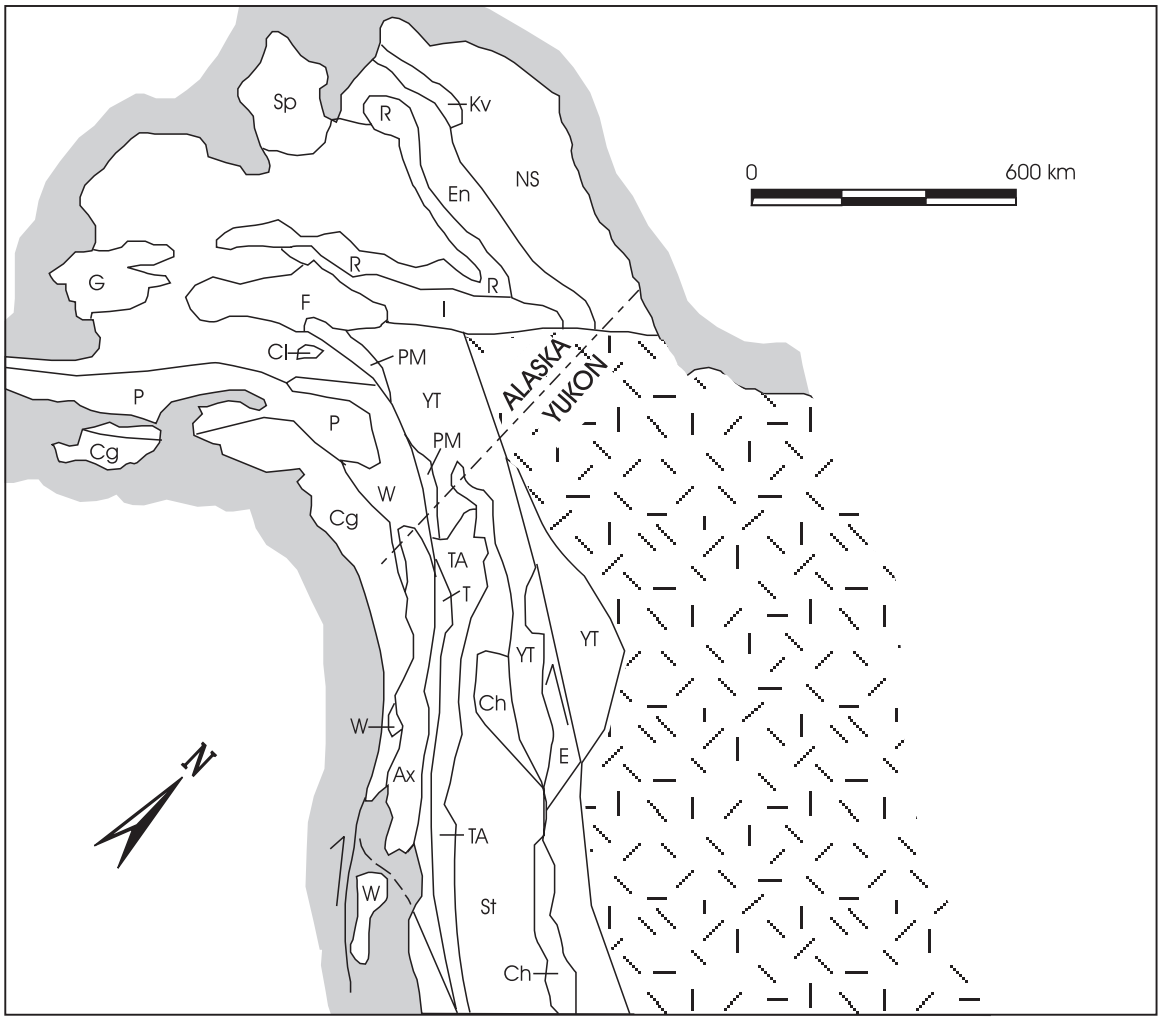

Figure 1. *Generalized map showing location of major tectonostratigraphic terranes in Alaska and northwestern Canada (modified from Coney and others, 1980). Dashed pattern, North American autochthonous basement. Barbed arrows indicate direction of major strike-slip movements. F - Farewell terrane; I - Innoko; R - Ruby; G - Goodnews; P - Peninsular; Cg - Chugach; Cl - Chulitna; W - Wrangellia; PM - Pingston & McKinley; Sp - Seward Peninsula; En - Endicott; Kv - Kagvik; NS - North Slope; YT - Yukon-Tanana; TA - Tracy Arm; Ax - Alexander; T - Taku; St - Stikine; Ch - Cache Creek; E - Eastern Assemblage.*

BIOGEOGRAPHICALLY DISTINCTIVE FAREWELL TERRANE EMSIAN FAUNAS

The first locality is from the Nixon Fork subterrane. It consists of a number of collections from three measured sections of a distinctive marker unit of limestone and minor shale of early Emsian age in the Medfra B-3 Quadrangle (fig. 2, loc. 1). This unit, which is about 150 m thick, is well exposed in a north-trending ridge, long known informally as "Reef Ridge" by mineral-company geologists. It is repeated twice by thrust faulting along this ridge, which is located in section 23, T. 24 S., R. 23 E. of that quadrangle. The entire succession is thought to represent shallow, subtidal to open shelf depositional environments (Chalmers and others, 1995). Carbonate rocks include packstone, wackestone, and mudstone; locally, favositid coral heads are common in the limy intervals, reaching up to 1 m in diameter. Some channels of probable tidal origin bearing reworked bioclasts and lithoclasts are present. Three prominent, richly fossiliferous shale intervals occur interbedded with the dominantly carbonate section; the shale intervals are thicker in the upper part of the section, as is characteristic of deepening-upward shelf sequences. This unit, bounded above and below by dolostone, forms a distinctive regionally mappable subunit within the Whirlwind Creek Formation of Dutro and Patton (1982), and should ultimately be given a separate stratigraphic name. Megafossils are especially abundant in the more shaly intervals, and include brachiopods, rugose and tabulate corals, leperditiid ostracodes, echinoderm ossicles, bivalves, gastropods, and trilobites. The brachiopod, rugose coral, and conodont faunal elements of this unit were briefly discussed by Blodgett and others (1995). Conodonts (identified by N.M. Savage) from throughout the unit indicate an early Emsian age (Polygnathus dehiscens Zone). Brachiopods and rugose corals (identified by R.B. Blodgett and A.E.H. Pedder, respectively) from this interval also indicate an early Emsian age.

Brachiopods are represented by over 30 species, of which the common element are rhynchonellids (notably uncinulids). Genera present include *Plicogypa, Stenorhynchia, Taimyrrhynx, "Uncinulus", Nordotoechia?, Spinatrypa, Nucleospira, Protathyris, Howellella,* and *Aldanispirifer*. Diagnostic species from this unit include *Plicogypa* cf. *kayseri* (Peetz), *Taimyrrhynx taimyrica* (Nikiforova), "*Uncinulus*" *polaris* Nikiforova, and *Howellella yacutica* Alekseeva. These species are known from various parts of Siberia (Kolyma, Taimyr, and Kuznetsk Basin) and Arctic Russia (Novaya Zemlya), and are unknown from equivalent age strata of east-central Alaska (Nation Arch area), or northwestern and Arctic Canada. Another strong Siberian linkage of the brachiopod fauna is shown by the presence of the brachiopod genus *Aldanispirifer*, described originally from northeastern Siberia, and also unknown from either northwestern or Arctic Canada. In fact, the now extensive collection of "Reef Ridge" brachiopods assembled by the author shows not even one species in common with equally extensive—but even more richly diverse—Emsian brachiopod fauna gathered by the author from the Ogilvie Formation of east-central Alaska and adjacent Yukon Territory. The latter formation forms a western terminus of the extensive carbonate platform that then constituted part of the miogeoclinal assemblage of the North American continent during late Early Devonian time.

Rugose corals identified by Pedder from the "Reef Ridge" unit consist mostly of solitary forms and dominated by relatively undiagnostic *Pseudoamplexus altaicus*, *Lithophyllum* spp., and rare *Zonophyllum* from 21.3 to 57.3 m. From 65.2 to 111.9 m corals include *Rhizophyllum schischkaticum*, *Lythophyllum* spp., *Pseudoamplexus altaicus*, new species of *Zelophyllum*, *Acathophyllum*, and a new species. Pedder noted that although undescribed, these higher faunas are related to early Emsian Kolymian loop coral faunas of Siberia. Both the brachiopod and rugose coral element of this fauna is distinctly Siberian in character. Thus, it is now proposed that during Emsian time the Nixon Fork subterrane of the Farewell terrane was biogeographically part of the Uralian Region, which included faunas of both Siberia and the Urals.

The second locality is situated in the Mystic Subterrane, and consists of a small (but biogeographically highly significant) collection made by Bruce L. Reed (his locality 75AR67) in 1975 from Emsian age limestones. The locality was described as a "locally derived slump block" (Reed and Nelson, 1980, table 1, locality 17) in the Shellabarger Pass area, Talkeetna C-6 Quadrangle. The author has had an opportunity to examine this collection and has noted abundant two-holed crinoid ossicles, atrypid brachiopods, and the brachiopods *Ivdelinia*, *Eospirifer*, and *Janius*. The gypidulid genus *Ivdelinia* is a typical Old World Realm taxon, and is common in the Rhenish-Bohemian and Uralian Regions but almost wholly unknown in the Cordilleran Region of the Old World Realm which, in the Emsian, included the areas of Arctic and western Canada and Nevada. Only two species of *Ivdelinia* have been described from Emsian-Eifelian strata of the Cordilleran Region: these are *Ivdelinia grinnellensis* Brice, 1982 and *Ivdelinia* (*Ivdelinella*) *ellesmerensis* Brice, 1982, both of which occur in the Canadian Arctic Islands. The Shellabarger Pass *Ivdelinia* is quite distinct from both of the above species and is

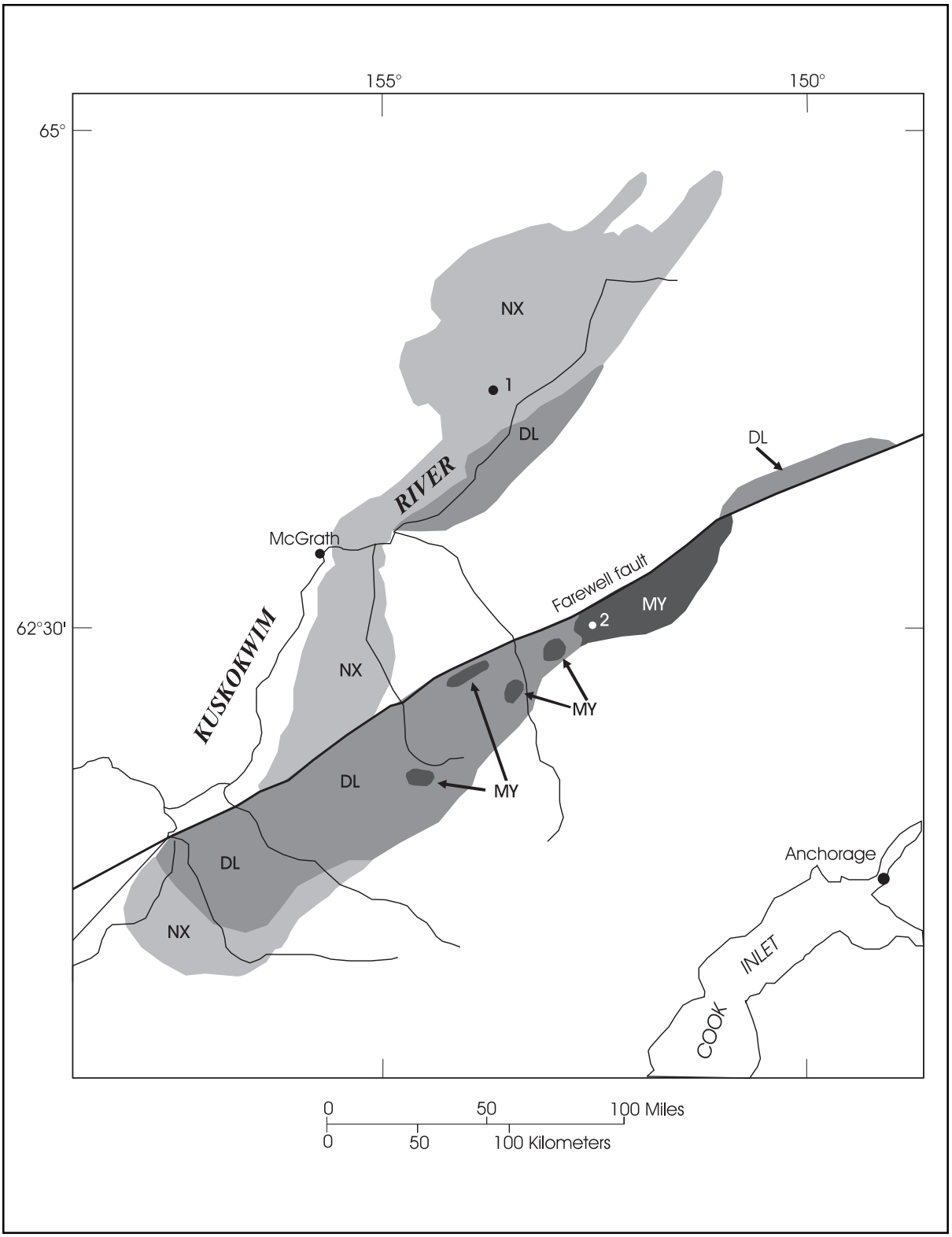

Figure 2. *Generalized geologic map of southwestern and west-central Alaska showing location of the two cited Emsian age fossil localities and component subterranes (Dillinger, Nixon Fork, and Mystic) of the Farewell terrane. Map modified from Blodgett and Gilbert (1992). Dillinger subterrane here includes East Fork terrane of Dutro and Patton (1982). Map symbols: 1, "Reef Ridge" area, Medfra B-3 Quadrangle; 2, Shellabarger Pass, Talkeetna C-6 Quadrangle; NX - Nixon Fork subterrane; DL - Dillinger subterrane; MY - Mystic subterrane.*

more closely related to species described from the Ural Mountains. Likewise, both *Eospirifer* and *Janius*, as well as the subfamily that includes them, the Eospiriferinae, are nearly totally unknown anywhere in Early Devonian or Eifelian strata of the Cordilleran Region of the Old World Realm. The only exception is the report of the genus *Janius* or *"Janius"* as an uncommon element in Emsian faunas of the Royal Creek area, Yukon Territory (Perry and Lenz, 1978; Savage and others, 1979, p. 196). In contradistinction, however, eospiriferinid brachiopods are reported as common elements in Emsian strata of Siberia (Kolyma, Kuznetsk Basin) and at numerous localities throughout the Uralian seaway. As with the Nixon Fork subterrane, the Emsian brachiopod fauna of the Mystic subterrane also appears to biogeographically belong to the Uralian, not the Cordilleran, Region of the Old World Realm.

BIOGEOGRAPHICALLY DISTINCTIVE FAREWELL TERRANE FAUNAS AND FLORAS OF OTHER AGES

In addition to the late Early Devonian examples discussed above, Farewell terrane fossil faunas and floras from other time intervals within the Paleozoic also indicate Siberian affinities and suggest a similar origin for this terrane. Two stratigraphically distinct, rich, diverse Middle Cambrian trilobite faunas were discovered in 1984 in Nixon Fork terrane strata of the Sleetmute A-2 Quadrangle. These were initially discussed by Palmer and others (1985), who considered both faunas to be representative of an outer-shelf environment and biogeographically of Siberian aspect, with faunal elements previously unrecognized in North America. Alternatively, it was later suggested by Babcock and Blodgett (1992) and Babcock and others (1993) that these southwestern Alaskan trilobite faunas of Siberian aspect may have dispersed in cool waters below the thermocline because they also show strong similarity to autochthonous outer-shelf faunas of North Greenland.

In Upper Ordovician (Ashgillian) strata of the Lone Mountain area (McGrath C-4 Quadrangle, west-central Alaska), a rich, diverse, silicified fauna of brachiopods and gastropods occurs, the most abundant element of which is the pentamerid brachiopod *Tcherskidium* (Rohr and Blodgett, 1985; Potter and others, 1988; Potter and Blodgett, 1992; Blodgett and others, 1992). This genus has not yet been unequivocally identified in North America, but is characteristic of Ashgillian faunas from Siberia (Kolyma, Taimyr, and Chukotka). The Lone Mountain form, occurring within strata previously assigned to the Nixon Fork subterrane, probably represents a new species of this genus, which is also present in the Shublik Mountains of the northeastern Brooks Range. Gastropods from the Lone Mountain section are most similar to species from the York Mountains of the Seward Peninsula (Blodgett and others, 1992), the latter area being considered to represent an eastward continuation of Chukotka.

Late Silurian (Ludlovian) algal reef complexes are widely recognized along the seaward outer margin of the Nixon Fork subterrane (Blodgett and others, 1984; Blodgett and Clough, 1985; Blodgett and Gilbert, 1992b; Clough and Blodgett, 1985, 1989) as well as in single isolated buildup present in Mystic subterrane (Rigby and others, 1994). The most abundant and characteristic faunal element of these peculiar algal buildups are aphrosalpingid sphinctozoans (Blodgett and others, 1984; Clough and Blodgett, 1985, 1989). These sponges previously had been recognized only in Upper Silurian strata of the Ural Mountains of Russia, but the occurrence of this group has recently been documented and illustrated by Rigby and others (1994) from southwestern and west-central Alaska (Nixon Fork and Mystic subterranes) and southeastern Alaska (Alexander terrane). Brachiopods co-occurring with aphrosalpingid sponges in algal buildups of both the Nixon Fork subterrane and Alexander terrane are also characterized by strong Uralian affinities (Blodgett and others, 1984).

Mamay and Reed (1984) briefly described and illustrated Permian plants from the conglomerate of Mt. Dall in the Talkeetna C-5 Quadrangle, central Alaska Range. They considered this flora to be derived from the Mystic terrane of Jones and others (1981). Although the flora shares some elements found in the southwestern part of the United States, its most distinctive element is the genus *Zamiopteris*, which is characteristic of Angaraland (Siberia) and is not known elsewhere in North America. On this basis, it was suggested by them that the Mystic terrane possibly was exotic and accreted to Alaska between post-Early Cretaceous and early Tertiary time.

CONCLUSIONS

Newly acquired biogeographic data on highly provincial late Early Devonian (Emsian) faunas from the Farewell terrane—which includes the previously defined Nixon Fork, Dillinger, and Mystic terranes—suggest that they probably had their origin as a rift block of the Siberian (or Angaraland) paleocontinent; alternatively, there was a separate tectonic entity in close enough proximity to the Siberian continent for reproductive communication to occur throughout most of the Paleozoic. Areas of close faunal ties include Kolyma, New Siberian Islands, Taimyr, Novaya Zemlya, the Uralian seaway, and the Kuznetsk Basin (fig. 3). Although the marine faunas of Siberia and nonaccreted

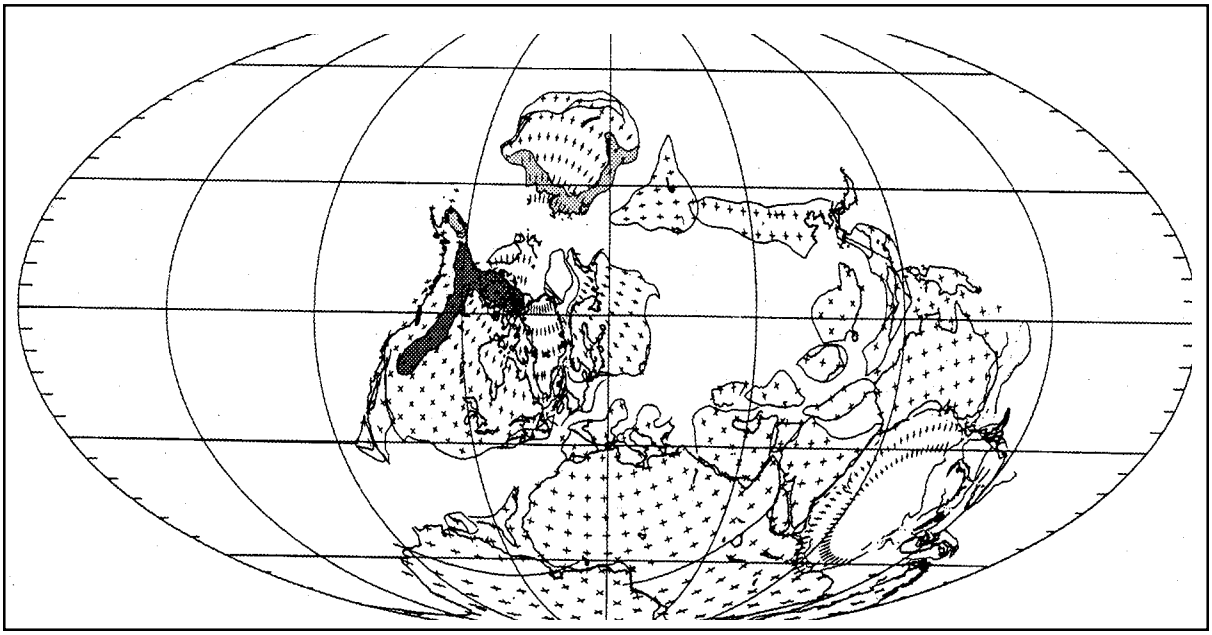

Figure 3. *Late Early Devonian (Emsian) global reconstruction showing areas of faunal linkage of Siberia (Kolyma, Taimyr, Kuznetsk Basin, Novaya Zemlya, and Uralian Seaway) and the Farewell terrane of Alaska (modified from Scotese and McKerrow, 1990). The dark-screened and light-screened areas indicate the distribution of Cordilleran Region and Uralian Region faunas, respectively. Although not included by these patterns, the Arctic Alaska terrane (shown in the figure as the block of northern Alaska and adjoining Chukotka, which has been rotated clockwise against the Canadian Arctic Islands) and the Alexander terrane of southeastern Alaska share many faunal affinities with the Farewell terrane during the Late Ordovician-Middle Devonian time interval, and likewise may represent Siberian rift blocks that have been subsequently accreted to North America.*

parts of northwestern North America are somewhat similar during the more cosmopolitan conditions that followed the Emsian in both the Middle and Late Devonian, the levels of provinciality are so high during the Emsian that most species—and many genera and even some families and subfamilies—of brachiopods are not shared at this time.

The strongly Siberian and Uralian cast to the Emsian brachiopod and coral faunas of the Farewell terrane suggest that this tectonostratigraphic entity was at that time either part of the Siberian continent or was close enough for close reproductive communication to occur. The frequent repetition of similar close faunal and floral ties both before and after agree with this interpretation and suggests possible close proximity between rocks of the Farewell terrane and the Siberian continent up until at least Permian time.

Extremely close faunal linkages also exist in the Emsian and Middle Devonian between the Farewell terrane and other tectonostratigraphic terranes of Alaska, most notably the Livengood, Arctic Alaska (including the Endicott, North Slope, and other terranes of earlier usage), and Alexander terranes (Blodgett, 1992; Blodgett and others, 1990; Baxter and Blodgett, 1994; Popov and others, 1994). These terranes, as with the Farewell terrane, also are probably of Siberian origin. Thus, the only truly North American part of Alaska during the late Early Devonian is represented by the Nation Arch area of east-central Alaska, where strata of the Ogilvie Formation contain typical species and genera characteristic of the similar-age North American miogeoclinal strata in the Yukon and Northwest Territories. Also, none of the Alaskan terranes bearing a major component consisting of Lower or Middle Paleozoic strata evince an “austral” or southwestern Pacific origin.

ACKNOWLEDGMENTS

The author thanks the Committee for Research and Exploration of the National Geographic Society for providing funds for both a detailed faunal and lithologic study of the “Reef Ridge” section in the Medfra B-3 Quadrangle and continuing fieldwork in the Shellabarger Pass area, Talkeetna C-6 Quadrangle. I also thank Arthur J. Boucot and David M. Rohr for their thoughtful reviews of this manuscipt.

REFERENCES CITED

Abbott, Grant, 1995, Does Middle Cambrian rifting explain the origin of the Nixon Fork terrane?: Geological Society of America Abstracts with Programs, v. 27, no. 5, p. 1.

Babcock, L.E., and Blodgett, R.B., 1992, Biogeographic and paleogeographic significance of Middle Cambrian trilobites of Siberian aspect from southwestern Alaska: Geological Society of America Abstracts with Programs, v. 24, no. 5, p. 4.

Babcock, L.E., Blodgett, R.B., and St. John, James, 1993, Proterozoic and Cambrian stratigraphy and paleontology of the Nixon Fork terrane, southwestern Alaska: Proceedings of the First Circum-Pacific and Circum-Atlantic Terrane Conference, Guanajuato, Mexico, 9-14 November, 1993, p. 5-7.

Baxter, M.E., and Blodgett, R.B., 1994, A new species of *Droharhynchia* (Brachiopoda) from the Lower Middle Devonian (Eifelian) of west-central Alaska: Journal of Paleontology, v. 68, p. 1235-1240.

Berdan, J.M., 1990, The Silurian and Early Devonian biogeography of ostracodes in North America, *in* McKerrow, W.S., and Scotese, C.R., eds., Palaeozoic palaeogeography and biogeography: Geological Society (London) Memoir 12, p. 223-231.

Blodgett, R.B., 1983, Paleobiogeographic affinities of Devonian fossils from the Nixon Fork terrane, southwestern Alaska, *in* Stevens, C.H., ed., Pre-Jurassic rocks in western North America suspect terranes: Pacific Section, Society of Economic Paleontologists and Mineralogists, Los Angeles, p. 125-130.

———1992, Taxonomy and paleobiogeographic affinities of an early Middle Devonian (Eifelian) gastropod faunule from the Livengood quadrangle, east-central Alaska: Palaeontographica Abteilung A, v. 221, p. 125-168.

Blodgett, R.B., and Clough, J.G., 1985, The Nixon Fork terrane - Part of an *in-situ* peninsular extension of the Paleozoic North American continent: Geological Society of America Abstracts with Programs, v. 17, no. 6, p. 342.

Blodgett, R.B., Clough, J.G., and Smith, T.N., 1984, Ordovician-Devonian paleogeography of the Holitna Basin, southwestern Alaska: Geological Society of America Abstracts with Programs, v. 16, no. 5, p. 271.

Blodgett, R.B., and Gilbert, W.G., 1992a, Upper Devonian shallow-marine siliciclastic strata and associated fauna and flora, Lime Hills D-4 quadrangle, southwest Alaska, *in* Bradley, D.C., and Dusel-Bacon, C., eds., Geologic Studies in Alaska by the U.S. Geological Survey, 1991: U.S. Geological Survey Bulletin 2041, p. 106-113.

———1992b, Paleogeographic relations of Lower and Middle Paleozoic strata of southwest and west-central Alaska: Geological Society of America Abstracts with Programs, v. 24, no. 5, p. 8.

Blodgett, R.B., Rohr, D.M., and Boucot, A.J., 1988, Lower Devonian gastropod biogeography, *in* McMillan, N.J., Embry, A.F., and Glass, D.J., eds., Devonian of the World, Volume III: Paleontology, Paleoecology and Biostratigraphy, Canadian Society of Petroleum Geologists Memoir 13, p. 281-294.

Blodgett, R.B., Rohr, D.M., and Boucot, A.J., 1990, Early and Middle Devonian gastropod biogeography, *in* McKerrow, W.S., and Scotese, C.R., eds., Palaeozoic Palaeogeography and Biogeography, Geological Society (London) Memoir 12, p. 277-284.

Blodgett, R.B., Rohr, D.M., and Clough, J.G., 1992, Late Ordovician brachiopod biogeography of Arctic Alaska and Chukotka: International Conference on Arctic Margins, Anchorage, Alaska, September 2-4, 1992, Abstract Volume, p. 11.

Blodgett, R.B., Savage, N.M., Pedder, A.E.H., and Rohr, D.M., 1995, Biostratigraphy of an upper Lower Devonian (Emsian) limestone unit at "Reef Ridge," Medfra B-3 quadrangle, west-central Alaska: Geological Society of America Abstracts with Programs, v. 27, no. 5, p. 6-7.

Boucot, A.J., 1974, Silurian and Devonian biogeography, *in* Ross, C.A., ed., Paleogeographic Provinces and Provinciality: Society of Economic Paleontologists and Mineralogists, Special Publication 21, p. 165-176.

———1975, Evolution and Extinction Rate Controls: Amsterdam, Elsevier, 427 p.

———1988, Devonian biogeography: An update, *in* McMillan, N.J., Embry, A.F., and Glass, D.J., eds., Devonian of the World, Volume III: Paleontology, Paleoecology and Biostratigraphy: Canadian Society of Petroleum Geologists Memoir 13, p. 211-227.

Boucot, A.J., Johnson, J.G., and Talent, J.A., 1969, Early Devonian brachiopod zoogeography: Geological Society of America Special Paper 119, 113 p.

Brice, D., 1982, Brachiopodes du Dévonien Inférieur et Moyen des Formations de Blue Fiord et Bird Fiord des Îles Arctiques Canadiennes: Geological Survey of Canada Bulletin 326, 175 p.

Chalmers, R.W., Measures, E.A., Rohr, D.M., and Blodgett, R.B., 1995, Depositional environments of an upper Lower Devonian (Emsian) limestone unit at "Reef Ridge," Medfra B-3 quadrangle, west-central Alaska: Geological Society of America Abstracts with Programs, v. 27, no. 5, p. 9.

Churkin, M., Jr., Wallace, W.K., Bundtzen, T.K., and Gilbert, W.G., 1984, Nixon Fork-Dillinger terranes: A dismembered Paleozoic craton margin in Alaska displaced from Yukon Territory: Geological Society of America Abstracts with Programs, v. 16, no. 5, p. 275.

Clough, J.G., and Blodgett, R.B., 1985, Comparative study of the sedimentology and paleoecology of Middle Paleozoic algal and coral-stromatoporoid reefs in Alaska: Proceedings of the Fifth International Coral Reef Congress, Tahiti, 1985, v. 3, p. 184-190.

———1989, Silurian-Devonian algal reef mound complex of southwest Alaska, *in* Geldsetzer, H., and James, N.P., eds., Reefs, Canadian and adjacent area: Canadian Society of Petroleum Geologists Memoir 13, p. 246-250.

Coney, P.J., Jones, D.L., and Monger, J.W.H., 1980, Cordilleran suspect terranes: Nature, v. 288, p. 329-333.

Copeland, M.J., and Berdan, J.M., 1977, Silurian and Early Devonian beyrichian ostracode provincialism in northeastern North America: Geological Survey of Canada Special Paper 77-1B, p. 15-24.

Decker, J., Bergman, S.C., Blodgett, R.B., Box, S.E., Bundtzen, T.K., Clough, J.G., Coonrad, W.L., Gilbert, W.G., Miller, M.L., Murphy, J.M., Robinson, M.S., and Wallace, W.K., 1994, Geology of southwestern Alaska, *in* Plafker, George, and Berg, H.C., eds., The Geology of Alaska: Boulder, Colorado, Geological Society of America, The Geology of North America, v. G-1, p. 285-310.

Dutro, J.T., Jr., and Patton, W.W., Jr., 1982, New Paleozoic formations in the northern Kuskokwim Mountains, west-central Alaska: U.S. Geological Survey Bulletin 1529-H, p. H13-H22.

Eldredge, N., and Ormiston, A.R., 1979, Biogeography of Silurian and Devonian trilobites of the Malvinokaffric Realm, *in* Gray, J., and Boucot, A.J., eds., Historical biogeography, plate tectonics, and the changing environment: Corvallis, Oregon State University Press, p. 147-167.

Forney, G.G., Boucot, A.J., and Rohr, D.M., 1981, Silurian and Lower Devonian zoogeography of selected molluscan genera, *in* Gray, J., Boucot, A.J., and Berry, W.B.N., eds., Communities of the Past: Stroudsberg, PA, Hutchinson Ross Publishing Company, p. 119-164.

Johnson, J.G., 1970, Taghanic onlap and the end of North American proviciality: Geological Society of America Bulletin, v. 2077-2105.

———1971, A quantitative approach to faunal province analysis: American Journal of Science, v. 270, p. 257-280.

Johnson, J.G., and Boucot, A.J., 1973, Devonian brachiopods, *in* Hallam, A., ed., Atlas of Palaeobiogeography: New York, Elsevier, p. 89-96.

Jones, D.L., Silberling, N.J., Berg, H.C., and Plafker, George, 1981, Map showing tectonostratigraphic terranes of Alaska, columnar sections, and summary descriptions of terranes: U.S. Geological Survey Open-File Report 81-792, 20 p., 2 sheets, scale 1:2,500,000.

Jones, D.L., Silberling, N.J., Coney, P.J., and Plafker, George, 1987, Lithotectonic terrane map of Alaska (west of the 141st Meridan): U.S. Geological Survey Map MF-1874-A, 1 sheet, scale 1:2,500,000.

Jones, D.L., Silberling, N.J., Gilbert, W.G., and Coney, P.J., 1982, Character, distribution, and tectonic significance of accretionary terranes in the central Alaska Range: Journal of Geophysical Research, v. 87, p. 3709-3717.

Jones, D.L., Silberling, N.J., and Coney, P.J., 1986, Collision tectonics in the Cordillera of western North America: examples from Alaska, *in* Coward, M.P., and Ries, A.C., eds., Collision Tectonics, Geological Society (London) Special Publication 19, p. 367-387.

Kobayashi, T., and Hamada, T., 1975, Devonian trilobite provinces: Proceedings of the Japan Academy, v. 51, p. 447-451.

Mamay, S.H., and Reed, B.L., 1984, Permian plant megafossils from the conglomerate of Mount Dall, central Alaska Range, *in* Coonrad, W.L., and Elliott, R.L., eds., The United States Geolgical Survey in Alaska: Accomplishments during 1981: U.S. Geological Survey Circular 868, p. 98-102.

Nokleberg, W.J., Moll-Stalcup, E.J., Miller, T.P., Brew, D.A., Grantz, Arthur, Reed, J.C., Jr., Plafker, George, Moore, T.E., Silva, S.R., Patton, W.W., Jr., with contributions on specific regions by Blodgett, R.B., Box, S.E., Bradley, D.C., Bundtzen, T.K., Dusel-Bacon, Cynthia, Gamble, B.M., Howell, D.G., Foster, H.L., Karl, S.M., Miller, M.L., and Nelson, S.W., 1994, Tectonostratigraphic terrane and overlap assemblage map of Alaska: U.S. Geological Survey Open-File Report 94-194, 53 p., scale 1:2,500,000, 1 sheet.

Oliver, W.A., Jr., 1973, Devonian coral endemism in eastern North America and its bearing on paleogeography, *in* Hughes, N.F., ed., Organisms and continents through time: Palaeontological Association, Special Papers in Palaeontology 12, p. 318-319.

———1976, Biogeography of Devonian rugose corals: Journal of Paleontology, v. 50, p. 365-373.

Oliver, W.A., Jr., 1977, Biogeography of Late Silurian and Devonian rugose corals: Palaeogeography, Palaeoclimatology, Palaeoecology, v. 22, p. 85-135.

Oliver, W.A., Jr., and Pedder, A.E.H., 1979, Rugose corals in Devonian stratigraphy correlation, *in* House, M.R., Scrutton, C.T., and Bassett, M.G., eds., The Devonian System: Palaeontological Association, Special Papers in Palaeontology 23, p. 233-248.

———1984, Devonian rugose coral biostratigraphy with special reference to the Lower-Middle Devonian boundary: Geological Survey of Canada Paper 84-1A, p. 449-452.

Ormiston, A.R., 1972, Lower and Middle Devonian trilobite zoogeography in northern North America: 24th International Geological Congress, Section 7, p. 594-604.

———1975, Siegenian trilobite zoogeography in Arctic North America, *in* Martinsson, A., ed., Evolution and morphology of the Trilobita, Trilobitoidea, and Merostomata: Fossils and Strata, no. 4, p. 391-398.

Palmer, A.R., Egbert, R.M., Sullivan, R., and Knoth, J.S., 1985, Cambrian trilobites with Siberian affinities, southwestern Alaska: American Association of Petroleum Geologists Bulletin, v. 69, no. 2, p. 295.

Pedder, A.E.H., and Oliver, W.A., Jr., 1990, Rugose coral distribution as a test of Devonian palaeogeographic models, *in* McKerrow, W.S., and Scotese, C.R., eds., Palaeozoic Palaeogeography and Biogeography, Geological Society (London) Memoir 12, p. 267-275.

Perry, D.G., and Lenz, A.C., 1978, Emsian paleogeography and shelly fauna biostratigraphy of Arctic Canada, in Stelck, C.R., and Chatterton, B.D.E., eds., Western and Arctic Canadian Biostratigraphy: Geological Association of Canada Special Paper, 18, p. 133-160.

Popov, L.Y., Blodgett, R.B., and Anderson, A.V., 1994, First occurrence of the genus *Bicarinatina* (Brachiopoda, Inarticulata) from the Middle Devonian in North America (Alaska): Journal of Paleontology, v. 68, p. 1214-1218.

Potter, A.W., and Blodgett, R.B., 1992, Paleobiogeographic significance of Ordovician brachiopods from the Nixon Fork terrane, west-central Alaska: Geological Society of America Abstracts with Programs, v. 24, no. 5, p. 76.

Potter, A.W., Blodgett, R.B., and Rohr, D.M., 1988, Paleobiogeographic relations and paleogeographic significance of Late Ordovician brachiopods of Alaska: Geological Society of America Abstracts with Programs, v. 20, no. 7, p. 339.

Reed, B.L., and Nelson, S.W., 1980, Geologic map of the Talkeetna quadrangle, Alaska: U.S. Geological Survey Miscellaneous Investigations Series Map I-1174, 15 p., 1 sheet, scale 1:250,000.

Rigby, J.K., Nitecki, M.H., Soja, C.M., and Blodgett, R.B., 1994, Silurian aphrosalpingid sphinctozoans from Alaska and Russia: Acta Palaeontologica Polonica, v. 39, p. 341-391.

Rohr, D.M., and Blodgett, R.B., 1985, Upper Ordovician Gastropoda from west-central Alaska: Journal of Paleontology, v. 59, p. 667-673.

Savage, N.M., Perry, D.M., and Boucot, A.J., 1979, A quantitative analysis of Lower Devonian brachiopod distribution, *in* Gray, J., and Boucot, A.J., eds., Historical biogeography, plate tectonics, and the changing environment: Corvallis, Oregon State University Press, p. 169-200.

Scotese, C.R., and McKerrow, W.S., 1990, Revised world maps and introduction, *in* McKerrow, W.S., and Scotese, C.R., eds., Palaeozoic Palaeogeography and Biogeography, Geological Society (London) Memoir 12, p. 1-21.

Wang Yu, Boucot, A.J., Rong Jia-Yu, and Yang Xue-Chang, 1984, Silurian and Devonian brachiopod biogeography of China: Geological Society of America Bulletin, v. 95, p. 265-279.

This page has intentionally been left blank.

GROWTH-POSITION PETRIFIED TREES OVERLYING THICK NANUSHUK GROUP COAL, LILI CREEK, LOOKOUT RIDGE QUADRANGLE, NORTH SLOPE, ALASKA

by
Paul L. Decker,[1] Gregory C. Wilson,[1] Arthur B. Watts,[1] and David Work[2]

ABSTRACT

Geologic reconnaissance conducted during 1996 in the National Petroleum Reserve in Alaska (NPRA) located an outcrop with remarkably well-preserved, growth-position petrified trees in a late Albian to Cenomanian fluvial sandstone-coal sequence from the Corwin Formation of the Nanushuk Group. The six upright trunks and trunk impressions found at the Lili Creek locality range from 10 to 70 cm in diameter, and are up to 4.5 m high. A very well preserved horizontal log at least 1.6 m long is also partially exposed. The petrified trees are encased in the overlying 6.5 m thick fluvial sandstone. Although no root balls are exposed, some of the trees appear rooted in the upper part of the underlying coal seam or transitional carbonaceous mudstone facies. The exposed thickness of the coal seam, including possible interbeds of carbonaceous shale, is at least 9 m, but the base is covered. No taxonomic classification has yet been made of the flora at this locality. The specific fluvial environment and processes responsible for the unit are open to interpretation, but preservation of trees of this height suggests high rates of sand deposition.

INTRODUCTION

While performing reconnaissance fieldwork across the west-central fold belt of the Alaska North Slope during July 1996, the authors encountered an exposure of Nanushuk Group sandstone containing six growth-position fossil trees overlying a thick coal seam. This short note summarizes observations gathered from examination of an approximately 0.4 hectare area during a single brief visit to the outcrop and from subsequent study of photographs taken there.

The outcrop is located near the headwaters of Lili Creek, a north-flowing tributary of the Meade River, in sec. 28, T. 1 S., R. 26 W., in the Lookout Ridge B-4 Quadrangle (lat 69° 19.310' N., long 158° 11.258' W.) (fig. 1). Exposures of the Nanushuk Group in this area are generally poor, but incision of the east-west-trending escarpment by north-draining tributaries of the Meade River affords fair outcrops. The upland to the south of Lili Creek is gently rolling and tundra covered. South of this upland, modest outcrops of Nanushuk Group rocks are again encountered along Lookout Ridge and the drainages that dissect it.

REGIONAL GEOLOGIC SETTING

The Albian-Cenomanian Nanushuk Group is mapped in a wide outcrop belt across the western North Slope of Alaska (Mayfield and others, 1988), including the Lili Creek area (fig. 2). No detailed geologic map has been published for the Lookout Ridge B-4 Quadrangle. Thorough reviews of the sedimentology, depositional history, and structural setting of the Nanushuk Group are provided by Ahlbrandt and others (1979), Bird and Andrews (1979), Huffman and others (1985, 1988), Molenaar (1985), and Mull (1979, 1985). Floral assemblages and age of the Nanushuk Group are discussed by Scott and Smiley (1979), May and Shane (1985), and Spicer and Herman (1995).

The main structural element underlying the Lookout Ridge and adjacent quadrangles is the Colville Basin, a foreland basin filled by dominantly east-northeast-directed progradation of Cretaceous syntectonic clastic sediments derived from the Brooks Range and the now-subsided Herald Arch (Bird and Andrews, 1979; Molenaar, 1985; Huffman and others, 1988). Superimposed on the basin are broad folds and thrust faults that developed as the Brooks Range compression moved into the foreland basin (fig. 2). The fold belt present in the southern part of the Lookout Ridge Quadrangle dies out into the coastal plain of the northern part of the quadrangle.

The lithic sandstones of the Nanushuk Group, the shale-dominated Torok Formation, and the turbidite-dominated Fortress Mountain Formation constitute a major Brookian clastic wedge of Aptian to Cenomanian age (Mull, 1979, 1985) that prograded into the Colville Basin with the advance of two major deltaic systems

[1]ARCO Alaska, Inc., P.O. Box 100360, Anchorage, Alaska 99510.
[2]Anadarko Petroleum Corporation, P.O. Box 100360, Anchorage, Alaska 99510.

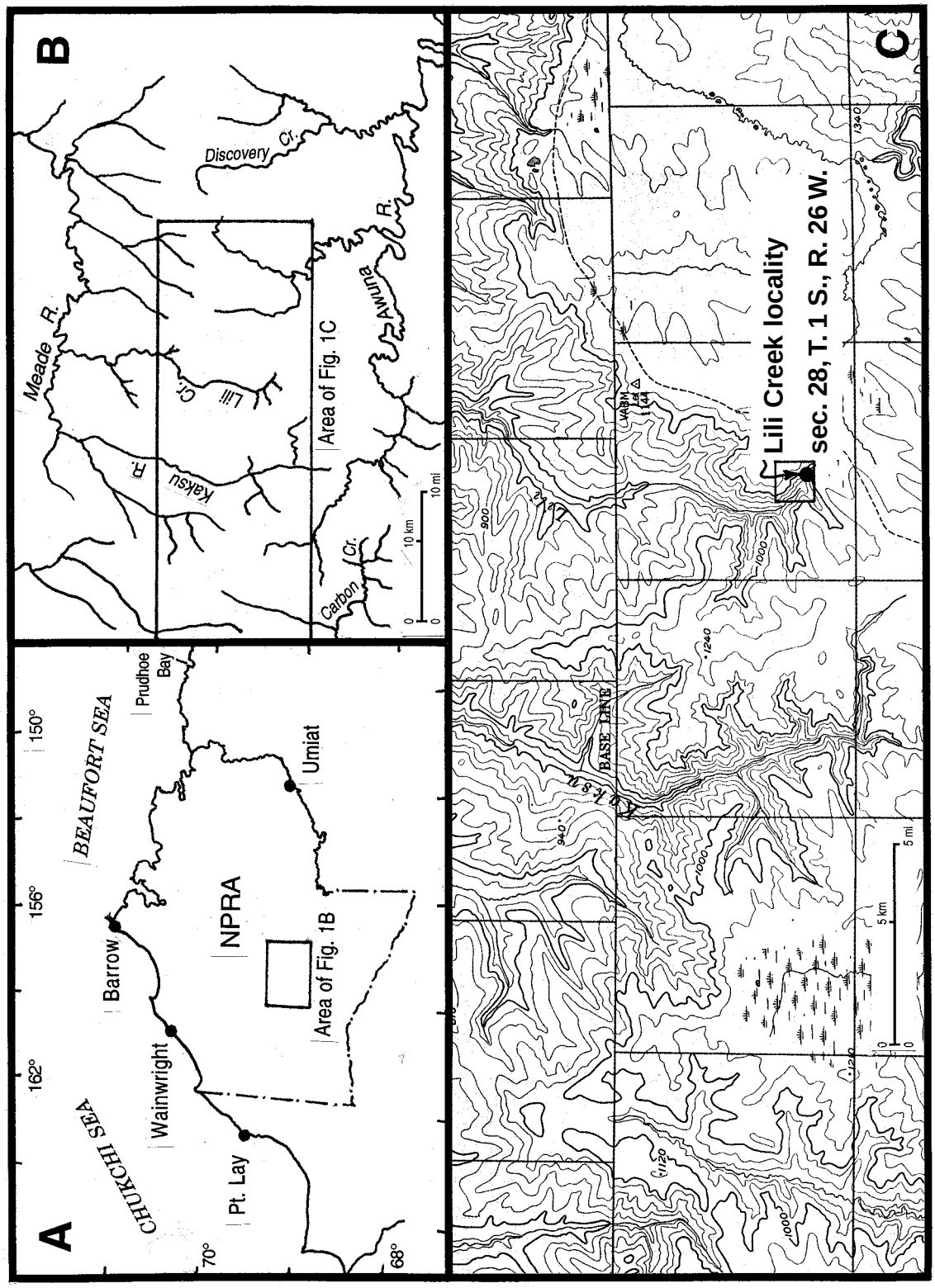

Figure 1. *Location map of the Lili Creek area. Topographic map from 1:250,000 Lookout Ridge Quadrangle.*

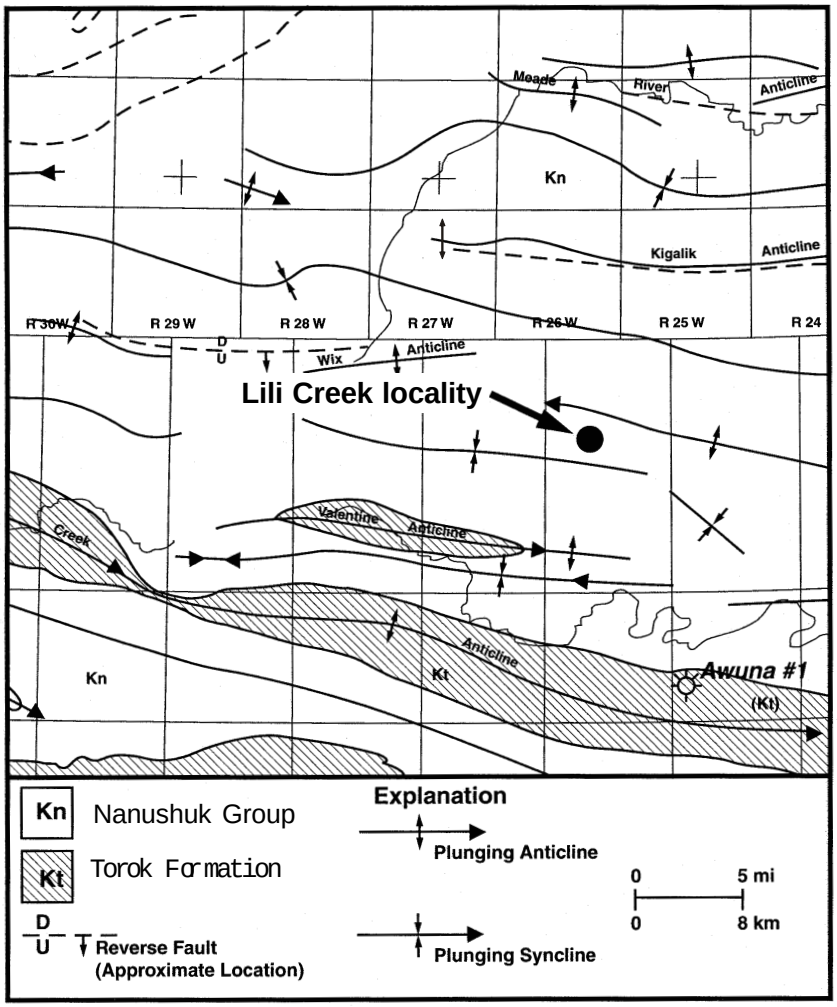

Figure 2. *Generalized geologic map of Northern Foothills area in the vicinity of Lili Creek fossil tree locality, after Mayfield and others (1988).*

from distinctly different provenance areas. The largest of these systems was the Corwin Delta (Ahlbrandt and others, 1979, Huffman and others, 1985), sourced farthest to the west. The Corwin Delta prograded to the east-northeast over the predominantly shaly prodelta facies of the Torok Formation to deposit the shallow marine sands of the Kukpowruk Formation, which grade upward through transitional facies into the nonmarine sands and coals of the Corwin Formation (fig. 3) (Ahlbrandt and others, 1979). Farther east, the smaller Umiat Delta prograded mainly northward from a somewhat more quartzose provenance area (Bartsch-Winkler, 1979; Fox, 1979), depositing the Grandstand, Chandler, and Ninuluk Formations (fig. 3) (Ahlbrandt and others, 1979; Huffman and others, 1985, 1988; Molenaar, 1985). In this location, the Lili Creek succession is considered Corwin Formation on the basis of its nonmarine facies assemblage, stratigraphic position high in the Nanushuk Group, and its setting within the Corwin Delta system, consistent with the interpretations of Nanushuk paleogeography discussed by Ahlbrandt and others (1979), Huffman and others (1985, 1988), Molenaar (1985), and other authors.

Coals are plentiful within the Corwin Formation. Chapman and Sable (1960) reported analyses of numerous Corwin Formation coals up to 4 m in exposed thickness from outcrops along Corwin Bluffs, Cape Beaufort, and the Utukok, Kokolik, and Kukpowruk Rivers. The thickest of these, located on the Kukpowruk River, has been measured in tunnel workings and by shallow drilling to vary from 5.5 to 7.2 m in true stratigraphic thickness (Warfield and Boley, 1966, 1969; Callahan and others, 1969). A high-quality Corwin Formation coal with an average thickness of about 5.5 m is the focus of an experimental mining operation conducted by Arctic Slope Regional Corporation at Deadfall Syncline, 25 km southeast of Point Lay (T. Imm, oral commun., 1996). Coals up to 9 m thick were penetrated in the upper parts of the U.S. Navy Meade and Kaolak test wells (Collins, 1958), located 86 km north-northeast and 107 km northwest of the Lili Creek locality, respectively. Collins (1958) considered

those coals to be part of the Killik Tongue of the Chandler Formation, rather than the largely equivalent Corwin Formation (fig. 3). However, recognizing the paleogeographic relationship of the these wells to the Corwin Delta (Ahlbrandt and others, 1979; Huffman and others, 1985, 1988; Molenaar, 1985), the present authors include their nonmarine Nanushuk Group section in the Corwin Formation.

DESCRIPTION OF LILI CREEK LOCALITY

From a distance, the most striking characteristic of the Lili Creek outcrop is the presence of an uncommonly thick coal seam which, although its lower parts are largely scree covered, forms a very steep to overhanging slope and appears to be well over 9 m thick in composite thickness (fig. 4). Because no measured section or thorough observation of the seam was made, it is unclear if carbonaceous shale or mudstones constitute some of this thickness. Certainly, much of the seam, particularly the upper several meters, consists of thick- to massive-bedded, very clean, vitrain-rich coal with widely spaced cleats (vertical fractures). Float blocks of massive vitreous coal more than 1 m on a side litter the base of the slope, indicating that noncoal partings are absent from beds at least that thick. The presence of thick beds of clean coal implies a stable backswamp environment, with little clastic input from floodwaters (Flores, 1981). Vitrinite reflectance measurements of 0.74 percent from cleated vitreous coal in the uppermost meter and 0.72 percent in the carbonaceous mudstone interval immediately above the seam indicate that the coal is likely of high volatile bituminous rank (see equivalency scales of Hood and others, 1975, and Sentfle and Landis, 1991), although no rank determinations were made with coal-analysis standards of the American Society for Testing and Materials. Clearly, future work will be required to determine the true thickness, lateral continuity, rank, and industrial characteristics of this seam.

Where observed, the contact between the top of the blocky coal and the overlying clean, fluvial sandstones

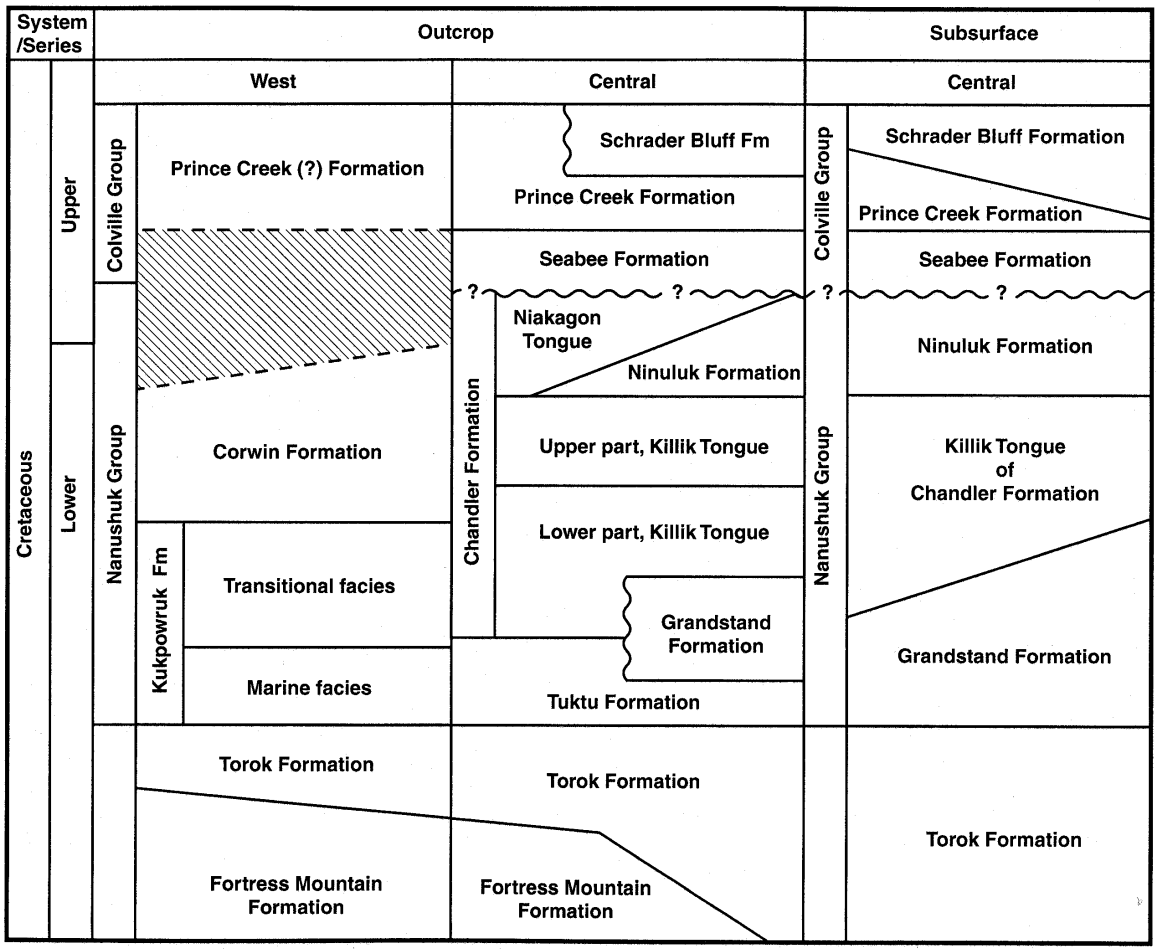

Figure 3. *Stratigraphic nomenclature for the Nanushuk Group and other Brookian Sequence units in NPRA and adjacent areas, North Slope, Alaska (from Huffman, 1985 after Ahlbrandt and others, 1979).*

is gradational over a recessive-weathering interval about 30 cm to 1 m thick. This interval consists of generally upward coarsening and thickening intercalations of soft flaky coal, dark olive-gray to black carbonaceous mudstone and siltstone, and lenticular-bedded, fine- to medium-grained sandstone. The irregular thickness is attributed to scouring of somewhat subtle channels occupied by the overlying sandstone. This assemblage is interpreted to represent the introduction of crevasse splay sediments into a poorly drained backswamp. No marine fossils or traces were observed, which suggests a depositional setting in the upper reaches of the delta plain, as previously proposed for the Corwin Formation by Callahan and Sloan (1978).

The resistant-weathering fluvial sandstone sequence containing the standing petrified trees and tree molds is about 6.5 m thick. Neither samples nor detailed descriptions were collected in this unit, but it generally resembles fine- to medium-grained sandstones associated with coal seams described elsewhere in the Corwin Formation. The sandstone is sharp based, is thinly to thickly bedded, and contains both channel profiles and lateral accretion surfaces. Sandstone bedding is distinctly troughlike adjacent to several of the growth-position trees (fig. 4), suggestive of scour-and-fill due to turbulence in the current flowing around the standing trunks.

Of the six growth-position trees, three of the largest trunks occur within 12 m of each other. The trunks are preserved as either impressions on the sandstone face, three-dimensional forms weathering out of the exposure, or as combinations of these types (fig. 4). The largest upright tree is preserved partly as a deeply concave, semicylindrical impression and partly as a three-dimensional segment of the petrified trunk, which together measure 4.5 m in height by 70 cm in diameter (fig. 5). A dark rind of what appears to be petrified bark is locally preserved on this specimen and could possibly aid in making a taxonomic classification. Other large petrified tree trunks found have diameters of 55 cm and 32 cm (figs. 6, 7). The smallest upright trunk measured is 11 cm in diameter and 1.5 m tall. Because the recessive-weathering transitional facies between the sandstone and the coal is partially covered, no root balls are exposed. Hence, it is not clear if the trees root in the transitional facies, or in the coal itself.

On the west end of the outcrop is a partially exposed log in a horizontal position, remarkable for its preservation (fig. 8). It exhibits a thin, carbonaceous bark veneer and minute details of the external wood grain and knot structure. As in the standing trees, the wood grain appears relatively straight and smooth. This specimen measures 11 cm in diameter, and is about 1.6 m long.

The tops of the two tallest trees are truncated at about the same channelized horizon about 5.5 m above the top of the clean, blocky coal (fig. 4). The pre-servation of standing trees of this height indicates a fairly high sedimentation rate for the fluvial sands. As an arbitrary example, if the largest trees remained standing for a decade after the initial influx of fluvial material before being broken off at the sediment surface, the average sedimentation rate would have been about 0.6 m per year. The facies succession probably reflects fluvial avulsion (autocyclic shift) into and rapid infilling of a local topographic low occupied by a long-lived, subsiding backswamp. Hence, the inferred sedimentation rates likely do not apply across the Corwin Delta plain as a whole.

RECOMMENDATIONS FOR FUTURE WORK

The unusual occurrence of this Albian to Cenomanian population of large, growth-position petrified trees and the associated thick coal seam merits further investigation. The provisional observations and interpretations of this report should be followed up by more thorough work, including a detailed measured section, paleobotany, coal analyses, and reconnaissance of the surrounding area. Though good exposures are very sparse in the upland terrain to the south of Lili Creek, Corwin Formation strata equivalent to the nearly flat-lying exposures at Lili Creek may crop out in the deep ravines of the upper Kaksu River about 10 km to the west. In addition, the authors have observed a meter-scale petrified bulbous stump, probably the flared base of a tree trunk, in a sandstone-coal succession on the upper Meade River about 26 km north of the Lili Creek outcrop. Detailed fieldwork may provide valuable information on the nature and extent of this “petrified forest,” and may help define the distribution, thickness, and resource potential of the thick coal facies with which these trees are associated.

ACKNOWLEDGMENTS

We thank ARCO Alaska, Inc. and Anadarko Petroleum Corporation for permission to publish this finding. We also thank C.G. Mull for suggesting that we publish the finding, J. Clough for editorial guidance, Bo Tye for technical discussions, and G. Stricker and R. Gangloff for their helpful reviews.

Figure 4. *The main outcrop of Corwin Formation sandstone-coal at the Lili Creek locality. Geologist at left center is approximately 2 m tall. The observed composite thickness of the coal seam is approximately 9 m. Three growth-position petrified tree fossils occur in the portion of the overlying fluvial sandstone shown in this view, the largest one at left and two more at right center, which may appear from this perspective as a single trunk because one is exposed directly behind the other. View to north.*

Figure 5. *Closeup of the largest exposed petrified tree at the Lili Creek locality, with a lower, three-dimensional exposure of the petrified trunk and an upper section of the impression of the trunk. This trunk is shown in figure 4. Hammer is 33 cm long. View to north.*

Figure 6. *The second-largest-diameter petrified tree trunk at the Lili Creek locality. This specimen is located at the top of the slope about 150 m northwest of the face shown in figure 4. Hammer is 33 cm long. View roughly southeast.*

Figure 7. *This trunk at the Lili Creek locality is broken into two sections. The lower part of this specimen, visible at right center in figure 4, is leaning slightly and appears to have broken off and fallen nearly straight down from the upper part, which is embedded in the overhanging face of the sandstone outcrop. Hammer is 33 cm long. View to east-northeast.*

Figure 8. *Closeup of petrified log exposed at ground level on bench near top of outcrop about 50 m northwest of the face shown in figure 4. Note details of wood grain, knot structure, and remnants of carbonized bark. Field of view is about 50 cm, looking roughly east.*

REFERENCES CITED

Ahlbrandt, T.S., Huffman, A.C., Jr., Fox, J.E., and Pasternack, Ira, 1979, Depositional framework and reservoir-quality studies of selected Nanushuk Group outcrops, North slope, Alaska, *in* Ahlbrandt, T.S., ed., Preliminary geologic, petrologic, and paleontologic results of the study of Nanushuk Group rocks, North Slope, Alaska: U.S. Geological Survey Circular 794, p. 14-31.

Bartsch-Winkler, S., 1979, Textural and mineralogical study of some surface and subsurface sandstones from the Nanushuk Group, western North Slope, Alaska, *in* Ahlbrandt, T.S., ed., Preliminary geologic, petrologic, and paleontologic results of the study of Nanushuk Group rocks, North Slope, Alaska: U.S. Geological Survey Circular 794, p. 61-76.

Bird, K.J., and Andrews, Jack, 1979, Subsurface studies of the Nanushuk Group, North Slope, Alaska, *in* Ahlbrandt, T.S., ed., Preliminary geologic, petrologic, and paleontologic results of the study of Nanushuk Group rocks, North Slope, Alaska: U.S. Geological Survey Circular 794, p. 32-41.

Callahan, J.E., Wanek, A.A., Schell, E.M., Zeller, H.D., and Rohrer, W.L., 1969, Geology of T. 15., R. 44 W., unsurveyed, Umiat Principal Meridian, in the Kukpowruk coal field, Alaska: U.S. Geological Survey Open-File Report (unnumbered), 19 p.

Callahan, J.E., and Sloan, E.G., 1978, Preliminary report on analyses of Cretaceous coals from northwestern Alaska: U.S. Geological Survey Open-File Report 78-319.

Chapman, R.M., and Sable, E.G., 1960, Geology of the Utukok-Corwin region, northwestern Alaska: U.S. Geological Survey Professional Paper 303-C, 167 p.

Collins, F.R., 1958, Test wells, Meade and Kaolak areas, Alaska, *with* Micropaleontologic study of Meade Test Well 1 and Kaolak Test Well 1, northern Alaska, by Bergquist, H.R.: U.S. Geological Survey Professional Paper 305-F, p. 341-376.

Flores, R., 1981, Coal deposition in fluvial paleoenvironments of the Paleocene Tongue River Member of the Fort Union Formation, Powder River area, Powder River Basin, Wyoming and Montana, *in* Etheridge, F.G., and Flores, R., eds., Recent and ancient nonmarine depositional environments: Models for exploration: Society of Economic Paleontologists and Mineralogists Special Publication 31, p. 169-190.

Fox, J.E., 1979, A summary of reservoir characteristics of the Nanushuk Group, Umiat test well 11, National Petroleum Reserve in Alaska, *in* Ahlbrandt, T.S., ed., Preliminary geologic, petrologic, and paleontologic results of the study of Nanushuk Group rocks, North Slope, Alaska: U.S. Geological Survey Circular 794, p. 42-53.

Hood, A., Gutjahr, C.C.M., and Heacock, R.L., 1975, Organic metamorphism and the generation of petroleum: American Association of Petroleum Geologists Bulletin, v. 59, p. 986-996.

Huffman, A.C., Jr., 1985, Introduction to the geology of the Nanushuk Group and related rocks, North Slope, Alaska, *in* Huffman, A.C., Jr., ed., Geology of the Nanushuk Group and related rocks, North Slope, Alaska: U.S. Geological Survey Bulletin 1614, p. 1-6.

Huffman, A.C., Jr., Ahlbrandt, T.S., Pasternack, I., Stricker, G.D., and Fox, J.E., 1985, Depositional and sedimentologic factors affecting the reservoir potential of the Cretaceous Nanushuk Group, central North Slope, Alaska, *in* Huffman, A.C., Jr., ed., Geology of the Nanushuk Group and related rocks, North Slope, Alaska: U.S. Geological Survey Bulletin 1614, p. 61-74.

Huffman, A.C., Jr., Ahlbrandt, T.S., and Bartsch-Winkler, S., 1988, Sedimentology of the Nanushuk Group, North Slope, *in* Gryc, George, ed., Geology and exploration of the National Petroleum Reserve in Alaska, 1974 to 1982: U.S. Geological Survey Professional Paper 1399, p. 281-298.

May, F.E., and Shane, J.D., 1985, An analysis of the Umiat Delta using palynologic and other data, North Slope, Alaska: *in* Huffman, A.C., Jr., ed., Geology of the Nanushuk Group and related rocks, North Slope, Alaska: U.S. Geological Survey Bulletin 1614, p. 97-120.

Mayfield, C.F., Tailleur, I.L., and Kirschner, C.E., 1988, Bedrock geologic map of the National Petroleum Reserve in Alaska, *in* Gryc, George, ed., Geology and exploration of the National Petroleum Reserve in Alaska, 1974 to 1982: U.S. Geological Survey Professional Paper 1399, p. 187-190.

Molenaar, C.M., 1985, Subsurface correlations and depositional history of the Nanushuk Group and related strata, North Slope, Alaska, *in* Huffman, A.C, Jr., ed., Geology of the Nanushuk Group and related rocks, North Slope, Alaska: U.S. Geological Survey Bulletin 1614, p. 37-59.

Mull, C.G., 1979, Nanushuk Group deposition and the late Mesozoic structural evolution of the central and western Brooks Range and Arctic Slope, *in* Ahlbrandt, T.S., ed., Preliminary geologic , petrologic, and paleontologic results of the study of Nanushuk Group rocks, North Slope, Alaska: U.S. Geological Survey Circular 794, p. 5-13.

Mull, C.G., 1985, Cretaceous tectonics, depositional cycles, and the Nanushuk Group, Brooks Range and Arctic Slope, Alaska, *in* Huffman, A.C., Jr., ed., Geology of the Nanushuk Group and related rocks, North Slope, Alaska: U.S. Geological Survey Bulletin 1614, p. 7-36.

Sentfle, J.T., and Landis, C.R., 1991, Vitrinite reflectance as a tool to assess thermal maturity, *in* Merrill, R.K., ed., Source and migration processes and evaluation techniques: Treatise of Petroleum Geology, Handbook of Petroleum Geology, American Association of Petroleum Geologists, p. 119-126.

Scott, R.A., and Smiley, C.J., 1979, Some Cretaceous plant megafossils and microfossils from the Nanushuk Group, northern Alaska: A preliminary report, *in* Ahlbrandt, T.S., ed., Preliminary geologic, petrologic, and paleontologic results of the study of Nanushuk Group rocks, North Slope, Alaska: U.S. Geological Survey Circular 794, p. 89-127.

Spicer, R.A., and Herman, A.B., 1995, *Nilssoniocladus* in the Cretaceous Arctic: new species and biological insights: Review of Palaeobotany and Palynology, v. 92, p. 229-243.

Warfield, R.S., and Boley, C.C., 1966, Sampling and coking studies of coal from the Kukpowruk River area, Arctic Northwestern Alaska: U.S. Bureau of Mines Report of Investigations 6767, 59 p.

———1969, Sampling and coking studies of several coalbeds in the Kokolik River, Kukpowruk River, and Cape Beaufort areas of Arctic northwestern Alaska: U.S. Bureau of Mines Report of Investigations 7321, 58 p.

PALEOTOPOGRAPHIC CONTROL ON DEPOSITION OF THE LOWER KAYAK SHALE, NORTHERN FRANKLIN MOUNTAINS, BROOKS RANGE, ALASKA

by
David L. LePain[1]

INTRODUCTION

In the northeastern Brooks Range of Alaska, Lower Carboniferous through Lower Cretaceous strata, assigned to the Ellesmerian sequence, are separated from an underlying deformed succession of pre-Middle Devonian sedimentary and igneous rocks by a regional surface of unconformity (fig. 1). The Ellesmerian sequence is interpreted to record sedimentation on the passive continental margin of the Arctic Alaska Plate. Situated at the base of the Ellesmerian sequence is a transgressive succession of Early Carboniferous age that is assigned to the Endicott Group and consists, in ascending order, of the Kekiktuk Conglomerate and the Kayak Shale (fig. 2). In the northeastern Brooks Range, the Endicott Group has been interpreted as an early postrift succession that records sedimentation in an upland region landward of the tectonic hinge zone in response to regional thermal subsidence (LePain and others, 1994).

In latest Tournaisian time, relative sea level rise shifted stream equilibrium profiles landward and upward and initiated deposition of the fluvial and marginal-marine Kekiktuk Conglomerate. LePain and others (1994) related the stratigraphic organization of the Kekiktuk to paleotopographic relief on the unconformity surface at its base. As relative sea level continued rising, fluvial dispersal systems were gradually drowned and replaced upsection by marginal- and shallow-marine depositional systems recorded by the lower and middle members of the Kayak Shale.

The Kayak Shale consists mainly of black shale with subordinate amounts of sandstone and carbonate rocks. Relatively thick successions of sandstones and carbonates are stratigraphically restricted to the lower and upper thirds of the Kayak Shale, respectively. Carbonates are present in the upper beds of the Kayak Shale throughout its geographic distribution in outcrop in the Brooks Range and in the North Slope subsurface. However, appreciable thicknesses of sandstone (that is, thicker than 2 m), while stratigraphically restricted to the lower beds of the Kayak Shale, are also geographically restricted to locations where the underlying Kekiktuk Conglomerate is relatively thick. The purpose of this paper is to briefly describe the stratigraphic organization and depositional setting of the basal Kayak Shale, which is informally referred to herein as the lower Kayak, and relate its geographic and stratigraphic distribution to paleotopographic relief on the sub-Mississippian unconformity and relative sea level rise during the late Tournaisian and Visean.

GEOLOGIC SETTING

In northern Alaska, a regional sub-Carboniferous surface of angular unconformity has been recognized throughout the North Slope subsurface and at widely spaced locations across the Brooks Range. This surface truncates rocks as young as Early Devonian (Blodgett and others, 1991). Rocks below the unconformity are characterized by a complex tectonic history that includes episodes of contraction and extension; above the unconformity, the rocks have been assigned to the Ellesmerian sequence and are largely the product of extensional tectonics (Moore and others, 1992). The Ellesmerian sequence consists of northward-onlapping terrigenous clastic and carbonate strata, which are interpreted as a Lower Carboniferous through Lower Cretaceous south-facing (present-day coordinates) passive continental margin succession (fig. 1).

The Endicott Group comprises the base of the Ellesmerian sequence and, in the northeastern Brooks Range consists of fluvial, marginal-marine, and shallow-marine terrigenous clastic and carbonate rocks that are latest Tournaisian to Visean and are exposed along east-west-trending outcrop belts (figs. 2, 3) (Armstrong and Mamet, 1977; Utting, 1990, 1991a, 1991b).

In the northeastern Brooks Range, the Kekiktuk Conglomerate is thickest (up to 128 m) above incised paleovalleys and progressively thins toward and eventually pinches out against adjacent paleotopographic highs (LePain and others, 1994). LePain and others (1994) recognized six lithofacies associations in the Kekiktuk and related their stratigraphic and

[1]Alaska Division of Geological & Geophysical Surveys, 794 University Avenue, Suite 200, Fairbanks, Alaska 99709-3645.

geographic distribution to paleotopographic relief on the sub-Carboniferous unconformity (table 1; fig. 4). These relationships indicate that where the Kekiktuk Conglomerate is thickest, fluvial systems were confined within incised paleovalleys cut into pre-Middle Devonian rocks and, where only a thin veneer of Kekiktuk is present, it is the record of deposition along the flanks of paleotopographic highs on the sub-Carboniferous unconformity (LePain and others, 1994). Paleocurrent indicators within the Kekiktuk generally show southerly transport directions (LePain, unpublished field notes; Nilsen and others, 1980).

Slow postrift subsidence of continental crust landward of the hinge zone (for example, Braun and Beaumont, 1989), combined with a possible eustatic sea level rise throughout Early Carboniferous time (Hallam, 1984), resulted in regional transgression, flooding of fluvial dispersal systems, and establishment of a broad suite of marginal- and shallow-marine depositional environments recorded in the Kayak Shale. As transgression continued, estuarine conditions developed above valley-filling fluvial successions of the Kekiktuk Conglomerate and locally resulted in deposition of quartzose sandstone bodies encased in black mudstone

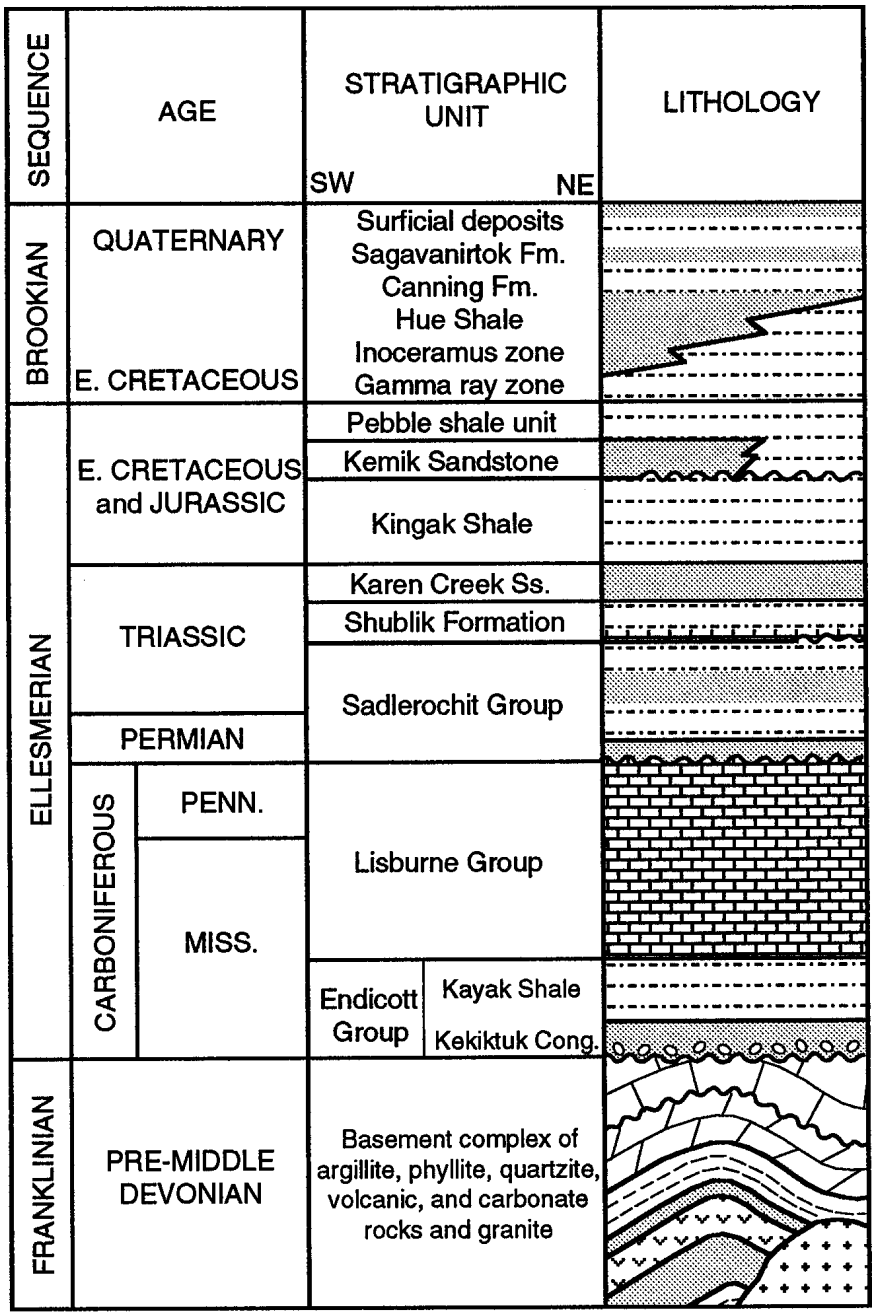

Figure 1. *Generalized stratigraphy of the Ellesmerian sequence in the northeastern Brooks Range, Alaska (modified from Bader and Bird, 1986). No scale intended.*

of the Kayak Shale. Local paleotopographic highs were onlapped and buried beneath a veneer of marginal-marine mud of the Kayak Shale.

The Kayak Shale onlaps and pinches out above a regional paleotopographic high in the Sadlerochit Mountains (fig. 3). The Sadlerochit high was transgressed and buried beneath shallow-water carbonate rocks of the Lisburne Group by late Visean time (zone 16i, earliest Chesterian; Armstrong, 1974). Around the exposed perimeter of the Okpilak batholith (fig. 3), thin discontinuous successions of the Kekiktuk Conglom-erate resting nonconformably above granite, sandy limestone of the Lisburne Group resting nonconformably above granite where the Kekiktuk is absent, and the absence of the Kayak Shale indicate that the batholith was also a paleotopographic high throughout much of the Visean. Armstrong (1974) and Armstrong and Bird (1974) extended the Sadlerochit high eastward, north of Leffingwell Ridge, to the Canadian border on the basis of foraminifera biostratigraphy of the Lisburne Group. Along Leffingwell Ridge the Kekiktuk Conglomerate is present in thin, discontinuous exposures and the Kayak Shale is laterally continuous, forming successions up to 285 m thick.

Paleogeographic reconstructions for Carboniferous strata in the northeastern Brooks Range show fluvial and marginal-marine sand of the Kekiktuk Conglomerate deposited to the north and carbonate sediments of the Lisburne Group deposited to the south (Armstrong, 1974; Armstrong and Bird, 1974). Between these areas, organic-rich terrigenous mud and argillaceous carbonate sediment of the Kayak Shale accumulated under restricted-marine conditions. Coeval carbonate rocks of the Lisburne Group deposited to the south probably formed an effective barrier to marine circulation during Kayak deposition. This paleogeographic configuration, combined with a steady influx of terrestrial organic material from the north, led to dysaerobic-to-anaerobic conditions and deposition of dark gray to black mudrock of the Kayak Shale.

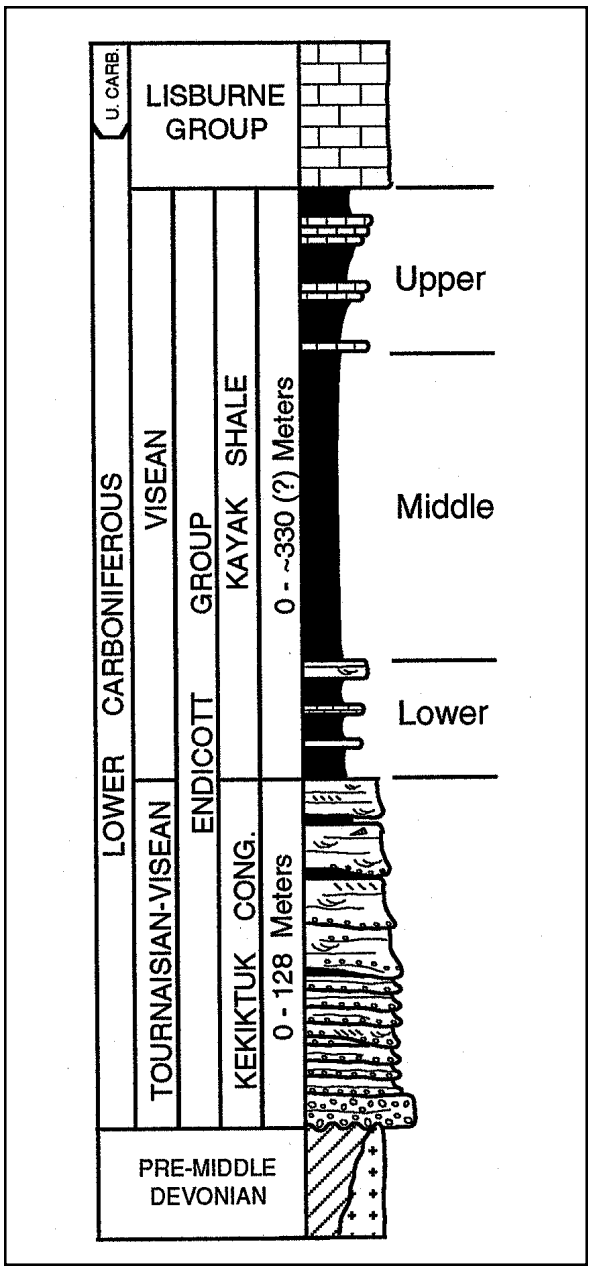

STRATIGRAPHIC ORGANIZATION OF THE KAYAK SHALE

I have divided the Kayak Shale in the northeastern Brooks Range into three informal members based on lithology and their relationship to the sub-Carboniferous unconformity, the Kekiktuk Conglomerate, and the overlying Lisburne Group (fig. 2). The lower member is geographically restricted to positions above thick, valley-filling fluvial to marginal-marine successions of the Kekiktuk Conglomerate. Consequently, it has been recognized only at a few locations in the northeastern Brooks Range. The contact between the lower member and the underlying Kekiktuk Conglomerate is typically poorly exposed, but appears to be gradational. The lower member consists predominantly of organic-rich mudstone, minor but prominent quartzose sandstone and quartzose bioclastic limestone, and rare anthracitic coal.

Figure 2. *Generalized column of the Carboniferous Endicott Group in the northeastern Brooks Range.*

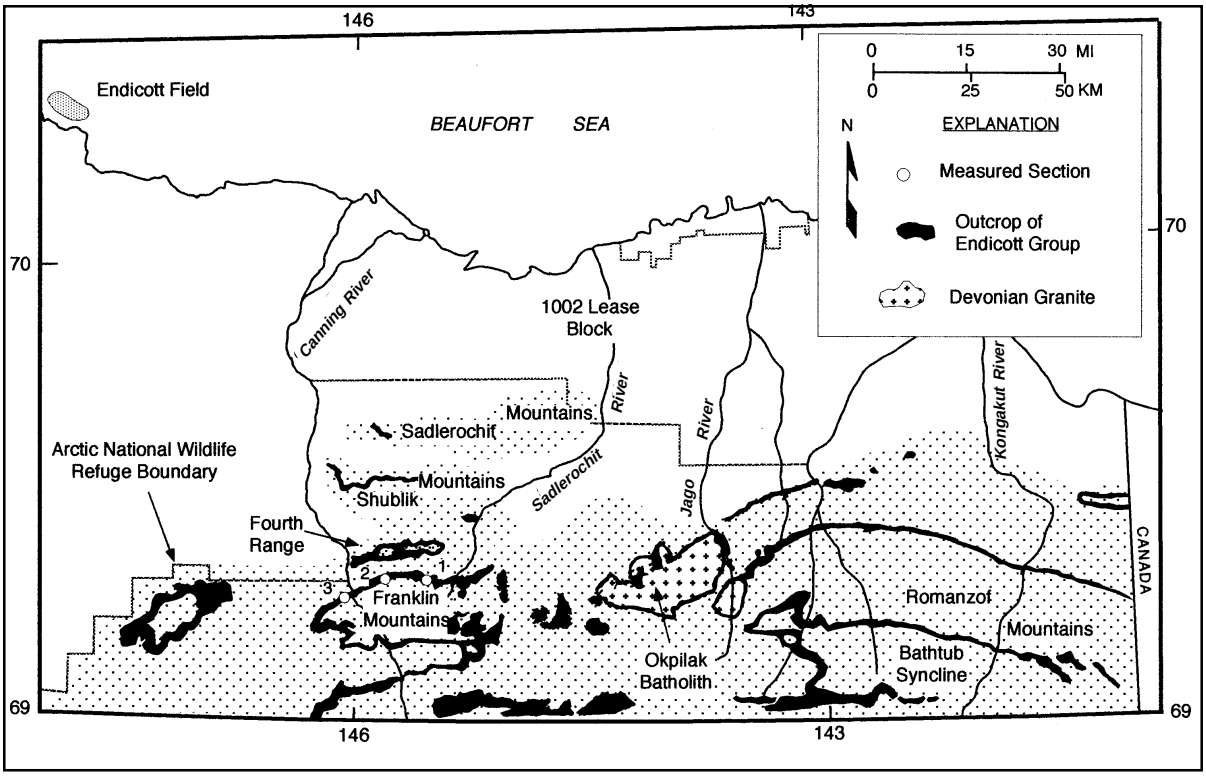

Figure 3. *Map showing distribution of Endicott outcrop belts in the northeastern Brooks Range, Alaska (modified from Bird, 1987). Circles show location of measured sections. Location 1 is Straight Creek; location 2 is Curve Creek; and location 3 is Plunge Creek.*

The middle member is present throughout the northeastern Brooks Range where a variety of contact relationships have been observed with underlying rocks. The contact between the lower and middle members is sharp. Where the lower member is absent, both sharp and gradational contacts have been observed between the middle member and the underlying Kekiktuk Conglomerate. Where the Kekiktuk Conglomerate is absent above paleotopographic highs, the middle member rests unconformably on pre-Middle Devonian rocks. The middle member consists predominantly of black to dark-gray shale. Minor coal and sharp-based sandstone beds and bedsets (<2 m thick) are locally present near the base of the middle member where it rests above pre-Middle Devonian rocks situated on paleotopographic highs.

The contact between the middle and upper Kayak Shale is gradational. The upper member consists of dark gray to black, organic-rich shale and a variety of carbonate lithologies and is commonly characterized by the arrangement of these lithologies in meter-scale thickening-upward parasequences. The upper member records the transition from terrigenous clastic-dominated environments of the Endicott Group to carbonate-dominated environments of the overlying Lisburne Group.

LITHOFACIES ASSOCIATIONS IN THE LOWER KAYAK SHALE

Seven lithofacies have been recognized in the lower Kayak Shale on the basis of lithology and sedimentary and biogenic structures. Brief descriptions and process interpretations for each lithofacies are presented below and summarized in table 2. These lithofacies are interpreted herein as the depositional record of a barred estuarine system. However, many of the physical attributes of the lithofacies presented herein are not unique to any specific environmental setting—estuarine or otherwise. The association of the lithofacies and their relationships to the underlying Kekiktuk Conglomerate and the pre-Mississippian unconformity suggests an estuarine depositional setting for the lower Kayak Shale.

ORGANIC-RICH MUDSTONE

The organic-rich mudstone lithofacies is up to 65 m thick, encases most of the other lithofacies in the lower Kayak, and has been recognized at both Straight and Curve Creeks (figs. 4, 5). The contact between this lithofacies and the underlying Kekiktuk Conglomerate is generally poorly exposed, but is likely gradational. This lithofacies consists of dark-gray to black, organic-rich siltstone, silty shale, and shale and weathers into

Table 1. *Summary of depositional unit characteristics in the Kekiktuk Conglomerate*

Unit	Texture	Structure	Geometry	Unit relations	Interpretation
A	Unsorted to poorly sorted, clast- and rare matrix-supported cobble and pebble conglomerate; minor poorly sorted, pebbly sandstone.	Thick- to very thick-bedded, unstratified to crude horizontal stratification, disorganized clast fabric; fining- and coarsening-upward trends.	Lenticular.	Unconformably overlies and onlaps pre-Middle Devonian rocks; sharp and gradational contact with unit B, C, or Kayak Shale.	Flood-generated, high sediment concentration flows, rare debris flows; local sediment sources, confined to incised valleys.
B	Poorly to moderately sorted, clast-supported pebble conglomerate and medium- to coarse-grained, pebbly sandstone.	Thin- to thick-bedded, unstratified to horizontally stratified conglomerate and sandstone; rare trough and planar cross bedding; fining-upward couplets 0.4-1.5 m thick.	Sheetlike is most common, less commonly lenticular.	Sharp or gradational contact with unit A, or unconformably above pre-Middle Devonian rocks; onlaps pre-Middle Devonian rocks; gradationally overlain by unit C.	Braid-bar complexes and shallow channel fills in low-sinuosity, bedload-dominated fluvial system, confined to incised valleys.
C	Moderately sorted, fine- to coarse-grained sandstone and clast-supported pebble conglomerate, minor organic-rich mudstone.	Multistory and multilateral fining-upward channel-fills from 1.0-3.4 m thick; thin- to thick-bedded; basal conglomerate, abruptly overlain by pebbly sandstone, abundant trough cross bedding and common planar cross bedding throughout channel-fills.	Broadly lenticular to sheetlike.	Gradational lower contact with unit B, sharp lower contact with unit A, or unconformably above pre-Middle Devonian rocks; onlaps pre-Middle Devonian rocks; gradational contact with overlying unit E. Where unit E is absent, sharp contact with Kayak Shale.	Mixed-load, low- to moderate-sinuosity fluvial system, incised valley fill.
D	Moderately sorted, fine- to coarse-grained sandstone, common organic-rich mud-stone, minor pebble-conglomerate with minor mudstone intraclasts, minor coal.	Single story and multistory channel-fills from 1.0-4.0 m thick; similar to unit C, only with mudstone intraclasts in basal conglomerate and planar cross bedding limited to top of channel fills; mudstone successions up to 9.0 m thick cap most channel-fills, organic-rich, coal-bearing, with thin interbeds of sandstone.	Sheetlike?	Unconformably above pre-Middle Devonian rock; gradational with overlying unit E. Where unit E is absent, sharp contact with Kayak Shale.	Mixed-load, moderate- to high-sinuosity fluvial system with adjacent perennial flood basins, incised valley fill.
E	Moderately to well-sorted, fine- to coarse-grained sandstone, minor to common pebble conglomerate, minor coal.	Thin- to thick-bedded multilateral and multistory channel-fills < 1.0 m thick; basal pebble conglomerate, abruptly overlain by sandstone and pebbly sandstone with common trough and planar cross bedding, low-angle lamina and pebble conglomerate stringers 1-2 clasts thick common near top of channel fills.	Broadly lenticular and sheetlike.	Gradational lower contact with either unit C or D; contact relations with overlying Kayak Shale are uncertain—the contact appears to be abrupt based on three locations in the northern Franklin Mountains.	Mixed-load, low- to moderate-sinuosity and moderate- to high-sinuosity distributary channel fills, distributary-mouth bars or adjacent beach-ridge deposits in marginal-marine setting, incised valley fill.
F	Moderately to well-sorted, fine- to medium-grained sandstone, organic-rich mudstone, minor coal.	Thin- to medium-bedded, unstratified to horizontally bedded and internally laminated, sandstone grades upward into interbedded, burrow-mottled sandstone, mudstone, and coal.	Sheetlike.	Unconformably above pre-Middle Devonian rocks; gradationally overlain by Kayak Shale.	Fluvial sheet flood and tidal flat-coastal swamp deposits above paleotopographic highs on sub-Mississippian unconformity.

Table 2. *Summary of lithofacies characteristics recognized in the lower Kayak Shale*

Lithofacies	Composition and texture	Sedimentary and biogenic structures	Geometry and position	Interpretation
Organic-rich mudstone (Orm)	Black, organic-rich siltstone, silty shale, and shale, minor fine-grained quartzose sandstone, + - plant fragments and coal.	Fissile mudstone, + - lenticular laminated sandstone.	Geometry unknown; valley-fill, lower contact with Kekiktuk not exposed, but appears gradational.	Estuary with fringing swamps or marshes on landward side.
Planar cross-bedded sandstone (Pcs)	Quartzarenite and chert-quartz sub-litharenite (lower unit), lithic wacke (upper unit).	Wavy, parallel beds up to 15 cm thick; planar cross beds in sets 6-15 cm thick, reactivation surfaces; trough cross beds in sets up to 10 cm thick; mudstone partings between most foreset beds; upper unit is burrow mottled.	Geometry unknown; encased in organic-rich mudstone, near base of lower Kayak.	Tidal sandflat and tidal creek.
Argillaceous sandstone (Ars)	Quartzarenite, chert-quartz sub-litharenite, and chert-quartz granule conglomerate.	Lower contact with organic-rich mudstone is erosive, upper is sharp to gradational; at least two fining-upward cycles; trough cross beds 10-30 cm thick; ripple cross-laminae; mudstone intraclasts throughout; scale of sedimentary structures decreased upward.	Lenticular geometry; encased within organic-rich mudstone, near base of lower Kayak.	Channelized fluvial-flood succession.
Bioclastic limestone (Bcl)	Quartzose bryozoan-pelmatozoan packstone and grainstone.	Sharp lower contact with organic-rich mudstone; normally graded; preferred orientation of skeletal grains; skeletal grains highly abraded; variably bioturbated.	Lenticular; encased within organic-rich mudstone, near middle and top of lower Kayak.	Distal storm-washover deposits.
Irregularly bedded sandstone (Ibs)	Quartzarenite.	Discontinuous, wavy beds up to 6 cm thick; trough cross beds up to 5 cm thick; horizontal traces on bedding planes—resemble *Thalassanoides* and *Ophiomorpha*.	Sharp lower contact with organic-rich mudstone, sharp upper contact with plane-bedded sandstone at top of lower Kayak, truncated laterally by trough cross-bedded sandstone; geometry unknown, broadly lenticular (?).	Back-barrier proximal washover deposits.
Plane-bedded sandstone (Pbs)	Quartzarenite.	Even parallel beds up to 3.0 cm thick; low-angle inclined lamination; low-relief scours; parting lineation on some bedding surfaces.	Sharp lower contact with irregularly bedded sandstone, sharp upper contact with middle Kayak, truncated laterally by trough cross-bedded sandstone.	Lower foreshore to upper shoreface deposits.
Trough cross-bedded sandstone (Tcs)	Quartzarenite.	Large-scale trough cross-beds in sets up to 1.0 m thick; plane-parallel beds at top of succession up to 20 cm thick.	Sharp lower contact with organic-rich mudstone, sharp upper contact with middle Kayak; lenticular.	Tidal inlet-fill deposits.

elongated, pencil-like fragments (table 2). Siltstone is most common in the lower beds. Lenticular laminae <0.5 cm thick of fine-grained quartzarenite are scattered throughout this lithofacies and minor anthracitic coal is present near the base. Moderately well-preserved plant fragments (branches and leaves) up to 15 cm long are restricted to the lower half of this lithofacies, whereas comminuted organic debris is common in mudstones of the upper half. Palynologic samples collected from this lithofacies contain abundant woody and coaly fragments and scolecodonts (Utting, 1990).

Relatively abundant siltstone near the base of this lithofacies likely records proximity to low-energy fluvial channels. Minor coal lenses and abundant plant fragments in the lower half of this lithofacies suggest that swamps existed on the landward side of the estuary and that deposition in these areas proceeded at, or very close to, sea level under anaerobic conditions (Galloway and Hobday, 1983). The progressively lower siltstone content and lack of coal upsection indicates a steadily decreasing supply of coarser grained detritus to the marginal-marine environment and deposition in shallow subtidal conditions. Thin lenticular laminae of fine-grained sandstone scattered throughout the lithofacies suggests fluctuating energy levels associated with tides. Lenticular bedding is not unique to any one depositional setting, although it is a common feature in many tidally influenced marginal-marine settings (Reineck and Wunderlich, 1968). The dark-gray and black coloration of siltstone and shale suggests an organic carbon content >1.0 percent (Hosterman and Whitlow, 1983; Potter and others, 1980) and that the estuary was characterized by an oxygen-depleted bottom layer (Heckel, 1972). Scolecodonts, the jaw apparati of marine annelids, are the only indigenous faunal remains recognized in this lithofacies, which suggests that bottom conditions were at least dysaerobic locally and capable of supporting some life (O'Brien and Slatt, 1990). The organic-rich mudstone lithofacies records deposition from suspension and relatively weak traction currents in a low-energy estuarine setting.

PLANAR CROSS-BEDDED SANDSTONE

The planar cross-bedded sandstone lithofacies is about 1.5 m thick, has only been recognized at one locality, and is poorly exposed near the base of the lower Kayak Shale (figs. 4, 5). This lithofacies consists of medium- to coarse-grained sandstone and argillaceous sandstone and can be divided into two units based on mudstone content (table 2). The lower unit is about 1.0 m thick and consists of moderately sorted, medium- to coarse-grained sandstone with both planar tabular and unidirectional planar-tangential cross-bedded sets from 6 to 15 cm thick, and minor trough cross-bedded sets up to 10 cm thick. Planar cross-beds overlie an erosion surface with up to 5 cm of relief and are unidirectional. Reactivation surfaces have been recognized that truncate some foresets. Mudstone drapes are commonly observed between foreset laminae, and small mudstone intraclasts are common throughout.

The upper unit is 0.5 m thick, rests in sharp contact with the lower unit, and is sharply overlain by the organic-rich mudstone lithofacies. This unit consists of highly bioturbated, poorly sorted, fine- to medium-grained argillaceous sandstone. Mudstone is present throughout; beds are wavy, discontinuous, and up to 4 cm thick.

Planar and trough cross-bedded sandstone in the lower unit records the migration of straight-crested sandwaves and sinuous-crested dunes, respectively, under lower flow-regime conditions. Mudstone drapes between some foreset laminae indicate deposition during slack-water periods in the middle of tidal cycles, when currents were weak or nonexistent. These are analogous to mud drapes observed in sand successions from modern tidal-flat environments by Raaf and Boersma (1971). Associated reactivation surfaces are consistent with deposition in a tidal-flat environment, where they are commonly associated with sandy successions deposited from reversing tidal currents with asymmetric time-velocity profiles (Raaf and Boersma, 1971; Reineck and Singh, 1980). The presence of mudstone drapes suggests deposition under fluctuating energy conditions in a tidally influenced setting. The highly bioturbated, argillaceous character of the upper unit is consistent with this interpretation and resembles highly bioturbated tidal deposits described by Raaf and Boersma (1971). Vertical successions resembling the planar cross-bedded lithofacies have been described from siliciclastic tidal flats by Raaf and Boersma (1971), Reineck (1972), and Weimer and others (1982). The vertical succession suggests progressive flooding and gradual drowning of a sandy tidal flat. However, poor exposure precluded tracing this lithofacies laterally, so it is unknown if it was deposited on a sandy tidal flat or in a tidal channel.

ARGILLACEOUS SANDSTONE

The argillaceous sandstone lithofacies is about 3.5 m thick, weathers to a dark red-brown color, and has only been recognized at one locality, where it is situated near the base of the lower Kayak Shale (figs. 4, 5). This lithofacies has a broad, lenticular geometry and consists of argillaceous, quartzose granule conglomerate and fine- to coarse-grained sandstone in beds from 4 to 50 cm thick (table 2). In vertical succession, this lithofacies is composed of at least two upward-thinning and -fining

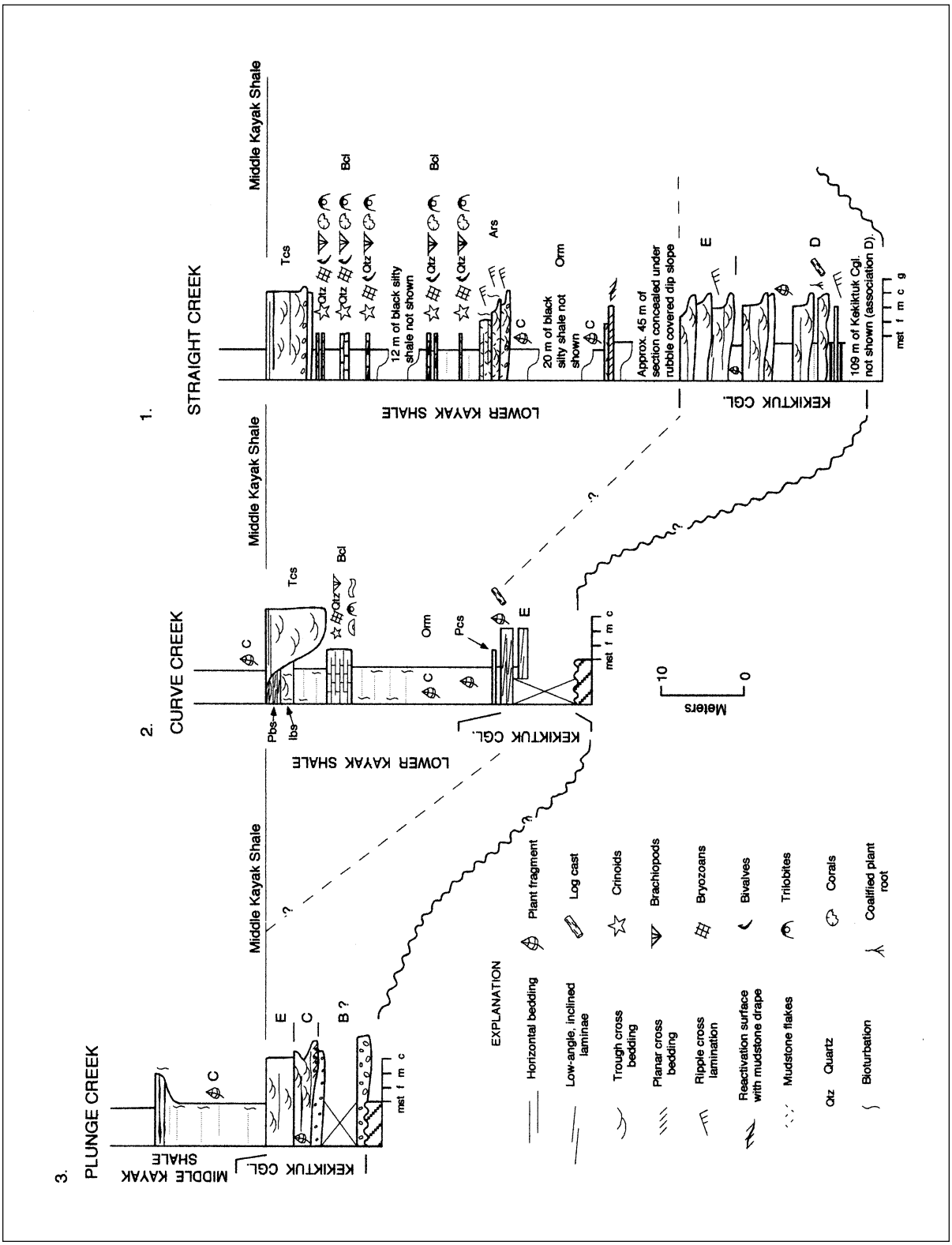

Figure 4. *Measured sections through the lower Kayak Shale in the northern Franklin Mountains. The locations of each measured section is shown in figure 3: location 1 is Straight Creek; location 2 is Curve Creek; and location 3 is Plunge Creek. The lower Kayak Shale is not present at Plunge Creek, which is located along approximate depositional strike from locations 1 and 2 (see fig. 3). The Plunge Creek succession is interpreted to represent deposition on a paleotopographic high, or along the flanks of a paleotopographic high.*

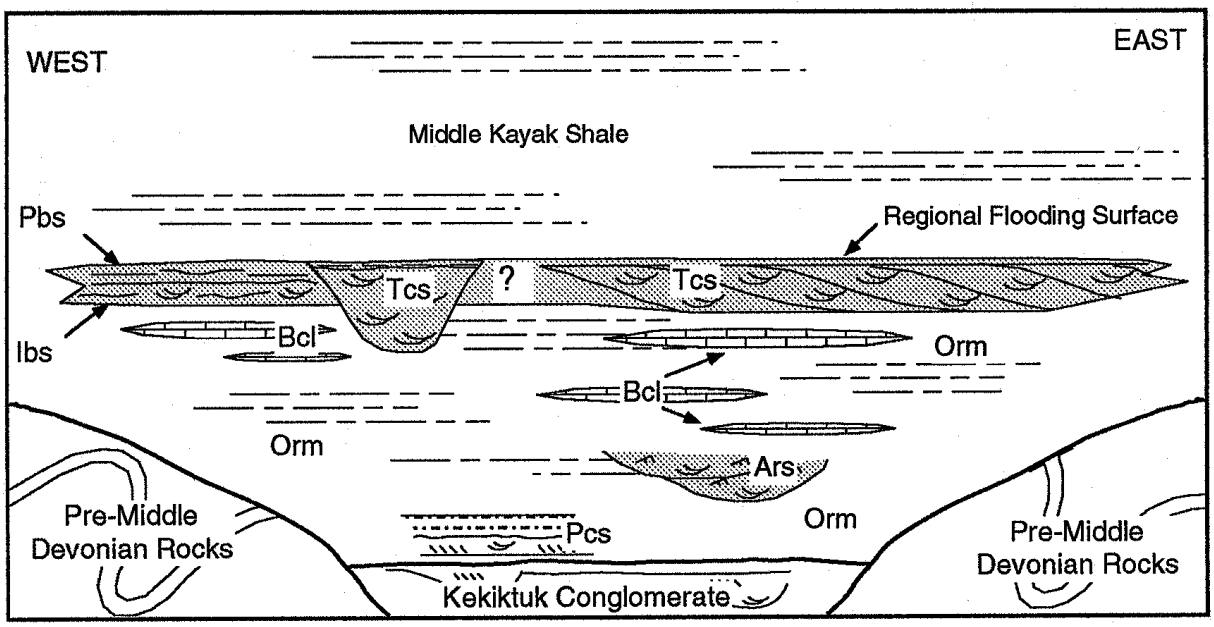

Figure 5. *Schematic cross section across valley-fill deposits in the northern Franklin Mountains summarizing lateral and vertical lithofacies relations in the lower Kayak Shale. Ars = argillaceous sandstone lithofacies; Bcl = bioclastic limestone lithofacies; Ibs = irregularly bedded sandstone lithofacies; Orm = organic-rich mudstone lithofacies; Pbs = Plane-bedded sandstone lithofacies; Pcs = planar cross-bedded sandstone lithofacies; Tcs = trough cross-bedded sandstone lithofacies.*

cycles from 1.0 to 2.5 m thick. The lower cycle consists of a basal, trough cross-bedded quartz-granule conglomerate that rests above a sharp, erosive contact with the underlying organic-rich mudstone lithofacies (fig. 4). Conglomerate is gradationally overlain by trough cross-bedded and ripple cross-laminated, fine- to coarse-grained sandstone. Elongated black, organic-rich mudstone intraclasts are common throughout the cycle and are oriented parallel to bedding. The higher cycle erosively overlies and is similar in all respects to the lower cycle, with the exception that a basal conglomerate is lacking and the cycle is sharply overlain by dark-gray to black mudstone. Within both cycles, the scale of sedimentation units gradually decreases upsection while the degree of bioturbation increases. Poorly preserved plant fragments are present on some bedding surfaces.

Within each cycle, coarse-grained detritus initially migrated as small- to medium-scale sinuous-crested dunes under lower flow-regime conditions. As flow strength gradually decreased, progressively finer-grained sediment was deposited in smaller-scale bedforms until, at the end of each cycle, fine-grained sandstone was deposited from migrating asymmetric, sinuous-crested ripples. Each cycle was characterized by an initial high-energy phase when turbulent currents reworked the underlying substrate. Currents traversed a cohesive, muddy substrate, as indicated by the ubiquitous presence of mudstone intraclasts. After the initial scour phase, the record is one of gradually waning flow strength. The close association between the argillaceous sandstone lithofacies and underlying coarse-grained valley-filling fluvial successions in the Kekiktuk Conglomerate suggests that the former records episodic transport of coarse-grained detritus into a marginal-marine setting during fluvial flood events. The vertical succession in the argillaceous sandstone lithofacies appears similar to proximal bayhead-delta channel-fill sequences described from estuarine settings by Dalrymple and others (1992); however, thin coarsening-upward successions typically associated with bayhead-delta successions have not been recognized in the lower Kayak.

BIOCLASTIC LIMESTONE

The bioclastic limestone lithofacies consists of red-brown weathering limestone lenses up to 1.2 m thick that extend 5 to >50 m laterally along local strike within the upper beds of the lower Kayak Shale (figs. 4, 5; table 2). Limestone lenses have sharp, erosive lower and sharp upper contacts with organic-rich mudstone. Stratal thicknesses in this lithofacies gradually increase upsection from lamina to thin-beds (up to 6 cm) of bioclastic limestone and, where well exposed, defines a distinctive thickening upward trend when viewed from a distance. Laminasets are up to 6 cm thick and separated by thin shale partings. Near the top of the thickening upward trend lenses are composed of bedsets with individual beds up to 6 cm thick that lack shale partings and have erosive bounding surfaces. Many of the thicker beds are normally graded. Limestones consist

primarily of bryozoan and pelmatozoan packstone and grainstone with subordinate brachiopods, pelecypods, rugose corals, ostracods, trilobites, calcispheres, mudstone intraclasts, and angular-to-subround sand- and granule-sized detrital quartz (table 2). Mudstone intraclasts and elongated skeletal grains have a strongly preferred orientation parallel to bedding, and the latter are broken and abraded. The upper surfaces of some lenses and stratal units comprising lenses are slightly bioturbated to completely burrow mottled.

Normal size grading, broken and abraded skeletal grains, mudstone intraclasts, and the strong preferred orientation of elongated grains parallel to bedding suggest transportation by strong currents, probably under upper flow-regime plane-bed conditions, and are features commonly recognized in storm-generated shell beds (Aigner, 1985; Kreisa and Bambach, 1982). The dark-gray to black, organic-rich mudstone lithofacies suggests that the estuarine environment was not a suitable habitat for the open-marine fauna contained in these deposits (Flugal, 1982; Heckel, 1972; Wilson and Jordan, 1983). Thus, skeletal grains were transported landward from nearby open-marine settings and deposited in an estuarine environment that was characterized by poor circulation and anaerobic-to-dysaerobic bottom conditions. Detrital quartz grains were entrained by these flows as they overtopped barrier islands located on the seaward side of estuaries. The quartzose bioclastic limestone lithofacies records episodic sedimentation from storm-generated surges as distal washover deposits (Elliot, 1986; Reinson, 1984). Similar storm-generated washover deposits with open-marine, allochthonous faunas have been described from Lower Silurian transgressive barrier-island successions in southwest Wales by Bridges (1976). Storm washovers are most common on microtidal to low mesotidal coasts (Hayes, 1979).

IRREGULARLY BEDDED SANDSTONE

The irregularly bedded sandstone lithofacies is up to 2 m thick and is situated near the top of the lower Kayak, where it gradationally overlies organic-rich mudstones and is sharply overlain by the plane-bedded sandstone lithofacies (figs. 4, 5). The irregularly bedded sandstone lithofacies consists of fine- to coarse-grained, moderately to well-sorted sandstone in discontinuous beds up to 6.0 cm thick that locally contain plane-parallel and trough cross stratification (table 2). Vertical and bed-parallel biogenic traces of uncertain affinity are present on many bedding surfaces. Bed-parallel traces are linear, stand in relief about 1.0 cm, and are up to 2.0 cm wide. Non-branching bed-parallel forms are most common, although branching forms have been observed. Traces resemble *Thalassanoides* and *Ophiomorpha* (Hantzschel, 1975).

In outcrop this lithofacies is characterized by irregularly shaped parting surfaces, which create a jumbled appearance. No distinct textural variations have been recognized in this lithofacies, so it unclear if these irregular surfaces correspond to bedding that has been disrupted by burrowing and grazing organisms.

The presence of plane-parallel and trough cross bedding suggests deposition under fluctuating energy conditions. Plane-parallel bedding probably originated under upper flow-regime plane-bed conditions, whereas trough cross bedding developed under lower flow-regime conditions from small- to medium-scale dune bedforms. The gradational lower contact with mudstone indicates progressive landward migration of the lithofacies with repeated depositional episodes. Trace fossils likely belong to the Skolithos ichnofacies, which is usually associated with shifting substrates in high-energy settings (Frey and Pemberton, 1984). The irregularly bedded sandstone lithofacies records episodic events that involved transport of medium- to coarse-grained sand and deposition as proximal washover deposits on the landward side of barrier islands. Similar sequences have been described from Holocene back-barrier settings by Kraft (1971), Kraft and John (1979), and Wilkinson (1975).

PLANE-BEDDED SANDSTONE

The plane-bedded sandstone lithofacies is situated at the top of the lower Kayak Shale, where it is sharply overlain by the middle Kayak Shale (figs. 4, 5). The lower contact with the irregularly bedded sandstone lithofacies is sharp and probably erosive, although no downcutting was observed. This lithofacies is up to 1.0 m thick and consists of medium- to coarse-grained sandstone (table 2). Beds are thin (up to 3.0 cm thick), laterally continuous, and commonly contain internal low-angle inclined lamination. Locally, beds are truncated by low-relief scour-and-fill structures. Parting lineations are visible on some bed surfaces.

Plane-parallel stratification in medium- to coarse-grained sand suggests upper flow-regime conditions (Collinson and Thompson, 1988). Low-angle inclined laminae are commonly observed in the foreshore and upper shoreface zones of beaches and are thought to form under upper flow-regime conditions associated with wave-swash runoff (Clifton, 1969). The stratigraphic position above organic-rich coal- and scolecodont-bearing mudstone (organic-rich mudstone lithofacies) and storm-generated quartzose bioclastic limestone and sandstone deposits (bioclastic limestone and irregularly bedded sandstone lithofacies, respectively) suggests deposition on the seaward side of a barrier island. Similar sequences have been described from barrier-island settings by Kraft (1971), Kraft and John (1979), and Wilkinson (1975).

TROUGH CROSS-BEDDED SANDSTONE

The trough cross-bedded sandstone lithofacies is situated at the top of the lower member, where it rests above the organic-rich mudstone lithofacies along an erosion surface (figs. 4, 5). At one locality, the trough cross-bedded sandstone lithofacies truncates both the irregularly bedded and plane-bedded sandstone lithofacies and extends several meters into the underlying mudstones (figs. 4, 5). At another locality, where the irregularly bedded and plane-bedded lithofacies are absent, the trough cross-bedded sandstone lithofacies forms a laterally extensive lithosome with large-scale lateral accretion surfaces (sandstone body at top of lower Kayak in figures 4 and 5). The trough cross-bedded sandstone lithofacies is up to 11 m thick and consists of medium- to coarse-grained, commonly granule-bearing sandstone and minor granule conglomerate.

Conglomerate beds are up to 1.0 m thick and are restricted to the base of the lithofacies. Where conglomerate is present, an upward-fining textural trend is apparent, grading from conglomerate to medium- to coarse-grained sandstone. Most clasts are of extrabasinal origin (quartz and minor chert); however, distinctive mudstone intraclasts are present as elongated chips up to 7.0 cm long and 1.0 cm thick oriented parallel to stratification. Trough cross bedding is ubiquitous with individual sets from 0.4 to 0.5 m thick. Foresets are 0.5 to 1.5 cm thick and usually separated by thin drapes of black mudstone.

Sandstone beds are up to 1.3 m thick and characterized by festoon trough cross bedding with sets from 0.4 to about 1.0 m thick. Mudstone intraclasts are common and are oriented parallel to stratification. Foreset beds are commonly separated by thin drapes of black mudstone. Scour troughs are 2.5 to 5.0 m wide and one was traced about 25 m in the transport direction. An interval of plane-parallel bedded sandstone from 0.3 to 0.5 m thick usually caps this lithofacies. Both grain size and the scale of stratification decrease slightly upsection.

Large-scale trough cross bedding and the coarse grain size typical of this lithofacies suggest deposition under upper low-flow-regime conditions from migrating dunes. Dunes are commonly recognized bedforms in tidal inlets (Elliot, 1986; Reinson, 1984). Mudstone drapes separating many foreset beds indicate fluctuating energy conditions between times when flow strength was great enough to transport granule-size clasts and times when flow strength was weak or nonexistent, thereby allowing silt- and clay-sized particles to settle out of suspension and form mudstone drapes. The close association between this lithofacies and the irregularly bedded and plane-bedded sandstone lithofacies and its position at the top of the lower Kayak Shale (fig. 4) suggests deposition in tidal inlets. Three-dimensional dunes and mudstone drapes are common features in sandstones deposited in tidally influenced settings (for example, Elliot, 1986; Raaf and Boersma, 1971; Dalrymple and others, 1992).

The trough cross-bedded sandstone lithofacies records deposition in two types of tidal inlets. A deep, stable inlet is indicated where the trough cross-bedded sandstone lithofacies has truncated the barrier-island succession and cut into underlying mudstones (fig. 4). Tidal channels that scour below the level of associated barrier-island deposits into underlying muddy substrates tend to migrate slowly or remain fixed in one place (Elliot, 1986). An unstable or laterally migrating inlet is indicated where the plane-bedded and irregularly bedded sandstone lithofacies (barrier island) are absent and the trough cross-bedded sandstone lithofacies is present as an extensive sheetlike lithosome (fig. 4). Inlet fill of this type contains large-scale lateral accretion surfaces that indicate an easterly migration direction. Lateral accretion surfaces are commonly observed in tidal-inlet successions and record migration of inlets in the direction of longshore currents (Hoyt and Henry, 1967). Tidal-inlet successions may dominate the depositional record of a barrier island along stretches of coastline with significant longshore currents (Elliot, 1986).

Swift (1968) suggested that transgressive disconformities bound landward-migrating tidal-inlet successions. Each disconformity represents a ravinement surface, and Swift referred to this situation as a double ravinement. Following Swift (1968), two transgressive disconformities are recognized where this lithofacies is present. The lower surface corresponds to the base of the trough cross-bedded sandstone lithofacies and was the result of scour associated with channelized tidal currents; the upper surface corresponds to the base of the plane-parallel bedded sandstone recognized at the top of the inlet fill succession, and resulted from wave reworking in the shoreface zone as the tidal-inlet system migrated landward and was gradually abandoned due to relative sea-level rise. Where the trough cross-bedded sandstone lithofacies is absent, only one disconformity is recognized and corresponds to the erosional contact between the irregularly bedded and plane-bedded sandstone lithofacies.

DEPOSITIONAL RECONSTRUCTION

A depositional model for the lower Kayak Shale is summarized in figure 6. Deposition of the Endicott Group was initiated by relative sea-level rise that began to affect the northeastern Brooks Range in latest

Tournaisian-earliest Visean time, based on the age of the basal Kekiktuk (Utting, 1991b). Prior to this, downcutting fluvial systems flowed over an uplifted terrane of pre-Middle Devonian sedimentary and igneous rocks and established a system of incised paleovalleys. Relative sea-level rise resulted in an upward and landward shift in stream equilibrium profiles. Fluvial detritus that had previously bypassed the northeastern Brooks Range to be incorporated into a thick clastic wedge at the basin margin south of the Franklin Mountains gradually became trapped within incised paleovalleys. Thus, the onset of transgression in the range-front region of the northeastern Brooks Range is recorded by fluvial deposits of the Kekiktuk Conglomerate.

The Kekiktuk is present in widespread but discontinuous exposures throughout the northeastern Brooks Range and is thickest in incised paleovalleys (LePain and others, 1994). The Kekiktuk either thins drastically or pinches out entirely away from the axial regions of paleovalleys, along the flanks of paleotopographic highs (paleointerfluves). The lower Kayak Shale has been recognized only above these thick paleovalley-filling successions of the Kekiktuk Conglomerate, which suggests that the distribution of the lower Kayak was directly controlled by paleotopographic relief on the sub-Carboniferous unconformity. Onlap relationships between the lower Kayak Shale and underlying pre-Middle Devonian rocks have not been observed; however, the association between the lower Kayak and thick valley-filling successions of the Kekiktuk Conglomerate suggests deposition in an estuarine system (figs. 5, 6). Thick paleovalley-filling successions of the Kekiktuk provided abundant terrigenous sand to the marginal-marine environment at the seaward end of incised valleys. The irregularly bedded sandstone, plane-bedded sandstone, and trough cross-bedded sandstone lithofacies and their stratigraphic relationships to each other suggest deposition in a barred estuary with a barrier island(s) at the seaward end (cf. Dalrymple and others, 1992).

The Kekiktuk Conglomerate and the overlying lower Kayak Shale were deposited on a surface characterized by significant local relief of at least 128 m (based on maximum thickness of the Kekiktuk Conglomerate) and possibly up to 248 m (maximum thickness of the Kekiktuk Conglomerate plus the thickness of lower Kayak Shale). Paleotopographic relief as a control on distribution of fluvial, estuarine, and barrier-island successions is well documented for Holocene sediments

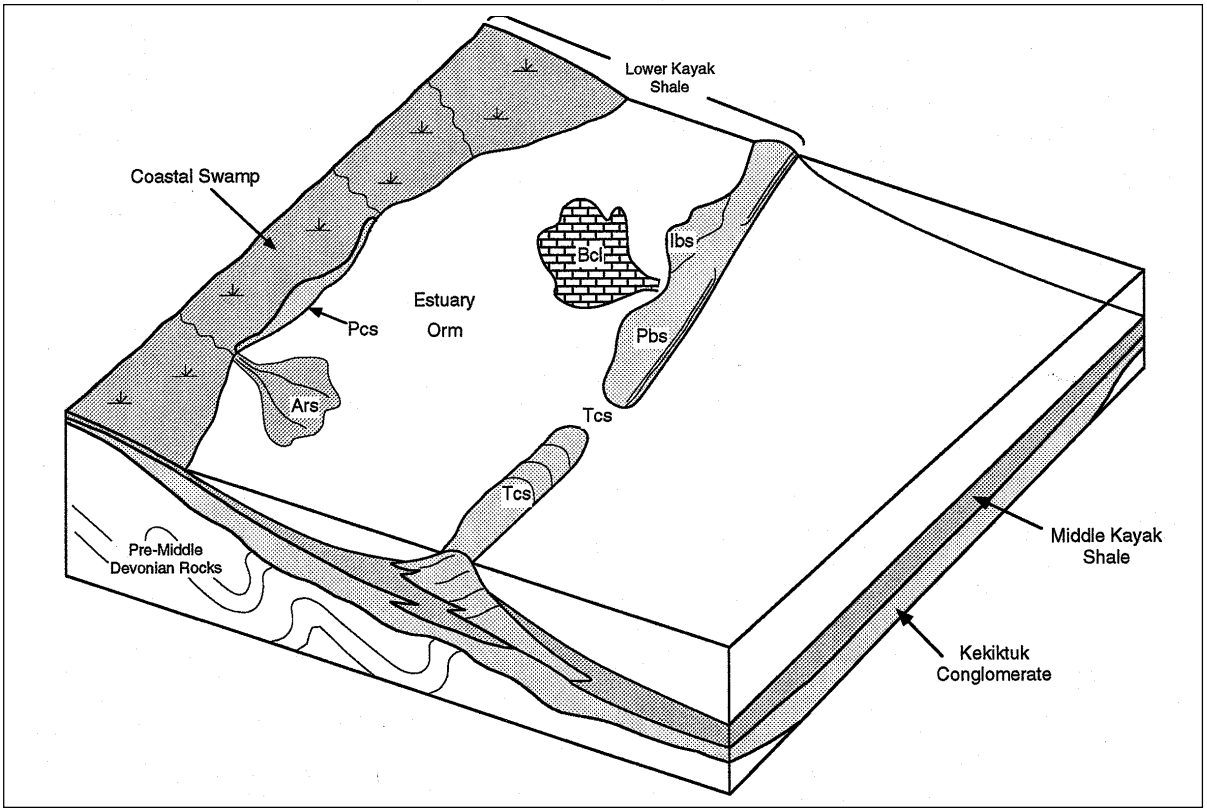

Figure 6. *Generalized block diagram showing a depositional reconstruction for the lower Kayak Shale. Refer to figure 5 for key to lithofacies abbreviations.*

in Delaware (Kraft, 1971), for Cretaceous marginal-marine rocks in Kansas (Franks, 1980), and the Texas Gulf Coast (Wilkinson, 1975). Heward (1981) states that barrier islands have the greatest preservation potential above paleotopographic lows, or drowned valleys. The preservation of barrier-island and shallow tidal-inlet deposits in the lower Kayak was likely enhanced by a paleogeographic position in an incised paleovalley.

The degree of preservation of barrier-island and shallow tidal-inlet deposits in the lower Kayak Shale also suggest deposition in an incised valley, as the preservation potential of transgressive barrier islands is usually low unless they are associated with drowned river valleys or if the rate of relative sea-level rise is high (Fischer, 1961; Swift, 1968; Kraft and John, 1979). No information is available on the rate of relative sea-level rise in the northeastern Brooks Range during the deposition of the lower Kayak. The contact between the lower and middle members of the Kayak is interpreted as a transgressive disconformity and a marine flooding surface that records drowning and shutdown of marginal-marine depositional systems, and the establishment of shallow-marine conditions on the seaward side (south) of estuaries (figs. 5, 6).

As sea level continued rising, barrier islands were initially able to retrograde and keep pace with the rise because of a readily available supply of coarse-grained sediment from reworked fluvial deposits and longshore currents along open stretches of the coast. During this initial phase, barrier islands migrated landward (northward) through a combination of storm-washover and shoreface-retreat processes in a manner analogous to Holocene barriers along the Delaware coast (Kraft, 1971; Kraft and John, 1979). This process continued until the supply of sediment was insufficient to maintain the barrier system as underlying fluvial sediment (Kekiktuk Conglomerate), and terrigenous clastic source areas (pre-Middle Devonian rocks) were buried due to continued transgression. Barrier islands probably responded by getting progressively smaller, until they were ultimately drowned and the surf zone skipped some distance to the north. Regional study of the Endicott Group suggests that barrier islands were probably not re-established at a more northerly position (for example, the Sadlerochit and Shublik Mountains and Leffingwell Ridge) because of the lack of a sufficient volume of sand. However, outcrop belts are widely spaced and oriented roughly parallel to the Carboniferous coastline (fig. 3), so this cannot be established with certainty.

Tidal-inlet deposits are a prominent feature in the lower Kayak Shale and, at one locality, lateral inlet migration has resulted in complete removal of barrier-island deposits. The presence of tidal inlets and the low abundance of distal storm-washover deposits suggest that tides were in the high microtidal to low mesotidal range (Hayes, 1979). Flood-tidal delta deposits have not been recognized in estuarine deposits of the lower Kayak Shale. Hayes (1979) noted that flood tidal deltas tend to be small or absent along microtidal and low mesotidal coasts. Ebb-tidal delta deposits, if originally present, would be expected to have a low preservation potential in transgressive settings because of their high stratigraphic position (McCubbin, 1982; Reinson, 1984).

CONCLUSIONS

Relative sea level rise in late Tournaisian time shifted stream equilibrium profiles upward and landward (north), and initiated fluvial deposition and preservation within incised paleovalleys. As relative sea level rise continued, the seaward portions of paleovalleys were flooded, fluvial dispersal systems of the Kekiktuk Conglomerate were drowned, and the estuarine conditions recorded in the lower Kayak Shale were established. The description of the lower Kayak Shale presented in the preceding sections suggests the following conclusions:

(a) Seven lithofacies have been recognized in the lower Kayak Shale that record deposition in barrier-island, tidal-inlet, and back-barrier environments.

(b) The association between the lower Kayak Shale with relatively thick underlying valley-fill fluvial successions of the Kekiktuk Conglomerate suggests that the distribution of the lower Kayak was controlled by paleotopographic relief on the sub-Carboniferous unconformity, and that the lower Kayak Shale records deposition in a barred estuarine system.

(c) Barrier-island and associated tidal-inlet environments migrated landward (present-day north) by a process of shoreface erosion and associated redistribution of sediment landward into the estuarine setting as storm-generated washovers.

(d) The steadily decreasing supply of coarse-grained detritus to the barrier island system, combined with a steady rise in relative sea level, ultimately led to drowning and shutdown of marginal-marine depositional systems (lower Kayak Shale) and establishment of shallow-marine conditions recorded by the middle and upper Kayak Shale.

(e) The degree of preservation of barrier-island and tidal-inlet deposits in the lower Kayak

Shale suggest deposition in incised paleovalleys in which valley margins of resistant bedrock protected the seaward lithofacies from complete destruction from shoreface erosion as transgression proceeded and the shoreline gradually migrated northward.

ACKNOWLEDGMENTS

My work on the Kayak Shale was carried out as a Ph.D. student in the Tectonics and Sedimentation Research Group at the University of Alaska, under the direction of Drs. Keith Crowder, Wes Wallace, and Keith Watts. I gratefully acknowledge the financial support provided to the Tectonics and Sedimentation Research Group from the petroleum industry. Industry sponsors included ARCO Alaska, ARCO Research, BP Exploration (Alaska), Chevron, Conoco, Elf Aquitane, Exxon, Japan National Oil Corporation, Marathon Oil, Mobil Exploration and Producing, Murphy Oil, Phillips Petroleum, Shell Western Exploration and Production, Texaco, and Unocal. Jim Clough (Alaska Division of Geological & Geophysical Surveys) and Evvy Goebel (BP Exploration) reviewed the manuscript and made significant suggestions for its improvement.

REFERENCES CITED

Aigner, T., 1985, Storm depositional systems: Dynamic stratigraphy in modern and ancient shallow-marine sequences, *in* Friedman, G.M., Neugebauer, H.J., and Seilacher, A., eds., Lecture notes in earth sciences: New York, Springer-Verlag, v. 3, 174 p.

Armstrong, A.K., 1974, Carboniferous carbonate depositional models, preliminary lithofacies and paleotectonic maps, Arctic Alaska: American Association of Petroleum Geologists Bulletin, v. 58, p. 621-645.

Armstrong, A.K., and Bird, K.J., 1974, Facies and environments of deposition of Carboniferous rocks, Arctic Alaska, *in* Miller, T.P., ed., Recent and ancient environments in Alaska: Alaska Geological Society Symposium, Anchorage, Alaska, p. A1-A16.

Armstrong, A.K., and Mamet, B.L., 1977, Carboniferous microfacies, microfossils, and corals, Lisburne Group, Arctic Alaska: U.S. Geological Survey Professional Paper 849, 144 p., 47 sheets.

Bader, J.W., and Bird, K.J., 1986, Geologic map of Demarcation Point, Mt. Michelson, Flaxman Island, and Barter Island quadrangles, northeastern Alaska: U.S. Geological Survey Miscellaneous Investigations Series Map I-1791, 1:250,000, 1 sheet.

Bird, K.J, and Molenaar, C.M., 1987, Stratigraphy, *in* Bird, K.J., and Magoon, L.B., eds., Petroleum geology of the northern part of the Arctic National Wildflife Refuge, northeastern Alaska: U.S. Geological Survey Bulletin 1778, p. 37-59.

Blodgett, R.B., Clough, J.G., Harris, A.G., and Robinson, M.S., 1991, The Mount Copleston Limestone, a new Lower Devonian formation in the Shublik Mountains, northeastern Brooks Range, Alaska, *in* Bradley, D.C., and Ford, A., eds., Geologic studies in Alaska by the U.S. Geological Survey in 1990: U.S. Geological Survey Bulletin 1999, p. 1-5.

Braun, J., and Beaumont, C., 1989, A physical explanation of the relation between flank uplifts and the breakup unconformity at rifted continental margins: Geology, v. 017, p. 760-764.

Bridges, P.H., 1976, Lower Silurian transgressive barrier islands, southwest Wales: Sedimentology, v. 23, p. 347-362.

Clifton, H.E., 1969, Beach lamination: Nature and origin: Marine Geology, v. 7, p. 553-559.

Collinson, J.D., and Thompson, D.B., 1988, Sedimentary structures (2nd ed.): London, Unwin and Hyman, 207 p.

Dalrymple, R.W., Zaitlin, B.A., and Boyd, R., 1992, Estuarine facies models: Conceptual basis and stratigraphic implications: Journal of Sedimentary Petrology, v. 62, p. 1130-1146.

Elliot, T., 1986, Siliciclastic Shorelines, *in* Reading, H.G., ed., Sedimentary environments and facies: Oxford, Blackwell, p.155-188.

Fischer, A.G., 1961, Stratigraphic record of transgressing sea in light of sedimentation on Atlantic coast of New Jersey: American Association of Petroleum Geologists Bulletin, v. 45, p. 1656-1666.

Flugal, E., 1982, Microfacies analysis of limestones: Berlin, Springer-Verlag, 633 p.

Franks, P.C., 1980, Models of marine transgression - examples from Lower Cretaceous fluvial and paralic deposits, north-central Kansas: Geology, v. 8, p. 56-61.

Frey, R.W., and Pemberton, S.G., 1984, Trace fossil facies models, *in* Walker, R.G., ed., Facies models (2nd ed.): Geoscience Canada Reprint Series 1, p. 189-207.

Galloway, W.E., and Hobday, D.K., 1983, Terrigenous clastic depositional systems: New York, Springer-Verlag, 423 p.

Hallam, A., 1984, Pre-Quaternary sea-level changes: Annual Review Earth and Planetary Science, v. 12, p. 205-243.

Hantzschel, W., 1975, Trace fossils and problematica, *in* Teichert, C., ed., Treatise of invertebrate paleontology, part W, Miscellanea, Supplement 1: Lawrence, University of Kansas Press and Geological Society of America, 269 p.

Hayes, M.O., 1979, Barrier island morphology as a function of tidal and wave regime, *in* Leatherman, S., ed., Barrier-islands from the Gulf of St. Lawrence to the Gulf of Mexico: Academic Press, p. 1-28.

Heckel, P.H., 1972, Recognition of ancient shallow-marine environments, *in* Rigby, K.J., and Hamblin, W.K., eds., Recognition of ancient sedimentary environments: Society of Economic Paleontologists and Mineralogists Publication 16, p. 226-286.

Heward, A.P., 1981, A review of wave-dominated clastic shoreline deposits: Earth-Science Reviews, v. 17, p. 223-276.

Hosterman, J.W., and Whitlow, S.I., 1983, Clay mineralogy of Devonian shales in the Appalachian Basin: U.S. Geological Survey Professional Paper 1298, 31 p., 1 sheet.

Hoyt, J.H., and Henry, V.J., 1967, Influence of island migration on barrier-island sedimentation: Geological Society of America Bulletin, v. 78, p. 77-86.

Kraft, J.C., 1971, Sedimentary facies patterns and geologic history of a Holocene marine transgression: Geological Society of America Bulletin, v. 82, p. 2131-2158.

Kraft, J.C., and John, C.J., 1979, Lateral and vertical facies relations of transgressive barrier: American Association of Petroleum Geologists Bulletin, v. 63, p. 2145-2163.

Kreisa, R.D., and Bambach, R.K., 1982, The role of storm processes in generating shell beds in Paleozoic shelf environments, *in* Einsele, G., and Seilacher, A., eds., Cyclic and event stratification: Heidelberg, Springer-Verlag, p. 200-207.

LePain, D.L., Crowder, R.K., Wallace, W.K., 1994, Early Carboniferous transgression on a passive continental margin: Deposition of the Kekiktuk Conglomerate, northeastern Brooks Range, Alaska: American Association of Petroleum Geologists Bulletin, v. 78, no. 5, p. 679-699.

McCubbin, D.G., 1982, Barrier-island and strand plain facies, *in* Scholle, P.A., and Spearing, D., eds., Sandstone depositional environments: American Association of Petroleum Geologists Memoir 31, 410 p.

Moore, T.E., Wallace, W.K., Bird, K.J., Karl, S.M., Mull, C.G., and Dillon, J.T., 1992, Stratigraphy, structure, and geologic synthesis of northern Alaska: U.S. Geological Survey Open-File Report 92-330, 183 p., 1 sheet.

Nilsen, T.H., Moore, T.E., Dutro, J.T., Brosgé, W.P., and Orchard, D.M., 1980, Sedimentology and stratigraphy of the Kanayut Conglomerate and associated units, central and eastern Brooks Range, Alaska - Report of the 1978 field season: U.S. Geological Survey Open-File Report 80-888, 40 p.

O'Brien, N.R., and Slatt, R.M., 1990, Argillaceous rock atlas: New York, Springer-Verlag, 141 p.

Potter, P.E., Maynard, J.B., and Pryor, W.A., 1980, Sedimentology of shale: Study guide and reference source: New York, Springer-Verlag, 306 p.

Raaf, J.F.M. de, and Boersma, J.R., 1971, Tidal deposits and their characteristic sedimentary stuctures: Geologie En Mijnbouw, v. 50, p. 479-504.

Reineck, H.E., 1972, Tidal flats, *in* Rigby, J.K., and Hamblin, W.K., eds., Recognition of ancient sedimentary environments: Society of Economic Paleontologists and Mineralogists Special Publication 16, p. 146-159.

Reineck, H.E., and Singh, I.B., 1980, Depositional Sedimentary Environments (2nd ed.): Springer-Verlag, 551 p.

Reineck, H.E., and Wunderlich, F., 1968, Classification and origin of flaser and lenticular bedding: Sedimentology, v. 11, p. 99-104.

Reinson, G.E., 1984, Barrier-island and associated strand-plain systems, *in* Walker, R.G., ed., Facies models, (2nd ed.): Geoscience Canada Reprint Series 1, p. 119-140.

Swift, D.P.J., 1968, Coastal erosion and transgressive statigraphy: Journal of Geology, v. 76, p. 444-456.

Utting, J., 1990, Palynological examination of 25 samples from the Kekiktuk and Kayak Formations of Alaska: Geological Survey of Canada Report 2-JU-90.

———1991a, Palynological examination of 26 outcrop samples from the Carboniferous of northeast Alaska: Geological Survey of Canada Report 5-JU-91.

———1991b, Palynological examination of 27 outcrop samples from the Carboniferous of northeast Alaska: Geological Survey of Canada Report 7-JU-91.

Weimer, R.J., Howard, J.D., and Lindsay, D.R., 1982, Tidal flats and associated tidal channels, *in* Scholle, P.A., and Spearing, D., eds., Sandstone depositional environments: American Association of Petroleum Geologists Memoir 31, p. 191-245.

Wilkinson, B.H., 1975, Matagorda Island: The evolution of a Gulf Coast barrier complex: Geological Society of America Bulletin, v. 86, p. 959-967.

Wilson, J.L., and Jordan, C., 1983, Middle Shelf, *in* Scholle, P.A., Bebout, D.G, and Moore, C.H., eds., Carbonate depositional environments: American Association of Petroleum Geologists Memoir 33, p. 298-343.

This page has intentionally been left blank.

COOLING HISTORY OF THE OKPILAK BATHOLITH, NORTHEASTERN BROOKS RANGE, AS DETERMINED FROM POTASSIUM-FELDSPAR THERMOCHRONOMETRY

by
Julie S. Paegle,[1] Paul W. Layer,[2,3] and Andrew W. West[2]

ABSTRACT

Detailed step-heat $^{40}Ar/^{39}Ar$ dating and potassium-feldspar thermochronometry of the Devonian Okpilak batholith, northeastern Brooks Range, refine its long thermotectonic history. Samples from two locations in the batholith yielded age spectra indicative of multidomain behavior of feldspar that can be modeled to determine the cooling history of the batholith, which is consistent with previous age information. The feldspar modeling provides a cooling history spanning a temperature range from ~450°C to 220°C and a time from ~130 Ma to ~30 Ma. This history is different at different elevations in the batholith, and may provide information on the Cretaceous paleogeothermal gradient (~20°C/km). These new data suggest that the batholith experienced slow cooling due to uplift and erosion from ~130 Ma to ~40 Ma, when the batholith underwent rapid uplift and cooling from a temperature of about 250°C to less than 100°C in a few million years, consistent with fission track studies. Thus, the rocks were uplifted from a depth of greater than 10 km (assuming a 20°C to 25°C/km geothermal gradient) in a relatively short period of time. These new data rule out a model of gradual uplift from greater than 10 km depth between 59 and 40 Ma.

INTRODUCTION

Analysis of $^{40}Ar/^{39}Ar$ age spectra has been shown to provide details about the geologic history of various regions and geologic settings (McDougall and Harrison, 1988). Whereas most dating methods can provide snapshots of the cooling history of a unit at particular times and temperatures, potassium feldspar thermochronometry (Lovera and others, 1989; 1991, 1993; Fitz Gerald and Harrison, 1993) has been developed to model the complete cooling history of a unit spanning a broad temperature range from ~400°C to ~150°C. This technique has produced cooling-uplift history models that are consistent with other geologic information in tectonic settings marked by simple cooling histories (that is, intrusion followed by a single cooling or uplift event). Examples of successful application of the technique include the Himalayas (Richter and others, 1991; Copeland and others, 1995) and the Alaska Range (West, 1994).

One of the basic assumptions of the technique of Lovera and others (1989) is that the feldspar has encountered a simple cooling history, without substantial reburial or reheating. It is unclear how applicable such modeling is in accurately determining the thermal history in more complicated geologic settings where, for example, intrusion is followed by a long and complex history marked by uplift, subsidence, and reheating events (Zeitler and Warnock, 1992). The Devonian Okpilak batholith, northeastern Brooks Range, is a granitic body which is believed to have encountered a long and complex history from intrusion (Devonian) to final uplift (Cenozoic) (Dillon and others, 1987; Hanks and Wallace, 1990; O'Sullivan and others, 1995). We have applied the technique of potassium feldspar thermochronometry to samples from this body to test the thermochronometry technique developed for simple cooling histories when applied to more complex ones.

GEOLOGIC SETTING

The Okpilak batholith is the largest igneous body in the northeastern Brooks Range (fig. 1) and has been described in detail elsewhere (Sable, 1977; Bader and Bird, 1986; Hanks and Wallace, 1990). It intrudes weakly metamorphosed Proterozoic and Paleozoic sedimentary and volcanic rocks of the Franklinian sequence, which are the oldest rocks exposed in the northeastern Brooks Range (Reiser and others, 1980). U-Pb zircon dating has yielded an initial crystallization age of 380 ± 10 Ma (Dillon and others, 1987) for the batholith. Both the batholith and the Franklinian sequence are unconformably overlain by Mississippian to Lower Cretaceous carbonate and clastic rocks of the Ellesmerian sequence (Sable, 1977; Bird and Molenaar, 1987). Geochronologic and depositional relationships

[1]Department of Geology and Geophysics, University of Utah, Salt Lake City, Utah 84112.
[2]Geophysical Institute University of Alaska Fairbanks, Fairbanks, Alaska 99775.
[3]Author to whom correspondence should be addressed.

clearly indicate that the batholith predates the unconformity. Granitic pebbles are found in Mississippian rocks at the base of the Ellesmerian sequence which implies that the batholith was at or near the surface at that time (LePain and others, 1994). The Ellesmerian sequence is, in turn, conformably overlain by Lower Cretaceous and younger sediments of the Brookian sequence. These sediments were derived from the uplift and erosion of the main axis of the Brooks range to the south (Mull, 1985; Molenaar and others, 1987).

All three sedimentary sequences and the batholith were involved in Cenozoic fold and thrust deformation. (Hanks and Wallace, 1990, Wallace and Hanks, 1990, Hanks, 1993). The northward-concave arcuate trend of structures around the batholith's southern margin suggests that the batholith initially acted as a structural buttress, delaying thrusting in its immediate vicinity (Hanks and Wallace, 1990). The northward propagation of a detachment resulted in the eventual involvement of the batholith in the thrusting event. This deformation and uplift of the batholith, as proposed by Hanks and Wallace (1990), could be accommodated in either the form of a series of discrete fault slices bounded by shear zones or by homogeneous simple shear at the mesoscopic and microscopic level, or by a combination of the two (Hanks and Wallace, 1990).

Geochronologic information that records this Cenozoic history includes a 61 ± 10 Ma zircon lead-loss event and a 59 ± 2 Ma K/Ar age from recrystallized biotites from the southern part of the batholith (Dillon and others, 1987). These ages have been interpreted to indicate isotopic resetting caused by metamorphism. Zircon fission track ages from the batholith are 45 ± 2 Ma, whereas apatite fission-track data have produced ages

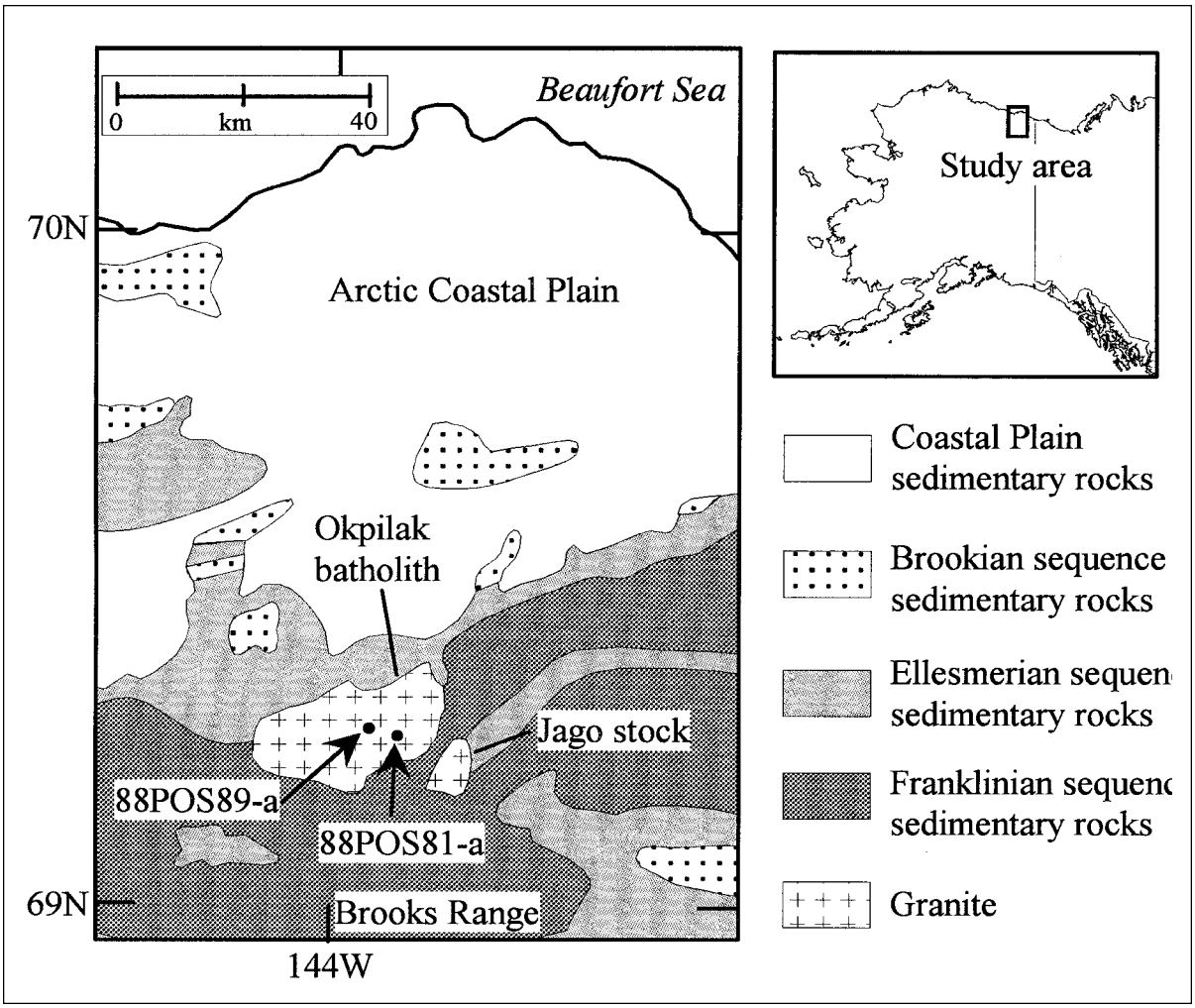

Figure 1. *General geologic map of the setting of the Okpilak batholith, northeastern Brooks Range, Alaska [adapted from Hanks and Wallace (1990) and O'Sullivan and others (1995)]. The samples dated in this study are from the center of the batholith, and from the summit and base of Mt. Michelson (not shown).*

from ~43 Ma at the top to ~23 Ma at the base for subsequent deformation, possibly in the form two discrete events of structural uplift at ~41-45 Ma and ~25 Ma (O'Sullivan, 1993; O'Sullivan and others, 1993; 1995).

Although the apatite fission-track study (O'Sullivan and others, 1995) provides a continuous cooling history for the latest history of the batholith, there are gaps in the thermal history of the batholith between 60 Ma and 45 Ma and between the time of batholith intrusion (380 Ma) and 60 Ma. We have attempted to document a more detailed, continuous cooling history through application of the $^{40}Ar/^{39}Ar$ thermochronometric method to address these gaps in the geologic history.

$^{40}Ar/^{39}Ar$ DATING

Two of 21 samples previously collected and dated by apatite and zircon fission-track techniques (O'Sullivan and others, 1995) were selected for this $^{40}Ar/^{39}Ar$ study. By using samples previously analyzed, the dating methods and determination of thermal histories at different locations in the batholith can be directly compared. The samples chosen are from the highest elevation (88POS81-a; 2,470 m) and lowest elevation (88POS89-a; 1,091 m) along a vertical transect in the center of the batholith (fig. 1). These two samples are separated by ~1,400 m of elevation and are roughly the same distance from the north margin of the batholith. The elevation difference should easily show the thermal gradients within the batholith.

For each sample, biotite and potassium feldspar separates were dated by the $^{40}Ar/^{39}Ar$ step-heating method by using a Nuclide mass-spectrometer system with an "on-line" resistance-style furnace (see Solie and Layer, 1993, and West, 1994, for analytical details). Samples were irradiated with the mineral standard MMhb-1 with an age of 513.9 Ma (Samson and Alexander, 1987; Lanphere and others, 1990) and processed by using the decay constants of Steiger and Jaeger (1977), following procedures outlined in McDougall and Harrison (1988). Analytical data for biotite and feldspar samples from 88POS81-a and 88POS89-a are shown in table 1. Biotite samples were step heated at seven to nine temperature steps from 400°C to sample fusion at 1,600°C. Potassium feldspar samples were step heated in a more complex fashion following procedures outlined in Lovera and others (1989) with ~45 fractions extracted. Key components of the heating schedule are isothermal steps that are repeat steps at the same temperature with a cycled heating schedule, where heating steps are gradually increased in temperature, reduced to a lower temperature step with a long heating time, and then once again followed by a gradual increase in temperature. This complex heating schedule (table 1) allows the structure of argon retention in feldspars to be more easily determined.

BIOTITE INTERPRETATION

$^{40}Ar/^{39}Ar$ analyses on biotites from all samples analyzed yield simple age spectra with flat plateaus of ~60 Ma with little or no argon loss (fig. 2; table 2). The biotite shows varying amounts of chlorite alteration, and the amount of chlorite present varies throughout the batholith. The plateau age is similar to previous K-Ar and U-Pb lower intercept ages (Dillon and others, 1987) and is interpreted to represent the time when biotite cooled through its argon closure temperature (~300°C) in response to an early Cenozoic thermal event. These ages are markedly older than apatite fission-track ages of ~41-25 Ma, which are interpreted to reflect two periods of rapid cooling below temperatures of ~110°C to ~60°C (O'Sullivan, 1993; O'Sullivan and others, 1995) (table 2).

POTASSIUM FELDSPAR THERMOCHRONOMETRY

The potassium feldspar age spectra show far more complexity than the biotite spectra (fig. 2). Characteristics of the spectra are very old ages at lower temperatures (generally at less than 0.2 fraction of ^{39}Ar released), lows or saddles at ~50 Ma (at ~0.2 to 0.3 fraction of ^{39}Ar released), and complex stair-step rises to a plateaus at 100 to 120 Ma. All these features have been observed in feldspars elsewhere and are indicative of complex thermal histories (for example, Lovera and others, 1989, 1991; West 1994).

THE EFFECT OF INCLUSIONS

The first 20 percent of gas release in both feldspar samples is marked by anomalously old ages characteristic of excess argon. Harrison and others (1994) have attributed this to the presence of fluid inclusions in feldspar that contain argon and chlorine, although the exact source of the fluid is not discussed. Through the use of isothermal steps at low temperatures, the effect of argon in these inclusions can be modeled. Harrison and others (1994) observed a quantitative correlation between the release of excess radiogenic argon ($^{40}Ar^*$) and of excess ^{38}Ar, which is produced from chlorine during the irradiation of the sample. The ratio of chlorine-derived ^{38}Ar to ^{39}Ar is proportional to $\Delta Cl/K$, allowing for a correction in the low-temperature part of the age spectra. Figure 3 shows a plot of excess argon ($\Delta^{40}Ar^*/K$) versus excess chlorine ($\Delta Cl/K$) in samples 88POS81-a and 88POS89-a. For each sample,

the slope is close enough to unity to merit application of the chlorine correction for excess argon in the low-temperature part of the age spectra. The ΔCl/K value for 88POS89-a is slightly higher than that of the other sample, indicative of a different (younger) cooling age for this sample. The effect of this "fluid inclusion" argon is much greater than that observed in simpler cases (for example, the McKinley pluton; West, 1994), perhaps attesting to the complex history (that is, involvement of hydrothermal fluids in a metamorphic event) of the

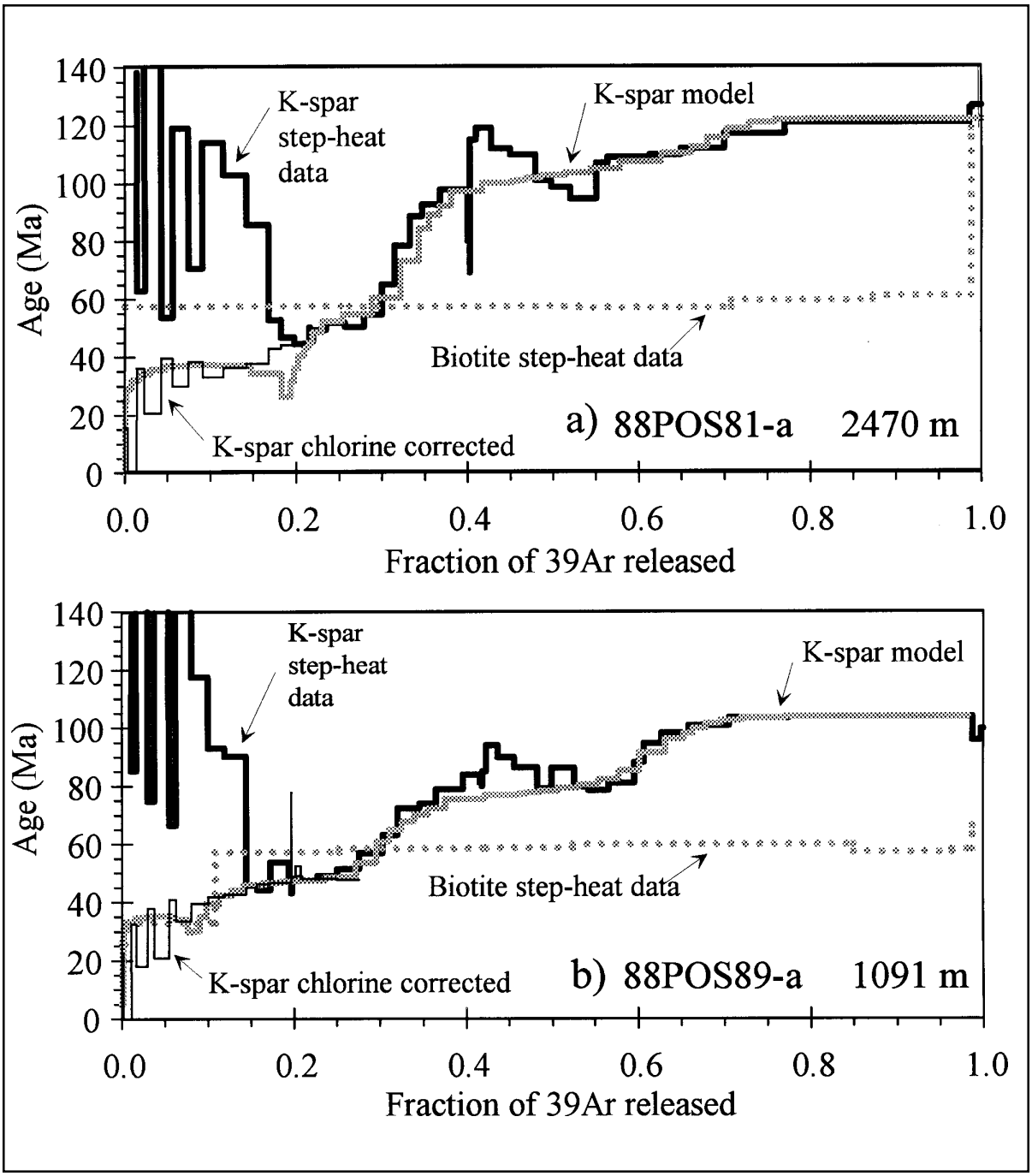

Figure 2. *Age spectra plots for biotite and potassium feldspar from samples 88POS81-a from 2,740 m (a) and 88POS89-a from 1,091 m (b). Anomalous old ages at <0.1 and between 0.4 and 0.5 fraction of ^{39}Ar released in the potassium feldspar age spectra (deviations from the model) are explained by argon trapped in inclusions in the mineral. Modeling of the relationship between chlorine and argon allows for correcting for this effect. The model spectrum represents the best fit to the data based on the diffusion parameters determined through thermochronometric modeling (Lovera and others, 1989; 1991).*

Table 1. *$^{40}Ar/^{39}Ar$ step heat analyses of biotite and potasium feldspar from the Okpilak Batholith*

88POS81-a Biotite
Mass=0.0854 g
Weighted average of J from standards = 0.007579 +/- 0.000054

Temp.[a] (°C)	Time[b] (min)	Cumulative[c] ^{39}Ar	$^{40}Ar/^{39}Ar$[d] measured	$^{37}Ar/^{39}Ar$[d] measured	$^{36}Ar/^{39}Ar$[d] measured	Volume ^{39}Ar[e] x 10^{-12} mol/g	% Atmos.[f] ^{40}Ar	$^{40}Ar^*/^{39}Ar_K$[g]	+/-	Age[h] (Ma)	+/- (Ma)
700	20	0.2624	4.546	0.015	0.001	36.158	6.441	4.226	0.017	56.9	0.2
800	20	0.5305	4.261	0.008	0.000	36.948	0.332	4.219	0.017	56.8	0.2
900	20	0.7082	4.244	0.015	0.000	24.495	0.444	4.197	0.025	56.5	0.3
1000	20	0.8727	4.424	0.044	0.000	22.665	0.559	4.371	0.027	58.8	0.4
1100	20	0.9881	4.531	0.207	0.000	15.899	0.028	4.502	0.038	60.5	0.5
1200	20	0.9960	9.177	4.921	0.002	1.089	2.746	8.926	0.550	118.1	7.0
1600	20	1.0000	18.092	9.247	0.013	0.553	16.635	15.150	1.087	196.1	13.3
Integrated			4.486	0.116	0.000	137.807	2.283	4.355	0.012	58.6	0.4

88POS81-a K-spar
Mass=0.2558 g
Weighted average of J from standards = 0.008060 +/- 0.000040

Temp.[a] (°C)	Time[b] (min)	Cumulative[c] ^{39}Ar	$^{40}Ar/^{39}Ar$[d] measured	$^{37}Ar/^{39}Ar$[d] measured	$^{36}Ar/^{39}Ar$[d] measured	Volume ^{39}Ar[e] x 10^{-12} mol/g	% Atmos.[f] ^{40}Ar	$^{40}Ar^*/^{39}Ar_K$[g]	+/-	Age[h] (Ma)	+/- (Ma)
450	20	0.0015	214.938	0.014	0.165	0.459	22.733	166.056	0.468	1532.6	2.9
525	20	0.0031	35.257	0.003	0.056	0.499	46.878	18.714	0.295	253.5	3.7
525	20	0.0138	47.909	0.000	0.044	3.256	27.372	34.774	0.062	445.8	0.7
565	20	0.0228	10.443	0.004	0.020	2.729	57.902	4.384	0.054	62.7	0.8
565	20	0.0429	15.550	0.001	0.016	6.119	29.569	10.931	0.027	152.3	0.4
600	20	0.0557	5.749	0.002	0.007	3.877	34.955	3.721	0.038	53.3	0.5
600	20	0.0741	10.710	0.002	0.008	5.624	21.348	8.401	0.028	118.2	0.4
600	20	0.0907	6.434	0.003	0.005	5.058	23.113	4.925	0.029	70.2	0.4
640	20	0.1147	9.879	0.002	0.006	7.291	18.102	8.068	0.022	113.7	0.3
670	20	0.1421	8.809	0.003	0.005	8.353	17.295	7.261	0.019	102.6	0.3
700	20	0.1684	7.133	0.003	0.004	7.988	15.446	6.007	0.019	85.3	0.3
700	20	0.1821	4.103	0.004	0.001	4.160	10.074	3.664	0.035	52.5	0.5
700	40	0.1980	3.565	0.003	0.001	4.851	8.828	3.224	0.030	46.3	0.4
700	75	0.2087	3.324	0.003	0.001	3.262	6.682	3.075	0.045	44.2	0.6
600	980	0.2151	4.523	0.002	0.005	1.937	31.520	3.078	0.075	44.2	1.1
675	20	0.2157	3.062	0.020	-0.001	0.184	-14.525	3.474	0.794	49.8	11.2
750	20	0.2205	3.425	0.002	0.001	1.458	7.184	3.152	0.100	45.3	1.4
790	20	0.2345	3.732	0.004	0.001	4.279	7.983	3.407	0.034	48.9	0.5
830	20	0.2575	3.979	0.005	0.001	6.980	9.463	3.577	0.021	51.3	0.3
860	20	0.2790	3.786	0.005	0.001	6.544	7.477	3.476	0.023	49.9	0.3
890	20	0.3000	4.176	0.007	0.001	6.417	8.711	3.786	0.023	54.2	0.3
890	20	0.3151	5.128	0.006	0.002	4.586	11.225	4.527	0.032	64.7	0.5
920	20	0.3333	6.483	0.005	0.003	5.542	15.004	5.486	0.027	78.1	0.4
920	20	0.3466	7.367	0.005	0.004	4.051	15.471	6.203	0.037	88.0	0.5
920	40	0.3676	7.849	0.004	0.004	6.382	16.938	6.496	0.024	92.1	0.3
920	210	0.4010	8.538	0.003	0.006	10.175	19.213	6.874	0.016	97.3	0.2
750	2010	0.4027	12.123	-0.001	0.022	0.506	53.598	5.612	0.289	79.8	4.0
840	30	0.4030	6.762	0.018	0.007	0.097	28.617	4.806	1.511	68.6	21.2
940	25	0.4105	10.132	0.004	0.007	2.274	19.962	8.087	0.065	113.9	0.9
980	20	0.4281	10.562	0.005	0.007	5.367	20.308	8.394	0.029	118.1	0.4
1010	20	0.4497	9.670	0.004	0.006	6.564	18.084	7.898	0.024	111.3	0.3
1040	20	0.4796	9.355	0.004	0.005	9.096	16.753	7.764	0.018	109.5	0.2
1040	20	0.4982	8.454	0.005	0.004	5.682	15.379	7.129	0.027	100.8	0.4
1040	40	0.5201	8.074	0.004	0.004	6.668	13.904	6.927	0.023	98.0	0.3
1040	80	0.5507	7.592	0.004	0.003	9.317	12.342	6.630	0.017	93.9	0.2
1070	20	0.5637	8.669	0.003	0.004	3.946	12.987	7.518	0.038	106.1	0.5
1100	20	0.5853	8.818	0.004	0.004	6.563	12.284	7.710	0.024	108.8	0.3
1125	20	0.6132	8.701	0.004	0.003	8.512	11.472	7.678	0.019	108.3	0.3
1150	20	0.6500	8.658	0.002	0.003	11.182	10.327	7.738	0.015	109.2	0.2
1175	20	0.7003	8.744	0.002	0.003	15.318	9.354	7.900	0.012	111.4	0.2
1200	20	0.7712	9.061	0.000	0.003	21.573	8.552	8.259	0.011	116.3	0.1
1300	20	0.9863	9.390	0.000	0.003	65.492	8.680	8.548	0.009	120.2	0.1
1450	20	0.9892	10.350	0.022	0.005	0.886	13.533	8.925	0.165	125.3	2.2
1650	20	1.0000	11.015	0.004	0.007	3.276	18.316	8.974	0.046	126.0	0.6
Integrated			9.051	0.002	0.005	304.381	15.364	7.636	0.004	107.8	0.5

88POS89-a Biotite
Mass=0.0908 g
Weighted average of J from standards = 0.007579 +/- 0.000054

Temp.[a] (°C)	Time[b] (min)	Cumulative[c] ^{39}Ar	$^{40}Ar/^{39}Ar$[d] measured	$^{37}Ar/^{39}Ar$[d] measured	$^{36}Ar/^{39}Ar$[d] measured	Volume ^{39}Ar[e] x 10^{-12} mol/g	% Atmos.[f] ^{40}Ar	$^{40}Ar^*/^{39}Ar_K$[g]	+/-	Age[h] (Ma)	+/- (Ma)
400	20	0.0037	12.917	0.204	0.037	0.338	85.026	1.930	1.661	26.2	22.4
600	20	0.1086	3.784	0.085	0.004	9.453	35.031	2.440	0.060	33.1	0.8
700	20	0.2516	4.768	0.122	0.002	12.900	10.021	4.265	0.044	57.4	0.6
800	20	0.4228	4.597	0.037	0.001	15.442	4.618	4.357	0.050	58.6	0.7
900	20	0.5234	4.639	0.056	0.001	9.076	5.224	4.370	0.062	58.8	0.8
1000	20	0.8489	4.636	0.060	0.000	29.349	3.086	4.465	0.020	60.0	0.3
1100	20	0.9644	4.392	0.443	0.000	10.420	2.141	4.271	0.054	57.5	0.7
1200	20	0.9876	4.847	2.735	0.002	2.090	10.219	4.334	0.270	58.3	3.6
1600	20	1.0000	6.528	2.244	0.006	1.121	24.291	4.928	0.501	66.2	6.6
Integrated			4.590	0.201	0.001	90.190	8.667	4.167	0.020	56.1	0.5

[a]Step-heating temperature.
[b]Duration of time at a particular temperature (in minutes).
[c]Normalized volume of ^{39}Ar released.
[d]Isotopic ratios corrected for system blank and decay of ^{37}Ar.
[e]Incremental volume of ^{39}Ar released in moles per gram of sample.
[f]Percentage of atmospheric argon in the sample assuming the atmospheric $^{40}Ar/^{36}Ar$ ratio = 295.5.
[g]Ratio of radiogenic ^{40}Ar to ^{39}Ar produced from potassium (with 1§ error).
[h]Radiometric age of sample in Ma (with 1§ error).

Table 1. *$^{40}Ar/^{39}Ar$ step heat analyses of biotite and potasium feldspar from the Okpilak Batholith—Continued*

88POS89-a K-Spar
Mass=0.2723 g
Weighted average of J from standards = 0.008060 +/- 0.000040

Temp.[a] (°C)	Time[b] (min)	Cumulative[c] ^{39}Ar	$^{40}Ar/^{39}Ar$[d] measured	$^{37}Ar/^{39}Ar$[d] measured	$^{36}Ar/^{39}Ar$[d] measured	Volume ^{39}Ar[e] x 10^{-12} mol/g	% Atmos.[f] ^{40}Ar	$^{40}Ar^*/^{39}Ar_K$[g]	+/-	Age[h] (Ma)	+/- (Ma)
450	20	0.0013	203.768	0.030	0.142	0.409	20.637	161.696	0.479	1505.3	3.0
450	20	0.0023	31.219	0.022	0.040	0.310	37.627	19.454	0.445	262.8	5.6
525	20	0.0107	56.365	0.005	0.033	2.592	17.155	46.672	0.075	576.1	0.8
525	20	0.0165	9.751	0.009	0.013	1.797	38.339	5.995	0.077	85.1	1.1
565	20	0.0298	17.678	0.005	0.010	4.093	17.328	14.591	0.037	200.6	0.5
565	20	0.0376	6.602	0.010	0.005	2.408	20.342	5.236	0.057	74.6	0.8
600	20	0.0547	15.690	0.009	0.007	5.295	12.763	13.663	0.030	188.5	0.4
600	20	0.0627	5.459	0.019	0.003	2.461	14.495	4.643	0.056	66.3	0.8
640	20	0.0810	13.374	0.021	0.006	5.668	12.219	11.714	0.027	162.8	0.4
670	20	0.0999	9.471	0.027	0.004	5.840	11.497	8.357	0.025	117.6	0.3
700	20	0.1191	7.357	0.013	0.003	5.927	10.543	6.555	0.024	92.9	0.3
730	20	0.1438	7.106	0.007	0.002	7.626	10.256	6.351	0.019	90.1	0.3
730	20	0.1567	3.371	0.006	0.001	3.972	4.438	3.194	0.035	45.9	0.5
730	40	0.1722	3.276	0.006	0.001	4.777	5.246	3.077	0.029	44.2	0.4
730	75	0.1935	3.996	0.004	0.001	6.582	5.850	3.735	0.021	53.5	0.3
600	995	0.1963	6.647	0.004	0.011	0.883	50.337	3.287	0.155	47.2	2.2
675	20	0.1967	2.766	0.016	-0.001	0.123	-9.417	2.995	1.119	43.0	15.9
750	20	0.2018	3.384	0.005	0.000	1.584	1.512	3.304	0.087	47.4	1.2
790	20	0.2068	3.240	0.004	-0.001	1.523	-4.728	3.363	0.090	48.3	1.3
830	20	0.2268	3.447	0.005	0.000	6.189	3.286	3.306	0.022	47.5	0.3
860	20	0.2497	3.568	0.005	0.000	7.081	3.559	3.414	0.020	49.0	0.3
890	20	0.2751	3.803	0.005	0.001	7.846	5.145	3.581	0.018	51.3	0.3
920	20	0.3023	4.291	0.006	0.001	8.397	6.780	3.973	0.017	56.9	0.2
920	20	0.3202	4.762	0.005	0.001	5.527	6.865	4.408	0.025	63.0	0.4
950	20	0.3456	5.588	0.005	0.002	7.854	8.861	5.066	0.018	72.2	0.3
950	20	0.3641	5.691	0.005	0.002	5.703	8.626	5.174	0.025	73.7	0.3
950	40	0.3956	6.158	0.005	0.002	9.725	9.753	5.532	0.015	78.7	0.2
950	160	0.4162	6.629	0.004	0.002	6.360	10.721	5.893	0.022	83.7	0.3
750	1030	0.4183	11.216	0.005	0.019	0.667	49.090	5.696	0.206	81.0	2.9
840	30	0.4187	4.953	0.015	-0.002	0.116	-13.680	5.598	1.178	79.6	16.4
940	25	0.4235	6.599	0.004	0.002	1.487	8.987	5.980	0.092	84.9	1.3
980	20	0.4362	7.433	0.006	0.003	3.924	10.537	6.624	0.036	93.8	0.5
1010	20	0.4559	7.077	0.006	0.002	6.074	10.061	6.339	0.023	89.9	0.3
1040	20	0.4826	6.761	0.006	0.002	8.261	9.622	6.085	0.018	86.4	0.2
1070	20	0.4995	6.107	0.005	0.002	5.194	8.497	5.562	0.027	79.1	0.4
1070	20	0.5254	6.660	0.006	0.002	8.007	8.419	6.073	0.018	86.2	0.3
1070	20	0.5420	6.071	0.006	0.002	5.126	7.469	5.591	0.027	79.5	0.4
1070	40	0.5654	5.927	0.004	0.001	7.226	6.603	5.509	0.020	78.4	0.3
1070	80	0.5951	6.078	0.004	0.001	9.171	6.081	5.681	0.016	80.8	0.2
1100	20	0.6065	6.615	0.003	0.001	3.526	5.838	6.202	0.039	88.0	0.5
1125	20	0.6266	7.126	0.004	0.001	6.227	6.005	6.671	0.023	94.5	0.3
1150	20	0.6579	7.415	0.003	0.002	9.660	6.217	6.927	0.016	98.0	0.2
1175	20	0.7052	7.614	0.002	0.002	14.600	6.105	7.122	0.012	100.7	0.2
1200	20	0.7746	7.829	0.001	0.002	21.434	6.172	7.319	0.010	103.4	0.1
1300	20	0.9871	7.876	0.000	0.002	65.658	6.363	7.348	0.008	103.8	0.1
1450	20	0.9969	7.991	0.007	0.004	3.002	15.150	6.756	0.046	95.7	0.6
1650	20	1.0000	10.937	0.011	0.013	0.971	35.506	7.035	0.142	99.5	1.9
Integrated			7.738	0.005	0.003	308.882	9.872	6.948	0.004	98.3	0.5

[a]Step-heating temperature.
[b]Duration of time at a particular temperature (in minutes).
[c]Normalized volume of ^{39}Ar released.
[d]Isotopic ratios corrected for system blank and decay of ^{37}Ar.
[e]Incremental volume of ^{39}Ar released in moles per gram of sample.
[f]Percentage of atmospheric argon in the sample assuming the atmospheric $^{40}Ar/^{36}Ar$ ratio = 295.5.
[g]Ratio of radiogenic ^{40}Ar to ^{39}Ar produced from potassium (with 1§ error).
[h]Radiometric age of sample in Ma (with 1§ error).

Okpilak batholith. By using the "chlorine correction," a model age spectrum can be constructed that removes the effect of excess argon (fig. 2). A similar effect of excess argon is also seen at ~0.4 fraction of ^{39}Ar released. This excess argon correlates well with chlorine (fig. 3) and is taken into account in the modeling discussed below.

MULTIPLE DIFFUSION DOMAINS

Once the age spectrum is "corrected" for the effects of excess argon, it can be modeled by using the techniques of Lovera and others (1989). This modeling involves calculating the diffusion of ^{39}Ar out of the sample as a function of temperature and determining diffusion parameters that best fit the data. Potassium feldspars consist of "diffusion domains," which trap and release argon independently. Analysis of feldspars has shown that there are discrete domain sizes in the minerals (Fitz Gerald and Harrison, 1993), and they can be used to calculate cooling histories and model age spectra—although there is some debate about the validity of the method (Villa, 1996).

Arrhenius diagrams were calculated for each sample by using the computer code developed by Lovera (1992) (fig. 4), which determines diffusion parameters and volume fractions for the various diffusion domains. In general, the best fits for both the Arrhenius plots and age spectra were for models with the same number (or one greater) of domains as heating cycles. The activation energy (E_a), frequency factor (D_0), and relative domain sizes are determined by fitting the Arrhenius plot. For each of the samples, four diffusional domains were isolated (fig. 4). The diffusion parameters for the two samples are very similar and are shown in table 3.

The results from modeling the Arrhenius plots were then used to fit the age spectra (fig. 2). For each domain, initial ages and cooling rates are assigned based on a visual fit to the age spectrum. The model will find the best fit ages, cooling rates, and volume fraction of each domain. The smallest domains were difficult to fit because of the presence of excess $^{40}Ar^*$ in the lowest temperature fractions. The age of the first domain was determined by using the minimum age fraction, although the overwhelming excess argon from inclusions makes that age identification less precise. Both the older age "humps" caused by excess $^{40}Ar^*$ from inclusions were ignored in the fitting. The fit of the Arrhenius plot was checked again with the new volume fractions. If the fit was still satisfactory, the modeling was then complete. If not, new diffusion parameters and ages were picked and the modeling was rerun. The final result of the age spectrum modeling was cooling histories spanning ~30 Ma to 140 Ma and from 200°C to 400°C. The resultant cooling histories are relatively insensitive to changes in domain size and domain volume (and also to small changes in the frequency factor and E_a). However, they are sensitive to ages assigned to each domain and to the excess argon modeling.

Table 2. *Biotite $^{40}Ar/^{39}Ar$ and apatite fission-track ages*

	88POS81-a	**88POS89-a**
Sample elevation	2,470 m	1,091 m
Biotite plateau age	58.6 ± 0.5 Ma	56.1 ± 0.5 Ma
Apatite fission track age[a]	43.4 ± 2.8 Ma	31.8 ± 2.2 Ma

[a]O'Sullivan and others, 1995.

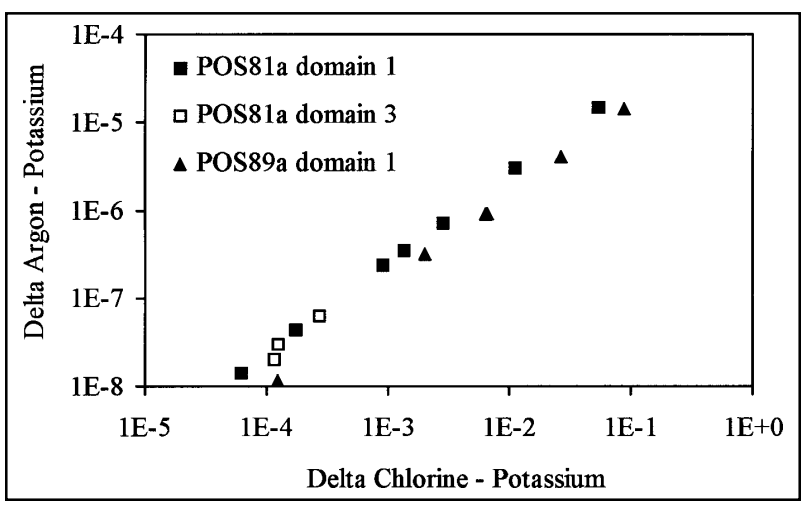

Figure 3. *Log-log plot of $\Delta^{40}Ar^*/K$ versus $\Delta Cl/K$ (Harrison and others, 1994) derived from samples 88POS81-a and 88POS89-a using isothermal steps between 450°C and 700°C.*

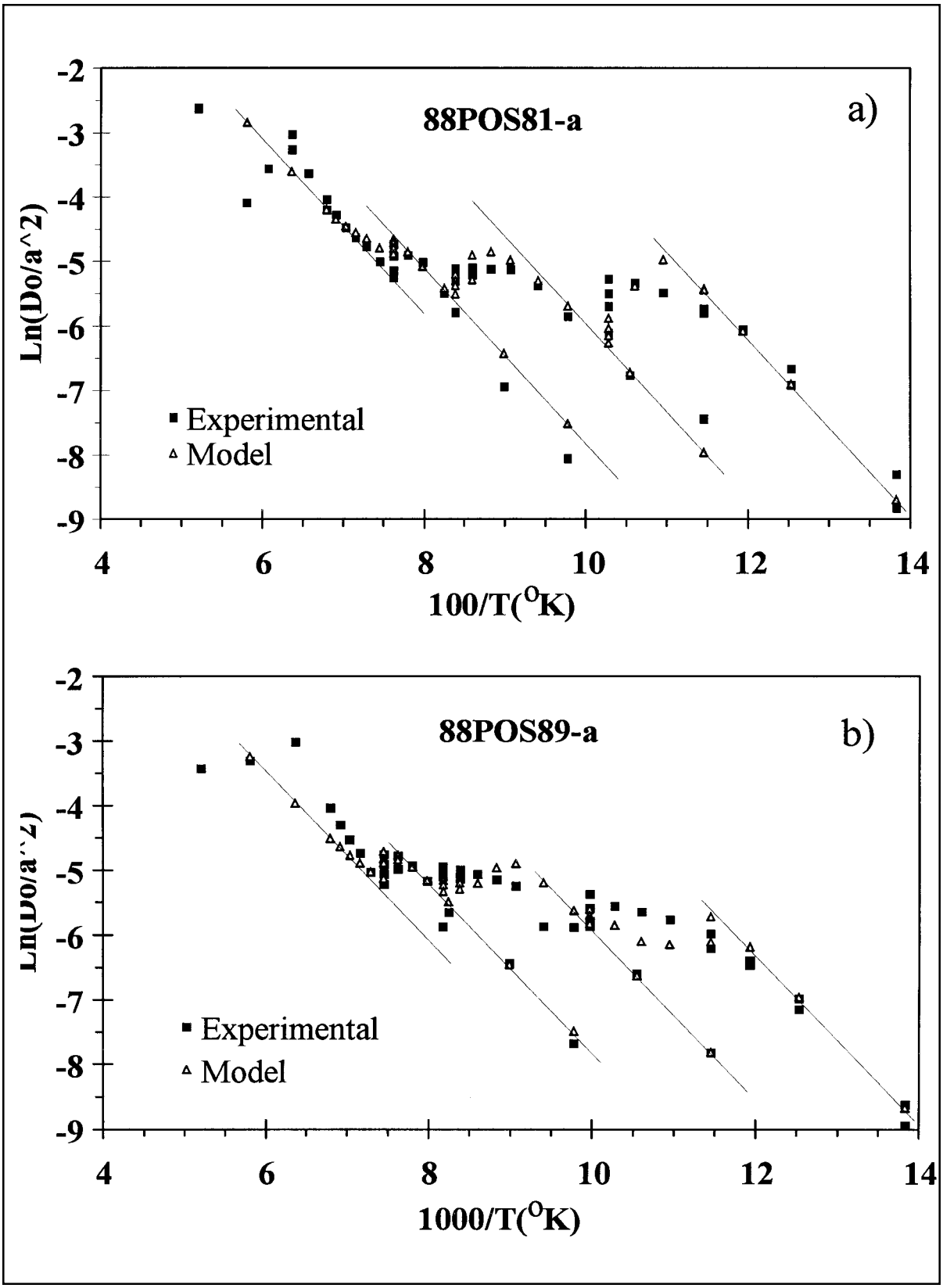

Figure 4. *Arrhenius plots for samples 88POS81-a (a) and 88POS89-a (b) determined from the cycled step heating experiments. The best-fit model Arrhenius plots are also shown. Line segments show trends for each domain.*

Table 3. *Best-fit diffusion parameters for Okpilak feldspars*

	88POS81-a	88POS89-a
Do (cm^2/s)	10.35	9.47
E (kcal/mol)	63	60
# of domains	4	4
Volume fraction in each domain		
domain 1	0.1134	0.0770
domain 2	0.1330	0.1871
domain 3	0.2060	0.2590
domain 4	0.5250	0.4770
Age of each domain (Ma)		
domain 1	38	37
domain 2	50	48
domain 3	100	75
domain 4	122	104
Size of domains relative to the first domain: $\log(r/r_1)$		
domain 1	0.00	0.00
domain 2	1.70	1.25
domain 3	2.45	2.25
domain 4	2.60	2.55

DISCUSSION

The diffusion parameters obtained from applying diffusion models proposed by Lovera and others (1989) to the feldspar age spectra result in cooling histories with different diffusion domains reflecting different parts of the cooling history (fig. 5a). These models can then be compared to each other and to other geologic and geochronologic information from the batholith. Samples 88POS81-a and 88POS89-a, which differ in elevation by ~1,400 m, show similar apparent cooling histories: an extended period of slow, gradual cooling for the more retentive domains, followed by more rapid cooling for the least retentive domain. Specifically, 88POS81-a shows gradual cooling from ~450°C at 140 Ma to ~300°C at ~40 Ma, followed by a period of rapid cooling to ~225°C at 30 Ma (fig. 5a). Similarly, 88POS89-a exhibits cooling from ~450°C at 130 Ma to ~270°C at 30 Ma, followed by rapid cooling from ~225°C at 30 Ma (fig. 5a).

The cooling histories for the two samples are statistically identical for the time period younger than 60 Ma and 300°C, which implies that the pluton was essentially isothermal (or cooling rapidly) during the time from ~60 Ma to 30 Ma. This is qualitatively similar to the results of O'Sullivan and others (1995); however, it indicates a cooling history that is different from that of O'Sullivan and others (1995) for ages younger than 45 Ma. The feldspar data indicate that rapid cooling occurred after 40 Ma, whereas the fission-track data indicate that cooling occurred before 40 Ma. For the K-spar, the model age of the youngest domain (with a closure temperature of ~225°C to 275°C) is most affected by excess argon in inclusions, as seen by the Cl/K analysis (fig. 3) and it is difficult to assign a reliable age to this domain. Therefore the age assigned to this domain may have been incorrect and the true age of this domain may be older. If this is the case and if the age of domain 1 is ~43 Ma to 45 Ma rather than ~37 Ma, the feldspar and fission-track cooling trajectories would be the same. In fact, it may be possible to use the detailed fission-track history to model the effect of inclusions on excess argon in the feldspar.

Excess argon is not present in domain 2 with an age of ~50 Ma, which allows us to have more confidence in the age assigned to that domain. Two models for the cooling history between 60 Ma and 45 Ma were proposed by O'Sullivan and others (1995). Our results from domains 2 and 3 imply that onset of uplift was rapid at ~45 Ma, thereby ruling out a model of gradual uplift from depth between 59 Ma and 43 Ma.

The cooling histories for the two samples for the time before 60 Ma follow parallel, but offset, paths. In figure 5a, the temperature for sample 88POS81-a is ~25°C below (cooler than) the temperature for sample 88POS89-a at any particular time. The elevation difference between the samples is 1.4 km. If we assume no tilting of the pluton, this elevation difference allows for calculation of a minimum geothermal gradient of ~20°C/km during that time. If the pluton was tilted during the thrusting event, the gradient would be higher.

As represented in figure 5a, the modeled cooling paths for domain 4 in the feldspar start at temperatures of ~450°C. This is a very high temperature and, based on geologic and petrologic evidence (for example, Hanks and Wallace, 1990), it is doubtful that the pluton was ever buried to a depth of 20 km or greater. The diffusion modeling programs of Lovera and others (1989) assume a simple cooling history for a feldspar from intrusion to uplift, which may not apply to the Okpilak batholith. An alternate explanation for age information in the highest temperature domains is that they preserve or retain radiogenic argon from the long history of the pluton from its intrusion at 380 Ma, its unroofing at ~340 Ma, and its subsequent reburial (fig. 5b). The sample from the higher elevation (88POS81-a) has older apparent ages for these domains, which would be consistent with the fact that this sample was cooler than the lower sample (88POS89-a) and, hence, lost less of this radiogenic argon. Additional "forward" modeling of the age spectra beginning with a thermal history is necessary to better unravel the "complete" thermal history of the Okpilak batholith (Zeitler and Warnock, 1992).

Thermochronometric modeling of the Okpilak batholith produces a cooling-history model that is

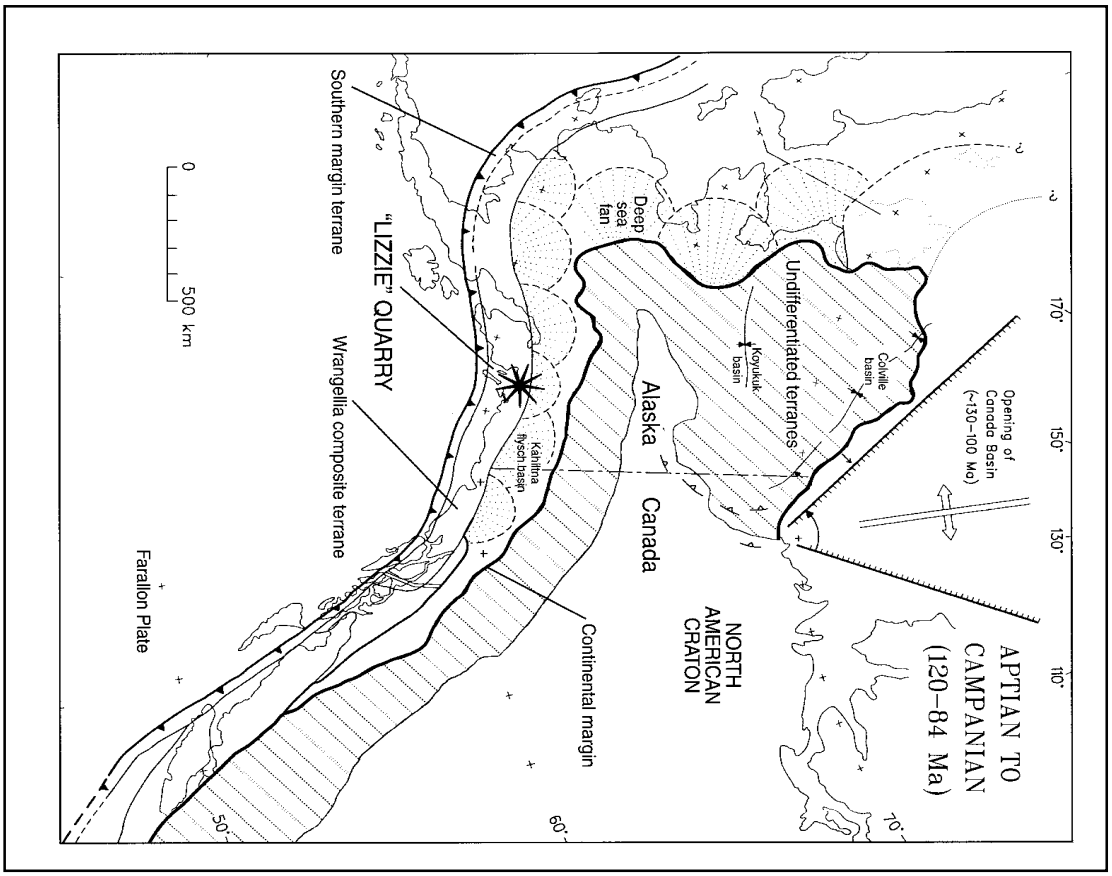

Figure 5. *(a) Cooling history for samples 88POS81-a and 88POS89-a from the Okpilak batholith obtained from feldspar thermochronometric modeling. For each sample, the cooling segments determined for the four diffusional domains from each sample are shown. The segments are not connected, however for each feldspar sample, a smoothly varying cooling path can be constructed. Also shown are the biotite $^{40}Ar/^{39}Ar$ plateau age (this study), and apatite and zircon fission track ages and cooling path from O'Sullivan and others (1995) using closure temperature values from Wagner and Van den Haute (1992). (b) Long-term cooling history from the time of batholith intrusion. U-Pb age is from Dillon and others (1987). Dashed line shows a possible cooling history reflecting exposure of the batholith at the surface in Mississippian time (LePain and others, 1994).*

qualitatively consistent with previous geochronologic evidence. The complex history of the batholith poses problems that make direct application of the technique difficult. Excess argon in the feldspar, perhaps in fluid inclusions, masks the preservation of the low-temperature part of the thermal history of the feldspar, whereas "memory" of intrusion and burial may complicate the high-temperature interpretation. Despite these complications, application of the thermochronometric approach to the Okpilak batholith more fully refines the history of this unique geologic setting.

ACKNOWLEDGMENTS

We thank Paul O'Sullivan and Wesley Wallace for providing samples for analysis, Oscar Lovera for the modeling code, Jeff Drake for laboratory assistance and moral support and Cathy Hanks for helpful discussions. We thank Chris Nye and Paul O'Sullivan for constructive reviews of the manuscript. This work was completed by J. Paegle under grant EAR93-22471 from NSF for the Research Experience for Undergraduates program at the Geophysical Institute, University of Alaska Fairbanks.

REFERENCES CITED

Bader, J.W., and Bird, K.J., 1986, Geologic map of the Demarcation Point, Mt. Michelson, Flaxman Island, and Barter Island quadrangles, northeastern Alaska: U.S. Geological Survey Miscellaneous Investigation Series I-1791, scale 1:250,000, 1 sheet.

Bird, K.J., and Molenaar, C.M., 1987, Stratigraphy, *in* Bird, K.J. and Magoon, L.B., eds., Petroleum geology of the northern part of the Arctic National Wildlife Refuge, northeastern Alaska: U.S. Geological Survey Bulletin 1778, p. 37-59.

Copeland, P., Harrison, T.M., Yun, P., Kidd, W.S.F., Roden, M., and Yuquan, Z., 1995, Thermal evolution of the Gangdese batholith, southern Tibet: A history of episodic unroofing, Tectonics, v. 12, p. 223-236.

Dillon, J.T., Tilton, G.R., Decker, J., and Kelly, M.J., 1987, Resource implications of magmatic and metamorphic ages for Devonian igneous rocks in the Brooks Range, *in* Tailleur, I.L., and Weimer, P., eds., Alaskan North Slope geology: Society of Economic Paleontologists and Mineralogists, Pacific Section Publication 50, p. 713-723.

Fitz Gerald, J.D., and Harrison, T.M., 1993, Argon diffusion domains in K-Feldspar I: Microstructures in MH-10, Contributions to Mineralogy and Petrology, v. 113, p. 367-380.

Hanks, C.L., 1993, The Cenozoic structural evolution of a fold and thrust belt, northeastern Brooks Range, Alaska: Geological Society of America Bulletin, v. 105, p. 287-305.

Hanks, C.L., and Wallace, W.K., 1990, Cenozoic thrust emplacement of a Devonian batholith, northeastern Brooks Range: Involvement of crystalline rocks in a foreland fold-and-thrust belt: Geology, v. 18, p. 395-398.

Harrison, T.M., Heizler, M.T., Lovera, O.M., Wenji, C., and Grove, M., 1994, A chlorine disinfectant for excess argon released from K-feldspar during step heating: Earth and Planetary Science Letters, v. 123, p. 94-104.

Lanphere, M.O., Dalrymple, G.B., Fleck, R.J., and Pringle, M.S., 1990, Intercalibration of mineral standards for K-Ar and $^{40}Ar/^{39}Ar$ age measurements (abstract): EOS, Transactions of the American Geophysical Union, v. 71, p. 1,658.

LePain, D.L., Crowder, R.K., and Wallace, W.K., 1994, Early Carboniferous transgression on a passive continental margin: Deposition of the Kekikutuk Conglomerate, northeastern Brooks Range, Alaska: American Association of Petroleum Geologists Bulletin, v. 78, p. 679-699.

Lovera, O.M., 1992, Computer programs to model $^{40}Ar/^{39}Ar$ diffusion data in multidomain samples: Computers and Geosciences, v. 18, p. 789-813.

Lovera, O.M., Heizler, M.T., and Harrison, T.M., 1993, Argon diffusion domains in K-feldspar II: Kinetic properties of MH-10: Contributions to Mineralogy and Petrology, v. 113, p. 381-393.

Lovera, O.M., Richter, F.M., and Harrison, T.M., 1989, The $^{40}Ar/^{39}Ar$ thermochronometry for slowly cooled samples having a distribution of diffusion domain sizes: Journal of Geophysical Research, v. 94, p. 17,917-17,935.

———1991, Diffusion domains determined by ^{39}Ar released during step heating: Journal of Geophysical Research, v. 96, p. 2,057-2,069.

McDougall, I., and Harrison, T.M., 1988, Geochronology and thermochronology by the $^{40}Ar/^{39}Ar$ method: New York, Oxford University Press, 212 p.

Molenaar, C.M., Bird, K.J., and Kirk, A.R., 1987, Cretaceous and Tertiary stratigraphy of northeastern Alaska, *in* Tailleur, I.L., and Weimer, P., eds., Alaskan North Slope geology: Society of Economic Paleontologists and Mineralogists, Pacific Section, Book 50, p. 513-528.

Mull, C.G., 1985, Cretaceous tectonics, depositional cycles, and the Nanushuk Group, Brooks Range, and Arctic Slope, Alaska, *in* Huffman, A.C., Jr. ed., Geology of the Nanushuk Group and related rocks, North Slope, Alaska: U.S. Geological Survey Bulletin 1614, p. 7-36.

O'Sullivan, P.B., 1993, Late Cretaceous and Tertiary thermal and uplift history of the North Slope foreland basin of northern Alaska and Canada: Ph.D. thesis, Latrobe University, Melbourne, Australia, 419 p.

O'Sullivan, P.B., Green, P.F., Bergman, S.C., Decker, J., Duddy, I.R., Gleadow, A.J.W., and Turner, D.L., 1993, Multiple phases of Tertiary uplift and erosion in the Arctic National Wildlife Refuge, Alaska, revealed by apatite fission track analysis: The American Association of Petroleum Geologists Bulletin, v. 77, p. 359-385.

O'Sullivan, P.B., Hanks, C.L., Wallace, W.K., and Green, P.F., 1995, Multiple episodes of Cenozoic uplift and erosion in the northeastern Brooks Range: Fission track data from the Okpilak batholith, Alaska, Canadian Journal of Earth Sciences, v. 32, n. 8, p. 1,106-1,118.

Reiser H.N., Brosgé, W.P., Dutro, J.T., Jr., and Detterman, R.L., 1980, Geologic map of the Demarcation Point quadrangle, Alaska: U.S. Geological Survey Miscellaneous Investigations Map I-1133, scale 1:250,000.

Richter, F.M., Lovera, O.M., Harrison, T.M., and Copeland, P., 1991, Tibetan tectonics from $^{40}Ar/^{39}Ar$ analysis of a single K-feldspar sample: Earth and Planetary Science Letters, v. 105, p. 266-278.

Sable, E.G., 1977, Geology of the western Romanzof Mountains, Brooks Range, northeastern Alaska: U.S. Geological Survey Professional Paper 897, 84 p.

Samson, S.D., and Alexander, E.C., Jr., 1987, Calibration of the interlaboratory ^{40}Ar-^{39}Ar dating standard, MMhb-1: Chemical Geology (Isotope Geoscience section), v. 66, p. 27-34.

Solie, D.N., and Layer, P.W., 1993, The Hayes Glacier fault, southern Alaskan Range: Evidence for post-Paleocene movement, *in* Solie, D.N, and Tannian, F., eds., Short notes on Alaskan geology 1993: Alaska Division of Geological & Geophysical Surveys Professional Report 113, p. 71-80.

Steiger R.H., and Jaeger E., 1977, Subcommission on geochronology: Convention on the use of decay constants in geo- and cosmochronology: Earth and Planetary Science Letters, v. 36, p. 359-362.

Villa, I.M., 1996, Why must 1000 km-scale tectonic models take into account 100 nm-scale recoil? The ^{39}Ar fairy tale (abstract): EOS, Transactions of the American Geophysical Union, Spring 1996 Supplement, p. S93.

Wagner, G., and Van den Haute, P., 1992, Fission track dating: Boston, Kluwer Academic Publishers, 285 p.

Wallace, W.K., and Hanks, C.L., 1990, Structural provinces of the northeastern Brooks Range, Arctic National Wildlife Refuge, Alaska: The American Association of Petroleum Geologists Bulletin, v. 74, p. 1,100-1,118.

West, A.W., 1994, A petrologic and geochronologic study of the McKinley pluton, Alaska: Fairbanks, M.S. thesis, University of Alaska, 181 p.

Zeitler, P.K., and Warnock, A., 1992, Monte-Carlo inversion of $^{40}Ar/^{39}Ar$ age spectra: EOS, Transactions of the American Geophysical Union, Fall Meeting Supplement, v. 73, p. 641.

This page has intentionally been left blank.

FIRST OCCURRENCE OF A HADROSAUR (DINOSAURIA) FROM THE MATANUSKA FORMATION (TURONIAN) IN THE TALKEETNA MOUNTAINS OF SOUTH-CENTRAL ALASKA

by
Anne D. Pasch[1] and Kevin C. May[1]

INTRODUCTION

The recent discovery of a hadrosaur ("Lizzie") in the Talkeetna Mountains about 150 km northeast of Anchorage is of special interest for several reasons. It is the first known occurrence of a hadrosaur in south-central Alaska, adding a new high latitude locality (62°N) for dinosaurs (fig. 1). Lizzie is unique in that she represents the only association of dinosaur bones in Alaska that can be attributed to a single individual. A closely associated assemblage of marine invertebrates provides a reliable age of middle Turonian (early Late Cretaceous), making it one of the few well-dated early hadrosaurs known in the world. Its location in the Matanuska Formation makes it one of only four vertebrate fossils known from the Wrangellia composite terrane in south-central Alaska (fig. 2). Although dinosaur remains are uncommon in marine deposits, this hadrosaur is the second dinosaur to be found in the marine mudstones of the Matanuska Formation. The first, *Edmontonia*, a nodosaur recently described by Gangloff (1995), is of Campanian-Maastrichtian age, or at least 10 million yrs younger than the new find (fig. 3).

[1]Geology Department, University of Alaska Anchorage, 3211 Providence Drive, Anchorage, Alaska 99508-8338.

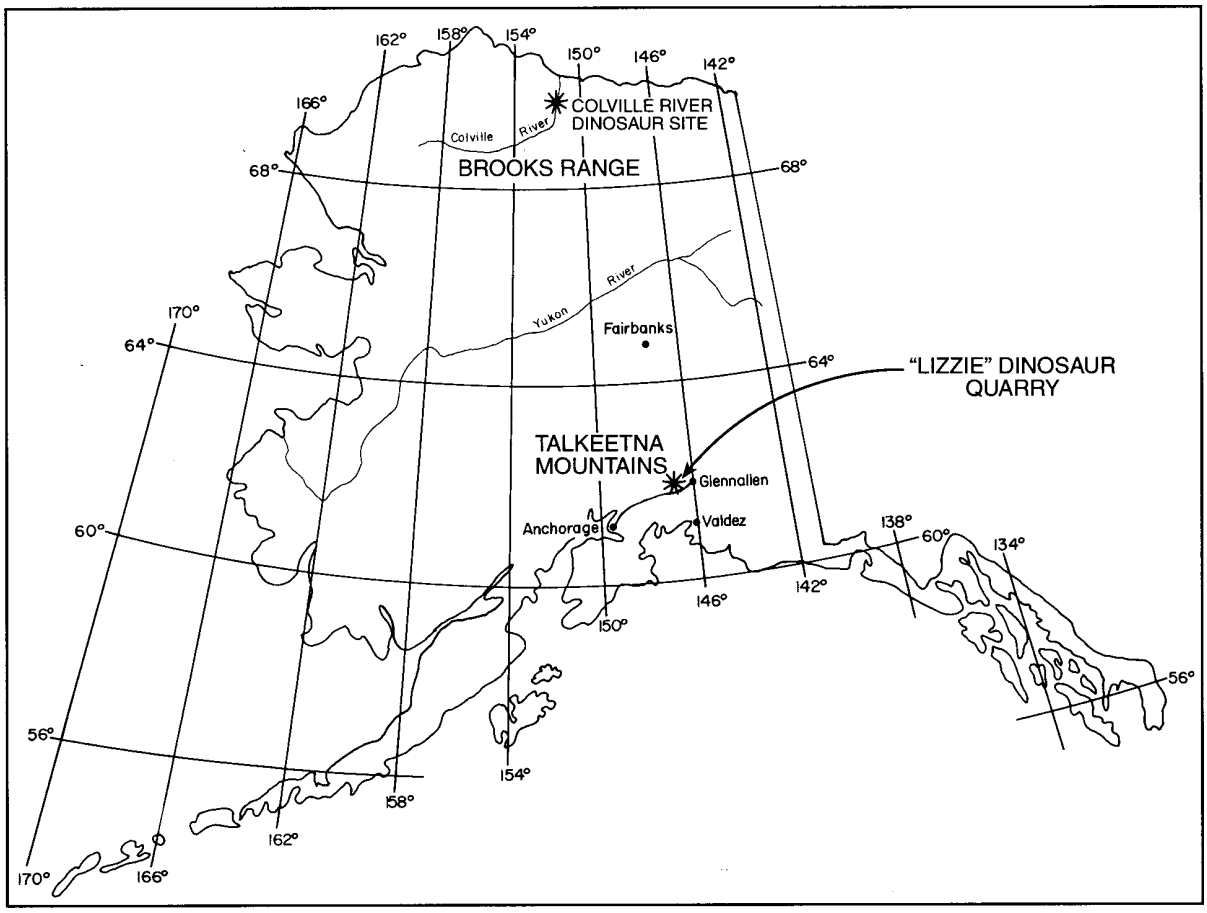

Figure 1. *Map of Alaska showing location of the Lizzie quarry in the Talkeetna Mountains of south-central Alaska.*

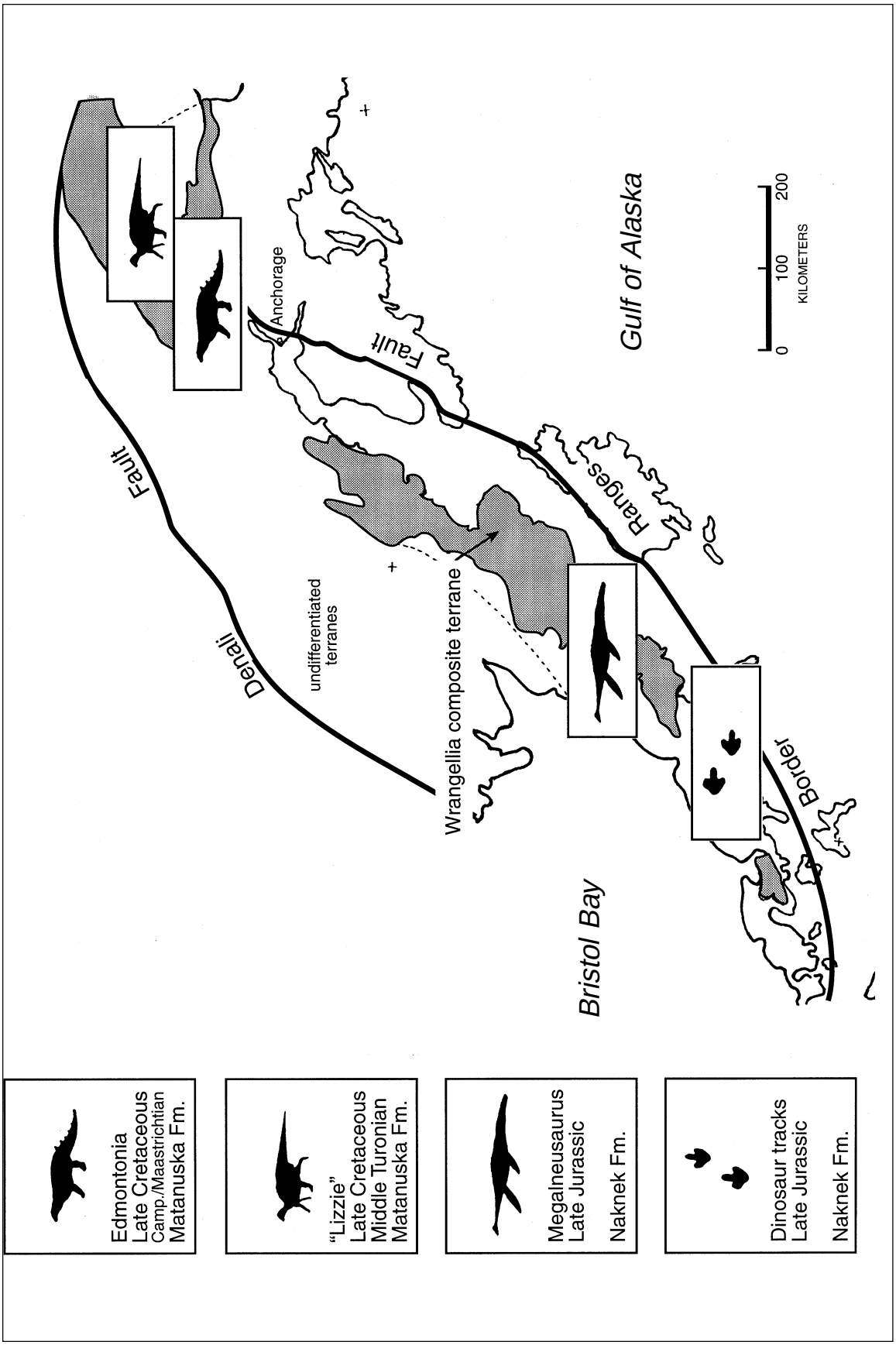

Figure 2. *The four fossil vertebrate localities in the Peninsular terrane of south-central Alaska (modified from Wallace, 1992, p. 53).*

BACKGROUND AND DISCOVERY

The hadrosaur fossil material was discovered by Virginia May in September 1994. Bone fragments lying in the rubble of a borrow pit led to the discovery of bone-bearing concretions in the bedrock. Centra of caudal vertebrae and distal elements of the limbs were later found in talus beneath the quarry face. During the summer of 1995 a quarry of 24 sq m was excavated. However, the main efforts were concentrated in a 4-sq-m quadrant containing a large concretion nearly 1 m long with bone fragments exposed along its edges. The alignment of the limb bones suggests that this concretion may contain pelvic bones. These would be the most diagnostic postcranial elements for identification to the generic level. Hundreds of invertebrate fossils were excavated along with the bone-bearing concretions.

Because of high public interest in this discovery, the fossil was given a popular name, Lizzie, after Kevin May's 12-yr-old daughter, who contributed many hours to the excavation project.

LOCATION AND GEOLOGIC SETTING

The privately owned borrow pit is situated in the Talkeetna Mountains in south-central Alaska near the Glenn Highway at about lat 61°52'N and long 147°21'W

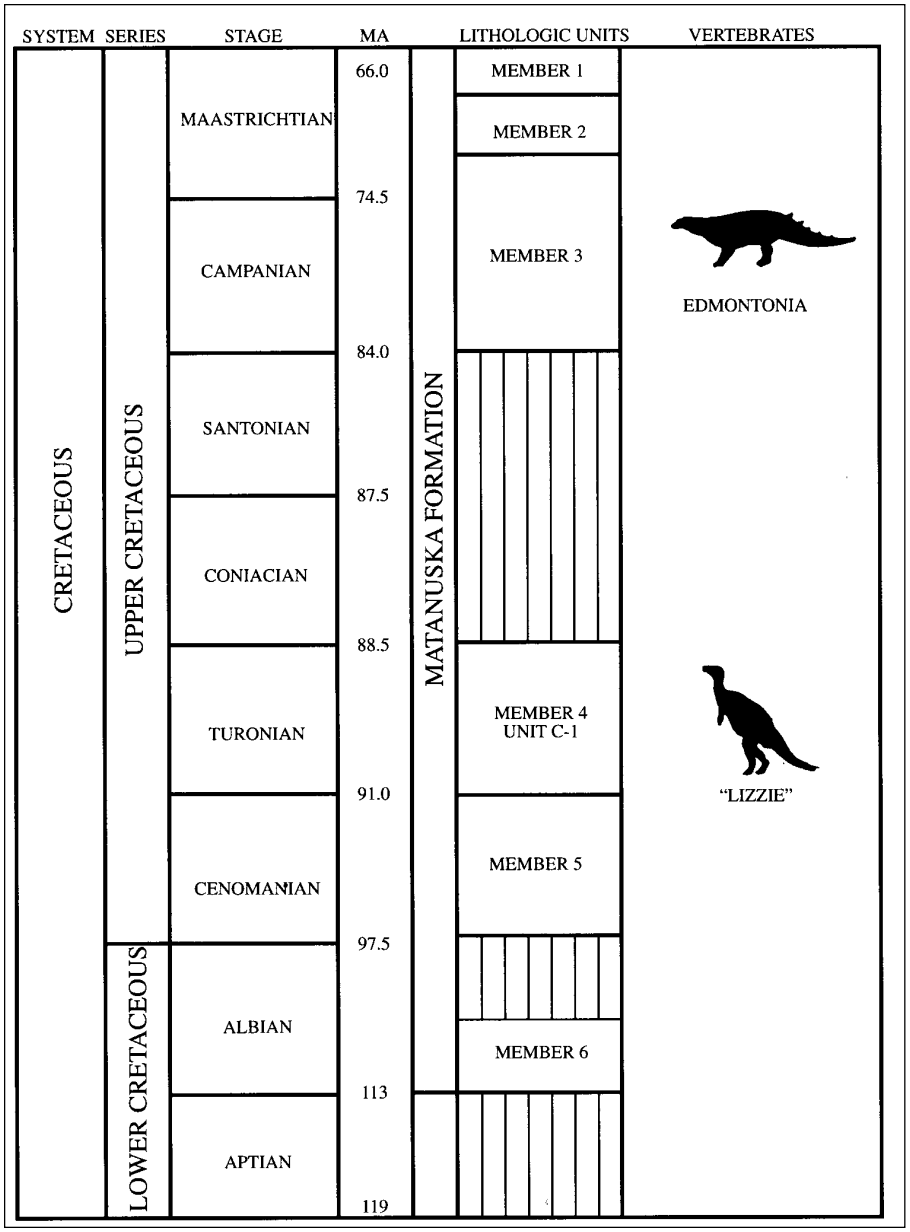

Figure 3. *Schematic columnar section of the Matanuska Formation showing positions of the dinosaur fossils (from Jones, 1963; Jones and Grantz, 1967).*

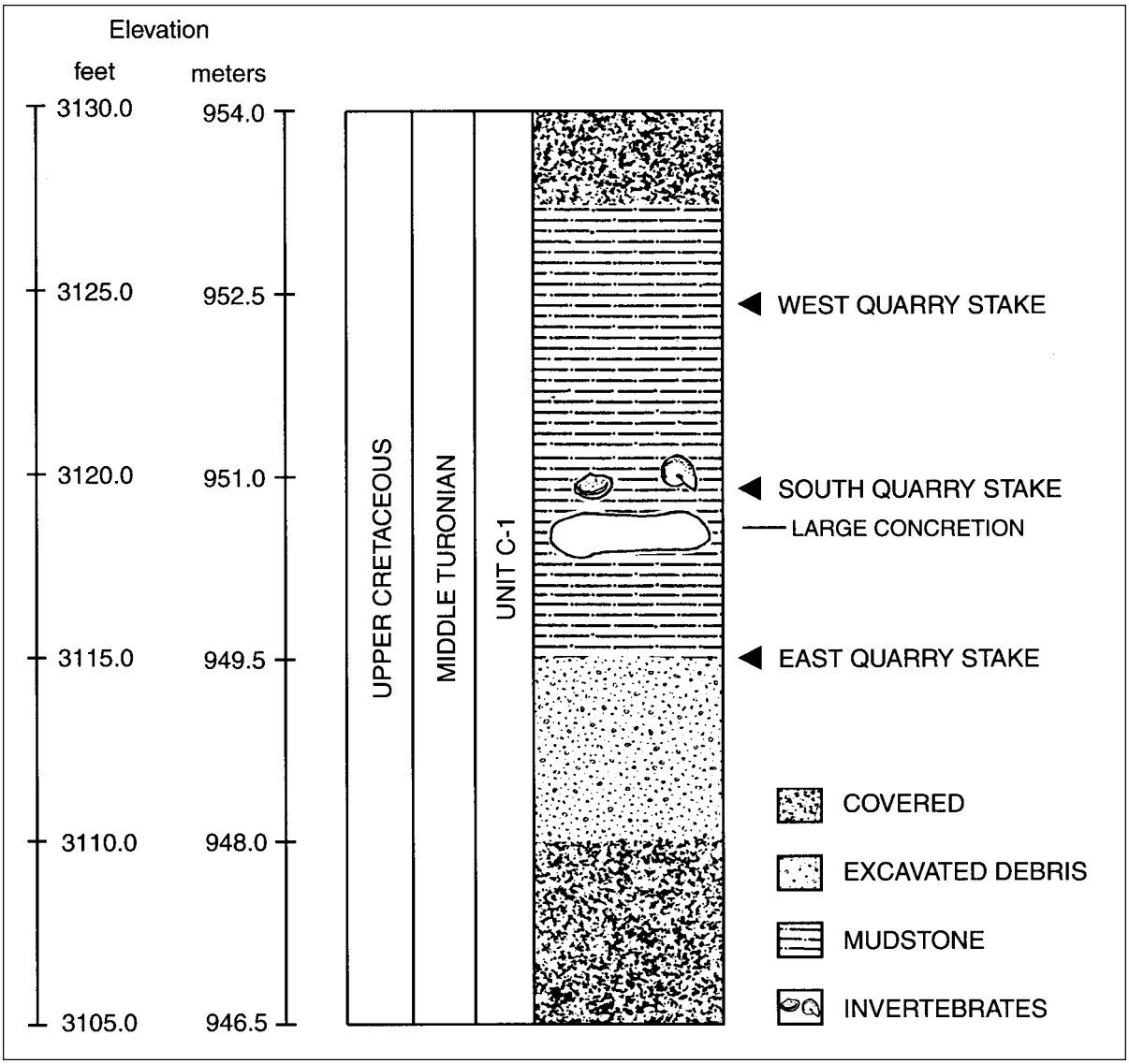

Figure 4. *Stratigraphic section of the Lizzie quarry.*

at an elevation of 950 m (fig. 1); the exact location is recorded at the Alaska Museum of Natural History in Anchorage. The nearest city is Glennallen.

The Mesozoic and Cenozoic sedimentary rocks underlying this region form an east-west-trending structural trough about 32 km wide and 112 km long northeast of Anchorage (Grantz, 1964). At the eastern margin of the trough Mesozoic rocks lie in an anticline that plunges to the northeast. The eastern end has been displaced along a north-south-trending fault. The Lizzie quarry lies in the Matanuska Formation on the southeast limb of the nose in the displaced part of the anticline (Grantz, 1961a, b). According to Jones and Grantz (1967) and Jones (1963), the Matanuska Formation sediments were derived from highlands to the north and deposited in a deep, subsiding, narrow trough. Their texture and mineralogy suggest deposition on a narrow shelf a few miles south of a shoreline to the north. Particles were rapidly buried and not subject to abrasion or winnowing by wave action.

The bone-bearing unit consists of an easily weathered dark-gray marine mudstone that contains highly indurated calcareous concretions and finely disseminated pyrite crystals (fig. 4). In outcrop it seems to be massive, lacking primary sedimentary features. However, fine laminations, possible ripples, and evidence of bioturbation are faintly visible on wet fresh surfaces. No rip-up clasts, graded beds, or sandstone units suggestive of classic turbidite deposits were noted at the site. The unit has been subject to postdepositional deformation as indicated by the joint sets, faults, secondary deposition of calcite, and degree of induration.

The beds in the quarry strike north; dip 22°00' to 26°50' east, and are cut by four joint sets. Two of the joint sets are planar and fairly well defined with steep dips of 50° to 70°; the other two are poorly defined and have undulating surfaces, one dipping steeply (40° to 89°), and one gently (6° to 35°). The latter set produces centimeter-scale offsets of the well-defined planar joints.

AGE

A well-preserved collection of fossil mollusks from the quarry provides a secure Turonian age and marine setting for the bone-bearing unit. The age was determined by Will P. Elder of the U.S. Geological Survey, who identified 7 species of ammonites, 6 species of bivalves, and 2 different gastropods. The presence of the ammonite *Muramotoceras* strongly suggests a Middle Turonian age, as this genus is known from only two species that occur in Middle Turonian sequences. This is the first noted occurrence of this unusual heteromorph outside of Japan (Matsumoto, 1977). The ammonite genus *Eubostrychoceras* is known from Japan, Germany, and Madagascar. *E. japonicum* is Turonian and probably Middle Turonian (Matsumoto, 1977). The inoceramids have a worldwide distribution and are used as guide fossils for the Late Cretaceous from the Albian through the Maastrichtian (Thiede and Dinkelman, 1977).

Other fossils include fish teeth, shark teeth, scaphopods, a solitary hexacoral, planktic forams, trace fossils, toredo-bored wood, and wood fragments. Both the lithology and the invertebrates of the bone-bearing unit strongly suggest that the quarry section belongs to the lower part of C-1, an informal stratigraphic unit of Turonian age in the lower half of the Matanuska Formation as defined by Jones and Grantz (1967), and Member 4 (Turonian), as defined by Jones (1963) (fig. 3). A comparison of fossils found in the Lizzie quarry with those in the equivalent units in the Matanuska Formation (Member 4 and C-1) is shown in table 1. Member 4 is estimated to be about 120 m thick and contains invertebrate fossils of the Indopacific faunal realm (Jones and Grantz, 1967; Matsumoto, 1988). The age of unit C-1 is based on the presence of the bivalve, *Inoceramus* aff. *I. cuvieri*, and the ammonite *Otoscaphites teshioensis* (Jones and Grantz, 1967; Jones, 1963).

PALEOGEOGRAPHY

The paleogeography of the quarry site is somewhat uncertain because of discrepancies between various models of the accretionary history of the tectonostratigraphic terranes in the southern Alaska margin. The Matanuska Formation lies within the Peninsular terrane (Grantz, 1964). In their overview of the tectonic history of Alaska, Plafker and Berg (1994) include it in the allochthonous Wrangellia composite terrane (WCT), a long narrow unit parallel to the southern curved shoreline of Alaska that lies between the Denali and Border Ranges faults (fig. 2). In both the Hillhouse (1987) and Plafker and Berg (1994) models, Turonian rock units were deposited prior to the counterclockwise rotation of southwestern Alaska and carried northward along the continental margin by oceanic plate motion. However, neither the mid-Cretaceous paleolatitude nor the time of accretion of the WCT have been firmly established. Plafker and Berg (1994) place the WCT close to its present latitude by Late Jurassic time and close to its present configuration in the Turonian. This would make the paleolatitude of the Lizzie site very close to the 62nd parallel. Hillhouse (1987) places the WCT 25 degrees south of its present location in Jurassic time with a northward migration, which doesn't place the WCT at its present latitude until Paleocene time (65-55 Ma).

The position of the WCT relative to the North American craton is also uncertain. McClelland and others (1992) suggest a middle Jurassic time for the accretion of the WCT to the mainland. However, Plafker and Berg (1994) favor an alternative model and place the WCT as an offshore fragment during the Aptian-Campanian interval (120-84 Ma) (fig. 5). If Lizzie can be shown to have affinities with early hadrosaurs in other parts of North America and Asia, a good argument for docking by Turonian time would be made. If Lizzie is unique, she could represent an isolated island community. A model for the "Turonian island" hypothesis is located in Romania, where one of the most primitive hadrosaurs known was found. Weishampel and others (1993) suggest that this animal occupied the trans-European archipelago of the Late Cretaceous and that this genus represents a population that was isolated from others in the world and highly specialized. It could not be a hadrosaurian ancestor because of its late Maastrichtian age. The taxonomic relationship of Lizzie to other early hadrosaurs might therefore put additional constraints on an accretionary model.

THE POSTCRANIAL SKELETAL MATERIAL

More than 60 elements of Lizzie's postcranial skeleton have been retrieved. Some required little preparation and some remain fully or partially encased in calcareous mudstone concretions. Axial and appendicular elements recovered in the fall of 1994 include articulated and isolated vertebrae and parts of all four limbs. Excavation was resumed during the

Table 1. *Comparison of the fauna of the Lizzie Quarry with that of Member 4 and the Turonian part of unit C-1 of the Matanuska Formation*

MEMBER 4 / UNIT C-1
(Jones, 1963; Jones and Grantz, 1967)

CEPHALOPODS
Gaudryceras denseplicatum
Mesopuzosia indopacifica
Neophylloceras sp. juv.
Scalarites sp.
Scaphites cf. *S. planusgiges*
Sciponoceras aff. *S. bohemicus*
Tetragonites aff. *T. glabrus*
Ostoscaphites sp.

PELECYPODS
Inoceramus cf. *I. corpulentus*
Inoceramus cf. *I concentricus*
Inoceramus aff. *I. cuvieri*
Inoceramus woods

"LIZZIE" QUARRY
(Elder, written commun.; Larson, oral commun.)

CEPHALOPODS
Eubostrychoceras cf. *japonicum*
Gaudryceras aff. *G. denseplicatum*
Mesopuzosia cf. *M. indopacifica*
Muramotoceras aff. *M. yezoense*
Sciponoceras sp.
Tetragonites aff. *T. glabrus*
Yezoites puerculus (Otoscaphites teshioensis)

GASTROPODS
Biplica sp.(or similar opisthobranch)
Naticid

CNIDARIANS
Solitary hexacoral

PROTISTS
Planktic forams
Arenaceous forams
Radiolarians
Dinoglagellates

PELECYPODS
Inoceramus aff. *I. cuvieri*
Inoceramus aff. *I. hobetsensis*
Inoceramus aff. *I. mamatensis*
Inoceramus aff. *I. teshioensis*
Acila (Truncacila) sp.
Nucula sp.
Toredo borings in wood

SCAPHOPODS
Dentalium sp.

ICHNOFOSSILS
Planolites (?)
Worm tubes (?)
Bioturbation

VERTEBRATES
Shark teeth
Fish teeth, jaw fragment, scales
Hadrosaurian postcranial elements

summer of 1995 to recover a large concretion that may contain pelvic elements. To date, 2 scapulae, 2 humeri, 2 ulnae, 1 radius, 6 rib fragments, parts of a femur, tibia, fibula, astragalus, 5 metatarsals, and 14 pedal phalanges from the appendicular skeleton have been identified along with 23 caudal centra, 2 chevrons, and a few centimeters of ossified tendon from the axial skeleton. They are shown diagrammatically in figure 6. All elements are closely associated and some are articulated. No elements are duplicated and the identified bones all fall within a narrow size range, suggesting they represent a single individual. Preliminary comparisons with other specimens suggest the animal was a juvenile about 3 m long. However, the possibility remains that she was an adult of a smaller species. Adult Late Cretaceous hadrosaurs were considerably larger than Lizzie, averaging 7 to 10 m in length and 3,000 kg in weight (Weishampel and Horner, 1990).

SYSTEMATICS

Class:	Reptilia
Superorder:	Archosauria
Order:	Ornithischia
Suborder:	Ornithopoda
Family:	Hadrosauridae
Genus:	unknown

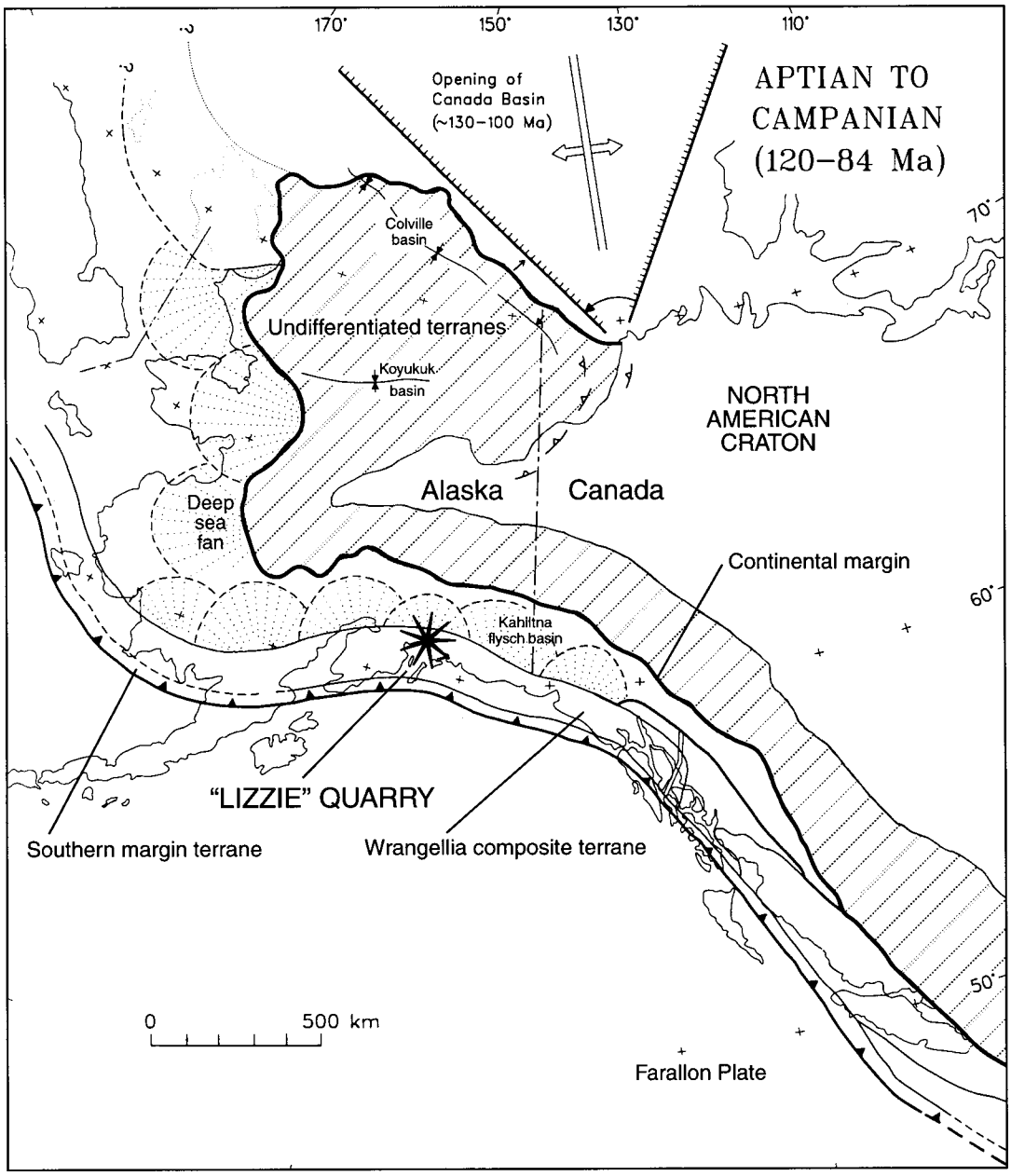

Figure 5. *Paleogeography of Alaska during the Aptian-Campanian (120-84 Ma) interval showing a possible configuration of the Wrangellia Composite Terrane and paleoposition of the Lizzie Quarry. It includes the Peninsular terrane and Wrangellia terranes (modified from Plafker and Berg, 1994, fig. 5E).*

Identification to the family level is based on three nearly complete phalanges (II-1, III-1, IV-1) of the right pes, which were compared with material at the University of Alaska Museum in Fairbanks and the Royal Tyrrell Museum of Palaeontology in Alberta, Canada. It is not known if this is a hadrosaurid (noncrested) or lambeosaurid (crested) duckbill. Pelvic bones or skull, if present, could allow assignment to the subfamilial and possibly the generic level.

PALEOECOLOGIC CONTEXT

Although dinosaur remains situated in rocks of marine origin are unusual, there are numerous reports of such finds. From a list of 95 individual dinosaurs found in marine Upper Cretaceous rocks in North America, 54 are hadrosaurs and the ratio of hadrosaurines (noncrested types) to lambeosaurines (crested types) in this setting is 17:1. About half of these

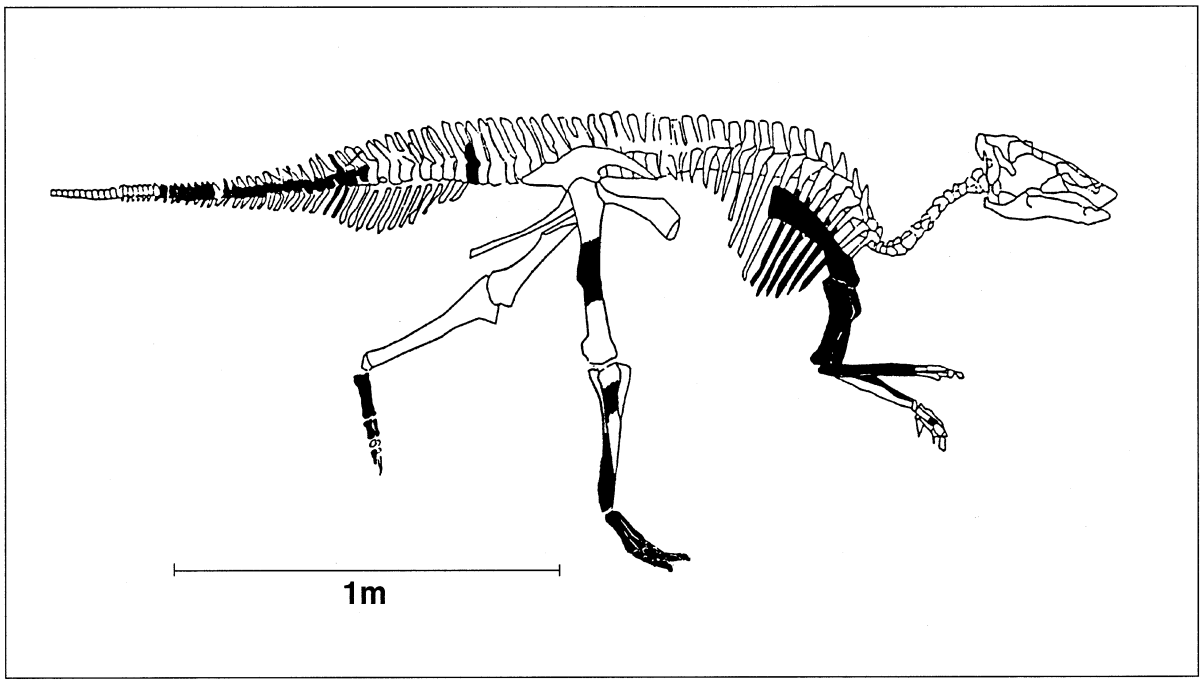

Figure 6. *Postcranial skeletal elements retrieved from Lizzie to date (modified from Norman, 1985, p. 118-119).*

hadrosaurs are young or juvenile individuals (Horner, 1979; Fiorillo, 1990). Nearly all were found articulated and in one case the animal was entombed in skin. Lizzie's skin and soft tissue may have controlled the formation of the concretions.

Deposition in a middle to outer shelf or upper bathyal environment below wave base appears to be suggested by the invertebrate assemblage, which is dominated by ammonites and inoceramid bivalves. The thin-shelled heteromorphic ammonites were probably inhabitants of the outer shelf (36 -183 m) (Tasch, 1973). Inoceramids are thought to have inhabited a wide range of depths, but seem to be confined to the upper bathyal and neritic environments close to continental or island margins (Thiede and Dinkelman, 1977). The lack of heavy-shelled, shallow-water pelecypods also suggests an outer neritic zone or deeper water location for the quarry (Jones, 1963).

The density of the invertebrates suggests that this was an environment where organisms were either very rare or arrived only after death. The preservation suggests rapid burial. The shells lack signs of postmortem biological activity such as borings or encrustations. They show no signs of abrasion, and broken surfaces are fresh. Some are nearly whole and undeformed, whereas others are fragmented, crushed, and greatly compressed. The orientation of the larger planar valves (up to 20 cm in diameter) in the quarry was always parallel to bedding. The lack of abrasion and the recovery of fragile heteromorph ammonites suggest that the invertebrates could not have been reworked. The proximity of the hadrosaur bones to each other implies that they were not disturbed a great deal by scavengers. The occurrence of pyrite suggests the organisms were buried in an anoxic environment. The lack of oxygen, low temperatures, and lack of scavengers provided excellent conditions for preservation.

Whether the fossil assemblage represents a living assemblage that can be used for the reconstruction of specific paleoecologic conditions is an open question. The muddy substrate may have been unstable and subject to submarine slides and slumps. Elder (written commun.) states that transport of delicate and complete shells in this type of environment is very common. The organisms, whether transported or not, show some ecological affinities to each other. Ecological interpretation is confounded by the possibility that ammonite shells can float long distances after death. This may be true for pelagic genera with normal planispiral shells such as *Mesopuzosia*, but it may not be true for the heteromorphs. In their recent paper, Seilacher and Labarbera (1995) suggest that the septum closing off the living chamber of heteromorph ammonites was not calcified and that it decomposed with other soft parts, thus limiting the drift of the shell. A benthic mode of life that has been suggested for heteromorphs of this type would also have placed limits on the distance of transport after death. Obviously heteromorph morphology is not conducive to a pelagic mode of life requiring the rapid locomotion of a predator. Matsumoto

(1977) suggests that *Eubostrychoceras*, with its open coiling, was not adapted for rapid swimming but for a benthic lifestyle and may even have been partly embedded in the substrate. The spinose flared ribs of the shell may have been used to stabilize the animal as it sat on the bottom. Ammonites were thought to live in marine vegetation or on a loose clay mud substrate (Tasch, 1973). Seilacher and Labarbera (1995) suggest the helical coil may have been covered by living tissue or another organism such as a sponge. They also suggest that heteromorph ammonites were "Cartesian divers" living as suspension feeders rather than active predators such as nautiloids. Their arms made up a delicate filter fan that removed small particles from the water more analogous to the feeding behavior of graptolites.

The most abundant bivalves in the borrow pit are inoceramids, an extinct group of bivalves thought to be related to modern oysters. An important guide fossil for the Late Cretaceous, they were benthic with large, relatively flat shells typical of species on soft, muddy substrates. They are characterized by large robust valves with lengths that can exceed 27 mm and thicknesses of 2 to 3 mm. The shells have multiple ligamental pits, which provided anchorage for threadlike ligaments that attached it to the substrate. They are common constituents of dark-gray calcareous laminated mudstones, which indicate reducing conditions below the sediment-water interface (Thiede and Dinkelman, 1977). They were probably filter feeders living below wave base, which harbored chemosynthetic symbionts to supplement their diet (MacLeod and Hoppe, 1992).

Nucula, represented by several specimens, is a ubiquitous genus of an infaunal detritus feeder often found in organic muds. It is an important component of ancient and modern deep-water communities. It is indicative of a low-diversity assemblage in a soft, water-saturated substrate, rich in organic matter with abundant hydrogen sulfide somewhat depleted in oxygen. Nine typical extant deep-water species live below bottom waters with temperatures from 2.3°C to 9.2°C (Kauffman, 1976).

Whether transported or not, the heteromorphs, inoceramids, and nuculids all indicate that Lizzie was buried at a paleodepth greater than 35 m.

EARLY HADROSAURS

Generally, hadrosaurs are a large, diverse, and well-known group of dinosaurs that were the dominant herbivores of the Campanian-Maastrichtian stages of the Late Cretaceous period. Their appearance is well documented in North and South America, Europe, and Asia. Most taxa are described from several individuals, including both juveniles and adults (Weishampel and Horner, 1990). However, hadrosaurs from pre-Campanian rocks are quite rare. In their summary of known hadrosaurs, Weishampel and Horner (1990) list 42 taxa. Of these, 35 species are Campanian-Maastrichtian. Of the seven taxa older than that, the ages of five are uncertain. Until recently, there were almost no well-dated hadrosaurs of early Late Cretaceous age. Now, however, early hadrosaurs are known from at least nine sites in Asia and North America (table 2). Systematic study of these new specimens may show evolutionary relationships between these widely separated fossils. Hadrosaurs are thought to have evolved in Asia from iguanodontids and spread to Europe and North America (Weishampel and Horner, 1990). Work from the recent Sino-Canadian Dinosaur Project showed there are striking similarities between the dinosaur faunas of Asia and North America (Currie, 1995). Lizzie provides a geographic link between Asia and North America for these faunas during the Turonian. Because she is younger than most iguanodontids and older than most hadrosaurines, Lizzie should contribute to the understanding of the relationship between these two groups.

CONCLUSIONS

Lizzie is the first hadrosaur to be found in south-central Alaska and one of the earliest hadrosaurs known in the world. This fossil has the potential to contribute to our understanding of the timing and direction of the spread of this group of ornithopods and of the evolutionary relationships between hadrosaurids and their iguanodontid ancestors. This discovery may also help place constraints on the timing of the docking of the Wrangellia composite terrane with the North American craton. Future work will include micro-osteological and systematic analysis of the postcranial skeleton to determine this hadrosaur's developmental stage and its affinities to known genera.

ACKNOWLEDGMENTS

We are especially indebted to Will Elder of the U.S. Geological Survey, who recognized the rare heteromorph ammonites and identified the invertebrates. We offer a special thanks to Roland A. Gangloff of the University of Alaska Museum, who reviewed the manuscript; this project could not have succeeded without his generous assistance over the past 3 yr. Art Grantz provided expert editorial comments as well as important questions in his thorough review of the manuscript. We thank Phil Currie and Darren Tanke of the Royal Tyrrell Museum of Palaeontology, Steve Nelson and George Plafker of the U.S. Geological

Table 2. *Earliest Hadrosaur localities*

Location	Stratigraphic unit	Age	Material	Source
Eastern Mongolia, People's Republic of China	Iren Dabasu Fm.	Early Senonian (may be as young as Campanian)	Two genera, over a thousand elements	Currie and Eberth (1993)
Kurile Islands Russia	Miho Group	Early Santonian or late Conacian	Skull, postcranial material, juvenile	Weishampel and Horner (1990)
Central Kazakhstan	Beleutinskaya Fm.	Santonian-Turonian (?)	Hadrosaurine skull	Rozhdestvinskii (1968)
Southern Kazakhstan	Darbazinskaya Fm.	Conacian-Santonian (?)	Lambeosaurine portion of a skull	Rozhdestvinskii (1968)
Italy	Borgo Grotta Gigante Member of "Trieste Karst Fm."	Turonian	Postcranial elements of one individual	Brazzatti and Calligaris (1995)
Alaska	Matanuska Fm.	Middle Turonian	Over 60 postcranial elements of one individual	Pasch and May (1995)
Central Honduras	Valle de Angeles Group	Cenomanian (?)	Femur (iguanodontid or hadrosaurid)	Horne (1994)
Texas	Woodbine Fm.	Cenomanian	Skull, postcranial bone fragments	Jacobs (1995)
Utah	Cedar Mountain Fm.	Albian-Cenomanian Boundary	Skull, teeth	Kirkland (1994)

Survey, David Stone of the University of Alaska Fairbanks, Jim Kirkland of Dinamation, Sabra Reid of the Alaska Museum of Natural History, Jack Miller of MB Construction, Pat Murray, and the members of the Kevin May family. We also thank David Gillette for his encouragement and Jim Clough and an anonymous reviewer, who suggested important revisions. Lastly, we thank the Dinosaur Society, the Eagle River Parks and Recreation Board, and the Joe Kapella Memorial Fund for grants and the University of Alaska Anchorage, which supported this work.

REFERENCES CITED

Brazzatti, T., and Calligaris, R., 1995, Studio preliminare di reperti ossei di dinosauri del Carso Triestino: Atti del Museo Civico di Storia Naturale di Trieste [Italy], v. 46, p. 221-226.

Currie, P.J., 1995, Wandering dragons, the dinosaurs of Canada and China: Sixth Symposium on Mesozoic Terrestrial Ecosystems and Biota, Short Papers, Sun, Ailing, and Wang, Yuanqing, eds., Beijing, China Ocean Press, p. 101.

Currie, P.J., and Eberth, D.A., 1993, Paleontology, sedimentology and palaeoecology of the Iren Dabasu Formation (Upper Cretaceous), Inner Mongolia, People's Republic of China: Cretaceous Research, v. 14, p. 127-144.

Fiorillo, A.R., 1990, The first occurrence of hadrosaur (Dinosauria) remains from the Marine Claggett Formation, Late Cretaceous of south-central Montana: Journal of Vertebrate Paleontology, v. 10, no. 4, p. 515-517.

Gangloff, R.A., 1995, *Edmontonia* sp., the first record of an ankylosaur from Alaska: Journal of Vertebrate Paleontology, v. 15, no.1, p. 195-200.

Grantz, Arthur, 1961a, Geologic map and cross sections of the Anchorage (D-2) Quadrangle and northeasternmost part of the Anchorage (D-3) Quadrangle, Alaska: U.S. Geological Survey Miscellaneous Geologic Investigations Map I-342, scale 1:48,000.

———1961b, Geologic map of the north two-thirds of Anchorage (D-1) Quadrangle, Alaska: U.S. Geological Survey Miscellaneous Geologic Investigations Map I-343, scale 1:48,000.

———1964, Stratigraphic reconnaissance of the Matanuska Formation in the Matanuska Valley, Alaska: U.S. Geological Survey Bulletin 1181-I, 33 p.

Hillhouse, J.W., 1987, Accretion of southern Alaska: *in* Kent, D.V., and Krs, M., eds., Laurasian paleomagnetism and tectonics: Tectonophysics, v. 139, p. 107-122.

Horne, G.S., 1994, A Mid-Cretaceous ornithopod from central Honduras: Journal of Vertebrate Paleontology, v. 14, no. 1, p. 147-150.

Horner, J.R., 1979, Upper Cretaceous dinosaurs from the Bearpaw Shale (marine) of south-central Montana with a checklist of Upper Cretaceous dinosaur remains from marine sediments in North America: Journal of Paleontology, v. 53, no. 3, p. 566-577.

Jacobs, Louis, 1995, Lone star dinosaurs: College Station, Texas, A & M University Press, 160 p.

Jones, D.L., 1963, Upper Cretaceous (Campanian and Maestrichtian) ammonites from southern Alaska: U.S. Geological Survey Professional Paper 432, 53 p., 41 pls.

Jones, D. L., and Grantz, Arthur, 1967, Cretaceous ammonites from the lower part of the Matanuska Formation, southern Alaska: U.S. Geological Survey Professional Paper 547, 49 p., 9 pls.

Kauffman, E.G., 1976, Deep-sea Cretaceous macrofossils: hole 317A, Manihiki Plateau *in* Jackson, E.D., and others, Initial reports of the Deep Sea Drilling Project: Washington, U.S. Government Printing Office, v. XXXIII, p. 503-535, 3 pls.

Kirkland, J.T., 1994, A large primitive hadrosaur from the lower Cretaceous of Utah: Journal of Vertebrate Paleontology, v. 14, supplement to no. 3, p. 32A.

MacLeod, K.G., and Hoppe, K.A., 1992, Evidence that inoceramid bivalves were benthic and harbored chemosynthetic symbionts: Geology, v. 20, p. 117-120.

McClelland, W.G., Gehrels, G.E., and Saleeby, J.B., 1992, Upper Jurassic-Lower Cretaceous basinal strata along the cordilleran margin: Implications for the accretionary history of the Alexander-Wrangellia-Peninsular terrane: Tectonics, v. 11, no. 4, p. 823-835.

Matsumoto, Tatsuro, 1977, Some heteromorph ammonites from the Cretaceous of Hokkaido: Memoirs of the Faculty of Science, Kyushu University, Fukuoka, Japan, Series D, Geology, v. XXIII, no. 3, p. 303-366.

———1988, A monograph of the Puzosiidae (Ammonoidea) from the Cretaceous of Hokkaido: Palaeontological Society of Japan, Special Papers, no. 30, 82 p.

Norman, David, 1985, The illustrated encyclopedia of dinosaurs: New York, Crescent Books, 208 p.

Pasch, A.D., and May, K.C., 1995, The significance of a new hadrosaur (Hadrosauridae) from the Matanuska Formation (Cretaceous) in southcentral Alaska: Journal of Vertebrate Paleontology, Abstracts of Papers, v. 15, supplement to no. 3, p. 48A.

Plafker, George, and Berg, H.C., 1994, Overview of the geology and tectonic evolution of Alaska, *in* Plafker, George, and Berg, H.C., eds., The Geology of Alaska: Boulder, Colorado, Geological Society of America, The Geology of North America, v. G-1, p. 989-1018.

Rozhdestvenskii, A.K., 1968, Hadrosauridae of Kazakhstan: "Nauka" Publishing House, Moscow, [English translation from Russian] *in* Tatarinov, L.P., and others, eds., Upper Paleozoic and Mesozoic Amphibians and Reptiles: Akademia Nauk S.S.S.R. Moscow, 120 p.

Seilacher, A., and Labarbera, M., 1995, Ammonites as cartesian divers, Palaios, v. 10, p. 493-506.

Tasch, Paul, 1973, Paleobiology of the invertebrates: New York, John Wiley & Sons, Inc., 946 p.

Thiede, J., and Dinkelman, M.G., 1977, Occurrence of *Inoceramus* remains in late Mesozoic pelagic and hemipelagic sediments, *in* Supko, P. R., and others, eds., Intitial Reports of the Deep Sea Drilling Project: Washington, U.S. Government. Printing Office, v. XXIX, p. 899-910.

Wallace, W.K., and Stone, D.B., 1992, Tectonic evolution of Alaska, Alaska Geological Society Short Course notes, Anchorage, Alaska, University of Alaska Fairbanks.

Weishampel, D.B., and Horner, J.R., 1990, Hadrosauridae, *in* Weishampel, D.B., Dodson, P., and Osmolska, H., eds., The Dinosauria: Berkeley, University of California Press, p. 534-561.

Weishampel, D.B., Norman, D.B., and Grigorescu, D., 1993, *Telmatosaurus transsylvanicus* from the Late Cretaceous of Romania: The most basal hadrosaurid dinosaur: Palaeontology, v. 36, pt. 2, p. 361-385.

This page has intentionally been left blank.

PETROGRAPHY OF THE TINGMERKPUK SANDSTONE (NEOCOMIAN), NORTHWESTERN BROOKS RANGE, ALASKA: A PRELIMINARY STUDY

by
Rocky R. Reifenstuhl,[1] Michael D. Wilson,[2] and Charles G. Mull[1]

ABSTRACT

The Tingmerkpuk Sandstone (Neocomian) in the northwestern Brooks Range consists of texturally and compositionally mature, very fine to medium-grained quartz arenite, interbedded with clay-shale. At its type locality on Tingmerkpuk Mountain in the western DeLong Mountains, the Tingmerkpuk is 130 m thick and consists of about 60 percent net sand with sandstone beds up to 3.5 m thick in amalgamated horizons up to 7 m thick. It crops out in imbricate thrust sheets along a 80-km-long belt in the DeLong Mountains and Misheguk Mountain Quadrangles (1:250,000) in the western Brooks Range. The coeval Kuparuk River Formation of the upper part of the Ellesmerian (or Beaufortian) sequence, occurs to the northeast in the Tunalik #1 well in the western part of the National Petroleum Reserve in Alaska (NPRA) and to the northwest in the Burger #1 and Klondike #1 wells in the Chukchi Sea, where it is hydrocarbon bearing. This suggests that subsurface equivalents of the Tingmerkpuk Sandstone may be a potential hydrocarbon exploration play in the western part of the Arctic Slope of northern Alaska. Petrographic examination of 13 thin sections of outcrop samples shows that the Tingmerkpuk consists of 96 percent quartzose grains (86 percent monocrystalline quartz, 6 percent polycrystalline quartz, 4 percent chert), 2.5 percent lithic grains including glauconite, non-glauconite clay pellets and white mica, 1 percent feldspar, and traces of phyllite, micaceous quartzite, carbonate, and locally volcanic rock fragments. Dead oil is present in one of the samples. The framework grains are similar to those in the Tunalik #1 well. Porosity is low and ranges from zero to 4.3 percent because of carbonate cement and quartz overgrowths and compaction. Secondary porosity is minor and occurs in plagioclase and chert grains. Unweathered glauconite and clay rims on quartzose grains suggest a generally low-energy environment of deposition. Provenance indicators suggest that the sand grains are second- or third-cycle sediments derived from low-chert pre-Mississippian rocks of the Franklinian sequence, which locally included volcanic rocks.

INTRODUCTION

This petrographic examination of the Tingmerkpuk Sandstone includes point-count data from 14 thin sections of the Tingmerkpuk Sandstone in the DeLong Mountains and Misheguk Mountain 1:250,000 quadrangles (fig. 1). Six of the thin sections are from sandstone beds in a 130-m-thick measured section on Tingmerkpuk Mountain (Crowder and others, 1994) and three thin sections are from the Tingmerkpuk on a structurally higher thrust sheet (table 1). Additional thin sections were examined from the Tingmerkpuk at other localities, including Ilingnorak Ridge, 40 km east of Tingmerkpuk Mountain, and from Thetis Creek, 90 km west of the Tingmerkpuk Mountain area. One sandstone from the lower part of the Brookian sequence just above the top of the Tingmerkpuk Sandstone was also analyzed for comparison with the Tingmerkpuk.

The samples were collected as part of a Alaska Division of Geological & Geophysical Surveys study of the Neocomian rocks of the northwestern Brooks Range; this study included detailed mapping of the outcrop belt of the Tingmerkpuk and adjacent rocks at a scale of 1:63,360, measurement of stratigraphic sections, and paleontological and geochemical studies (Crowder and others, 1994; Mickey and others, 1995; Mull, 1995). A more extensive discussion of the petrography of the Brookian sandstones from the northwestern DeLong Mountains is given by Wartes and Reifenstuhl (1997, this volume).

Thin sections were impregnated with blue-dye epoxy to highlight porosity and stained for calcite, but were not stained for potassium feldspar. For modal analyses, 300 grains were counted per thin section for eight of the sections, and 120 grains counted per section on the remaining seven of the sections. In the discussions that follow, the framework grain compositions are reported as percentages of the total framework fraction, whereas the figures for porosity and pore-filling material represent percentages of the total rock.

[1]Alaska Division of Geological & Geophysical Surveys, 794 University Avenue, Suite 200, Fairbanks, Alaska 99709-3645.
[2]Consultant, 674 Tamarac Drive, Golden, Colorado 80401.

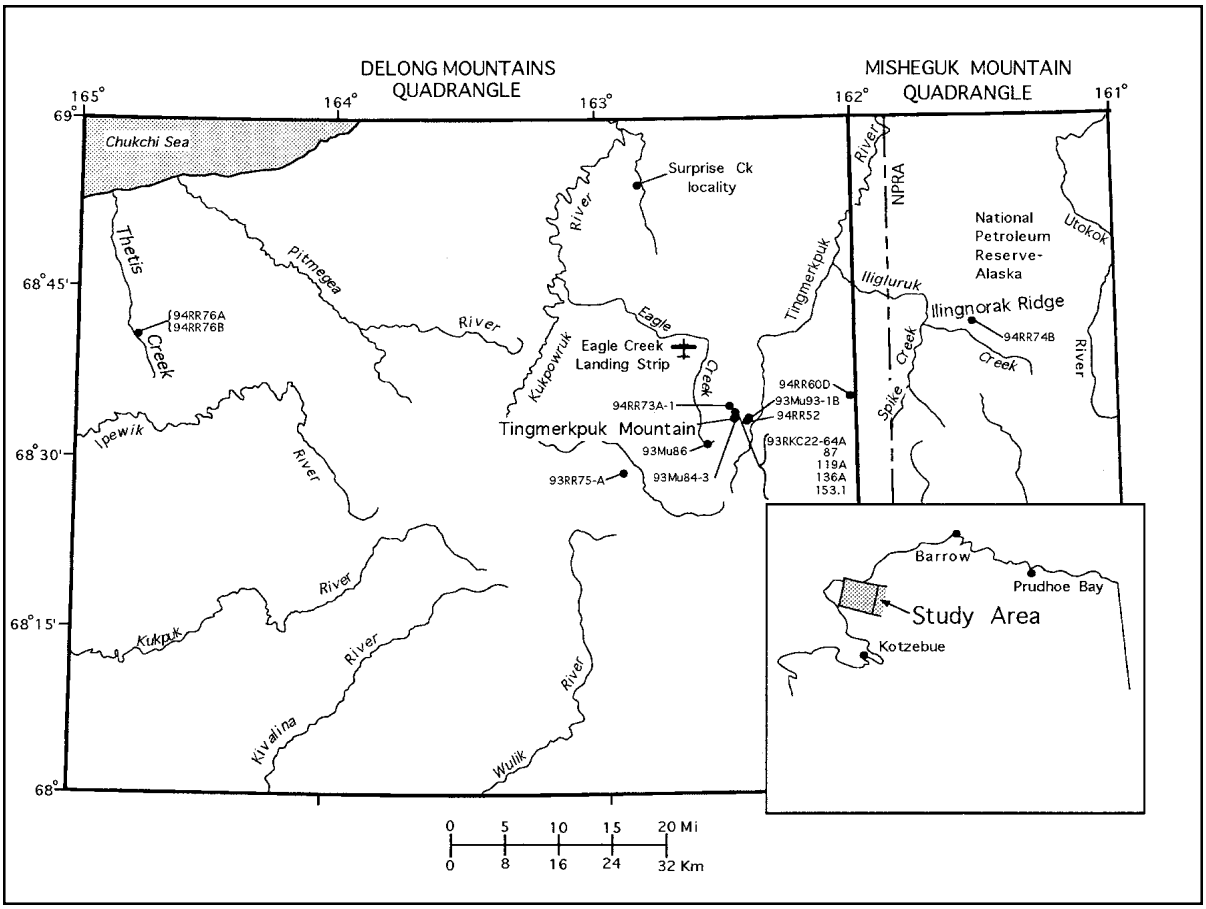

Figure 1. *Location map of samples and geographic localities discussed in text.*

REGIONAL GEOLOGY

The Tingmerkpuk Sandstone crops out in thrust sheets along an 80-km-long trend in the northwestern DeLong Mountains of the Brooks Range fold and thrust belt (fig. 2). The Tingmerkpuk on these thrust sheets is typically underlain by the Jurassic to Neocomian Kingak Shale and overlain by upper Neocomian lower Brookian shales that grade upward into the Mount Kelly Graywacke Tongue of the Fortress Mountain Formation of Aptian to Albian(?) age (Mull, 1985) (fig. 3). The Tingmerkpuk is similar to other Neocomian sandstones of the upper part of the Ellesmerian (or Beaufortian) sequence, such as the Kuparuk River Formation, Put River sandstone, and Pt. Thomson sandstone in the subsurface of the Arctic Slope, and the Kemik Sandstone in surface exposures of the Arctic National Wildlife Refuge in the northeastern Brooks Range. All these units contain similar quartz-rich sandstone derived from a northern source and deposited in shallow shelf settings. However, unlike these other Neocomian sandstones, the Tingmerkpuk was deposited in a deeper setting, either as storm deposits on a deeper part of the shelf or off the shelf as turbidites (Crowder and others, 1994).

Detailed mapping in the course of the current studies of the Neocomian has delineated two discrete facies belts of Tingmerkpuk in the Tingmerkpuk Mountain area. Between the Kukpowruk and Tingmerkpuk Rivers, thick Tingmerkpuk Sandstones that form conspicuous linear ridges in the northern part of the outcrop belt are overlain by thrust sheets that contain petrographically similar, but more distal, finer grained and more thinly bedded facies of the Tingmerkpuk.

Paleontologic data (Mickey and others, 1995; Mull, 1995) suggest that the Tingmerkpuk Sandstone straddles the time interval of the Lower Cretaceous unconformity (LCU). The lower part of the Tingmerkpuk contains pelecypods, foraminifera, and palynomorphs of Valanginian age, whereas shale in the upper part of the Tingmerkpuk contains abundant palynomorphs characteristic of the Hauterivian to Barremian rocks that overlie the LCU in the subsurface of the Arctic Slope (Mickey and others, 1995). However, no unconformity is evident within the Tingmerkpuk.

Geochemical analyses indicate that the shales interbedded with the Tingmerkpuk as well as the underlying Kingak Shale and at least the lower part of

Table 1. *Sample locations*

Sample[a]	Location	Formation	Comments
93RKC22-153.1	Tingmerkpuk Mountain measured section	Tingmerkpuk Sandstone	Sandstone 117 m above base of Tingmerkpuk Sandstone
93RKC22-136A	Tingmerkpuk Mountain measured section	Tingmerkpuk Sandstone	Sandstone 100 m above base of Tingmerkpuk Sandstone
93RKC22-119A	Tingmerkpuk Mountain measured section	Tingmerkpuk Sandstone	Sandstone 83 m above base of Tingmerkpuk Sandstone
93RKC22-87	Tingmerkpuk Mountain measured section	Tingmerkpuk Sandstone	Sandstone 51 m above base of Tingmerkpuk Sandstone
93RKC22-64A	Tingmerkpuk Mountain measured section	Tingmerkpuk Sandstone	Sandstone 28 m above base of Tingmerkpuk Sandstone
93RR73A-1	Tingmerkpuk Mountain measured section	Tingmerkpuk Sandstone	Basal sandstone of Tingmerkpuk Sandstone
93Mu84-3	Tingmerkpuk Mountain	Tingmerkpuk Sandstone, thin-bedded facies	Tingmerkpuk Sandstone, thin-bedded, southern facies on overlying thrust sheet
93Mu86	Eagle Creek	Tingmerkpuk Sandstone, thin-bedded facies	Tingmerkpuk Sandstone, thin-bedded, southern facies on overlying thrust sheet
94RR52A	Tingmerkpuk River	Tingmerkpuk Sandstone, thin-bedded facies	Tingmerkpuk Sandstone, thin-bedded, southern facies on overlying thrust sheet
94RR74B	Ilingnorak Ridge	Tingmerkpuk Sandstone	Eastern end of Tingmerkpuk Sandstone outcrop belt, gradationally overlies coquinoid limestone
94RR60D	Kokolik River	Tingmerkpuk Sandstone	Thin-bedded, fine-grained; contains glauconite
94RR75A	Thetis Creek tributary	Tingmerkpuk Sandstone	Carbonate in matrix; coquinoid limestone down(?) section
94RR76A	Thetis Creek	Tingmerkpuk Sandstone	Western end of Neocomian outcrop belt, isolated exposure of Tingmerkpuk Sandstone
94RR76B	Thetis Creek	Tingmerkpuk Sandstone	Western end of Neocomian outcrop belt, isolated exposure of Tingmerkpuk Sandstone
93Mu931B	South side of Tingmerkpuk Mountain	Brookian sandstone	Thin bedded sandstone in lower part of Brookian sequence

[a]RKC = R.K. Crowder, RR = R.R. Reifenstuhl, Mu = C.G. Mull.

the overlying Brookian shales are potential hydrocarbon source rocks with up to 1.8 percent total organic carbon (TOC). In the Tingmerkpuk Mountain area these rocks are thermally overmature for liquid hydrocarbons and yield vitrinite reflectance values of up to 1.57 percent Ro (Dow and Talukdar, 1995; Mull, 1995). However, coeval source rocks in the Surprise Creek area north of the Tingmerkpuk outcrop belt are thermally mature and have vitrinite reflectance values of 0.7 percent to 0.9 percent Ro.

Stratigraphic data indicate orogenesis in the western Brooks Range throughout the Aptian, Albian, and Cenomanian (115 to 90 Ma). Apatite fission-track data from several Tingmerkpuk localities in the thrust belt indicate major uplift and cooling at about 50-60 Ma, followed by minor uplift later in the Tertiary (J.M. Murphy, unpublished data). These ages are compatible with other data from the Brooks Range mountain front which indicate a regional cooling episode at about 60 Ma (Murphy and others, 1994; O'Sullivan, 1994).

Current geological studies began with a regional framework of geological mapping and stratigraphic studies by Chapman and Sable (1960), R.C. Crane and others (unpub. data, 1981), Mayfield and others (1988), and Curtis and others (1990).

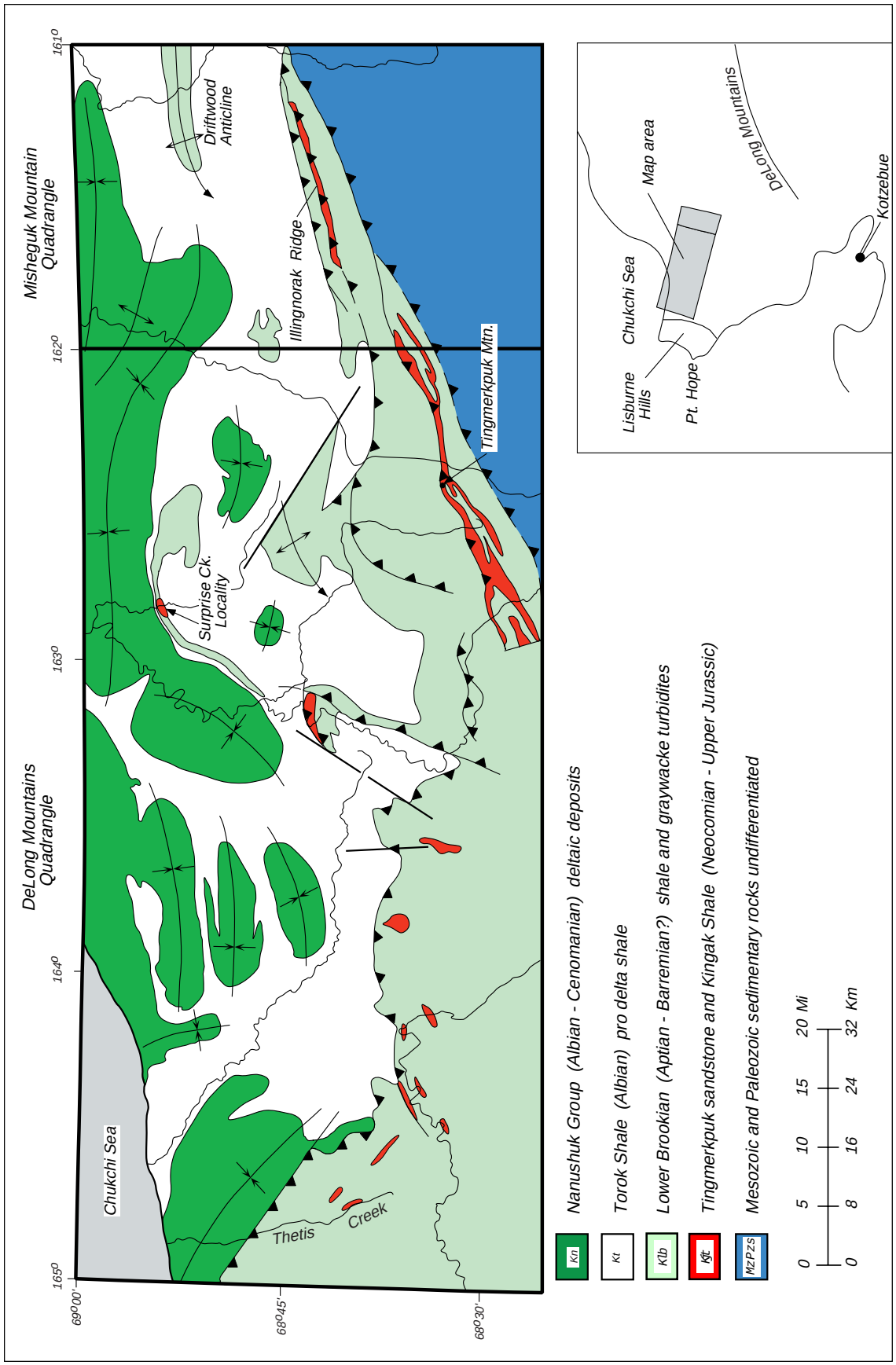

Figure 2. *Generalized geologic map of the northern DeLong Mountains and northwestern Misheguk Mountain 1:250,000 quadrangles, modified from Mull (1995), showing distribution of Tingmerkpuk Sandstone, other associated Jurassic to Neocomian rocks, and overlying formations.*

PETROLOGY

FRAMEWORK MINERALOGY

The Tingmerkpuk Sandstone consists mostly of monocrystalline quartz, with lesser amounts of polycrystalline quartz, chert, plagioclase, carbonate, white mica, and clay pellets. Average framework grain percentages for the Tingmerkpuk are shown on figure 4 and the modal compositions of individual samples are compared in the triangular QFL (quartz-feldspar-lithic) plot of figure 5.

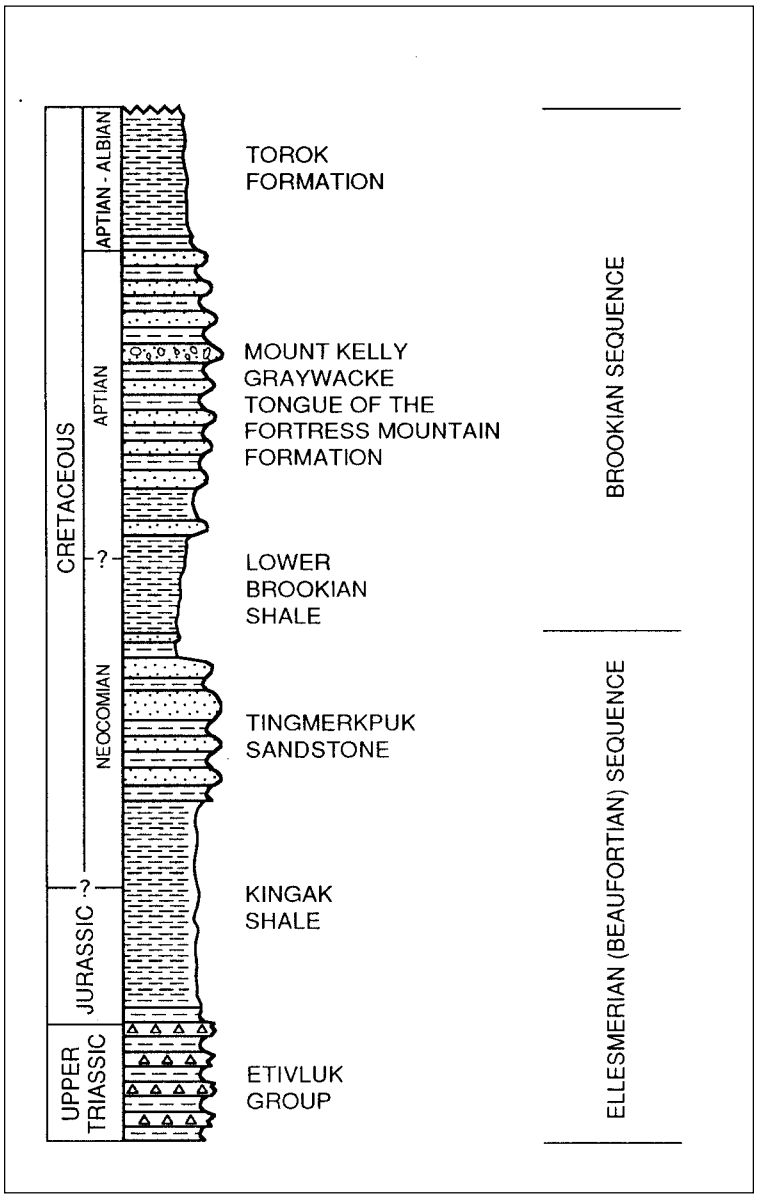

Figure 3. *Generalized stratigraphic column of rocks in thrust sheets of northwestern DeLong Mountains, modified from Mull (1995).*

QUARTZOSE COMPONENTS

Quartzose components average 95 percent of the framework grains and range from 84 percent to 100 percent (fig. 5). These consist dominantly of monocrystalline quartz, with lesser amounts of polycrystalline quartz and chert. Monocrystalline quartz ranges from 68 percent to 91 percent and averages 82 percent of the framework grains; nondescript polycrystalline quartz and traces of stretched polycrystalline quartz range up to 18 percent and average 10 percent of the framework grains (fig. 4). The monocrystalline grains are relatively free of lines of inclusions and strain lamellae. Although most grains display straight or very slight wavy extinction, a significant number of grains display strong wavy extinction (>5°), which was probably produced in situ by folding or faulting. A high percentage of the polycrystalline quartz grains contain from two to five subunits. Chert is a minor constituent ranging from 1.5 to 6.1 percent and an average of 4 percent of the framework grains. The chert grains are structureless except for inclusions of small blebs or rhombs of carbonate. Exceptions are one highly elongate grain in sample 93Mu84-3, which may be a sponge spicule, and grains in samples 93RKC22-119A and 93RKC22-64A, which contain circular voids that may be sponge spicules or radiolarians. Also grouped with the quartzose components are trace amounts of brown phosphatic ovules (featureless grains) and stable heavy minerals: zircon, rutile, and green-brown and colorless tourmaline.

FELDSPARS

Plagioclase is the only feldspar observed in the Tingmerkpuk, and ranges from a trace to 5 percent of the framework grains, with an average of 2 percent. Most plagioclase grains are unaltered and exhibit albite twinning; a few are slightly sericitized, and some may be partially albitized. In a few samples (for example, 93RKC22-119A), some of the plagioclase grains are partially dissolved and have collapsed, leaving an irregular arrangement of disoriented elongate fragments.

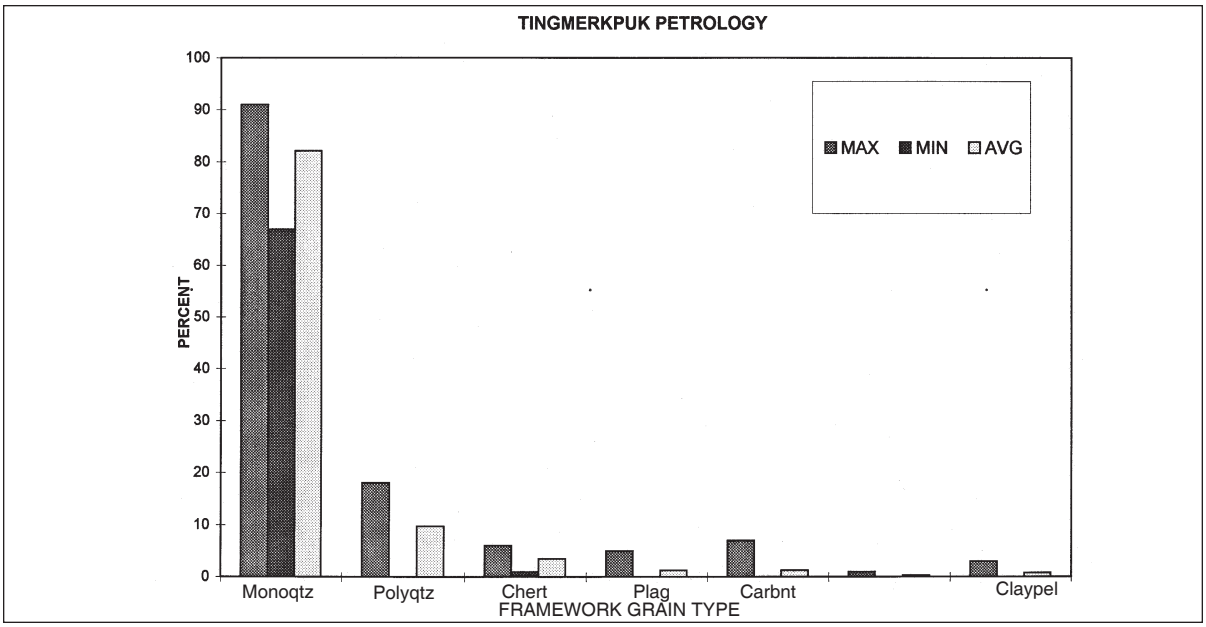

Figure 4. *Histogram summarizing composition of framework grains in Tingmerkpuk Sandstone showing maximum, minimum, and average values for seven grain types. Monoqtz—monocrystalline quartz; Polyqtz—polycrystalline quartz; Chert—chert grains; Plag—plagioclase feldspar; Carbnt—limestone+dolomite grains; W.M.—white mica and muscovite; Claypel—glauconitic and nonglauconitic clay pellets.*

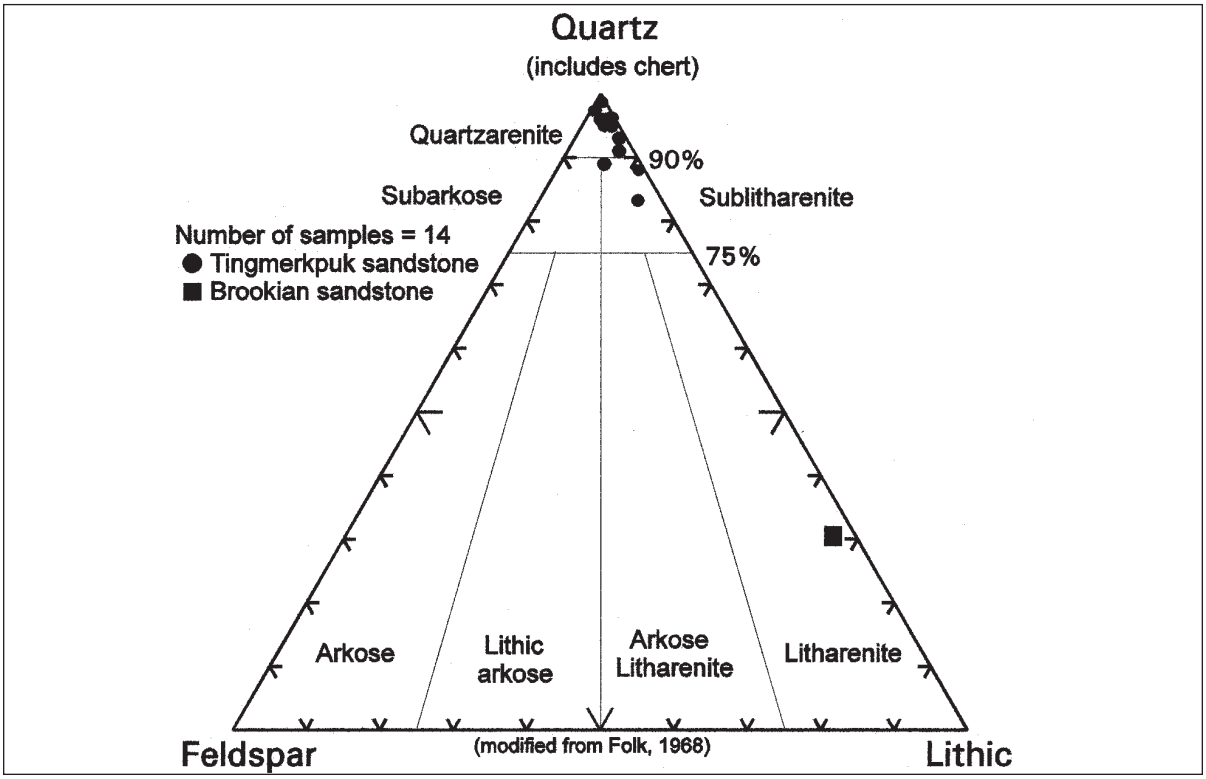

Figure 5. *Triangular quartz-feldspar-lithic (QFL) plot displaying framework compositions of 13 Tingmerkpuk sandstones and one Brookian sandstone. Plot is modified from Folk (1968) QFL plot, with lower quartzarenite boundary placed at 90 percent rather than 95 percent quartzose components, and chert included with the quartzose rather than lithic components. Most of the Tingmerkpuk samples lie in the quartzarenite field; three samples from Thetis Creek and Ilingnorak Ridge lie in the sublitharenite field.*

LITHIC GRAINS

Lithic grains in most of the Tingmerkpuk range from 0 to 7.9 percent and average 1.8 percent of the framework grains (fig. 5). An exception is an outcrop from Thetis Creek at the west end of the outcrop belt (samples 94RR76A, 76B), which contains up to 17 percent lithic grains. Ductile grains compose the bulk of the lithic fraction in most of the Tingmerkpuk, with carbonate fragments constituting the rest in three samples—93RKC22-64A, 94RR74B, and 94RR76B. The latter two localities have significantly more and different lithic grains than all remaining samples; these differences show well in a plot of total quartz vs chert/chert+lithics. This graphically accentuates lithic variability in the sample group (fig. 6). Sample 94RR74-B from Ilingnorak Ridge, at the east end of the outcrop belt, directly overlies a thin limestone coquina bed and contains pelecypod shell material. Compared to the Tingmerkpuk from other localities, the Thetis Creek locality at the west end of the Neocomian outcrop belt (94RR76A, 76B) contains an anomalously high 17 percent lithic grains. These consist of 6 percent chert, 7 percent carbonate, and 3 percent volcanic rock fragments, which were the only volcanic grains observed in the Tingmerkpuk.

The carbonate grains in sample 93RKC22-64A from Tingmerkpuk Mountain consist of detrital dolomite and possible detrital calcitic fragments that may be replacement of plagioclase. Partial calcitic replacements of plagioclase are present in this sample, and some calcitic material that might normally be counted as detrital calcitic fragments locally covers quartz overgrowths and thus is at least partially authigenic. There are no indications, either in grain geometries or internal structures, that the calcitic fragments in this sample represent fossil debris. The basal sandstone (94RR73A-1) from the Tingmerkpuk Mountain measured section contains 6.5 percent carbonate grains, also of unknown affinity (Wartes and Reifenstuhl, 1997; this volume). The carbonate fragments in sample 94RR74B from Ilingnorak Ridge are clearly fossil debris, as noted above, whereas the carbonate in sample 94RR76B is of unknown affinity.

Ductile grains occur in minor amounts ranging from

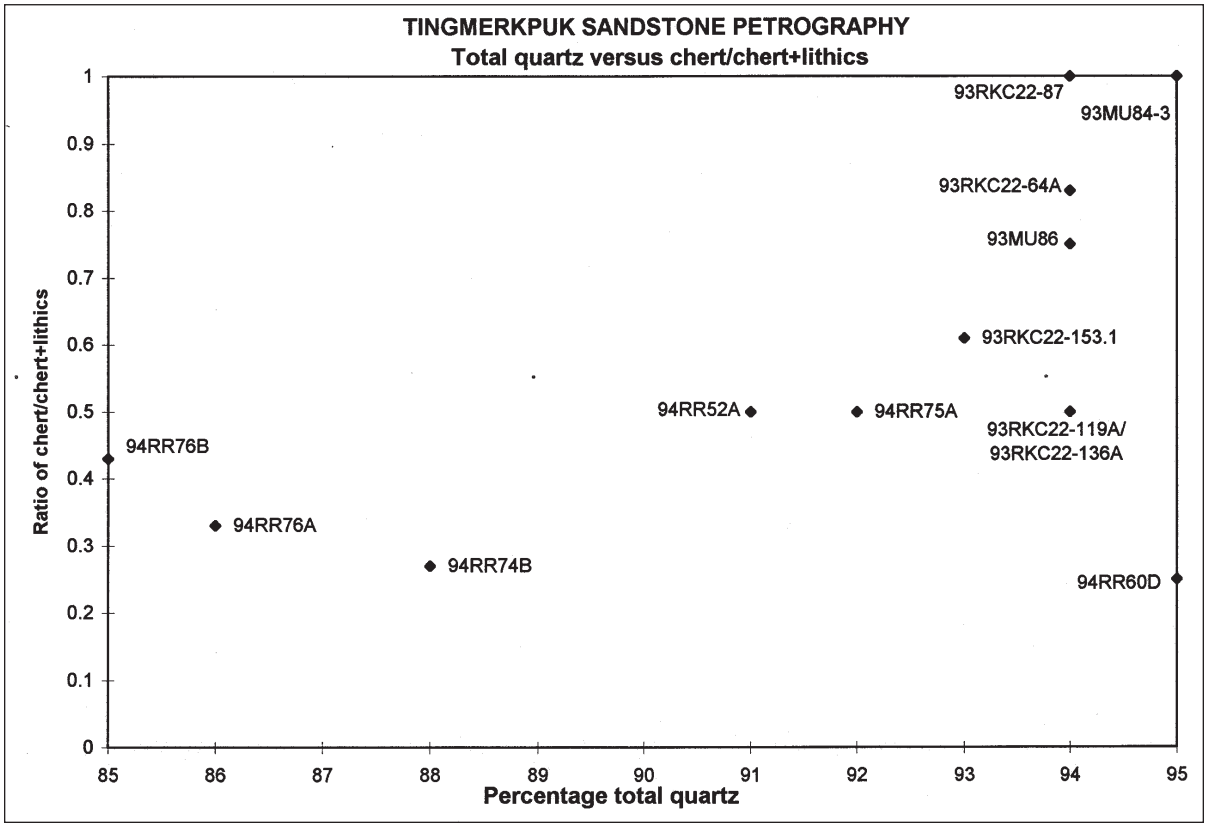

Figure 6. *Plot of total quartz vs chert/chert+lithic rock fragments for 13 Tingmerkpuk Sandstone samples. Plot accentuates nonchert lithic variability between samples from Ilingnorak Ridge (94RR 74B) and Thetis Creek (94RR 76A and (94RR 76B), one of which contains relatively more abundant lithic grains than other Tingmerkpuk samples and is the only Tingmerkpuk sample with volcanic rock fragments. Samples from southern fine-grained facies belt (93Mu 84-3, 93Mu 86, 94RR 52A) show no significance difference from remaining samples of Tingmerkpuk Sandstone.*

0 to 2.4 percent with an average of 0.7 percent, and consist almost entirely of muscovite and glauconitic and nonglauconitic clay pellets. The glauconite pellets are grass green, yellow green, or olive green; most pellets are extensively deformed. Trace amounts of pale-brown nonglauconitic pellets are also present. Traces of phyllite and rare chlorite occur locally, as do opaque heavy minerals. A few opaque grains, now altered to iron oxides or iron hydroxides, are probably weathered pyrite or magnetite grains.

TEXTURAL PROPERTIES

GRAIN SIZE AND SORTING

The Tingmerkpuk Sandstone is dominantly very fine to fine grained. Estimated grain size averages in the thin sections examined reveal 10 upper very fine grained or lower fine grained sandstones (0.12 to 0.17 mm) and four fine- to medium-grained sandstones (<0.5 mm). In the measured section on Tingmerkpuk Mountain, mean grain size increases upward from 0.12 to 0.13 mm in the lower part of the section (at 27 m and 50 m above the base), to 0.16 mm in a sample at 116.1 m.

The sands are well sorted and there is no significant variation in sorting with stratigraphic position. Grain sphericity and rounding are difficult to estimate because of the moderate to extensive grain suturing (interpenetration) that has affected most samples; however, grains not significantly modified by suturing are highly rounded (fig. 7). Moderate alignment of elongate quartz grains and muscovite flakes is evident in most samples. Although elongated quartz grains are common in the Tingmerkpuk Sandstone, similar grains are rare in coeval sandstone in the Tunalik #1 well (M.D. Wilson, unpublished data) .

CLAY RIMS

Pale-green clay rims are present on the quartz grains in most of the thin sections (fig. 7). The rim morphologies suggest that they were probably present on the framework grains at the time of deposition (Wilson, 1992). The rims are best developed in samples 93RKC22-64A and 93Mu84-3, where they are locally

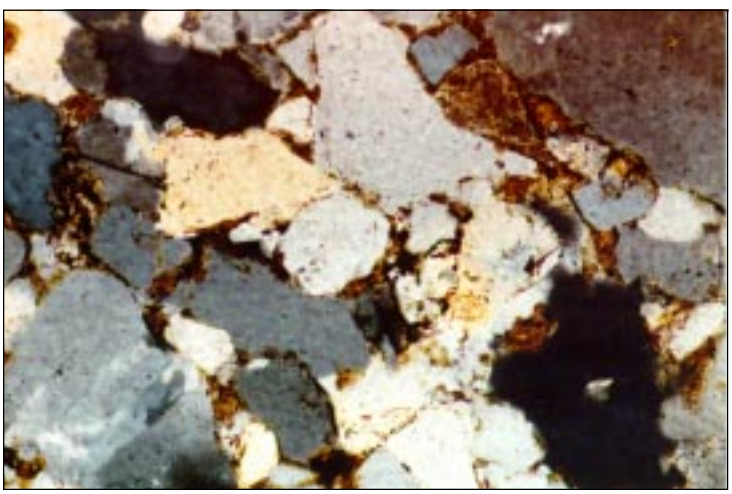

Figure 7. *Photomicrographs of fine-grained to very fine grained Tingmerkpuk Sandstone. A—crossed nicols. B—plane light. Photomicrographs show abundance of well-rounded, clay-rimmed monocrystalline and polycrystalline quartz framework grains. Grains show moderate to extensive grain suturing. Porosity is less than 4 percent due to quartz overgrowths, carbonate cement, and compaction. Bottom of photos are 0.7 mm long.*

A

B

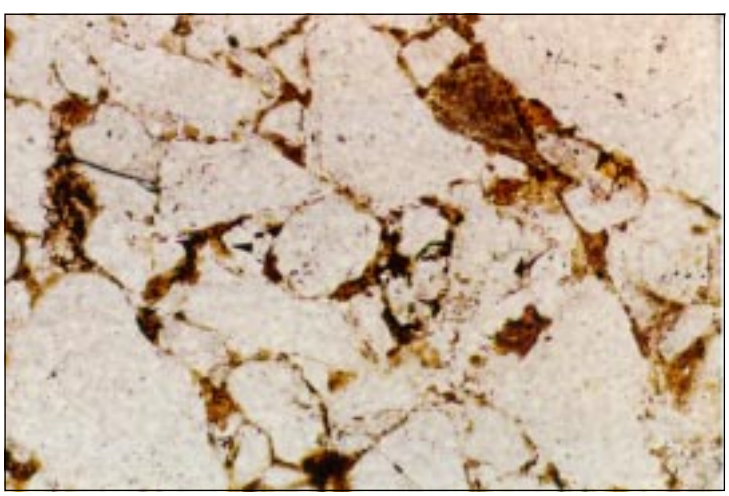

up to 0.001 to 0.002 mm thick. Although most of the rims were probably relatively complete coats when formed, they appear to have been partially removed by abrasion during transport and appear to decrease in thickness and abundance upward in the Tingmerkpuk Mountain measured section. The clay rims are interpreted to be inherited rims on the basis of their irregular thickness, commonly greater thickness in grain embayments, and local occurrence at points of grain-to-grain contact.

Clay rims are probably formed during bioturbation of the sands in a marine shelf environment, but alternatively, some clay rim coatings may represent syndepositional rims generated in relatively shallow water in close proximity to a major deltaic river system (Ehrenberg, 1993). The pale-greenish coloration suggests that they may originally have been partially glauconitized, but they now probably consist largely of illitic clays. An illitic composition for these inherited clay rims is suggested by the stronger yellowish birefringence (93RKC 22-119A, 93RKC 22-153.1). In other intervals, the rims may have been partially altered to, or replaced by, chlorite (93RKC22-64A, 93Mu86). However, because of grain suturing and compactive deformation of rims, it is commonly difficult to differentiate these rims from detrital matrix clays. In one sample (93RKC 22-87), few clay rims were recognized because of masking by abundant siderite and hematite cements. A brown color of the clay rims in another sample (93Mu84-3) is due to dead-oil stain.

POROSITY

Visible porosity is very low to nil in the thin sections from outcrop samples examined in this study, and range from 0 to 4.3 percent (fig. 7). However, because of low permeability, the blue-dye epoxy may not have penetrated throughout the sandstone. On the basis of both this and comparison with previous microscope and laboratory studies of similar sandstone, our visible porosity estimates from point counts are almost certainly on the low side, possibly by as much as 4 to 6 percent.

Measured porosities of five samples from the Tingmerkpuk Mountain measured section are tabulated in table 2.

Samples with visible porosity in thin section in the Tingmerkpuk Mountain section (93RKC22-64A, 93RKC22-119A, 93RKC22-136A) have thin, partial to complete clay rims. These rims are complete enough to prevent total cementation by quartz overgrowths but not thick enough to have filled a significant amount of the pore network. Other samples, such as 93RKC22-87 and 93Mu86, have either extensive carbonate cement or thick clay rims. These clay rims have severely inhibited development of quartz overgrowths and have promoted extensive grain suturing and infilling of pores by carbonate. In addition, some of the intergranular porosity has been enhanced by trace amounts of dissolution of some plagioclase and chert grains (samples 93RKC22-119A, 93RKC22-136). Whether this dissolution is a result of subsurface processes or surface weathering of the plagioclase and chert is unknown. Dissolution observed in the samples with minor intergranular porosity may be the result of surface weathering.

MECHANISMS OF POROSITY REDUCTION

The major mechanism of porosity reduction is pressure-solution suturing due to compaction in all but one Tingmerkpuk sample. Four samples record porosity loss of 18 to 22 percent due to compaction. Porosity loss by compaction is calculated by subtracting present intergranular volumes (determined from point-count data) from stabilized initial porosities estimated by using a size-sorting-porosity relationship generated from the data of Beard and Weyl (1973). The calculated values are not corrected for changes in bulk volume during compaction. The calculated stabilized initial porosities represent approximate porosities at shallow depth (about 100 to 300 m) in relatively quartzose sandstones with extensive grain rearrangement. With additional burial, further grain rearrangement generally destroys an additional 5 to 6 percent of the porosity, but this occurs slowly over the next few thousand meters of burial.

One sample from Tingmerkpuk Mountain (93RKC22-87) contains abundant siderite (27 percent) and hematite (11.7 percent) cements and has a calculated porosity loss of -1.8 percent due to compaction. This negative porosity loss implies cementation at a very early stage of diagenesis, probably at a very shallow depth (less than 100 m) prior to normal framework stabilization. Much of the hematite in this sample

Table 2. *Measured porosities from the Tingmerkpuk Mountain*

Sample	Distance above formation base (m)	% porosity (Helium)	Permeability (MD)
93RKC 22-136B	100	11.4	0.33
93RKC 22-119B	83	11.3	0.12
93RKC 22-110B	74	11.3	0.32
93RKC 22-86B	50	11.6	0.17
93RKC 22-64B	28	7.2	0.02

Analyses by Core Laboratories, Inc.

exhibits rhombic outlines and is interpreted as a surface-weathering residue of siderite, inasmuch as the hematite is concentrated as a rind along one side of the thin section.

Quartz overgrowths are present in minor amounts in most samples of the Tingmerkpuk and range from 0 to 8.7 percent of the rock volume, with an average of 4.9 percent. Clay rims have extensively inhibited overgrowth development in samples where rims are relatively complete (for example 93RKC22-64A, 93RKC22-119A, 93Mu86). Overgrowth abundance is inversely proportional to a combination of content of clay rims, carbonate cement (including that replaced by hematite in sample 93RKC22-87), and matrix (fig. 8).

Two sandstone samples from the southern facies belt of the Tingmerkpuk have significantly lower loss of porosity due to compaction than those from the northern facies belt. The sand in sample 93Mu84-3, which has a calculated porosity loss of 10.6 percent, contains abundant clay rims (15.7 percent), moderate quartz overgrowths (7 percent), and minor dead oil (3.7 percent). Loss of porosity due to compaction in this sample is limited by the fact that the inherited clay rims, although quite thick, are discontinuous and are commonly absent at points of grain-to-grain contact. Sample 93Mu86 contains abundant carbonate cement, 2 percent pore-filling quartz overgrowths, and >1 percent dead oil. Carbonate cementation at moderate depths of burial has apparently significantly limited the extent of porosity loss.

The absence of alteration of muscovite or plagioclase to kaolinite in any of the sandstones indicates that these samples were not subjected to extensive meteoric water during either early burial or outcrop weathering, or to acidic waters during later stages of burial.

The low visible and measured porosity, locally extensive plastic deformation, grain-to-grain suturing, and extensive loss of porosity due to compaction of the Tingmerkpuk Sandstone suggest exposure to high pressure and temperature. Such conditions are expected in the deeply buried and highly deformed northwest

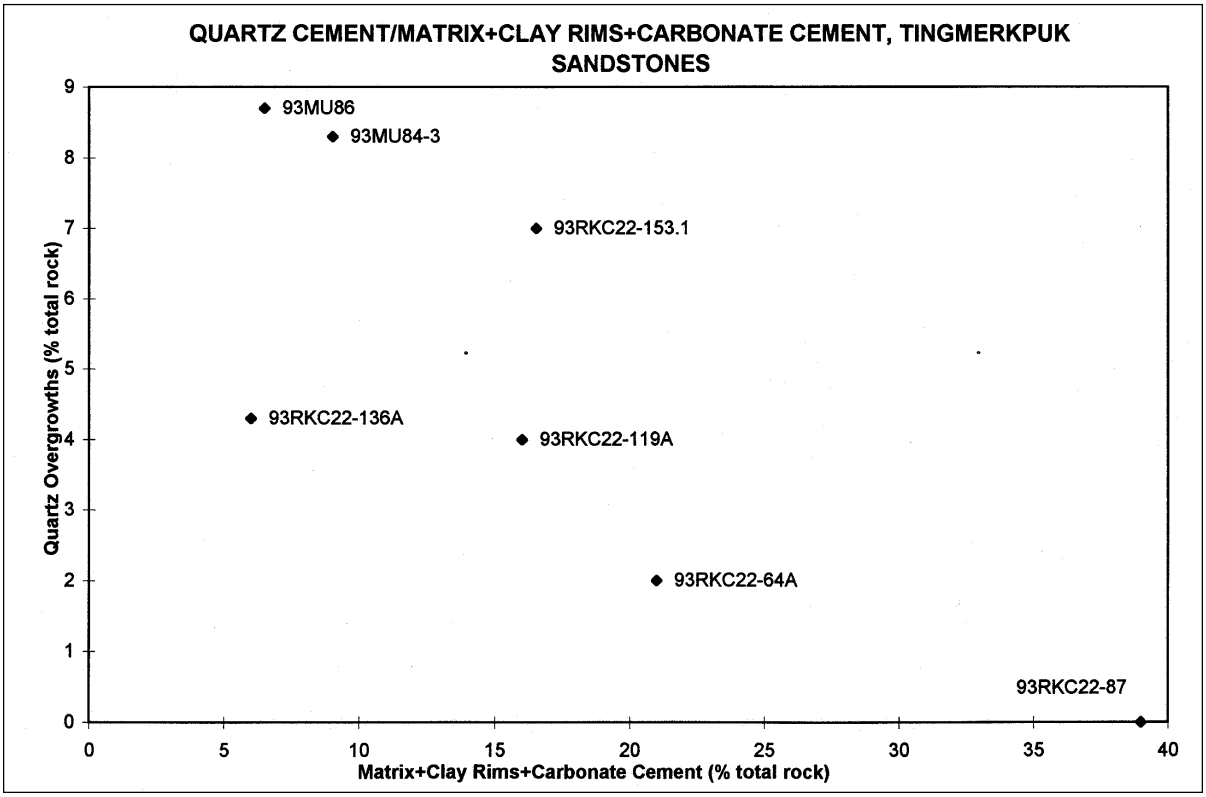

Figure 8. *Plot of quartz overgrowths (percent of total rock volume) vs matrix+clay rims+carbonate cement (percent of total rock volume) showing strong inverse relationship between quartz overgrowths and abundance of clay rims, matrix, and early carbonate cement for seven Tingmerkpuk Sandstone samples. Matrix, clay rims, and carbonate cement combine to severely limit quartz overgrowth content. In sample 93RKC 22-87 (lower right), hematite is a weathering product of early diagenetic siderite and included with carbonate cements. Although limitation of quartz overgrowths is beneficial for preservation of reservoir quality, samples with lower amounts of quartz overgrowths instead have abundant carbonate matrix or have encountered extensive pressure-solution suturing.*

Brooks Range fold and thrust belt and may not be representative of conditions in the subsurface of the Colville Basin, where the rocks have been subjected only to sedimentary burial and have not encountered tectonic deformation and burial due to imbrication of thrust sheets. Improved reservoir quality can be expected in areas in which one or more of the following conditions may exist:

(a) Areas of reduced sedimentological or tectonic burial, in which the residence time of exposure to elevated temperature or pressure is significantly reduced.
(b) Areas of early migration of hydrocarbons into the sandstones.
(c) Areas in which thin and complete clay rims have completely inhibited development of quartz overgrowths without significant cementation by other mechanisms of porosity reduction.
(d) Areas in which sandstones were extensively cemented during early diagenesis and in which most or all of this cement has subsequently been removed by dissolution without filling of the secondary porosity by later cements.
(e) Areas in which the sandstones were overpressured as they were uplifted from moderate depth of burial to their present exposure at the surface.

TINGMERKPUK ENVIRONMENT OF DEPOSITION

Environments of deposition are best determined by using sedimentary structures, data concerning the stratigraphic sequences, and paleontological evidence (see Regional Geology). The petrographic data from this study suggest some constraints for the interpretations of depositional environment of the Tingmerkpuk. The presence of unweathered glauconite in all samples indicates a marine environment. Glauconite abundance is low and ranges from a trace to 1.2 percent. Glauconite suggests that low rates of sedimentation and low oxidation during its formation (Odin and Fullagar, 1989).

Clay rims on sands are commonly generated by bioturbation in shelf environments (Wilson, 1992). However, clay-rimmed grains are commonly reworked into shelf shoreface transitional environments and deeper water slope and deep-sea fan environments. Reworking of these grains into deeper parts of the shelf by storms is suggested for the Tingmerkpuk. The well-sorted nature of the sands and low matrix content imply at least moderate energy during deposition and suggest a lack of extensive biogenic reworking. A low-energy environment characterized by a low rates of sedimentation and abundant bioturbation is unlikely for the Tingmerkpuk.

COMPARISON OF TINGMERKPUK SANDSTONE IN NORTHERN AND SOUTHERN FACIES BELTS

Mapping of the Tingmerkpuk at a scale of 1:63,360 has revealed the presence of two parallel belts of thrust sheets of Tingmerkpuk between the Kukpowruk and Tingmerkpuk Rivers (figs. 1, 2). These two belts contain the same stratigraphic sequence of Triassic Otuk Formation overlain by Kingak Shale, Tingmerkpuk Sandstone, and Brookian shale, but are characterized by a marked contrast in bed thickness and, to a lesser extent, by average grain size in the Tingmerkpuk. The northern belt, which contains the 130 m-thick Tingmerkpuk Mountain measured section (Crowder and others, 1994), forms high, resistant rubble-covered ridges formed by thick-bedded units of Tingmerkpuk. The Tingmerkpuk in the southern belt, which structurally overlies the northern belt, appears to have about the same interval thickness as in the northern belt, but is much thinner bedded and contains a higher ratio of shale to sandstone. The modal analyses of samples 93Mu84-3, 93Mu86, and 94RR52A from the thin-bedded southern-facies belt show no significant difference in the composition of framework grains from those in the northern belt from which the remaining samples were collected (figs. 5, 6).

COMPARISON OF TINGMERKPUK SANDSTONE WITH BROOKIAN SANDSTONE

Comparison of the Tingmerkpuk Sandstone mineralogy with data from one Brookian sandstone sample (93Mu93-1B) that overlies the Tingmerkpuk of the southern-facies belt shows major differences in composition between the two units (fig. 5). In the Brookian sandstone, quartzose grains compose 39.4 percent of the total framework grains, which is much lower than in the Tingmerkpuk Sandstone. Feldspar grains, which are entirely plagioclase, constitute 3.3 percent (slightly higher than in the Tingmerkpuk), and lithic grains compose 57.3 percent, which is much higher than in the Tingmerkpuk. The quartzose fraction contains a much larger proportion of polycrystalline quartz grains than in the Tingmerkpuk; some of these contain trace to minor amounts of aligned white mica or chlorite and were probably derived from phyllitic metasiltstone or microschist. Chert content of about 4 percent is similar to that of the Tingmerkpuk.

The composition of lithic grains in the Brookian sandstone also contrasts markedly with the lithic grains in the Tingmerkpuk. In the Brookian sandstone, the lithic grains consist predominantly of monocrystalline and polycrystalline dolomite fragments, with lesser amounts of phyllite, muscovite, and mudstone or shale fragments, and a trace of chlorite and silicic volcanic rock fragments. The dolomite grains are commonly twinned, which suggests a highly tectonized provenance.

Texturally, the Brookian sandstone grains have significantly lower sphericity and roundness than the Tingmerkpuk sands. Matrix and laminar clays are relatively abundant, and cement is a combination of plastic deformation of ductile grains, grain suturing, and dolomite (or ankerite ?) cementation. For a more extensive discussion of Brookian sandstones see Wartes and Reifenstuhl (this volume).

PROVENANCE

Although the petrographic data provide no definitive identification of provenance for the Tingmerkpuk Sandstone, they do provide insight into the *nature* of the provenance. Inasmuch as the Tingmerkpuk Sandstone was deposited during the Neocomian coeval with development of the Lower Cretaceous unconformity (LCU) and rifting of the northern Alaska margin, it has always been assumed that rocks similar to those near the rift margin may represent the Tingmerkpuk provenance.

The abundance of well-rounded monocrystalline quartz in the Tingmerkpuk indicates source rocks that consisted of quartz-rich sandstones, metasandstones, or metaquartzites. The Tingmerkpuk Sandstones are thus at least second- or third-cycle sandstones. Although no grains of sandstone, metasandstone, or metaquartzite were observed in thin section, this may be attributable to the relatively fine grain size of the Tingmerkpuk. Trace amounts of phyllite and muscovite imply at least minor amounts of low-grade metamorphic rocks in the source terrane.

The low chert content of most of the Tingmerkpuk sandstones suggests that they were not derived from rocks similar to most of the Ellesmerian sequence of the northern Arctic Slope. In the Ellesmerian sequence, the sands of the Triassic Sag River Sandstone and Ivishak Formation and of the Permian Echooka Formation contain up to 35 percent detrital chert grains (Bird, 1991; van de Kamp, 1988), and the Carboniferous Lisburne Group carbonates contain abundant chert nodules. However, the sandstones in other possible source units that underlie the Lisburne Group, such as the Lower Mississippian Kekiktuk Conglomerate at the base of the Ellesmerian sequence and pre-Mississippian Franklinian sequence, contain only minor chert, and might be considered a source.

In the lithic grain fraction of the Tingmerkpuk sands, the occurrence of dolomite and possibly calcitic fragments (samples 93RKC22-64A, 94RR76B, 94RR73A-1) and their absence in all other samples (fig. 6) is somewhat anomalous. Dolomite grains can withstand moderately extensive transport, but calcitic fragments are typically eliminated by dissolution and abrasion during relatively short transport. Questionable calcitic fragments in the sands may represent plagioclase-grain replacement (see discussion above), fossil fragments indigenous to the environment of deposition, or entrainment of grains from nearby environments during sediment transport or reworking, perhaps as tempestites. A number of stratigraphic units, including the Lisburne Group, the Katakturuk Dolomite, and some units within the Franklinian sequence, contain dolomite fragments that could have been the source of the minor amount of dolomite in the Tingmerkpuk. However, the low chert content of the Tingmerkpuk in the eastern part of its outcrop belt seems to rule out the Lisburne Group—with its abundant chert—as a significant component of the provenance for most of the Tingmerkpuk.

The volcanic rock fragments and higher percentage of chert in the Tingmerkpuk at Thetis Creek indicate the presence of a different component in the provenance of the Tingmerkpuk in the western part of the Neocomian outcrop belt than in the Tingmerkpuk to the east. Volcanic rocks are locally present in the Lisburne Group in both the Tunalik #1 test well in western NPRA and in the eastern Brooks Range. Volcanic rocks are also locally present in the Franklinian sequence in the northeastern Brooks Range (Reiser and others, 1980), but have not been reported in the subsurface of the Arctic Slope.

In contrast to the Tingmerkpuk Sandstone, the Brookian sandstone examined in this study contains abundant chert, volcanic rock fragments, metamorphic rock fragments, carbonate, and white mica (fig. 5). Rocks of this type are widespread in the pre-Mississippian rocks of the schist belt of the southern Brooks Range, in the structurally higher allochthons that regionally overlie the Tingmerkpuk, and in the Angayucham terrane, all of which lie south of the Tingmerkpuk area. Generalized discussions of the rocks in these areas are given by Dillon (1989), Mull (1989), Mayfield and others (1988), and Moore and others (1994).

In summary, the petrographic data suggest that rocks similar to those of the Franklinian sequence or the basal part of the Ellesmerian sequence of northern Alaska were probably the source of the Tingmerkpuk Sandstone. The absence of significant amounts of chert, volcanic rock fragments, metamorphic rock fragments, carbonate, or

white mica in the Tingmerkpuk, all of which are abundant in the pre-Cretaceous rocks of the Brooks Range to the south of the Tingmerkpuk outcrop belt, precludes a southern source for the Tingmerkpuk. However, these components are abundant in the Brookian sediments that directly overlie the Tingmerkpuk and indicate a significant change in provenance following the end of Tingmerkpuk deposition.

SUMMARY AND CONCLUSIONS

Petrographic study of the Tingmerkpuk Sandstone shows that:

(a) The Tingmerkpuk is dominantly a quartz-arenite with local sublitharenite (<90 percent quartz). Petrographically, the Tingmerkpuk is similar to the Kuparuk River Formation in the Tunalik #1 well of NPRA and other upper Ellesmerian (Beaufortian) sandstones of Neocomian age in northern Alaska.

(b) Framework grains in most of the Tingmerkpuk consist of an average of 87 percent monocrystalline quartz, 7 percent polycrystalline quartz, 4 percent chert, 1 percent plagioclase, 0.1 percent carbonate, 0.4 percent white mica, and 0.3 percent clay pellets. A single Tingmerkpuk locality at the western end of the Neocomian outcrop belt contains 3 percent volcanic rock fragments.

(c) The compositional and textural maturity of the Tingmerkpuk suggests that most of its sands are at least second- or third-order sands.

(d) Partially abraded clay rims are common on most of the quartz grains in the Tingmerkpuk, and were probably present at the time of deposition of the sands. These clay rims in the Tingmerkpuk were probably formed as a result of bioturbation of the sands in a shallow marine shelf environment prior to transport of the sand to a deeper depositional setting.

(e) Porosity and permeability in the Tingmerkpuk Sandstone in outcrop is low and ranges from 4 to 6 percent, due to quartz overgrowths on the grains, carbonate cementation, and compaction. Quartz overgrowths compose up to 8.8 percent of the total rock volume, and the sum of matrix+clay rims+carbonate cement+hematite cement ranges from 6 to 39 percent of the total rock volume. The dominant mechanism of porosity degradation in the Tingmerkpuk in outcrop is pressure solution due to compaction and may not be characteristic of conditions in the subsurface.

(f) The provenance for the Tingmerkpuk sands probably included rocks similar to the pre-Mississippian Franklinian sequence and possibly the Lower Mississippian part of the Ellesmerian Group that are present in the subsurface of the Arctic Slope north of the Tingmerkpuk outcrop belt. Minor volcanic rocks were part of the provenance for the Tingmerkpuk in its present-day westernmost exposure.

(g) Comparison of the petrography of the Tingmerkpuk with the basal sands in the overlying Brookian sequence documents an abrupt change to a dramatically different and presumably southern provenance that included abundant chert- and volcanic-bearing components as well as other metamorphic rocks.

ACKNOWLEDGMENTS

The field and analytical studies of the Neocomian rocks of the western DeLong Mountains were partially funded by grants from Anadarko Petroleum, Inc., ARCO Alaska, Inc., Arctic Slope Regional Corporation, BP Alaska, Inc., North Slope Borough, Phillips Petroleum Company, and Alfred James, Consultant. We thank reviewers D.L. LePain and G.C. Wilson for their thoughtful review comments.

REFERENCES CITED

Beard, D.C., and Weyl, P.K., 1973, Influence of texture on porosity and permeability of unconsolidated sand: American Association of Petroleum Geologists Bulletin, v. 57, p. 349-369.

Bird, K.J., 1991, North Slope of Alaska, *in* R.B. Taylor and others, eds., Economic geology, the geology of North America: Geological Society of America, v. P-2, p. 447-461.

Chapman, R.M., and Sable, E.G., 1960, Geology of the Utukok-Corwin region, northwestern Alaska: U.S. Geological Survey Professional Paper 303-C, p. 47-174.

Crowder, R. K., Adams, K.E., and Mull, C.G., 1994, Measured stratigraphic section of the Tingmerkpuk Sandstone (Neocomian), western Brooks Range, Alaska: Alaska Division of Geological & Geophysical Surveys Public-Data File 94-29, 5 p., 1 sheet.

Curtis, S.M., Ellersieck, Inyo, Mayfield, C.F., and Tailleur, I.L., 1990, Reconnaissance geologic map of the DeLong Mountains A-1 and B-1 quadrangles and part of C-1 quadrangle, Alaska: U.S. Geological Survey Map I-1930, 2 sheets, scale 1:63,360.

Dillon, J.T., 1989, Structure and stratigraphy of the southern Brooks Range and northern Koyukuk basin near the Dalton Highway, *in* Mull, C.G., and Adams, Karen, eds., Dalton Highway, Yukon River to Prudhoe Bay, Alaska: Bedrock

Geology of the eastern Koyukuk basin, central Brooks Range, and eastcentral Arctic Slope, Alaska: Alaska Division of Geological & Geophysical Surveys Guidebook 7, v. 2, p.157-188.

Dow, W.G., and Talukdar, S.C., 1995, Geochemical analysis of outcrop samples, western DeLong Mountains, Brooks Range, Alaska: Alaska Division of Geological & Geophysical Surveys Public-Data File 95-29, 40 p.

Ehrenberg, S.N., 1993, Preservation of anomalously high porosity in deeply buried sandstones by grain-coating chlorite: Examples from the Norwegian continental shelf: American Association of Petroleum Geologists Bulletin, v. 77, p. 1260-1286.

Folk, R.L., 1968, Petrology of sedimentary rocks: Austin, TX, Hemphill's, 170 p.

Mayfield, C.F., Tailleur, I.L., and Ellersieck, Inyo, 1988, Stratigraphy, structure, and palinspastic synthesis of the western Brooks Range, northwestern Alaska, *in* Gryc, George, ed., Geology and exploration of the National Petroleum Reserve in Alaska, 1974-1982: U.S. Geological Survey Professional Paper 1399, p. 143-186.

Mickey, M.B., Haga, Hideyo, and Mull, C.G., 1995, Paleontologic data: Tingmerkpuk Sandstone and related units, northwestern DeLong Mountains, Brooks Range, Alaska: Alaska Division of Geological & Geophysical Surveys Public-Data File 95-31, 42 p.

Moore, T.E., Wallace, W.K., Bird, K.J., Karl, S.M., Mull, C.G., and Dillon, J.T., 1994, Geology of Northern Alaska, *in* Plafker, George, and Berg, H.C., eds., The Geology of Alaska: Geological Society of America, Boulder, Colo., v. G1, p. 49-140.

Mull, C.G., 1995, Preliminary evaluation of the hydrocarbon source rock potential of the Tingmerkpuk Sandstone (Neocomian) and related rocks, northwestern DeLong Mountains, Brooks Range, Alaska: Alaska Division of Geological & Geophysical Surveys Public-Data File 95-30, 20 p.

———1989, Generalized stratigraphy and structure of the Brooks Range and Arctic Slope, *in* Mull, C.G., and Adams, Karen, eds., Dalton Highway, Yukon River to Prudhoe Bay, Alaska: Bedrock Geology of the eastern Koyukuk basin, central Brooks Range, and eastcentral Arctic Slope, Alaska: Alaska Division of Geological & Geophysical Surveys Guidebook 7, v. 1, p. 31-46.

Murphy, J.M., O'Sullivan, P.B., and Gleadow, A.J.W., 1994, Apatite fission-track evidence of episodic Early Cretaceous to late Tertiary cooling and uplift events, central Brooks Range, Alaska, *in* Thurston, D.K., and Fujita, K., eds., 1992 proceedings of the International Conference on Arctic Margins: U.S. Dept. of Interior, Minerals Management Service OCS Study MMS 94-0040, p. 257-262.

Odin, G.S., and Fullagar, P.D., 1989, Geological significance of the glaucony facies, *in* Odin, G.S., ed., Green marine clays: Amsterdam, Elsevier, p. 295-332.

O'Sullivan, P.B., 1994, Fission track evidence indicates that the present-day Brooks Range, Alaska is a Cenozoic, not Early Cretaceous, physiographic feature: EOS, v. 75(44), p. 646.

Reiser, H.N., Brosgé, W.P., Dutro, J.T., Jr., and Detterman, R.L., 1980, Geologic map of the Demarcation Point quadrangle, Alaska: U.S. Geological Survey Miscellaneous Investigations Series Map I-1133, scale 1:250,000.

van de Kamp, P.C., 1988, Stratigraphy and diagenetic alteration of Ellesmerian sequence siliciclastic rocks. North Slope, Alaska, *in* Gryc, George, ed., Geology and exploration of the National Petroleum Reserve in Alaska, 1974 to 1982: U.S. Geological Survey Professional Paper 1399, p 833-854.

Wartes, M.A., and Reifenstuhl, R.R., 1997, Preliminary petrography on the provenance of six Neocomian to Albian sandstones, northwestern Brooks Range, Alaska, *in* Clough, J.G. ed., Short Notes on Alaska Geology, 1997: Alaska Division of Geological & Geophysical Surveys Professional Report 118, p. 131-140.

Wilson, M.D., 1992, Inherited grain-rimming clays in sandstones from Eolian and shelf environments: Their origin and control on reservoir properties, *in* Houseknecht, D.W., and Pittman, E.D., eds., Origin, diagenesis, and petrophysics of clay minerals in sandstones: Society of Economic Paleontologists and Mineralogists Special Publication 47, p. 209-225.

LOWER TO MIDDLE DEVONIAN (LATEST EMSIAN TO EARLIEST EIFELIAN) CONODONTS FROM THE ALEXANDER TERRANE, SOUTHEASTERN ALASKA

by
Norman M. Savage[1] and Constance M. Soja[2]

INTRODUCTION

The thick Paleozoic sequences that occur in the southern Alexander Archipelago of southeastern Alaska include abundant deposits of Devonian age. Although various good Early Devonian conodont faunas of Lochkovian, Pragian, and early Emsian were recovered from several localities on the western and eastern sides of Prince of Wales Island and nearby adjacent islands, late Emsian conodonts have been notably rare (Savage, 1977, 1988; Savage and Gehrels, 1984.) Abundant conodonts of Middle Devonian (middle and late Eifelian) age are known from Wadleigh Island and farther northeast on Prince of Wales Island (Savage, 1995), but no faunas of earliest Eifelian age have been described. Thus, for many years the available evidence suggested a late Emsian to early Eifelian regression. More recently, *Pandorinellina expansa* was recovered by one of us (NMS) from samples collected on Kupreanof Island, to the north, indicating the possible presence of marine deposits during at least part of the missing interval (McLelland and Gehrels, 1990, table 1).

Herein we are reporting the occurrence of several species in an 18-m-thick section exposed on "Harlequin Duck" rock (informally named), at the north end of Karheen Passage (fig. 1), indicating that more of the previously missing marine sequence across the Early to Middle Devonian boundary may be present.

[1]Department of Geological Sciences, University of Oregon, Eugene, Oregon 97403.
[2]Department of Geology, Colgate University, Hamilton, New York 13346.

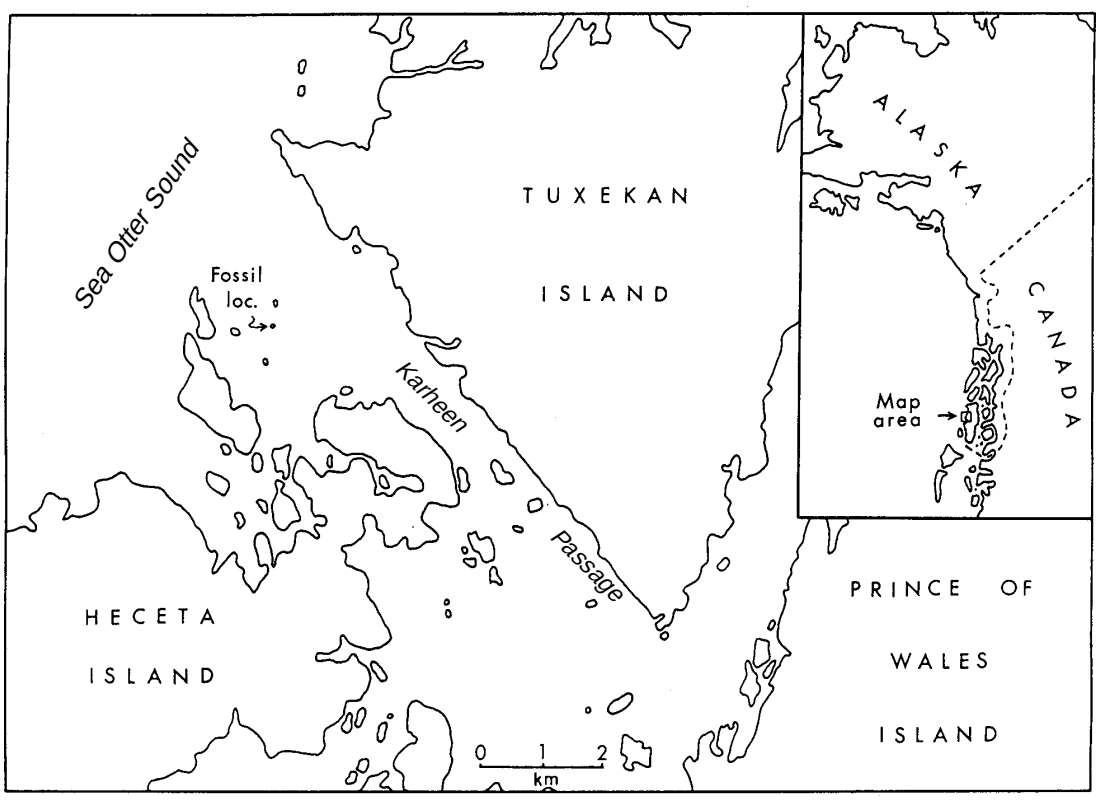

Figure 1. *Map of the Karheen Passage, and adjacent islands, southeastern Alaska, showing the position of the fossil locality on Harlequin Duck rock.*

OCCURRENCE AND AGE OF COLLECTIONS

The short section exposed on Harlequin Duck rock was measured by one of us (CMS) and shown to consist of a basal breccia that is 5 m thick, overlain by a "bioherm" (resedimented reef) that is about 13 m thick (fig. 2). The basal breccia has now yielded the conodonts *Ozarkodina carinthiaca* (Schulze), *Polygnathus linguiformis* cf. *l. bultyncki* Weddige, and *Polygnathus serotinus* Telford. *Ozarkodina carinthiaca* is known elsewhere from the *inversus* to *patulus* Zones, and *Polygnathus serotinus* and *Polygnathus linguiformis bultyncki* from the *serotinus* to *costatus* Zones (Klapper and Johnson, 1980). The oldest dated clasts in the basal breccia are thus likely to be no older than *inversus* Zone age, the youngest dated clasts no younger than *costatus* Zone age, and the breccia itself no older than *inversus* Zone age.

The bioherm has also yielded *Polygnathus serotinus*, together with *Pandorinellina expansa* Uyeno and Mason, and *Polygnathus angusticostatus* Wittekindt. *Pandorinellina expansa* is known elsewhere from the *inversus* to *costatus* Zones, and *Polygnathus angusticostatus* from the *patulus* to *ensensis* Zones (Klapper and Johnson, 1980). The occurrence of *Pandorinellina expansa* together with *Polygnathus angusticostatus* at locality 1.11 indicates an age for that horizon within the *patulus* to *costatus* Zones.

These occurrences on Harlequin Duck rock thus indicate the presence of beds of *inversus* to at least *patulus* and possibly as young as *costatus* age and show that the late Emsian to early Eifelian interval is probably present in marine limestones in this part of southeastern Alaska. Conodonts collected by one of the authors (NMS) from the Alberto Islands, farther south near the town of Craig, also show the occurrence of limestones of approximately this time interval. Thus there is now evidence from three different parts of southeastern Alaska that suggests marine deposition across the Lower to Middle Devonian boundary. Earlier indications of an unconformity or hiatus toward the end of the Emsian and into the Eifelian may be more the result of concealment of section beneath the sea than of regional regression.

SYSTEMATIC PALEONTOLOGY

In this paper the multielement notation and suprageneric classification used are those of Sweet (1988).

Family SPATHOGNATHODONTIDAE Hass, 1959
Genus OZARKODINA
Branson and Mehl, 1933

Type species. Ozarkodina confluens (Branson and Mehl, 1933).

OZARKODINA CARINTHIACA
(Schulze, 1968)
Figure 3.1-2

Discussion. This species has a distinctive Pa element with a high anterior blade that descends to a point about one third the unit length. The posterior two-thirds of the unit is gently arched and bears nodular subequal denticles above a wide, symmetrical basal cavity. In the type material from the Karawanken Alps there are alternating large and small denticles above the basal expansion. Klapper and others (1978) note that some of the specimens from the Barrandian area of the Czech

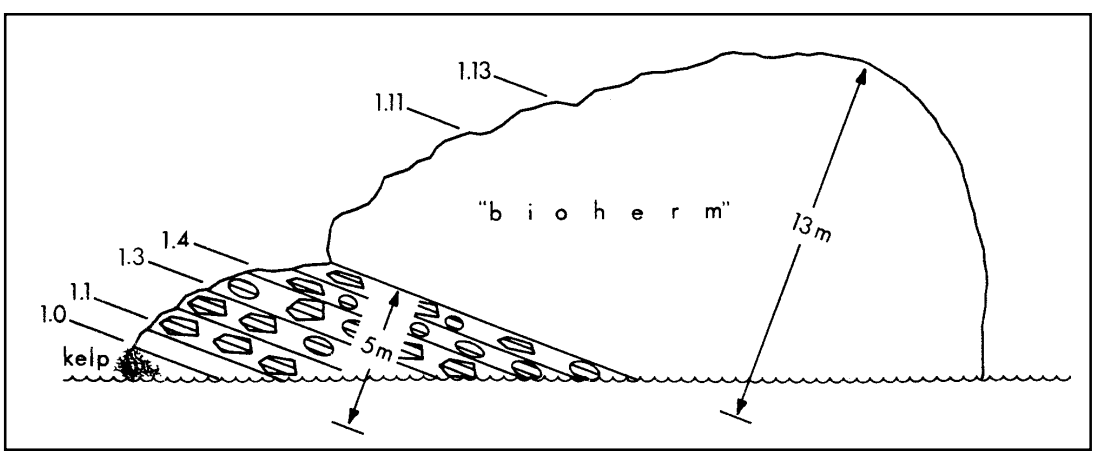

Figure 2. *Schematic section of exposure on Harlequin Duck rock showing localities 1.0, 1.1, 1.3, and 1.4 in the basal breccia, and localities 1.11 and 1.13 in the bioherm.*

Republic lack the smaller denticles and this is also the case with the Alaskan material. An additional feature of the Alaskan specimens is a more gradual descent of the anterior blade from the highest anterior denticles to the point above the front of the basal expansion. If additional specimens of the Alaskan form are obtained, and the lack of the alternating small denticles and more gradual descent of the upper blade margin prove to be consistent characteristics, these features may be enough to warrant recognition of a distinct subspecies. Despite these differences, the specimens from southeastern Alaska should be assigned to *Ozarkodina carinthiaca*, and are of interest as the first representatives of the species recorded from North America. Previously the species has been recorded from the Karawanken Alps (Schulze, 1968), the Carnic Alps (Pölser, 1969; Schönlaub, 1986), Bohemia (Klapper and others, 1978), Spain (Bultynck, 1976, 1979), the Armorican Massif, France (Lardeux and Weyant, 1993), and the Zeravshan Range, central Asia (Apekina and Mashkova, 1978).

Material. Two Pa elements, from locality 1.0.

Family POLYGNATHIDAE
Bassler, 1925
Genus POLYGNATHUS
Hinde, 1879
Type species. Polygnathus dubius Hinde, 1879.

POLYGNATHUS ANGUSTICOSTATUS
Wittekindt, 1966
Figures 3.6-8

Discussion. The species is characterized by platform margins that do not reach the posterior tip of the unit. It is a species that occurs most commonly in the Eifelian but can extend down into the latest Emsian. In southeastern Alaska it is fairly common in collections from the westernmost of the Alberto Islands and from Prince of Wales Island in beds assigned to the middle to late Eifelian *kockelianus* Zone (Savage, 1995).

Material. Two Pa elements from locality 1.11.

POLYGNATHUS LINGUIFORMIS cf. L. BULTYNCKI
Weddige, 1977
Figures 3.3-5

Discussion. This single Pa element is close to *Polygnathus linguiformis bultyncki* Weddige, but has more rounded platform margins and a less flexed posterior tongue. If more specimens were available, it would be easier to decide if these are consistent differences.

Material. One Pa element from locality 1.1.

POLYGNATHUS SEROTINUS
Telford, 1975
Figures 3.11-22

Discussion. These Pa elements, from horizons in the basal breccia and the bioherm, have the characteristic flange on the outer side of the basal pit and an upper platform that has a high outer margin and a sharply flexed posterior tongue.

Material. A total of 44 Pa elements (11 from locality 1.1, 6 from locality 1.3, 5 from locality 1.4, and 22 from locality 1.13).

Genus PANDORINELLINA
Müller and Müller, 1957
Type species. Pandorina insita Stauffer, 1940.

PANDORINELLINA EXPANSA
Uyeno and Mason, 1975
Figures 3.9-10

Discussion. The two Pa elements of *Pandorinellina expansa* recovered from locality 1.11 in the upper part of the section are characteristic of the species, exhibiting an expanded basal cavity that extends the whole length of the unit, a high anterior blade with three or four high denticles, and a precipitous drop from the anterior blade to the much lower, arched posterior part of the unit.

Material. Two Pa elements from locality 1.11.

ACKNOWLEDGMENTS

We thank Barbara Savage for processing the samples and picking the conodont residues. Dale R. Sparling and Thomas T. Uyeno kindly reviewed the submitted manuscript and made valuable suggestions for its improvement.

REFERENCES CITED

Apekina, L.S., and Mashkova, T.V., 1978, Conodonts, *in* Sokolov, B.S., and Garkovets, V.G., eds., Field Session, International Subcommission on Devonian Stratigraphy, Samarkand, USSR, Atlas of Paleontology, pls. 73-78.

Bassler, R.S., 1925, Classification and stratigraphic use of conodonts: Geological Society of America Bulletin, v. 36, p. 218-220.

Branson, E.B., and Mehl, M.G., 1933, Conodont studies: University of Missouri studies, v. 8, n. 1, p. 1-349.

Bultynck, P., 1976, Le Silurien supérieur et le Devonien inférieur de la Sierra de Guadarrama (Espagne centrale). Troisieme partie: elements icriodiformes, pelekysgnathiformes et polygnathiformes: Institut Royal des Sciences Naturelles de Belgiques, Bulletin, v. 49 (Sciences de la terre, 5), 74 p.

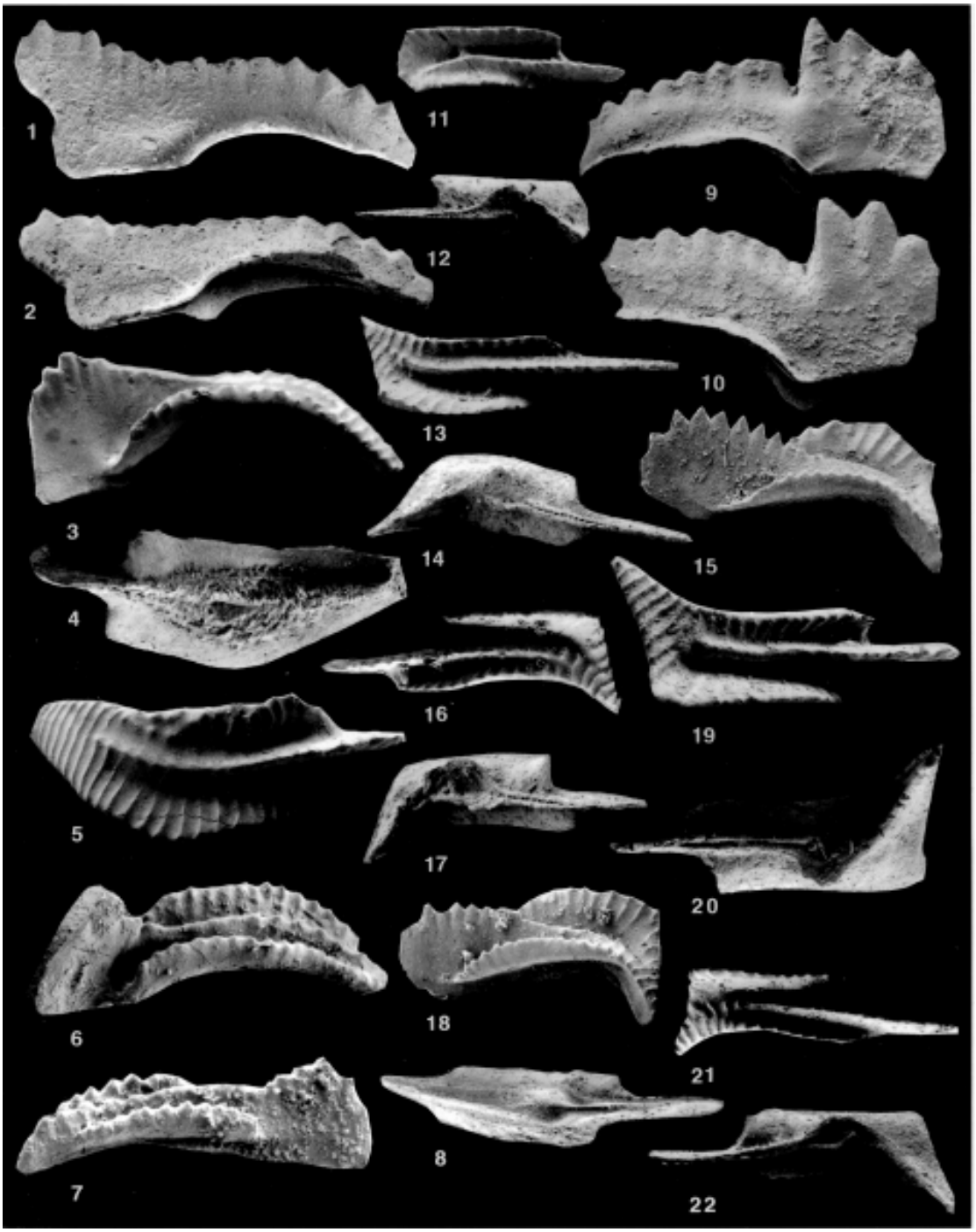

Figure 3. *1-2,* Ozarkodina carinthiaca *(Schulze, 1968). Lateral and lower lateral views of Pa element USNM 481686, from locality 1.0, x 90. 3-5,* Polygnathus linguiformis *cf.* l. bultyncki *Weddige, 1977. Lateral, lower, and upper views of Pa element USNM 481687, from locality 1.1, x 48. 6-8,* Polygnathus angusticostatus *Wittekindt, 1966. 6, upper lateral view of Pa element USNM 481688, from locality 1.11, x 90; 7-8, lateral and lower views of Pa element USNM 481689, from locality 1.11, x 90. 9-10,* Pandorinellina expansa *Uyeno and Mason, 1975. 9, lateral view of Pa element USNM 481690, from locality 1.11, x 90; 10, lateral view of Pa element USNM 481691, from locality 1.11, x 90. 11-22,* Polygnathus serotinus *Telford. 1975. 11-12, upper and lower views of Pa element USNM 481692 from locality 1.1, x 90; 13-15, upper, lower, and lateral views of Pa element USNM 481693, from locality 1.4, x 90; 16-18, upper, lower, and lateral views of Pa element USNM 481694, from locality 1.1, x 90; 19-20, upper and lower views of Pa element USNM 481695, from locality 1.13, x 90; 21-22, upper and lower views of Pa element USNM 481696, from locality 1.1, x 90.*

Bultynck, P., 1979, Excursion in the Devonian of the Sierra de Guadarrama between Cercadillo and La Riba de Santiuste (with minor contributions by H. Hollard, J.L. Garcia-Alcalde, M. House and F. Soto), *in* Garcia-Alcade, J.L., Arbizu, M.A., Garcia-Lopez, S., and Mendez-Bedia, I., eds., Guidebook, Meeting of the International Subcommission on Devonian Stratigraphy, Spain, Servicio de Publicacaciones, Universidad de Oviedo, p. 32-34.

Hass, W.H., 1959, Conodonts from the Chappel Limestone of Texas: U.S. Geological Survey Professional Paper 295-J, p. 365-369.

Hinde, G.J., 1879, On conodonts from the Chazy and Cincinnati Group of the Cambro-Silurian, and from the Hamilton and Genesee-Shale of the Devonian, in Canada and the United States: Quarterly Journal of the Geological Society of London, v. 35, p. 351-369.

Klapper, G., and Johnson, J.G., 1980, Endemism and dispersal of Devonian conodonts: Journal of Paleontology, v. 54, p. 400-455.

Klapper, G., Ziegler, W., and Mashkova, T.V., 1978, Conodonts and correlation of Lower-Middle Devonian boundary beds in the Barrandian area of Czechoslovakia: Geologica et Palaeontologica, v. 12, p. 103-116.

Lardeux, H., and Weyant, M., 1993, Conodontes et tentaculites (dacryoconarides) du Calcaire de Valet en Chaudeefonds: Dévonien Micropaléontologie, v.36, p. 19-28.

McClelland, W.C., and Gehrels, G.E., 1990, Geology of the Duncan Canal shear zone: Evidence for Early to Middle Jurassic deformation of the Alexander terrane, southeastern Alaska: Geological Society of America Bulletin, v. 102, p. 1378-1392.

Müller, K.J., and Müller, E.M., 1957, Early Upper Devonian (Independence) conodonts from Iowa, Part 1: Journal of Paleontology, v. 31, p. 1069-1108.

Pölser, P., 1969, Conodonten aus dem Devon der Karnischen Alpen (Findenigkofen, Österreich): Jahrbuch der Geologischen Bundesanstalt, v. 112, p. 399-440.

Savage, N.M., 1977, Lower Devonian conodonts from the Karheen Formation, southeastern Alaska: Canadian Journal of Earth Sciences, v. 14, p. 278-284.

———1988, Devonian faunas and major depositional events in the southern Alexander terrane, southeastern Alaska, *in* McMillan, M.J., Embry, A.F., and Glass, D.J., eds., Devonian of the World, Second International Symposium on the Devonian System, v. 3, Paleontology, paleoecology, and biostratigraphy: Canadian Society of Petroleum Geologists Memoir 14, p. 257-264.

Savage, N.M., 1995, Middle Devonian conodonts from the Wadleigh Limestone, southeastern Alaska: Journal of Paleontology, v. 69. p. 540-555.

Savage, N.M., and Gehrels, G.E., 1984, Early Devonian conodonts from Prince of Wales Island, southeastern Alaska: Canadian Journal of Earth Sciences, v. 21, p. 1415-1425.

Schönlaub, H.P., 1986, Devonian conodonts from Section Oberbuchach II in the Carnic Alps (Austria), *in* Ziegler, W., and Werner, R., eds., Devonian Series boundaries - Results of world-wide studies, Courier Forschungsinstitut Senkenberg, v. 75, p. 353-374.

Schulze, R., 1968, Die conodonten aus dem Paläozoikum der mittleren Karawanken (Seeberggebiet): Neues Jahrbuch Geologie und Paläontologie, Abhandlungen, v. 130, p. 133-245.

Stauffer, C.R., 1940, Conodonts from the Devonian and associated clays of Minnesota: Journal of Paleontology, v. 14, p. 417-435.

Sweet, W.C., 1988, The Conodonta: Morphology, taxonomy, paleoecology, and evolutionary history of a long-extinct animal phylum: Oxford Monographs on Geology and Geophysics, no.10, Oxford, Oxford University Press, 212 p.

Telford, P.G., 1975, Lower and Middle Devonian conodonts from the Broken River Embayment, north Queensland, Australia: London, Special Papers in Palaeontology, no. 15, 96 p.

Uyeno, T.T., and Mason, D., 1975, New Lower and Middle Devonian conodonts from northern Canada: Journal of Paleontology, v. 49, p. 710-723.

Weddige, K., 1977, Die Conodonten der Eifel-Stufe im Typusgebiet und in benachbarten Faziesgebieten: Senckenbergiana lethaea, v. 58, p. 271-419.

Wittekindt, H., 1966, Zur Conodontenchronologie des Mitteldevons: Fortschritte in der Geologie von Rheinland und Westfalen, v. 9, p. 621-646 [imprint 1965].

This page has intentionally been left blank.

PRELIMINARY PETROGRAPHY AND PROVENANCE OF SIX LOWER CRETACEOUS SANDSTONES, NORTHWESTERN BROOKS RANGE, ALASKA

by
Marwan A. Wartes[1] and Rocky R. Reifenstuhl[2]

ABSTRACT

The orogenic history of the western-most Brooks Range is poorly understood. This study presents new petrographic data for six Lower Cretaceous sandstones which will be used to constrain models for the geologic development of the western Brooks Range. Modal data, plotted on standard sandstone ternary diagrams, show significant differences between various Lower Cretaceous units, outlining changes through time in the provenance and tectonic environment of western Arctic Alaska as the Brooks Range evolved.

The oldest sample in this study, the Okpikruak Formation, appears to represent the earliest erosion of the volcanic and plutonic-rich Copter Peak and Misheguk Mountain allochthons. A nearly coeval unit, the Tingmerkpuk Sandstone, probably represents some of the last sediment derived from the north and was deposited within the stable passive margin setting which preceded the Brooks Range orogeny. The basal Brookian sandstone and the two young Mount Kelly Graywacke samples are rich in detrital carbonate and other lithic fragments. They were both deposited in the asymmetric foredeep on the north flank of the Brooks Range and are likely derived principally from the Paleozoic calcareous schist belt to the south. The Nanushuk Group sandstone probably had a mixed source area to the west with possible epeirogenic uplift exposing the Lisburne platform carbonates as a main source for chert and carbonate detritus.

INTRODUCTION

This preliminary study is part of a larger project undertaken by the Alaska Division of Geological & Geophysical Surveys to determine the hydrocarbon potential of the western Arctic Slope. The impetus for this study was a general lack of knowledge regarding the provenance and lithologic composition of the Lower Cretaceous sandstones of the western Brooks Range. This paper presents the petrography of six sandstones from five Lower Cretaceous rock units in the western Brooks Range and interprets their provenance and tectonic environment. Samples were collected in 1993 and 1994 from the northwestern DeLong Mountains (fig. 1) during a detailed mapping project in the western Brooks Range. The rock units represented range in age from Neocomian to Albian and were deposited in a foreland basin as turbidites, shelf storm deposits, and a nonmarine to marginal-marine deltaic environment. The five lithologic units from oldest to youngest are the Okpikruak Formation, the Tingmerkpuk Sandstone, an unnamed lower Brookian unit, the Mount Kelly Graywacke Tongue of the Fortress Mountain Formation, and the Nanushuk Group. General information on the location and ages of the samples is shown in table 1; figure 2 illustrates their relative stratigraphic and structural positions. Data on the depositional environments, paleontology, and organic geochemistry of some of these rocks are presented by Crowder and others (1994), Mickey and others (1995), Dow and Talukdar (1995), and Mull (1995).

GENERAL GEOLOGY

The western Brooks Range is an extension of the Cordilleran orogenic belt and was deformed from Late Jurassic through Early Cretaceous time. In the development of the orogenic belt, extensive thrusting displaced sheets of dominantly sedimentary rock hundreds of kilometers northward. These sheets have been termed allochthons (Mayfield and others, 1988; Mull and others, 1987a) and are composed of Late Devonian to Mesozoic rocks of the Ellesmerian sequence. Ellesmerian rocks were derived dominantly from a northern source and deposited in various stable platform environments. In the DeLong Mountains, the Brookian sequence consists of synorogenic and postorogenic sediments that were derived from the Brooks Range orogen and shed into the Colville Basin, an asymmetric foredeep to the north (Mull and others,

[1]Department of Geology and Geophysics, University of Alaska, Fairbanks, Alaska 99775. Now at Department of Geology and Geophysics, University of Wisconsin, Madison, Wisconsin 53706.
[2]Alaska Division of Geological & Geophysical Surveys, 794 University Avenue, Suite 200, Fairbanks, Alaska 99709-3645.

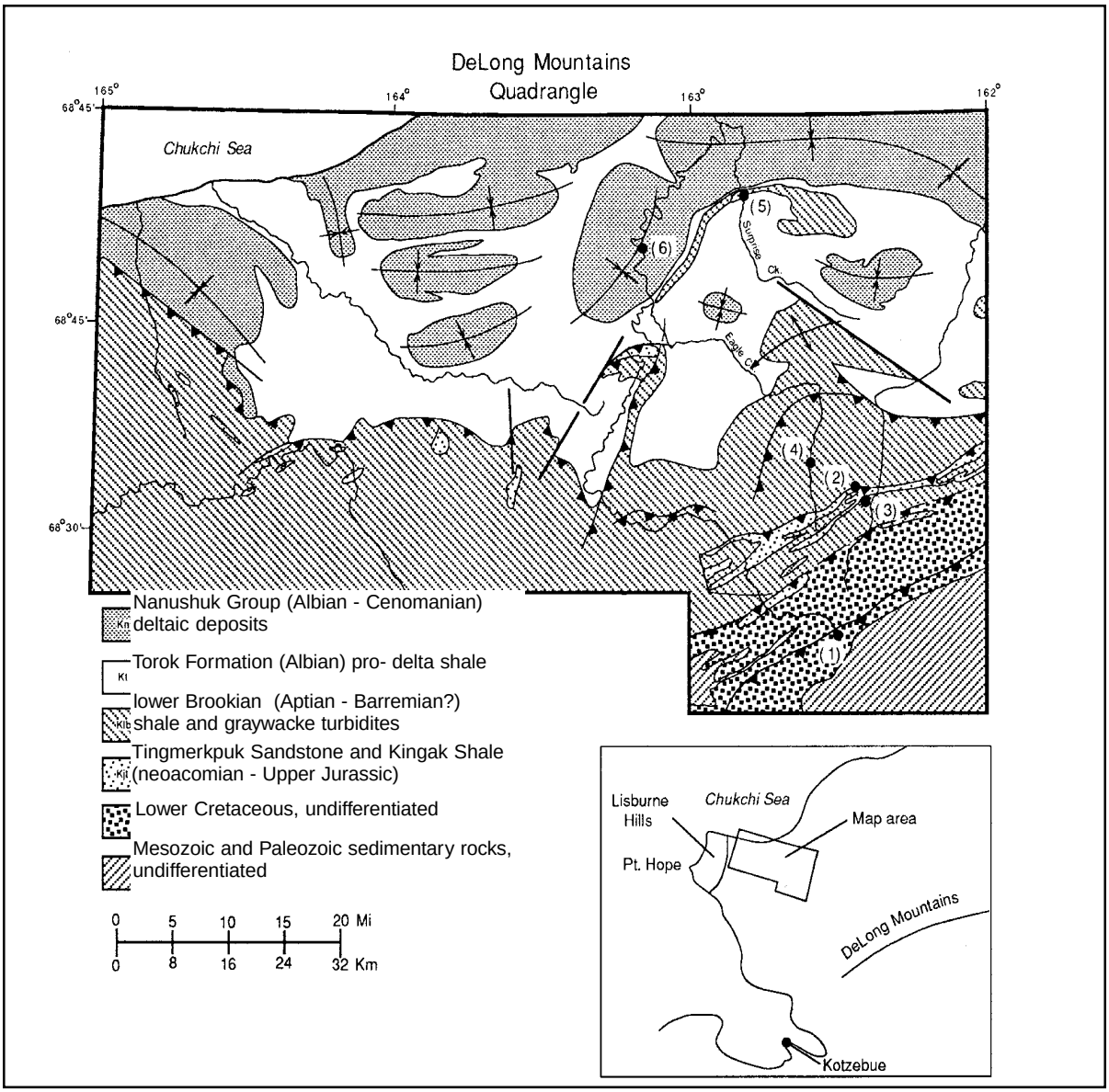

Figure 1. *Generalized geologic map of the northern DeLong Mountains 1:250,000 Quadrangle showing sample locations (modified from Mull, 1995). See table 1 for data on samples 1-6.*

Table 1. *General sample age and location*

Sample	Field	Formation	Age	Location
1	94 Mu 71	Okpikruak Formation	Valanginian	Upper Kukpowruk River
2	94 RR 73A-1	Tingmerkpuk Sandstone	Valanginian-Barremian	Tingmerkpuk Mt.
3	93 Mu 93	lower Brookian Formation	Hauterivian-Barremian	S. Side of Tingmerkpuk Mt.
4	93 Ha 152	Mt. Kelly Graywacke	Aptian	Eagle Creek
5	93 RR 64B	Mt. Kelly Graywacke	Aptian	Surprise Creek
6	93 RR 63A	Nanushuk Group	Albian	Coke Basin

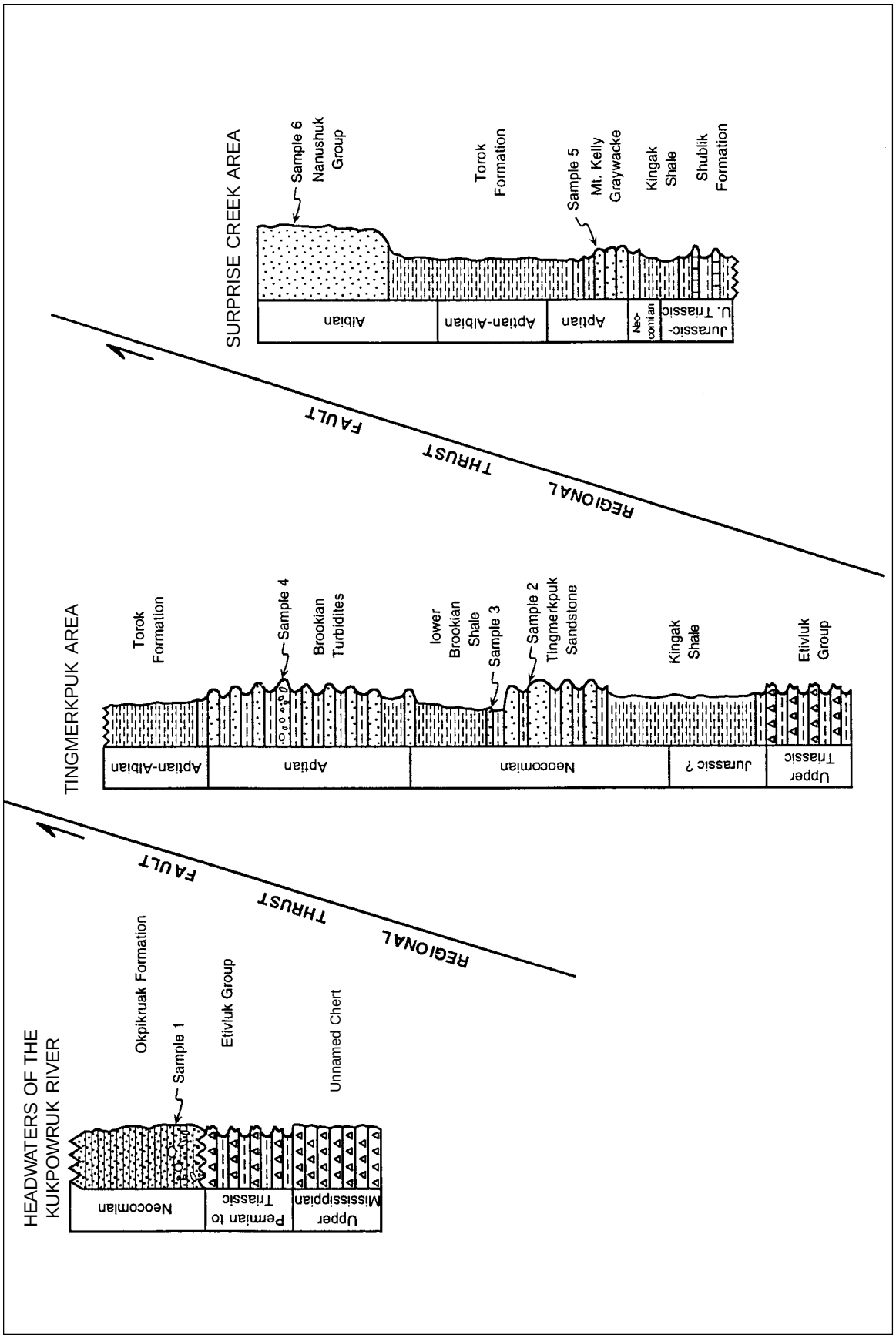

Figure 2. *Stratigraphic columns showing generalized sample stratigraphy and relative structural position.*

1987b). For a more detailed discussion of the geology of northern Alaska see Moore and others (1994), and for a palinspastic synthesis of the western Brooks Range see Mayfield and others (1988).

METHODS

Detrital modes were determined by using thin-section petrography for the six sandstone samples. To increase understanding of the provenance, altered grains were related to their detrital parent composition. Modal analysis followed the procedures of Decker (1985). A minimum of 400 points per thin section were counted for a statistically valid estimate of percent by volume for each grain category (table 2) (Van Der Plas and Tobi, 1965). Grain size in the thin sections varied from very fine (0.0625 to 0.125 mm) to course (0.5 to 1.0 mm), and the skip distance varied accordingly. However, skip distance was never less than 95 percent of the largest grain-size fraction within the sample.

The summarized petrographic data in table 2 include 18 types of detrital grains, 2 types of matrix, and 3 types of cement. These data are plotted on the triangular classification schemes of Dickinson and Suczek (1979) and Dickinson and others (1983) by using various framework modes or grain populations (table 3) to emphasize source-area characteristics (figs. 3A-3D, 4).

DIAGRAMS OF DETRITAL GRAIN POPULATIONS

Relative proportions of framework grains can be illustrated on triangular diagrams to display compositional variations in sandstones. These ternary plots use various poles representing proportions of grain types calculated from either the entire detrital population, as with the QFL and QmFLt plots, or as a smaller group, such as QpLvLs. The relative abundances of these recalculated proportions (table 3) are useful in interpreting provenance character and tectonic setting of Phanerozoic sandstones (Dickinson and others, 1983).

QFL diagrams (figs. 3A, 3B) plot all quartzose grains (Q=polycrystalline+chert+monocrystalline), total feldspars (F=plagioclase, potassium feldspar, etc.), and total lithic grains (L=unstable rock fragments). This plot emphasizes grain stability, which also gives information about the relief of the source area, the transport mechanism, and weathering processes (Dickinson and Suczek, 1979). QmFLt diagrams (figs. 3C, 3D) also use the entire grain population, but emphasize the grain size of the provenance by separating the fields into monocrystalline quartz (Qm), feldspar (F), and total detrital lithic components (Lt=polycrystalline quartz, chert, and other unstable rock fragments). The emphasis of grain size is due to the tendency of lithic fragments to accumulate in the sand-size range (Dickinson and Suczek, 1979). Figures 3A and 3C include carbonate grains as lithic detritus and figures 3B and 3D exclude carbonate grains from the framework constituent. The plots show the respective recalculated modal ratios. This exclusion of carbonate grains in figures 3B and 3D is discussed below.

The QpLvLs plot (fig. 4) uses only a part of the framework modes by comparing the relative abundances of polycrystalline quartz and chert (Qp) to lithic volcanic and metavolcanic rock fragments (Lv) to unstable sedimentary and metasedimentary rock fragments (Ls). This diagram, by excluding monocrystalline quartz, portrays the relative abundance of the less stable constituents, which are often more important in discriminating a provenance than recycled monocrystalline quartz.

The ternary plots are a powerful tool for interpreting provenance, but there are some inherent limitations. The most important limitation affecting this study is the deliberate omission of carbonate grains from the framework constituents, as suggested by Dickinson and others (1983). Mack (1984) notes that this omission is one of the major drawbacks in this technique and argues that nondetrital carbonate grains should be excluded because of their authigenic or intrabasinal nature. Such grains are not indicative of the sediment in the source area and thus, as with matrix, should also be excluded from the framework modes for provenance analysis. However, if carbonate rock fragments are derived from extrabasinal sources, they are detrital and hence should be included as an unstable lithic fragment. The special problem of coping with such hybrid sandstones can be only partially resolved because the distinction between intrabasinal carbonate allochems and detrital grains is often quite difficult. This question is particularly important in this study inasmuch as samples 1 through 5 have carbonate grains in their modes and samples 1 through 4 have greater than 28 percent carbonate grains. These latter four significantly influence the plots when carbonates are included or omitted and thus both calculated populations, QFL_1, $QmFLt_1$ (with) and QFL_2, $QmFLt_2$ (without), are shown in (figs. 3A-3D) and are taken into consideration for provenance determination.

PETROGRAPHY AND PROVENANCE

SAMPLE 1-OKPIKRUAK FORMATION

This sample from the Okpikruak Formation is from a sandstone horizon that is part of an olistostrome containing coarse boulder conglomerates. The outcrop

Table 2. *Point-count analyses*[a]

Sample names[b]	Detrital grains	Qm	Qp	Qpf	Qu	K	P	Vrf	S/P	Sch	Mic	Qca	Qc	Ss	Ca	G	Org	HM	Oth	Ma	Mu	Cs	Cc	Cu
1	389	35	12	0	0	0	45	0	0	0	0	0	0	0	0	0	0	0	8	0	0	2	0	1
2	384	64	26	0	t	0	t	0	0	0	t	0	2	0	5	0	0	t	t	0	0	0	4	0
3	339	24	17	t	2	0	t	1	t	9	3	t	t	0	41	0	0	t	t	12	0	t	3	0
4	382	13	21	2	t	0	3	5	t	10	t	3	9	0	33	t	t	t	t	t	t	0	3	0
5	375	19	17	t	t	0	2	2	t	6	1	6	7	t	36	0	t	0	t	0	1	t	4	t
6	377	18	12	1	1	0	t	3	0	2	0	14	21	0	28	0	t	0	t	t	t	t	4	0

Explanation of symbols

Ca	carbonate	Mic	white mica
Cc	carbonate cement	Mu	undifferentiated matrix
Cs	siliceous cement	Org	organics
Cu	undifferentiated cement	Oth	detrital others
F	all feldspathic grains	P	plagioclase feldspar
G	glauconite	Q	all quartzose grains
Hm	heavy minerals (zircon, tourmaline, rutile, garnet)	Qc	chert
		Qca	argillaceous chert
K	potassium feldspar	Qm	monocrystalline quartz
L	all unstable rock fragments	Qp	composite polycrystalline quartz
Ls	all unstable sedimentary and metasedimentary rock fragments	Qpf	foliated polycrystalline quartz
		Qu	undifferentiated quartz
Lt	all rock fragments including Qp, Qpf, Qc, Qca	S/P	slate/phyllite
		Sch	schist
Lv	all volcanic and metavolcanic rock fragments	Ss	sandstone
		t	trace amount
Ma	argillaceous matrix	Vrf	volcanic rock fragment

Table 3. *Calculated values for ternary plot axes*

Sample names[b]	Detrital grains	Q	F	L	Qm	Lt	Qp	Lv	Ls
Carbonate detritus included in lithic grains									
1	377	65	t	35	18	82	60	4	36
2	382	45	2	53	13	85	47	6	47
3	375	51	2	47	19	79	44	3	53
4	339	43	t	57	24	76	31	2	67
5	384	92	t	8	64	36	n/a	n/a	n/a
6	389	47	45	8	35	20	n/a	n/a	n/a
Carbonate detritus excluded from modal analysis									
1	270	92	t	8	25	75	n/a	n/a	n/a
2	256	69	5	26	20	75	n/a	n/a	n/a
3	241	79	3	18	30	67	n/a	n/a	n/a
4	201	74	1	25	41	58	n/a	n/a	n/a
5	364	98	t	2	69	31	n/a	n/a	n/a

n/a = Not applicable

[a]Values for detrital grains are total counts; values for framework components are percent of total detrital grains. Matrix and cement are calculated as percent of total rock volume.
[b](1) Okpikruak Formation; (2) Tingmerkpuk Sandstone; (3) lower Brookian sandstone; (4) Mount Kelly Graywacke (Eagle Creek); (5) Mount Kelly Graywacke (Surprise Creek); (6) Nanushuk Group sandstone.

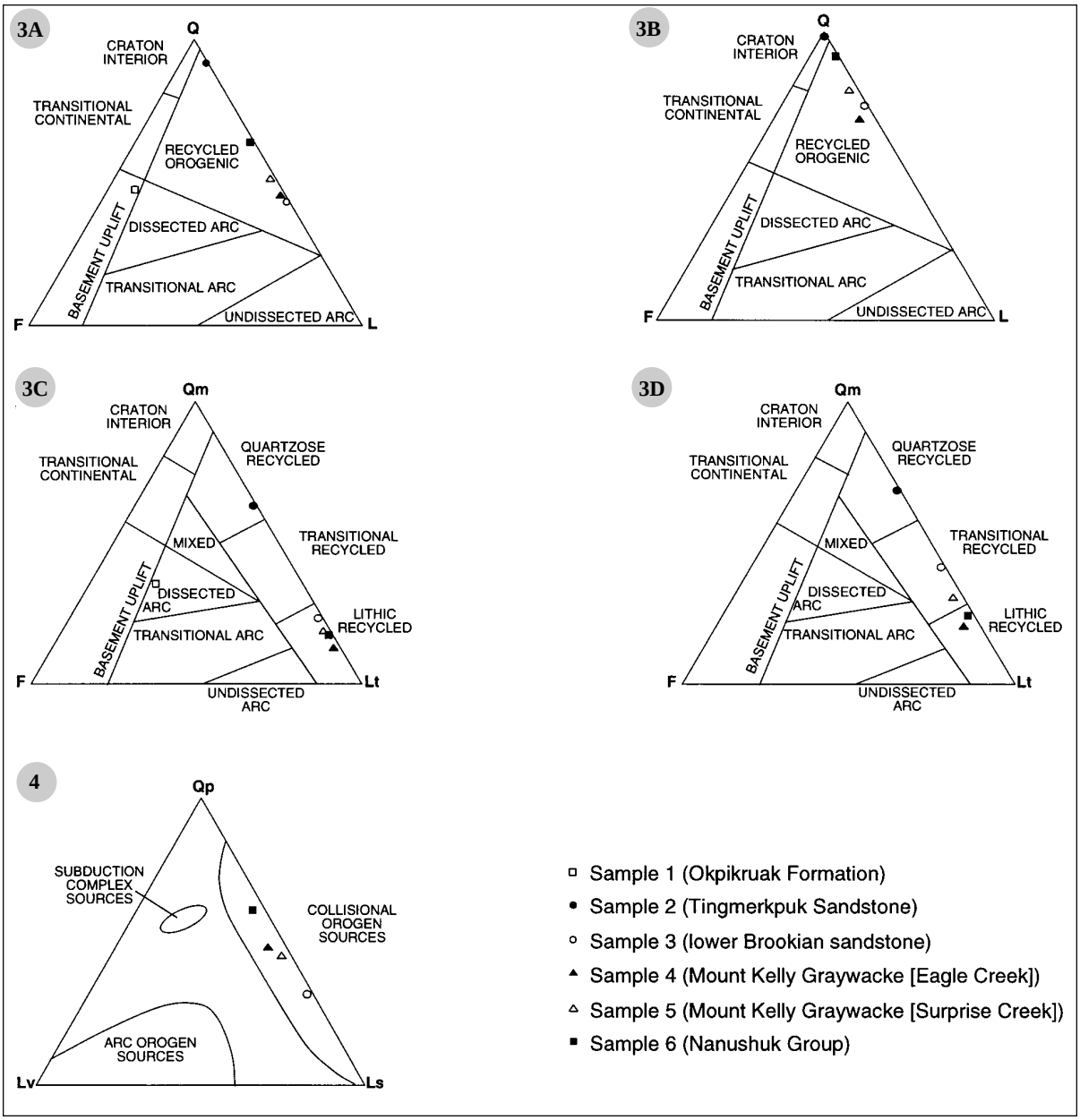

Figures 3 A-D. *Ternary diagrams (above) of total detrital grain populations. Figures A (AFL1) and C (QmFLt1) include carbonate detritus as a lithic fragment. Figures B (QmFLt2) and D (QFL2) exclude carbonate grains as a framework component and show recalculated modal ratios. See table 1 and 2 for values and symbol explanations. Provenance fields after Dickins and others (1981).*

Figure 4. *Ternary diagram (above) of partial grain populations. Plot shows mean proportions of the lithic fragments with tectonic environment fields after Dickinson and Suczek (1979). See table 1 and 2 values and symbol explanations.*

is part of a complex of thrust sheets that overlie the Tingmerkpuk Sandstone (sample 2) and lower Brookian sandstone (sample 3) and represent a more southerly part of the Colville basin (fig. 2). This sample is a very coarse to course-grained, poorly sorted, plagioclase-rich sandstone. Its framework modes consisted of only five grain types: monocrystalline quartz, polycrystalline quartz, plagioclase, hornblende (counted as "other"), and composite plagioclase rock fragments. The quartz grains are well-sutured, often obscuring grain boundaries. Plagioclase grains are either well zoned or twinned and were "dusky," indicating early stages of alteration. The hornblende detritus is also slightly altered.

The Okpikruak sandstone lacks carbonate detritus and is plotted only on QFL_1 (fig. 3A) and $QmFLt_1$ (fig. 3C). The QFL diagram (fig. 3A) indicates an uplifted basement of continental material. However, the QmFLt diagram (fig. 3C) indicates a dissected arc provenance. Either field adequately explains the high modal values for plagioclase (45 percent). The plagioclase may be plutonic or volcanic; based on the discrete morphologies of the various plagioclase grains, they could be derived from either source. Dickinson (1983) suggests deep-seated thrusting as a plausible tectonic scenario which explains sandstones with compositions such as the Okpikruak. Both arc volcanism and large-scale thrust faulting are recognized elements of Brookian tectonics, the latter often responsible for foredeep basins such as the Colville. Therefore, either interpretation of the tectonic regime for the source is probably valid. Petrographic studies of the Okpikruak in the central Brooks Range (Wilbur and others, 1987; Wilbur, 1989) have yielded more lithic-rich petrologies, which provided a more definitive relationship with magmatic arc provenances.

The two structurally highest allochthons in the central and western Brooks Range consist of the Copter Peak allochthon and the Misheguk Mountain allochthon. The Copter Peak igneous sequence is dominantly pillow basalt, but does contain numerous large-scale quartz diorite dikes and other finer-grained igneous rocks varying from dacitic to andesitic compositions (Curtis and others, 1990). The Misheguk Mountain igneous sequence consists of a fairly well developed ophiolite suite of mafic and ultramafic rocks (Roeder and Mull, 1978). However, the Misheguk Mountain sequence also contains a variety of course-grained dikes or plugs with compositions such as diorite, quartz diorite, and granite with significant amounts of quartz, plagioclase, hornblende, and biotite (Curtis and others, 1984). Either or both of the felsic to intermediate igneous rocks found in these allochthons could have been the source for the abundant plagioclase and hornblende grains in the Okpikruak.

SAMPLE 2-TINGMERKPUK SANDSTONE

The Tingmerkpuk Sandstone from Tingmerkpuk Mountain is a very fine grained, relatively clean quartzose sandstone. Quartzose grains compose most (92 percent) of the framework constituents. Chert is uncommon (2 percent), but composite polycrystalline quartz accounts for just over a quarter of the framework grains (26 percent). Monocrystalline quartz is the largest fraction (64 percent) and consists of stable, well-rounded grains, many of which are sutured. This suturing, combined with quartz overgrowths and minor amounts of carbonate cementation, creates a dense, low-porosity sandstone. Data on measured porosities and permeabilities for the Tingmerkpuk are given in Mull (1995). Feldspar occurs only in trace amounts as plagioclase. The remaining framework grains are carbonate (5 percent). Reifenstuhl and others (1997; this volume) present a more in-depth treatment of the Tingmerkpuk Sandstone.

On the QFL_1 diagram (fig. 3A), the Tingmerkpuk Sandstone plots as a sediment derived from a recycled orogenic provenance. However, when the carbonate fraction is excluded in QFL_2 (fig. 3B), the sandstone plots as an interior cratonic sand derived from a continental block provenance. Both QmFLt diagrams (figs. 3C, 3D) place the Tingmerkpuk in the recycled orogen field as well, but more specifically as a recycled quartzose sand. The most likely interpretation involves using the two diagrams (QFL_2 and $QmFLt_2$) that exclude carbonate grains from the framework constituent. This conclusion is based on the observation that other comparable Ellesmerian sands from the north are not derived from provenances containing carbonate rocks. In addition, surface outcrops of the Tingmerkpuk Sandstone contain scattered *Buchia sublaevis* pelecypods, and at least one layer of *Buchia* coquina (Mull, 1995); Reifenstuhl and others (this volume; 1997) identified pelecypod shell material in thin sections counted in a companion study. These occurrences suggest that the carbonate in the Tingmerkpuk is derived from the shelf and not from extrabasinal sources.

SAMPLE 3-LOWER BROOKIAN SANDSTONE

The lower Brookian sandstone is a medium-grained, poorly sorted, subangular, carbonate-rich sandstone that has the highest non-quartzose lithic volume (57 percent) of the sandstones described here. The compositional immaturity of this sandstone is most readily illustrated by its lithic constituents, especially the relatively abundant schist fragments (9 percent). Carbonate grains

are also the highest noted in this study (41 percent). Though still framework supported, this sample contains significant amounts of argillaceous material as depositional matrix (12 percent).

The lower Brookian sandstone plots as a recycled orogenic sandstone on both QFL and both QmFLt diagrams (figs. 3A-3D). The $QmFLt_1$ plot (fig. 3C) further classifies the sample as a recycled lithic sandstone, whereas the $QmFLt_2$ plot (fig. 3D) places it in the transitional recycled field. The QpLvLs plot (fig. 4) suggests that the lower Brookian was probably derived from a collisional orogenic front. These data indicate that this unit has a distinctly different provenance than the underlying Tingmerkpuk sandstone and must have been shed shortly after the onset of the Brookian orogeny. None of the carbonate grains noted in this sample portrayed any bioclastic structure, suggesting that these grains were not derived from the fossiliferous Lisburne platform carbonates. In fact, palinspastic models suggest that during Neocomian time erosion is unlikely to have exposed the Lisburne Group carbonates (Mull, oral commun., 1996). The abundance of schist fragments, white mica, and the morphology of the pervasive carbonate detritus suggest that much of the detritus in the lower Brookian sands was derived from erosion of the schist belt and Lower Paleozoic Baird Group carbonates, which are widespread in the southern Brooks Range.

SAMPLES 4 AND 5-MOUNT KELLY GRAYWACKE

Two samples of the Mount Kelly Graywacke, from Eagle Creek and from Surprise Creek, are medium-grained, poorly sorted, subangular, carbonate-rich sandstone. The major lithic grains include volcanic rock fragments (5 and 2 percent, respectively), schist (10 and 6 percent), and high modal values of carbonate (33 and 36 percent). Most of the volcanic rock fragments and plagioclase grains are in late stages of alteration to chlorite. Sample 5, from Surprise Creek, has a more mature monocrystalline quartz fraction (19 percent vs 13 percent in sample 4), but the samples had equal values for the sum of composite polycrystalline quartz and chert (30 percent). For a more detailed treatment of the Mount Kelly Tongue and the Fortress Mountain Formation see Molenaar and others (1988).

Both samples of the Mount Kelly Graywacke plot on the QFL diagrams (figs. 3A, 3B) as recycled orogenic sandstones. Sample 4, from Eagle Creek, plots as a lithic recycled orogenic sandstone on both QmFLt diagrams (figs. 3B, 3D), whereas sample 5 (from Surprise Creek) plots as a lithic recycled sandstone in $QmFLt_1$ (fig. 3C) and as transitional recycled in $QmFLt_2$ (fig. 3D). Both sandstones plot within the collisional orogen field of the QpLvLs diagram (fig. 4). These data indicate an unstable orogenic setting whose sedimentary basin was the evolving Colville foredeep. The carbonate grains were probably derived from the erosion of the quartz muscovite schist and associated calcareous schist that form the southern margin of the Brooks range (Mull, 1985). The remaining sedimentary lithic grains, such as chert, were likely derived from the allocthonous rocks of the DeLong and Endicott mountains.

SAMPLE 6-NANUSHUK GROUP

The sample from the Nanushuk Group of the Coke Basin is a medium-grained litharenite. Quartzose grains are abundant (65 percent), and are composed largely of polycrystalline varieties (73 percent of total quartzose population). Chert is abundant in this sample (35 percent), ranging from cherty-argillite to clean, very fine grained chert. Much of the chert is partially obscured by the interstitial growth of authigenic dolomite rhombs. Detrital carbonate is also a large fraction (28 percent) of the framework mode. Minor amounts of other unstable lithic grains, such as schist and volcanic fragments, suggest proximity to the source terrane.

The Nanushuk Group sandstone plots in the recycled orogenic field on both QFL diagrams (figs. 3A, 3B). Both QmFLt diagrams (figs. 3C, 3D) also portray the provenance as consisting largely of orogenic, lithic-rich material. The position of this sandstone sample at the lithics pole is largely due to high modal values of chert (35 percent) and carbonate detritus (28 percent). These two constituents strongly indicate a sedimentary source area. Carbonates of the Lisburne Group crop out in the Tigara uplift west of the Coke basin (Grantz and others, 1976; Mull, 1979), and may be present in the Herald arch, a possible offshore extension of the uplift. General mapping and paleocurrent indicators of Ahlbrandt and others (1979) suggest that the Nanushuk Group in the western Arctic Slope was deposited as part of a large delta, termed the Corwin Delta. Their data indicate a derivation of the delta from the west in the area of the Herald arch. Although it does not change the field in which this sample plots, the carbonate grains are probably detrital and thus sedimentary lithics. The QpLvLs plot (fig. 4) places the sandstone in a collisional orogen source field, suggesting deposition as a result of the Brookian orogeny.

SUMMARY

A petrographic analysis of a suite of Neocomian through Albian sandstones (table 1) sampled from the DeLong Mountains Quadrangle reveals provenance and likely tectonic environments.

The sandstone sampled from the Okpikruak Formation (sample 1) is unusually rich in plagioclase (45 percent). The provenance is probably the result of early erosion of the volcanic and plutonic-rich Copter Peak and Misheguk Mountain allochthons, which now exist largely as disparate klippen (Roeder and Mull, 1978). Felsic and intermediate sources present within these upper-most thrust sheets adequately account for the high modes of plagioclase relative to the other four Brookian sands deposited later.

The Tingmerkpuk Sandstone (sample 2) is the only sand in this study whose genesis was within the relatively stable tectonic setting of the Ellesmerian passive margin. On the basis of this setting, the provenance was an interior craton, in this case the Franklinian sequence.

The basal Brookian sandstone (sample 3) was derived from a carbonate-rich source area. The Lisburne platform carbonates are excluded as a possible source, and the calcareous rocks of the schist belt are the likely source, though they currently crop out only along the southern margin of the Brooks Range.

The Mount Kelly Graywacke (samples 4 and 5) probably had a mixed source area. The modal values for chert (9 and 13 percent, respectively) suggest sources related to the DeLong and Endicott mountains allochthons. In addition, the abundance of detrital carbonate (33 and 36 percent, respectively) indicates deposition proximal to the source area, which was probably the schist belt.

The sandstone of the Nanushuk Group (sample 6) has high modal values of sedimentary lithics. Geologic evidence suggests the Lisburne carbonates were epeirogenically uplifted and later served as a potential western source for the Nanushuk. This sample was the youngest of those examined here and was clearly a product of the Brooks Range orogeny.

The preliminary nature of this study and the sampling spread make any correlations and regional inferences tentative. However, some petrographic trends through time and space are noteworthy and may provide a basis for further investigation.

The Okpikruak Formation probably records the early unroofing of the highest allochthons during Valanginian time. Therefore, a detailed regional study of lateral and vertical variation in Okpikruak petrography and provenance, combined with good age control, may provide further data for a palinspastic synthesis. Such a study could improve understanding of the early tectonic evolution of the Brooks Range orogenic belt.

The Mt. Kelly Graywacke (samples 4 and 5) and the lower Brookian sandstone (sample 4) are quite similar petrographically. The Mt. Kelly is younger (Aptian) than the lower Brookian unit (Hauterivian-Barremian), but this study suggests that their tectonic environment and provenance are similar. Their differentiation at the hand-sample level is problematic, and without the benefit of stratigraphic succession, they are nearly impossible to tell apart. Earlier studies based identification of the Mount Kelly on visible mica. However, this study found more mica and comparable values of schist fragments in the lower Brookian sandstone. More detailed petrography of both units is planned to establish if the two units exhibit any diagnostic petrographic differences.

The petrographic data presented in this study help to detail the changes through time in provenance and tectonic environment of Arctic Alaska as the Brooks Range orogenic belt evolved. The observed compositional variation of sediments in the Colville Basin from Valanginian to Albian time record the progressive erosion of the maturing Brooks Range fold and thrust belt.

ACKNOWLEDGMENTS

The authors thank the Alaska Division of Geological & Geophysical Surveys (DGGS) for the use of their microscope facilities and the University of Alaska Fairbanks, Department of Geology and Geophysics for the use of their thin-section making equipment. We especially thank Gil Mull for suggesting this project and providing continuous input throughout the study. Graduate student Tom Douglas (UAF) helped with the arduous task of making several thin sections. We are indebted to Erin Parcher for both early editorial work on the manuscript and help with the creation of tables 1-3. And, of course, we especially thank Gil Mull (DGGS) and David LePain (Shannon and Wilson) for their insightful comments and suggestions.

REFERENCES CITED

Ahlbrandt, T.S., Huffman, A.C., Fox, J.E., and Pasternack, I., 1979, Depositional framework and reservoir-quality studies of selected Nanushuk Group outcrops, North Slope, Alaska, *in* Ahlbrandt, T.S., ed., Preliminary geologic, petrologic, and paleontologic results of the study of the Nanushuk Group rocks, North Slope Alaska: U.S. Geological Survey Circular 794, p. 14-31.

Crowder, R.K., Adams, K.E., and Mull, C.G., 1994, Measured stratigraphic section of the Tingmerkpuk Sandstone (Neocomian), western Brooks Range, Alaska: Alaska Division of Geological & Geophysical Surveys, Public-Data File 94-29, 8 p., 1 sheet (measured sections).

Curtis, S.M., Ellersieck, Inyo, Mayfield, C.F., and Tailleur, I.L., 1990, Reconnaissance Geologic Map of the DeLong Mountains A-1 and B-1 quadrangles and part of the C-1 quadrangle, Alaska: U.S. Geological Survey Miscellaneous Investigation 1930, 2 sheets.

Decker, J.E., 1985, Sandstone modal analysis procedure: Alaska Division of Geological & Geophysical Surveys, Version 2, Public-Data File Report 85-3a, 38 p.

Dickinson, W.R., and Suczek, C.A., 1979, Plate tectonics and sandstone compositions: American Association of Petroleum Geologists Bulletin, v. 63, p. 2164-2182.

Dickinson, W.R., Beard, L.S., Brakenridge, G.R., Erjavec, J.L., Fergusun, R.C., Inman, K.F., Knepp, R.A., Lindberg, F.A., and Ryberg, P.T., 1983, Provenance of North American Phanerozoic sandstones in relation to tectonic setting: Geological Society of America Bulletin, v. 94, p. 222-235.

Dow, W.G., and Talukdar, S.C., 1995, Geochemical analysis of outcrop samples, western DeLong Mountains, Brooks Range: Alaska Division of Geological & Geophysical Surveys, Public-Data File 95-29, 40 p.

Grantz, Arthur, Holmes, M.L., and Kososki, B.A., 1976, Geologic framework of the Alaskan continental terrace in the Chukchi and Beaufort Seas, *in* Yorath, C.J., Parker, E.R., and Glass, D.J., eds., Canadian continental margins: Canadian Society of Petroleum Geologists Memoir 4, p. 669-700.

Lerand, M., 1973, Beaufort Sea, *in* McCrossam, R.G., ed., The future petroleum provinces of Canada—Their geology and potential: Canadian Society of Petroleum Geology Memoir 1, p. 315-386.

Mack, G., 1984, Exceptions to the relationship between plate tectonics and sandstone composition: Journal of Sedimentary Petrology, v. 54, p. 212-220.

Mayfield, C.F., Tailleur, I.L. and Ellersieck, I.F., 1988, Stratigraphy, structure and palinspastic synthesis of the Western Brooks Range, Northwest Alaska, *in* Gryc, G., ed., Geology and exploration of the National Petroleum Reserve in Alaska, 1974 to 1982: U.S. Geological Survey Professional Paper 1399, p. 143-186.

Mickey, M.B., Haga, H., Mull, C.G., 1995, Paleontologic data: Tingmerkpuk sandstone and related units, northwestern DeLong Mountains, Brooks Range, Alaska: Alaska Division of Geological & Geophysical Surveys, Public-Data File 95-31, 42 p.

Molenaar, C.M., Egbert, R.M., and Krystinik, L.F., 1988, Depositional facies, petrography, and reservoir potential of the Fortress Mountain Formation (Lower Cretaceous), central North Slope, Alaska, *in* Gryc, G., ed., Geology and exploration of the National Petroleum Reserve in Alaska, 1974 to 1982: U.S. Geological Survey Professional Paper 1399, p. 257-280.

Moore, T.E., Wallace, W.K., Bird, K.J., Karl, S.M., Mull, C.G., and Dillon, J.T., 1994, Geology of northern Alaska, *in* Plafker, George, and Berg, H.C., eds., The Geology of Alaska: Boulder Colorado, Geological Society of America, The Geology of North America, v. G-1, p. 49-140.

Mull, C.G., 1979, Nanushuk Group deposition and the Late Mesozoic structural evolution of the central and western Brooks Range and Arctic Slope, *in* Ahlbrandt, T.S., ed., Preliminary geologic, petrologic, and paleontologic results of the study of the Nanushuk Group rocks, North Slope Alaska: U.S. Geological Survey Circular 794, p. 5-13.

Mull, C.G., 1985, Cretaceous tectonics, depositional cycles, and the Nanushuk Group, Brooks Range and Arctic Slope, Alaska, *in* Huffman, A.C., Jr., ed., Geology of the Nanushuk Group and related rocks, North Slope, Alaska: U.S. Geological Survey Bulletin 1614, p. 7-36.

Mull, C.G., 1995, Preliminary evaluation of the hydrocarbon source rock potential of the Tingmerkpuk sandstone (Neocomian) and related rocks, northwestern Brooks Range, Alaska: Alaska Division of Geological & Geophysical Surveys Public-Data File 95-30, 20 p.

Mull, C.G., Crowder, R.K., Adams, K.E., Siok, J.P., Bodnar, D.A., Harris, E.E., and Alexander, R.A., 1987a, Stratigraphy and structural setting of the Picnic Creek allochthon, Killik River Quadrangle, central Brooks Range, Alaska: A summary, *in* Tailleur, I.L., and Weimer, P., eds., Alaskan North Slope geology: Bakersfield, California, Society of Economic Paleontologists and Mineralogists, Pacific Section, and Alaska Geological Society, Book 50, p. 649-662.

Mull, C.G., Roeder, D.H., Tailleur, I.L., Pessel, G.H., Grantz, Arthur, and May, S.D., 1987b, Geologic sections and maps across Brooks Range and Arctic Slope to Beaufort Sea: Geological Society of America Map and Chart Series MC-28S, scale 1:500,000.

Reifenstuhl, R.R., Wilson, M.D., and Mull, C.G. 1997, Petrography of the Neocomian Tingmerkpuk Sandstone, a hydrocarbon play, northwestern Brooks Range, Alaska, *in* Clough, J.C., ed., Short Notes on Alaska Geology 1997, Alaska Division of Geological & Geophysical Surveys Professional Report 118, p. 131-140.

Roeder, D., Mull, C.G., 1978, Tectonics of Brooks Range ophiolites, Alaska: AAPG Bulletin, v.62, no. 9, p. 1696-1702.

Van Der Plas, L., and Tobi, A.C., 1965, A chart for judging the reliability of point counting results: American Journal of Science, v. 263, p. 87-90.

Wilbur, S.C., Siok, J.P., and Mull, C.G., 1987, A comparison of two petrographic suites of the Okpikruak Formation: A point count analysis, *in* Tailleur, I.L, and Weimer, P., eds., Alaskan North Slope Geology: Bakersfield California, Society of Economic Paleontologists and Mineralogists, Pacific Section, and Alaska Geological Society, Book 50, p. 441-447.

Wilbur, S.C., 1989, Stratigraphy and petrology of the Okpikruak Formation, Cobblestone Creek, northcentral Brooks Range, *in* Mull, C.G., and Adams, K.E., eds., Dalton Highway, Yukon River to Prudhoe Bay, Alaska: Bedrock geology of the eastern Koyukuk basin, central Brooks Range, and eastcentral Arctic Slope, Alaska Division of Geological & Geophysical Surveys Guidebook 7, v. 2, p. 285-292.

SHORT NOTES ON ALASKA GEOLOGY 1997
PREVIOUS EDITIONS OF SHORT NOTES ON ALASKA GEOLOGY

Short Notes on Alaskan Geology 1976: **DGGS Geologic Report 51 (out of stock, $3.50 photocopied)**

Reconnaissance geology along the Variegated Glacier, Saint Elias Mountains
Evidence for early Cenozoic orogeny in central Alaska Range
The Shumagin-Kodiak batholith: A Paleocene magmatic arc?
Speculative tectonic evolution of the Cenozoic Shelikof Trough, south-central Alaska
Discovery of blueschists on Kodiak Island
Large kaolinite crystals in the Chignik Formation (Upper Cretaceous), Herendeen Bay
Occurrence of sodic amphibole-bearing rocks in the Valdez C-2 Quadrangle
High-quality coal near Point Hope, northwestern Alaska

Short Notes on Alaskan Geology 1977**: DGGS Geologic Report 55 (out of stock, $5.00 photocopied)**

A Givetian (Late Middle Devonian) fauna from Healy B-4 Quadrangle, central Alaska Range
Probable karst topography near Jade Mountains, southwestern Brooks Range
Tectonic significance of the Knik River schist terrane, south-central Alaska
Geochronology of southern Prince of Wales Island Katmai caldera: Glacier growth, lake rise, and geothermal activity
Geology and K-Ar age of mineralized intrusive rocks from the Chulitna mining district, central Alaska
The Richardson lineament: A structural control for gold deposits in the Richardson mining district, interior Alaska
Boulder Creek tin lode deposits
Comparison of mercury-antimony-tungsten mineralization of Alaska with strata-bound cinnabar-stibnite-scheelite deposits of the Circum-Pacific and Mediterranean regions
Earthquake recurrence and location in the western Gulf of Alaska

Short Notes on Alaskan Geology 1978**: DGGS Geologic Report 61 ($2.00)**

Holocene displacements measured by trenching the Castle Mountain fault near Houston
Bluff Point landslide, a massive ancient rock failure near Homer
Recurrent late Quaternary faulting near Healy
Glaciation of Indian Mountain, west-central Alaska
The Cantwell ash bed, a Holocene tephra in the central Alaska Range
Geochronology of metamorphic and igneous rocks in the Kantishna Hills, Mount McKinley Quadrangle
The Chilikadrotna Greenstone, an Upper Silurian metavolcanic sequence in the central Lake Clark Quadrangle
Tectonic and economic significance of Late Devonian and late Proterozoic U-Pb zircon ages from the Brooks Range

Short Notes on Alaskan Geology 1979-80**: DGGS Geologic Report 63 ($1.00)**

Lead isotope ratios from the Red Dog and Drenchwater Creek lead-zinc deposits, De Long Mountains, Brooks Range
^{40}K-^{40}Ar ages from rhyolite of Sugar Loaf Mountain, central Alaska Range: Implications for offset along the Hines Creek strand of the Denali fault system
Multiple glaciation in the Beaver Mountains, western interior Alaska
Fossil algae in Lower Devonian limestones, east-central Alaska
Tertiary tillites(?) on the northeast flank of Granite Mountain, central Alaska Range
Evidence for suprapermafrost ground-water blockage, Prudhoe Bay oil field

Short Notes on Alaskan Geology 1981: **DGGS Geologic Report 73 ($3.00)**

Alkaline igneous rocks in the eastern Alaska Range
Shear moduli and sampling ratios for the Bootlegger Cove Formation as determined by resonant-column testing
Clinoptilolite and mordenite deposits of possible economic value at Iliamna Lake, Alaska
The Keete Inlet thrust fault, Prince of Wales Island
Two Holocene maars in the central Alaska Range
Radiometric-age determinations from Kiska Island, Aleutian Islands, Alaska
Geochemical signature of the Goon Dip Greenstone on Chicagof Island, southeastern Alaska
Uranium mineralization in the Nenana Coal Field, Alaska
Reconnaissance of rare-metal occurrences associated with the Old Crow batholith, eastern Alaska - north-western Canada
A recent earthquake on the Denali fault in the southeast Alaska Range
Triassic paleomagnetic data and paleolatitudes for Wangellia, Alaska

***Short Notes on Alaskan Geology 1982-83*: DGGS Professional Report 86 ($2.50)**

An unconformity with associated conglomeratic sediments in the Berners Bay area of southeast Alaska
An iron-rich lava flow from the Nenana coal field, central Alaska
Results of shallow seismic survey for ground water at McGrath
Evaluation of a shallow sand-and-gravel aquifer at Eagle River
Correlation of geophysical well logs for a water development in south Anchorage
Garnet compositional estimates as indicators of progressive regional metamorphism in polymetamorphic rocks, Kantishna Hills
Geology of the Miss Molly molybdenum prospect, Tyonek C-6 Quadrangle Glacial geology of the Mt. Prindle area, Yukon-Tanana Upland

***Short Notes on Alaskan Geology 1991*: DGGS Professional Report 111 ($8.00)**

Tin placers associated with the downcutting of fissure basalts, Ray River drainage, Alaska
Geology and geochemistry of the Gagaryah barite deposit, western Alaska Range, Alaska
Geology and geochemistry of Tatlawiksuk Hot Springs, a newly discovered geothermal area in western Alaska
Geology and geochemistry of the Sleitat Mountain tin deposit, southwestern Alaska
Native mercurian-silver, silver, and gold nuggets from Hunter Creek, Alaska
Late Pleistocene volcanic deposits near the Valley of Ten Thousand Smokes, Katmai National Park, Alaska
Deglaciation of the Allison-Sawmill Creeks area, southern shore of Port Valdez, Alaska
Dating Holocene moraines of Canwell Glacier, Delta River valley, central Alaska Range
Gilead sandstone, northeastern Brooks Range, Alaska: An Albian to Cenomanian marine clastic succession
Kikiktat Mountain klippe: A link between the Copter Peak and Nuka Ridge allochthons, northcentral Brooks Range, Alaska
Sample media useful for a systematic geochemical survey of upper Valdez Creek, Alaska

***Short Notes on Alaskan Geology 1993*: DGGS Professional Report 113 ($6.00)**

Mississippian terrigenous clastic and volcaniclastic rocks of the Ellesmerian sequence, upper Sheenjek River area, eastern Brooks Range, Alaska
The penultimate great earthquake in southcentral Alaska: evidence from a buried forest near Girdwood
Geology, alteration, and mineralization of the Vinasale Mountain gold deposit, west-central Alaska
Fumarolic gas chemistry (1982) and thermal spring water chemistry (1985), Crater Peak, Mount Spurr, Alaska
Organic-rich shale and bentonite in the Arctic Creek unit, Arctic National Wildlife Refuge: implications for stratigraphic and structural interpretations
Dating Holocene moraines of Black Rapids Glacier, Delta River valley, central Alaska Range
Paleomagnetism of the Fairbanks basalts, interior Alaska
The Hayes Glacier fault, southern Alaska Range: evidence for post-Paleocene movement
Detachment folds and a passive-roof duplex: examples from the northeastern Brooks Range, Alaska

***Short Notes on Alaskan Geology 1995*: DGGS Professional Report 117 ($15.00)**

Radiocarbon age of probable Hayes tephra, Kenai Peninsula, Alaska
Geochemistry of saline lakes of the northeastern Yukon Flats, eastcentral Alaska
Geometry and deformation of a duplex and its roof layer: Observations from the Echooka anticlinorium, northeastern Brooks Range, Alaska
Late-Wisconsin events in the Upper Cook Inlet region, southcentral Alaska
Stratigraphy and implications of a lakeside section, Glacial Lake, southwestern Kigluaik Mountains, Seward Peninsula, Alaska
Lithofacies, petrology, and petrophysics of the Kemik Sandstone (Lower Cretaceous), eastern Arctic Slope, Alaska
A new species of the conodont *amydrotaxis* From the Early Devonian of southwestern Alaska
Early Devonian and Late Triassic conodonts from Annette and Hotspur Islands, southeastern Alaska
Mineralization and zoning of polymetallic veins in the Beaver Mountains volcano-plutonic complex, Iditarod Quadrangle, westcentral Alaska
Possible thrust windows on the central Seward Peninsula, Alaska

View of boudinaged white marble within metapelite in the Kigluaik Mountains, Seward Peninsula. Light gray granite dike at lower right intrudes upward through metapelite until it hits the marble-metapelite contact, where it then becomes a sill. Photography by J.M. Amato.